SYNTHESIS OF ANTIMICROBIAL PEPTIDES DERIVED FROM BP100 AND BPC194

Imma GÜELL COSTA

Dipòsit legal: GI-255-2012
http://hdl.handle.net/10803/69920

Universitat de Girona

Doctoral dissertation

SYNTHESIS OF ANTIMICROBIAL PEPTIDES DERIVED FROM BP100 AND BPC194

Imma Güell Costa

2011

Programa de doctorat en Ciències Experimentals i Sostenibilitat

PhD supervisors:

Dra. Marta Planas Grabuleda

Dra. Lidia Feliu Soley

Memòria presentada per optar al títol de Doctora per la Universitat de Girona

Universitat de Girona

Les doctores Marta Planas Grabuleda i Lidia Feliu Soley, professores de l'àrea de Química Orgànica de la Universitat de Girona,

CERTIFIQUEM:

Que aquest treball, titulat *"Synthesis of antimicrobial peptides derived from BP100 and BPC194"*, que presenta la Sra. Imma Güell Costa per a l'obtenció del títol de Doctora, ha estat realitzat sota la nostra direcció i que compleix els requeriments per poder optar a Menció Europea.

Signatura

Dra. Marta Planas Grabuleda

Dra. Lidia Feliu Soley

Girona, 08 de Novembre de 2011

A person who never made a mistake, never tried anything new.

Albert Einstein

Tot està per fer i tot és possible.

Miquel Martí Pol

A la meva família i a l'Òscar

Agraïments / Acknowledgements

La veritat és que no sé per on començar... Fer una tesi és un camí personal... però no es pot fer tot sol, per tant, no em puc deixar d'agrair a totes les persones que en algun moment o altre m'han acompanyat al llarg d'aquests anys, tant en el camp universitari com personal.

Dins el camp universitari, vull començar agraïnt a les meves directores, la Dra. Lidia Feliu i Dra. Marta Planas, la seva ajuda i els seus valuosos consells així com també vull agrair que m'hagin donat l'oportunitat de fer el doctorat permetent-me créixer com a persona.

També m'agradaria donar les gràcies al Dr. Eduard Bardají el qual m'ha permès incorporar-me al grup LIPPSO i, per tant, portar a terme aquesta recerca, i a la Dra. Montse Heras per haver-me donat suport i bons consells durant el temps que he estat aquí.

En segon lloc m'agradaria donar les gràcies a totes les persones que formen part dels Serveis Tècnics de Recerca, especialment al Dr. Vicenç Oliveras pel seu ajut amb el MALDI, a la Dra. Lluïsa Matas per la seva ajuda en les ressonàncies i a la senyora Anna Costa pel seu ajut amb l'ESI/MS. A més, també vull agrair als membres del Grup de Patologia Vegetal de la UdG els quals han realitzat les proves biològiques, concretament a la Dra. Esther Badosa, que també m'ha ajudat molt quan he tingut dubtes "biològics", i al Dr. Jordi Cabrefiga.

Com no, també m'agradaria agrair als meus companys de grup (LIPPSIANS!!) que són les persones amb qui al final acabem passant més hores junts al llarg del dia. Amb tots ells compartim feina però també bones estones. A la Vane (Cherry) i en Rafael, que tot i que no he compartit molts moments amb ells, són la veu de l'experiència i, per això, els voldria agrair els consells que m'han donat els quals m'han ajudat a tirar endavant. A la Marta i la Montse, que tot i que la major part del temps han estat al parc, he tingut la seva ajuda incondicional. A més, també li volia agrair a la Montse la paciència que va tenir en ensenyar-me en els meus inicis. A l'Anna Díaz (super vital i optimista a l'hora de fer les coses) i a en

Tyffa que tot i que últimament no ens hem vist tant també han contribuït amb la seva alegria i positivisme. Dels "veteranos" ja només em queda l'Ana que li he d'agrair la seva paciència en explicar-me les coses. I com no a les "xaties" actuals i a les noves incorporacions dels laboratoris, la Cristina (La mangui), l'Iteng (Sra. Choi), la Sílvia (Xumi?), la Marta Soler (rrrrrrrrrrrrrr) i la Camó (*peró mujer.... que haces???)* els vull agrair els bons moments passats al laboratori i al despatx compartint històries, bromes, xerrades "filosòfiques" per salvar el món i el suport donat. No em podia deixar en Lluís (el iogurin) que amb esforç i dedicació però també amb sentit de l'humor ha ajudat a fer una part d'aquesta tesi amb els seus treballs experimental i acadèmicament dirigit. Finalment no em vull oblidar de les companyes que encara que ja no són aquí hem compartit laboratori o despatx, a la Laura, per les llargues estones que vam passar fent treballs de màster i a la Gemma Moiset, que espero que li vagi molt bé per Groningen.

A més, vull fer extensiu el meu agraïment a la resta de persones del departament de química "Les cats" pels dinars i per l'ajuda que m'han donat, els inorgànics que tot i que molts no volten ara per aquí sempre creaven ambient i els que encara que el seu nom no figuri de forma explícita en aquestes línies m'han ajudat d'una manera o altra; sense tots ells tampoc hauria estat possible.

Now I would like to express my appreciation for the collaboration, help, advice and good moments shared with me during the months I've been in Copenhagen. First, I would like to express my sincere thanks to prof. Knud Jensen for giving me the opportunity to work in his group and also for his support, guidance and patience throughout this project. I also would like to thank all the people from KVL, Kasper, Thomas, Renee, Søren, Masood, Nicolai… for helping me in the lab during all these months and also for the good moments with some of them outside the lab and in that nice bar *a-vej*. Thank you all of you to make me feel like I was at home. Antes de terminar con los buenos momentos vividos en CPH no me quiero olvidar de Vicky por estar siempre allí, gracias por los buenos momentos vividos por las "spanish girls". Tampoco me puedo olvidar de Ester i José (los Suecos) que me han ayudado mucho y hecho pasar muy buenos

momentos (vaya fiestas nos pegamos… ;p). La estancia no hubiera sido igual sin vosotros.

Per continuar amb els agraïments dins el camp universitari però que també són una part molt important en el camp personal, no em puc deixar les meves "nenes" l'Ester (altre cop), l'Alicia, l'Àngels i la Mireia. Qui ens havia de dir quan ens vam conèixer que acabaríem així... Moltes gràcies per ajudar-me en els moments més difícils i sobretot per compartir tants bons moments juntes. Sé que sempre puc comptar amb vosaltres. Gràcies per ser-hi!!!

Dins el camp personal, vull donar les gràcies als meus amics (la colla tutsworld i als "Bascus") per les estones que hem passat junts; les escapades de càmping, els viatges, els sopars... en definitiva per ser com són.

I no em podia deixar a la meva família que sempre ha estat al meu costat de manera incondicional quan l'he necessitat (i quan no també :p). A La meva mare li vull agrair tot el seu recolzament i sobretot que sempre tingui un moment per escoltar-me, encara que jo no en tingui gaires per a ella. A la meva germana (l'Anna, apa perquè no puguis dir que no és una dedicació nominal) la seva ajuda amb les seves idees boges i creatives i com no els *tuppers* que la mama li obligava a preparar-me, gràcies (jeje). A més, també voldria donar les gràcies al meu pare per la seva ajuda i als sogres pels seus tàpers i el fet que em cuidin com si fos una filla més. Com no també vull donar les gràcies a en David (el *cunyiiiiii*) pel super disseny de la portada de la tesi, gràcies! Finalment, a tu Òscar t'agraeixo la comprensió i el recolzament que m'has donat al llarg d'aquests anys i que espero que en siguin molts més ara que hem començat un nou camí junts. Gràcies per tot de tot cor, sé que no és fàcil aguantar-me però amb el vostra suport tot ha estat molt més senzill.

Us estimo molt!

ABBREVIATIONS

AA	Amino acid
Ac	Acetyl
ACN	Acetonitrile
Ahx	2-Aminohexanoic acid
Al	Allyl
AMP	Antimicrobial peptide
Aoa	Aminooxyacetyl
Bn	Benzyl
Boc	*tert*-Butyloxycarbonyl
^{t}Bu	*tert*-Butyl
Bz	Benzoyl
cDTE	Cyclo-dithioerythritol
CM	ChemMatrix
COMU	1-[(1-(Cyano-2-ethoxy-2-oxoethylideneaminooxy)-dimethylamino-morpholinomethylene)] methanaminium hexafluorophosphate
d	Doublet
dd	Doublet of doublets
DCE	1,2-Dichlorethane
DIPEA	*N,N'*-Diisopropylethylamine
DIPCDI	*N,N'*-Diisopropylcarbodiimide
DMF	*N,N'*-Dimethylformamide
DMSO	Dimethylsulfoxide
dt	Doublet of triplets
DVB	Divinylbenzene
EDC	Ethyl-(*N,N'*-dimethylamino)propylcarbodiimide hydrocloride
equiv	Equivalent
ESI/MS	Electrospray ionization-mass spectrometry

Et	Ethyl
Fmoc	9-Fluorenylmethyloxycarbonyl
Gal*p*	α-D-Galactopyranoside
HBTU	*O*-(Benzotriazol-1-yl)-*N,N,N',N'*-tetramethyluronium hexafluorophosphate
HOBt	1-Hydroxybenzotriazole
HPLC	High performance liquid chromatography
HRMS	High resolution mass spectrometry
IR	Infrared spectroscopy
J	Coupling constant
LC/MS	Liquid chromatography-mass spectrometry
m	Multiplet
MALDI-TOF	Matrix-assisted laser desorption/ionization-time-of-flight
MBHA	*p*-Methylbenzylhydrylamine
Me	Methyl
MIC	Minimun inhibitory concentration
Mtt	4-Methyltrityl
m/z	Mass-to-charge ratio
NMM	*N*-Methylmorpholine
NMP	*N*-Methylpyrrolidone
NMR	Nuclear Magnetic Resonance
***o*-BAL**	4,6-Dimethoxy-2-hydroxybenzaldehyde
Oxyma	Ethyl cyanoglyoxylate-2-oxime
Ph	Phenyl
Prg	Propargylglycine
PS	Polystyrene
PyOxim	*O*-[(1-Cyano-2-ethoxy-2-oxoethylidene)amino]-oxytri(pyrrolidin-1-yl) phosphonium hexafluorophosphate
Rink	4-[Amino(2,4-dimethoxyphenyl)methyl]phenoxyacetic acid

s	Singlet
t	Triplet
td	Triplet of doublets
TFA	Trifluoroacetic acid
TFE	Trifluoroethanol
THF	Tetrahydrofuran
TIS	Triisopropylsilane
TLC	Thin layer chromatography
t_R	Retention time
TRIS	Tris(hydroxymethyl)aminomethane
Ts	Tosyl
TSB	Trypticase Soy Broth

AMINO ACIDS

Name	Three letter code	One letter code
Aspartic acid	Asp	D
Glutamic acid	Glu	E
Alanine	Ala	A
Arginine	Arg	R
Asparagine	Asn	N
Cysteine	Cys	C
Phenylalanine	Phe	F
Glycine	Gly	G
Glutamine	Gln	Q
Histidine	His	H
Isoleucine	Ile	I
Leucine	Leu	L
Lysine	Lys	K
Methionine	Met	M
Norleucine	Nle	-
Proline	Pro	P
Serine	Ser	S
Tyrosine	Tyr	Y
Threonine	Thr	T
Tryptophan	Trp	W
Valine	Val	V

TABLE OF CONTENTS

General abstract

Antimicrobial peptides play an important role in the host defence system of the majority of species ranging from bacteria to plants, including mammals. Most of them are cationic and have the ability to adopt an amphiphatic conformation. Moreover, it is believed that their mode of action involves membrane permeation. These peptides have emerged as excellent candidates for the development of new antibacterial agents because they are unlikely to cause rapid emergence of resistance. Another advantage of antimicrobial peptides is the selectivity towards the bacterial membrane versus the eukaryotic cell membrane, which confers them a low toxicity. However, natural antimicrobial peptides present long sequences, poor bioavailability and low stability towards protease degradation.

This thesis was focused on the development of analogs of the lead antimicrobial peptides **BP100** (KKLFKKILKYL-NH_2) and **BPC194** c(KKLKKFKKLQ). Our aim was to obtain sequences with improved antimicrobial activity, low hemolysis and high stability to protease degradation. One of the strategies used was centered on the introduction of non-proteoinogenous amino acids in the peptide sequence such as D-amino acids. It has been reported that the incorporation of D-amino acids maintains structural peptide properties (hydrophobicity, side-chains and the distribution of the peptide charge) and increases the stability to protease digestion. We also studied the introduction of a 1,2,3-triazole moiety in the peptide sequence. This nitrogen heterocycle has been described to be resistant to metabolic degradation and it is considered as a powerful pharmacophore. Moreover, the formation of this heterocycle can be easely achieved through alkyne-azide cycloaddition under mild conditions that can be applied to derivatize peptide sequences. The last approach used in this thesis for designing antimicrobial peptides is based on the concept of multivalency. It has been reported that an improved binding to microbial membranes and thus an improved antimicrobial activity can be achieved if several copies of antmicrobial peptides are linked together to form multimeric species. It is proposed that these multivalent peptides interact more easily with the membrane than the corresponding monomer, which means that the minimum concentration required might be reduced.

First, we synthesized antimicrobial peptides derived from **BP100** containing D-amino acids with moderate to good purities. Peptides active against the plant pathogenic bacteria *Erwinia amylovora, Xanthomonas vesicatoria* and *Pseudomonas syringae*, and the human bacteria *Escherichia coli*, *Salmonella typhimurium*, *Staphylococcus aureus* and *Listeria monocytogenes* were identified. Some of these sequences were more active, less hemolytic and more stable to protease degradation than **BP100**. One of the peptides, **BP143** (KKLfKKILKYL-NH_2), showed an efficacy *in planta* comparable to streptomycin and higer than that of **BP100**.

We also prepared **BP100** analogs containing the 1,2,3-triazole ring on an amino acid side-chain. This heterocycle was formed by reaction of an alkynyl resin and an azide. All peptidotriazoles were obtained in moderate to good purities. We identified sequences active against the bacteria *Erwinia amylovora, Xanthomonas vesicatoria* and *Pseudomonas syringae* and the fungi Fusarium oxysporum and *Penicillium expansum*, displaying low hemolysis and with higher stability to proteases than **BP100**.

Additionally, we prepared cyclic peptidotriazoles based on the structure of **BPC194** containing a triazolylalanine, a triazolyl-modified glutamine or a tryazolyllysine at positions 3 or 5. The synthesis was achieved via a cycloaddition reaction either between an alkynyl peptidyl resin and an azide in solution or between an azidopeptidyl resin and an alkyne in solution. Both strategies afforded the cyclic peptidotriazoles in good purities. Beside, we synthesized a conjugated peptidotriazole in excellent purity by linking a cyclic alkynyl peptidyl resin and an azidopentapeptide. The use of microwave irradiation reduced the reaction time from 7 h to 30 min. We identified cyclic peptidotriazoles with high activity against *X. vesicatoria*, *P. syringae*, *E. amylovora* and *E. coli*, and low hemolysis. In addition, these compounds were not active against the biocontrol agents *L. mesenteroides* and *B. subtilis*. Therefore, these sequences can be considered as good candidates for plant protection. It has been observed that the introduction of a triazole moiety in **BPC194** did not significantly influence the antibacterial activity. Peptidotriazoles resulting from the substitution of an apolar residue of **BPC194** by a triazolyl-modified amino acid were less hemolytic than those resulting from the substitution of a polar residue. Among these

peptidotriazoles, the ones bearing a polar substituent at the triazole ring were the least hemolytic.

Moreover, we prepared carbopeptides through oxime ligation of C-terminal peptide aldehydes with tetra-aminooxyacetyl functionalized monosaccharide templates. The C-terminal aldehydes were derived from the lead antimicrobial peptides **BP100** and **BP143**. The carbohydrates used in this study were cyclo-dithioerythritol (cDTE) and α-D-Galactopyranoside (Gal*p*). Carbopeptides **cDTE(BP100)$_2$**, **cDTE(BP1430)$_2$** and **Gal*p*(BP100)$_4$** were obtained in moderate yields and good purities. These carbopeptides were active against *E. amylovora*, *X. vesicatoria*, *P. syringae*, *E. coli*, *L. monocytogenes* and *S. typhimurium*. However, they were highly hemolytic. For **Gal*p*(BP100)$_4$** and **cDTE(BP100)$_2$** a multimeric effect was observed against the plant pathogens.

This thesis shows that the biological profile of lead antimicrobial peptides can be improved by the incorporation of D-amino acids and triazolyl-modified amino acids.

Resum General

Els pèptids antimicrobians tenen un paper important en el sistema de defensa de l'innat d'una gran diversitat d'espècies que van des dels bacteris fins a les plantes, inclosos els mamífers. La majoria d'ells són catiònics i tenen la capacitat d'adoptar una conformació amfipàtica. A més, segons estudis realitzats fins al moment es creu que el seu mecanisme d'acció consisteix en la permeabilització de la membrana. Aquests pèptids han esdevingut excel·lents candidats pel desenvolupament de nous agents antibacterians, ja que fan difícil l'aparició de soques resistents. Un altre dels avantages dels pèptids antimicrobians és la selectivitat pels bacteris respecte a les cèl·lules eucariotes, conferint així una baixa toxicitat. No obstant això, els pèptids antimicrobians presents en la natura tenen llargues seqüències, poca biodisponibilitat i baixa estabilitat a la degradació per proteases.

Aquesta tesi doctoral es centra en el desenvolupament d'anàlegs als pèptids antimicrobians *lead* **BP100** (KKLFKKILKYL-NH_2) i **BPC194** c(KKLKKFKKLQ). Concretament, aquest treball es basa en l'obtenció de seqüències amb una millor activitat antimicrobiana, una baixa hemòlisi i una alta estabilitat a la degradació per proteases. Una de les estratègies utilitzades es va centrar en la introducció d'aminoàcids no proteinogènics a la seqüència del pèptid com ara D-aminoàcids. S'ha descrit que la incorporació de D-aminoàcids manté les propietats estructurals de pèptids (hidroficitat, cadenes laterals i la distribució de la càrrega de pèptids) i augmenta l'estabilitat a la digestió per proteases. A més, també es va estudiar la introducció d'un anell de 1,2,3-triazole en la seqüència del pèptid. Aquests heterocicles nitrogenats són resistents a la degradació metabòlica i són considerats uns potents farmacòfors. D'altra banda, la formació d'aquest heterocicle es pot aconseguir fàcilment a través d'una cicloaddició alquí-azida en unes condicions molt suaus aplicables a la derivatització de seqüències peptídiques. L'última metodologia utilitzada en aquesta tesi pel disseny de pèptids antimicrobians està basada en el concepte de multivalència. S'ha descrit que una millor unió a les membranes microbianes i per tant una millora en l'activitat antimicrobiana es pot aconseguir si diverses còpies de pèptids antimicrobians estan units entre si formant espècies multimèriques. S'ha proposat que aquests pèptids multivalents poden interactuar més fàcilment amb la membrana que

el corresponent monòmer, la qual cosa implica que la concentració mínima requerida es pot reduir.

En primer lloc, es van sintetitzar pèptids antimicrobians derivats de **BP100** contenint D-aminoàcids amb bones i moderades pureses. Es van identificar pèptids actius contra els bacteris fitopatògens *Erwinia amylovora*, *Xanthomonas vesicatoria* i *Pseudomonas syringae*, i els patògens humans *Escherichia coli*, *Salmonella typhimurium*, *Staphylococcus aureus* i *Listeria monocytogenes*. Algunes d'aquestes seqüències van resultar ser més actives, menys hemolítiques i més estables a la degradació per proteases que **BP100**. Un dels pèptids, **BP143** (KKLfKKILKYL-NH_2), va mostrar una eficàcia *in planta* comparable a l'estreptomicina i superior a **BP100**.

Altrament, es van preparar pèptids anàlegs a **BP100** contenint un anell de 1,2,3-triazole a la cadena lateral d'un aminoàcid. Aquest heterocicle es va formar per reacció d'una alquinil resina and azida. Tots els peptidotriazoles es van obtenir amb moderades i bones pureses. Es van identificar les seqüències actives contra els bacteris *Erwinia amylovora*, *Xanthomonas vesicatoria* i *Pseudomonas syringae* i els fongs *Fusarium oxysporum* i *Penicillium expansum*, mostrant una baixa hemòlisi i una major estabilitat a les proteases que **BP100**.

A més, es van preparar peptidotriazoles cíclics basats en l'estructura de **BPC194** contenint una triazolil-alanina, una triazolil-glutamina modificada o una triazolil-lisina a les posicions 3 i 5. La síntesi es va portar a terme a través d'una reacció de cicloaddició, ja sigui entre una alquinil peptidil resina i una azida en solució o entre una azidopeptidil resina i un alquí en la solució. Ambdues estratègies van proporcionar peptidotriazoles cíclics amb bones pureses. A banda d'això, es va sintetitzar un peptidotriazole conjugat amb una puresa excel·lent mitjançant la unió d'una alquinil resina cíclica i un azidopentapèptid. L'ús de la irradiació de microones va reduir el temps de reacció de 7 h a 30 min. Es van identificar peptidotriazoles cíclics amb una elevada activitat contra *X. vesicatoria*, *P. syringae*, *E. amylovora* i *E. coli*, i una baixa hemòlisi. A més, aquests compostos no eren actius contra els agents de control biològic *L. mesenteroides* i *B. subtilis*. Per tant, aquestes seqüències es poden considerar bons candidats per a la protecció de les plantes. En base a això, es va

observar que la introducció d'un anell de triazole en **BPC194** no va influir significativament en l'activitat antibacteriana. Els peptidotriazoles resultants de la substitució d'un residu apolar de **BPC194** per un aminoàcid triazolil-modificat eren menys hemolítiques que les resultants de la substitució d'un residu polar. Entre aquests peptidotriazoles, els que tenien un substituent polar en l'anell de triazole van resultar ser els menys hemolítics.

Finalment, es van preparar carbopèptids a través d'una unió oxima entre pèptids aldehid C-terminal i monosacàrids tetra-aminooxiacetil funcionalitzats. Els pèptids aldehid C-terminal són derivats dels pèptids *lead* antimicrobians **BP100** and **BP143**. Els carbohidrats utilitzats en aquest estudi van ser el ciclo-ditioeritritol (cDTE) i α-D-galactopiranosa (Gal*p*). Els carbopèptids **cDTE(BP100)$_2$**, **cDTE(BP143)$_2$** i **Gal*p*(BP100)$_4$** es van obtenir amb uns rendiments moderats i unes bones pureses. Aquests carbopèptids van resultar ser actius contra *E. amylovora*, *X. vesicatoria*, *P. syringae*, *E. coli*, *Listeria monocytogenes* i *S. typhimurium*. No obstant això, van ser molt hemolítics. Pels carbopèptids **Gal*p*(BP100)$_4$** i **cDTE(BP100)$_2$** un efecte multimèric es va observar enfront els patògens vegetals.

Aquesta tesi mostra que el perfil biològic dels pèptids *lead* antimicrobians pot ser millorat mitjançant la incorporació de D-aminoàcids i triazolil-aminoàcids modificats.

1. INTRODUCTION

1.1. Control of plant and human diseases

Pathogenic bacteria can cause diseases in different organisms such as plants, humans or animals. The LIPPSO group, in collaboration with the Plant Pathology group of the UdG, studies the development of sustainable and effective agents to control plant diseases for which no effective methods are currently available. In particular, the research project of this PhD thesis has been mainly focused on economically important plant pathogenic bacteria and fungi. Moreover, this project has also included human pathogenic bacteria.

1.1.1. Plant diseases

Phytopathogenic bacteria are responsible for a wide range of plant diseases causing large economic losses in fruit and vegetable crops. Their control is mainly based on copper derivatives and antibiotics such as kasugamycin and streptomycin. Although these compounds are highly efficient to treat these diseases, many of them are not allowed in Europe due to environmental concerns. In addition, the emergence of antibiotic-resistant strains has been reported, which limits the effectiveness of these compounds (Montesinos 2001). Therefore, there is a need of new antimicrobial compounds in agriculture for plant-disease control, with low toxicity and reduced negative environmental impact.

The framework of this thesis is focused on the development of new agents useful to control plant diseases caused by the bacteria *Erwinia amylovora*, *Pseudomonas syringae,* and *Xanthomonas vesicatoria* and the fungi *Fusarium oxysporum* and *Penicillium expansum* (Bardají P200601098, Monroc 2006, Ferre 2006, Badosa 2007, Badosa 2009).

E. amylovora is a gram-negative quarantine bacterium which is responsible of fire blight. Pears are the most susceptible to this bacterium, but apples, loquat and some other rosaceous plants of great economic and commercial interest are also vulnerable. Infection occurs via natural plant openings such as nectaries in flowers and wounds on leaves or on succulent shoots. The causal bacterium multiplies and rapidly spreads

through the plant via vascular tissues and can cause cell death (tissue necrosis). Fire blight control is not very effective in infected plants, so new measures are being implemented to prevent the spread of the pathogen and the introduction of the disease in endemic regions (Milčevičová 2010, Cabrefiga 2005) (Scheme 1.1).

Scheme 1.1. *Fire blight symptoms in an infected pear shoot.*

P. syringae is a rod shaped gram-negative bacterium with polar flagella which can infect a wide range of horticultural crops causing many diseases known as bacterial canker. This bacterium is responsible for the surface frost damage in plants exposed to the environment. The freezing causes injuries in the epithelia and makes the nutrients in the underlying plant tissues available to the bacteria. As a result, spots are formed on the leaves and fruits which prevent their growth (Agrios 2005) (Scheme 1.2).

Scheme 1.2. *Bacterial canker symptoms in an infected trunk.*

X. vesicatoria is a gram-negative bacterium causing bacterial spot in the family of solanaceous plants such as tomatoes and peppers, leading to considerable losses in productivity and quality of harvests. Infected plants in the seed bed usually have small, irregular, black or water-soaked spots along the edges of the first leaves. Older plants

develop small, pale green or water-soaked lesions that are raised on the underside of the leaf eventually causing plant death (Bajpai 2010).

Scheme 1.3. *Bacterial spot symptoms in infected tomatoes.*

P. expansum causes blue mould which is the most important postharvest decay of stored apples. This agent not only causes fruit decay but also has potential public health significance, due to the production of the carcinogenic mycotoxin patulin. This toxin may rise to unacceptable levels in fruits destined for processing and may also result in off flavours (Rutberget 2004, Sanzani 2009) (Scheme 1.4).

Scheme 1.4. *Bulb infected with blue mould.*

F. oxysporum is the causal agent of vascular wilt disease in a wide variety of economically important crops. Vascular wilt disease is a major limiting factor in the production of many agricultural and horticultural crops. The typical symptoms are yellowing, vascular wilt and root rot. This fungus is also known as a serious emerging pathogen of humans, causing a broad spectrum of infections ranging from superficial to locally invasive or disseminated (Ortoneda 2004).

1.1.2. Human diseases

The fight against bacterial infections represents one of the striking points in modern medicine. The discovery and the development of antibiotics during the mid-twentieth century provided potent antimicrobial drugs with high specificity. However, as a consequence of the frequent use of antibiotics, bacterial resistance to known classes of antibiotics has become a severe global problem, resulting in diminished effectiveness of current therapies. Consequently, there is an obvious need to search for alternative natural antimicrobial agents with a mode of action different from that of classical antibiotics. Based on this, this thesis also studies the use of peptides to control bacteria responsible of human diseases such as *Escherichia coli, Staphylococcus aureus, Salmonella typhimurium and Listeria monocytogenes.*

E. coli is a gram-negative bacterium and it is part of the normal gastrointestinal microflora which exerts a barrier effect against enteropathogens and also it is necessary for proper digestion of food. Most *E. coli* strains are harmless, but some can cause serious food poisoning in humans. Virulent strains of *E. coli* can cause gastroenteritis, urinary tract infections, and neonatal meningitis. In rare cases, virulent strains are also responsible for hemolytic-uremic syndrome (HUS), peritonitis, mastitis and septicemia (Boyen 2009).

S. aureus is a gram-positive bacterium which is a major human pathogen responsible for both community- and hospital-acquired infections with a significant morbidity and mortality. Today, the prevalence of methicillin-resistant *S. aureus* (MRSA) is steadily increasing, and treatment of staphylococcal infections has become more difficult due to the emergence of multidrug-resistant strains. Infections caused by *S. aureus* range from mild skin and wound infections to acute life-threatening diseases such as endocarditis, pneumonia, arthritis, and osteomyelitis. However, this bacterium can also cause a chronic type of disease with recurrent infections, as demonstrated for osteomyelitis and cystic fibrosis (Kahl 2003).

S. typhimurium is a gram-negative bacterium and is the major cause of salmonellosis in humans, which is characterized by acute intestinal inflammation and diarrhea. Animals and birds are the natural reservoirs of this bacterium and, consequently, meat, dairy

products and eggs are the most commonly implicated sources in salmonellosis outbreaks (Winter 2009).

L. monocytogenes is a gram-negative bacterium responsible for listeriosis, a fatal disease of public health concern. This disease is primarily a mild gastroenteritis but may end up causing more severe invasive syndromes such as septicemia or meningitis. Infections of these bacteria are particularly dangerous to certain risk groups, including pregnant women, the elderly, newborns and immunocompromised patients. The infectious dose of these bacteria has not been clearly established, being highly variable & depending on the degree of susceptibility of each individual. This pathogen is widely distributed on raw fruits and vegetables. Plants and vegetables consummed as salad play a role in disseminating the pathogen through human food supply. Because of its particular characteristic to survive at low temperatures, it is especially threatening for the dairy industry if fast and reliable methods are not employed (Vanegas 2009).

1.1.3. Bacteria as biocontrol agents

Pathogenic microorganisms affecting plant health are a major and chronic threat to food production and ecosystem stability worldwide. As agricultural production intensified over the past few decades, producers became more and more dependent on agrochemicals as a relatively reliable method of crop protection. However, the increasing use of chemical inputs causes several negative effects, *i.e.,* development of pathogen resistance to the applied agents and their nontarget environmental impacts (Montesinos 2001). Furthermore, the growing cost of pesticides, particularly in less-affluent regions of the world, and consumer demand for pesticide-free food has led to a search for substitutes for these products. There are also a number of fastidious diseases for which chemical solutions are few, ineffective or nonexistent (Gerhardson 2002).

Biological control is being considered as an alternative or a supplemental way of reducing the use of chemicals in agriculture (Gerhardson 2002, Cabrefiga 2011). It can be defined as the use of natural enemies to reduce the damage caused by a pest population. According to most biological control practitioners, biological control differs from natural control. Natural control is what occurs much of the time, natural enemies

keeping populations of potential pests in check without intervention. Biological control, on the other hand, requires intervention rather than simply letting nature take its course. Biocontrol agents include a wide variety of life forms, including vertebrates, invertebrates, fungi, and microorganisms. These beneficial species are common in most natural communities and, although their presence is often unnoticed, they help to maintain the "balance of nature" by regulating the density of their host or prey population.

The Plant Pathology group of the UdG studies de use of *Bacillus subtilis* and *Leuconostoc mesenteroides* as biocontrol agents for the plant diseases caused by the previously mentioned phytopathogenic bacteria and fungi. Therefore, in this thesis we decided to evaluate the activity of the synthesized peptides against these bacteria.

B. subtilis is a gram-positive bacterium commonly recovered from water, soil, air, and decomposing plant residues. This bacterium produces an endospore that allows it to endure extreme conditions of heat and desiccation in the environment. *B. subtilis* produces a variety of proteases and other enzymes that enable it to degrade a variety of natural substrates and contribute to nutrient cycling. However, under most conditions this organism is not biologically active and exists in the spore form (Alexander 1977). *B. subtilis* is considered a benign organism as it does not possess traits that cause disease. It is not considered pathogenic or toxigenic to humans, animals, or plants. The potential risk associated with the use of this bacterium in fermentation facilities is low.

L. mesenteroides is a gram-positive epiphytic bacterium widely spread in the natural environment which plays an important role in several industrial and food fermentations. This bacterium initiates growth in vegetables more rapidly over a range of temperatures and salt concentrations than any other lactic acid bacteria. It produces carbon dioxide and acids which rapidly decrease the pH and inhibit the development of undesirable microorganisms. The carbon dioxide produced replaces the oxygen, making the environment anaerobic and suitable for the growth of subsequent species of lactobacillus. Removal of oxygen also helps to preserve the colour of vegetables and stabilises any ascorbic acid that is present.

1.2. Antimicrobial peptides

The problems associated with the use of antibiotics, such as the emergence of resistant-strains and environmental concerns has prompted the search for new alternative treatments. Antimicrobial peptides (AMPs), also known as genetically encoded antibiotic peptides, are conserved components of the innate immune response of many organisms and, for this reason, they have emerged as good candidates for the development of effective antimicrobial agents in pathogenic bacteria and fungi protection.

They have been isolated from many living organisms such as bacteria, insects, plants and vertebrates (Zasloff 2002, Brodgen 2005, Zaiou 2007, Diamond 2009). In mammals, these peptides act mainly in phagocytic cells of the immune system to kill invasive bacteria. Moreover, they function in mucosal epithelial cells to prevent the colonization of host tissues by pathogens. The inventory of AMPs comprises a huge amount of peptides, which have been listed in a database in Trieste (http://www.bbcm.univ.trieste.it/~tossi/pag1.htm). These peptides display a wide range of biological activities such as antibacterial, antifungal, antiviral or antitumor (Otvos 2000, Hancock 2001, Brodgen 2003, Hancock 2006, Jenssen 2006, Zaiou 2007). Thus, AMPs have been widely studied for the treatment of major diseases in diverse areas such as medicine, veterinary and plant pathology.

AMPs have general features in common, which modulate their activity and specificity. They have a chain length most often between 10-50 residues and consist of a strategic combination of cationic and hydrophobic amino acids. Most of these peptides have a net positive charge and can adopt secondary structures under the appropriate conditions, such as α-helix and antiparallel β-sheet (Scheme 1.5). In addition, they are often amphipathic with one side of the secondary structure being hydrophilic and the other being hydrophobic (Brogden 2005, Jenssen 2006).

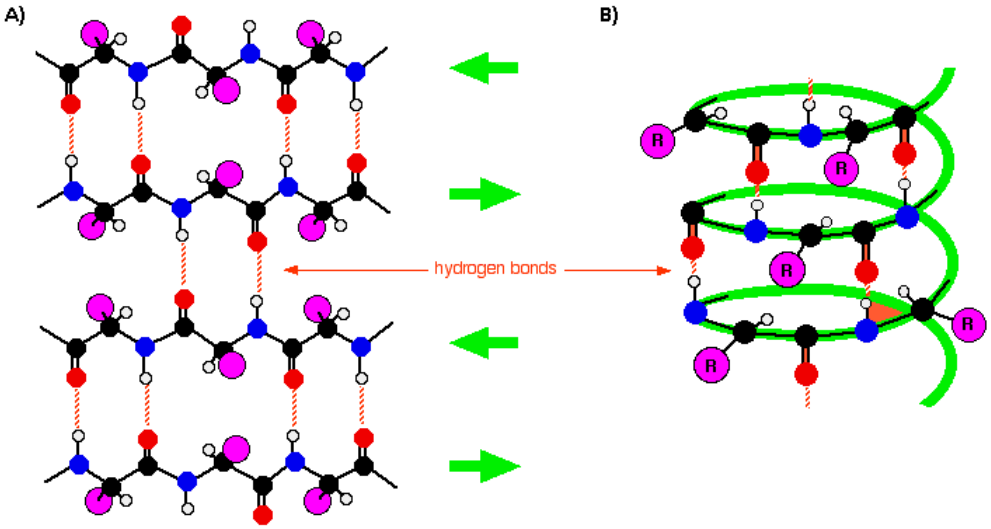

Scheme 1.5. *Types of secondary structures.* ***A)*** *Antiparallel β-sheet.* ***B)*** *α-Helix. Carbon atoms are shown in black, oxygen in red and nitrogen in blue. Hydrogen bonds are indicated as a red dashed line.*

Although the mechanism of action of AMPs has not been fully elucidated, it has been postulated that many work primarily by compromising the membrane of the target organism (Bechinger 2006, Hancock 2006, Huang 2006, Marcos 2009). It has been proposed that the net positive charge of AMPs facilitates the interaction with the negatively charged phospholipids of the bacterial membrane, while their amphypathic structure favors their insertion into the membrane bilayer (Tossi 2000, Zasloff 2002b, Glukhov 2005). When a critical concentration is reached, peptides are inserted into the membrane disturbing the bilayer integrity either by disruption or pore formation (Power 2003, Brogden 2005, Nicolas 2009, Melo 2009). Moreover, there have also been identified other phenomena related with the activity such as charge neutralization, permeability and translocation (Ferre 2009).

There are currently three general models that explain how AMPs disrupt membranes and are depicted in Scheme 1.6. In the *toroidal-pore* model, the attached AMPs aggregate and induce the lipid monolayers to bend continuously through the pore so that the water core is lined by both the inserted peptides and the lipid head groups. In the *barrel-stave model*, the attached AMPs aggregate and insert into the membrane bilayer so that the hydrophobic peptide regions align with the lipid core region and the hydrophilic peptide regions form the interior region of the pore. Unlike the toroidal-

pore, the phosphate groups remain on the bilayer surface. Finally, in the *carpet-like* model, peptides place parallel to the surface of the lipid bilayer forming an extensive layer or carpet. At high peptide concentrations, it is thought that the AMPs disrupt the bilayer in a detergent-like manner, leading to the formation of micelles. These mechanisms make the emergence of resistant strains difficult as this would involve drastic changes in the composition of bacterial membrane phospholipids.

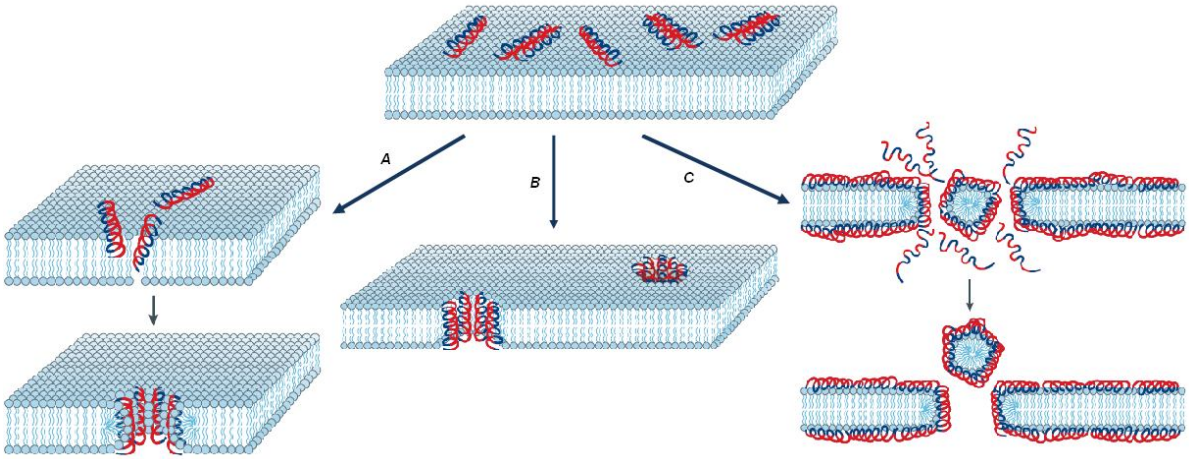

Scheme 1.6. *Schematic model of the mechanisms of membrane disruption by AMPs. Hydrophilic regions of the peptides are shown in red, hydrophobic regions of the peptides are shown in blue.* ***A)*** *Toroidal pore model,* ***B)*** *Barrel-stave pore model and* ***C)*** *Carpet-like model (Brogden 2005).*

Another advantageous feature of AMPs is a certain selectivity to bacterial with respect to mammalian cells. The most important factor for this selectivity seems to be the different lipid composition between bacterial and eukaryotic cell membranes (Toke 2005, Rotem 2009). In particular, the greater presence of anionic phospholipids in the outer leaflet of bacteria and the absence of cholesterol in bacterial membranes is considered a major factor for selectivity (Scheme 1.7).

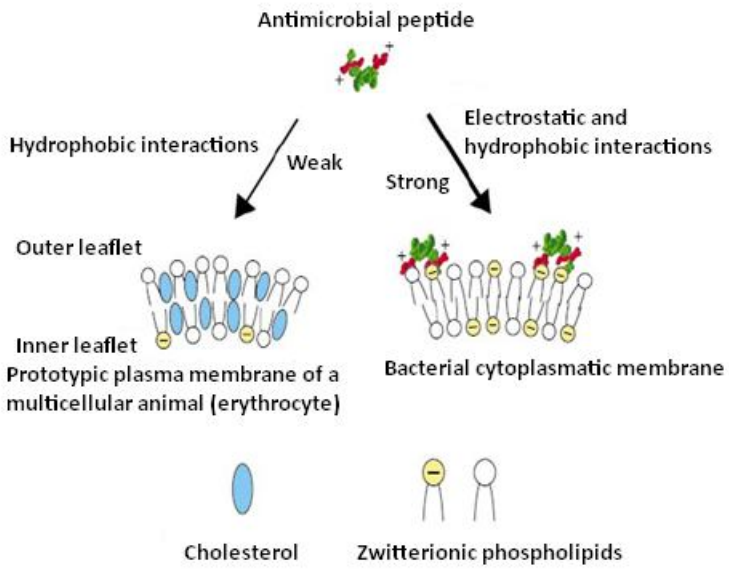

Scheme 1.7. *The basis for AMP specificity (Zasloff 2002b).*

1.3. Design and synthesis of AMPs: LIPPSO background

Despite the existence of a large number of natural potent AMPs, they show some disadvantages that limit their use. They usually have long amino acid sequences, display poor bioavailability, are prone to protease degradation and might be toxic to animals and plants. Thus, different strategies are used to overcome these drawbacks. Below are described some of the strategies developed in the LIPPSO group.

1.3.1. Cecropin A-melittin hybrid peptides

Cecropins are a family of cationic AMPs that are a key component of the immune response of insects. They were first isolated from the hemolymph of the giant silk moth *Hyalophora cecropia* and, subsequently, they have been isolated from other animal species including mammals. Cecropins have a potent antibacterial activity against many gram-negative and gram-positive bacteria, but show no cytotoxic activity against eukaryotic cells. In particular, cecropin A is a 37-amino acid linear peptide which consists of a strongly basic N-terminal amphypathic α-helical domain connected to a hydrophobic α-helix by a flexible hinge (Andreu 1983, Steiner 1981) (Table 1.1). Melittin is an antimicrobial peptide whith a structure similar to that of cecropins and contains 26 residues. It was isolated from bee venom, and has a potent antibacterial activity, but also a high hemolytic activity (Table 1.1).

Major concerns about the use of cecropin A and melittin as pesticides in plant protection are the high production cost of such long peptides and their sensitivity to protease degradation. Searches for shorter, more potent, nontoxic, and more stable peptides led to the identification of synthetic peptides with broader and higher activity than their natural counterparts. Specifically, the 11-residue sequence WKLFKKILKVL-NH_2 (Pep3), derived from the well-known cecropinA(1-7)-melittin(2-9) hybrid peptide, has a good profile of antifungal and antibacterial activities (Cavallarin 1998) (Table 1.1).

Table 1.1. *Sequences of selected AMPs.*

Peptide	Sequence
Cecropin A	KWKLFKKIEKVGQNIRDGIIKAGPAVAVVGQATQIAK-NH_2
Melittin	GIGAVLKVLTTGLPALISWIKRKRQQ-NH_2
Cecropin A(1-7)-melittin(2-9)	KWKLFKKIGAVLKVL-NH_2
Pep3	WKLFKKILKVL-NH_2

Based on the ideal α-helical wheel diagram of Pep3, the LIPPSO group prepared a library of 125 undecapeptides (Scheme 1.8). These peptides were designed by varying the amino acids at positions X1 and X10 by residues with different degrees of hydrophilicity and hydrophobicity. Moreover, the derivatization of the N-terminus was studied. In general, it was observed that the most active peptides contained a basic N-terminus and hydrophobic residues at the C-terminus, mainly aromatic amino acids (Ferre 2006).

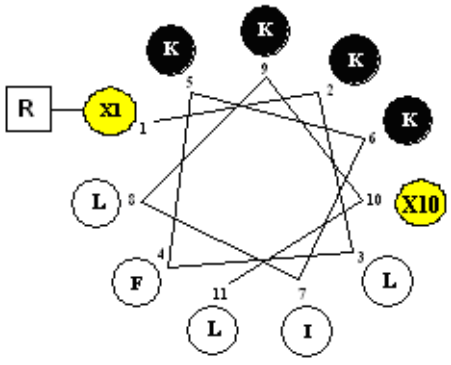

Scheme 1.8. *Edmunson wheel projection of peptides derived from Pep3. Black background, hydrophilic amino acids; white background, hydrophobic amino acids; yellow background, residues that can be either hydrophilic (Lys) or hydrophobic (Leu, Trp, Tyr, Val and Phe); R corresponds to H, Ac, Ts, Bz or Bn (Badosa 2007).*

These peptides were tested for *in vitro* growth inhibition of the bacteria *E. amylovora*, *P. syringae* and *X. vesicatoria* and the fungi *F. oxysporum* and *P. expansum* and for toxicity against eukaryotic cells. Peptide susceptibility to degradation by proteases was also evaluated. Several sequences were found to have a best biological profile than the parent peptide **Pep3**. Peptides with antifungal or antibacterial activity were identified (Table 1.2). Among the antifungal peptides, **BP33** and **BP15** were the most active against *F. oxysporum* while **BP21** was the most active against *P. expansum* (Badosa 2009). Among the antibacterial peptides, **BP76** and **BP100** were the best (MIC of 2.5 to 7.5 μM), showing an excellent *in vitro* biological profile. Moreover, **BP100** showed the highest *in vivo* activity (Badosa 2007).

Table 1.2. *Antimicrobial activity and cytotoxicity of Cecropin A-melittin hybrid undecapeptides being considered as a good candidates for the development of effective antimicrobial agents for plant protection.*

Peptide	Sequence	MIC[a] (μM)					H (%)[c]
		Ps[b]	*Xv*[b]	*Ea*[b]	*Pe*[b]	*Fo*[b]	
BP15	KKLFKKILKVL-NH_2	2-5	12-15	5-7	12.5-25	0.6-1-2	16 ± 2.9
BP33	LKLFKKILKVL-NH_2	5-7	10-12	5-7	25-50	0.3-0.6	37 ± 2.7
BP21	Ac-FKLFKKILKVL-NH_2	>7.5	2.5-5	>7.5	<6.2	3.1-6-2	85 ± 1.4
BP76	KKLFKKILKFL-NH_2	2.5-5.0	2.5-50	2.5-50	25-50	0.6-1.2	34 ± 2.1
BP100	KKLFKKILKYL-NH_2	2.5-5.0	5.0-7.5	2.5-5.0	25-50	<6.2[d]	22 ± 2.8

[a]Minimum inhibitory concentration.
[b]*Ps: P. syringae; Xv: X. vesicatoria; Ea: E. amylovora; Pe: P. expansum; Fo: F. oxysporum.*
[c]Percent hemolysis at 150 μM plus confidence interval (α = 0.05).
[d]Minimum concentration tested.

1.3.2. Peptides containing D-amino acids

Among the several strategies to improve the biological profile of peptides, the introduction of non-proteoinogenous amino acids, including D-isomers, in the peptide sequence is widely used. Although the introduction of D-amino acids destabilizes the secondary structure, other structural properties such as hydrophobicity and charge distribution are mantained. In addition, more stable sequences are obtained since only few enzymes are known to digest amide bonds involving a D-configuration (Matsuzaki

2009). This strategy has been used to improve the biological activity profiles of synthetic AMPs, not only increasing the resistance to proteolytic enzymes but also reducing the hemolytic activity while maintaining the antimicrobial activity (Hong 1999, Adessi 2002, Papo 2002, Zhu 2007, Sharma 2010).

Previously, the LIPPSO group synthesized several **BP100** analogues in order to study the influence of replacing an L-amino acid by the corresponding D-isomer on the biological activity. A total of 11 sequences were prepared containing one D-amino acid (**BP138-BP148**) and were tested for *in vitro* growth inhibition of *E. amylovora*, *P. syringae* and *X. vesicatoria*, for toxicity against eukaryotic cells and for their susceptibility to degradation by proteases (Table 1.3).

Table 1.3. *Antibacterial activity (MIC) cytotoxicity and stability to protease degradation of linear undecapeptides with one D-amino acid.*

Peptide	Sequence[a]	MIC[b] (μM)			H (%)[d]	Digestion (%)[e]
		Xv[c]	*Ps*[c]	*Ea*[c]		
BP100	KKLFKKILKYL-NH_2	5-7.5	2.5-5	2.5-5	54	75
BP138	KKLFKKILK**Y**L-NH_2	>7.5	>7.5	>7.5	7	53
BP139	KKLFKKILKY**L**-NH_2	>7.5	>7.5	>7.5	23	6
BP140	KKLFKKIL**K**YL-NH_2	>7.5	5-7.5	>7.5	0	1
BP141	KKLFKK**I**LKYL-NH_2	>7.5	2.5-5	2.5-5	4	1
BP142	KKLF**K**KILKYL-NH_2	>7.5	2.5-5	5-7.5	3	35
BP143	KKL**F**KKILKYL-NH_2	5-7.5	2.5-5	2.5-5	5	18
BP144	KK**L**FKKILKYL-NH_2	>7.5	2.5-5	>7.5	7	50
BP145	K**K**LFKKILKYL-NH_2	5-7.5	2.5-5	2.5-5	51	61
BP146	KKLFK**K**ILKYL-NH_2	>7.5	2.5-5	>7.5	53	24
BP147	**K**KLFKKILKYL-NH_2	2.5-5	2.5-5	2.5-5	71	47
BP148	KKLFKK**I**LKYL-NH_2	>7.5	>7.5	>7.5	0	0

[a]Underlined and bold amino acids are D-enantiomers.
[b]Minimum inhibitory concentration.
[c]*Ps: P. syringae; Xv: X. vesicatoria; Ea: E. amylovora*
[d]Percent hemolysis at 250 μM plus confidence interval (α = 0.05).
[e]Percentage of degraded peptide determined by HPLC.

Peptides **BP143**, **BP145** and **BP147** (MIC ≤ 5 μM) showed a good profile of antibacterial activity. Except for **BP147**, all sequences exhibited a low hemolytic character. In addition, these peptides were more stable to degradation by proteases than **BP100**.

1.3.3. Cyclic AMPs

Linear peptides have a conformational flexibility which limits their target selectivity, bioavailability, and stability towards protease degradation (Scheme 1.9).

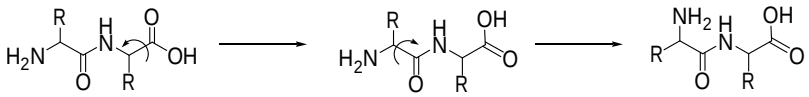

Scheme 1.9. *Linear peptide conformations.*

Cyclic peptides are more conformationally constrained structures and, generally, have a higher metabolic stability than linear peptides due to the limited accessibility to proteases. In addition, it has been shown that peptide cyclization could promote an increase of the selectivity for bacterial versus mammalian cells. In fact, peptide cyclization could result in a suitable amphipathicity that could enhance electrostatic interactions in the initial peptide binding with the negatively charged bacterial membranes, so that interactions with the neutral lipids of the membrane of red blood cells are reduced (Monroc 2006).

Cyclic peptides can be obtained following four main approaches. In all cases the cyclization is performed by the formation of a covalent bond, mainly an amide or a disulfide. These cyclizations, as illustrated in Scheme 1.10, involve bridging between **(A)** the side chain functional groups of two amino acids; **(B)** the N- and C-teminus of the peptide, which is called “head-to-tail” cyclization; **(C)** one amino acid side-chain and the N- or C-terminus of the peptide; or **(D)** two backbone residues (Fung 2005).

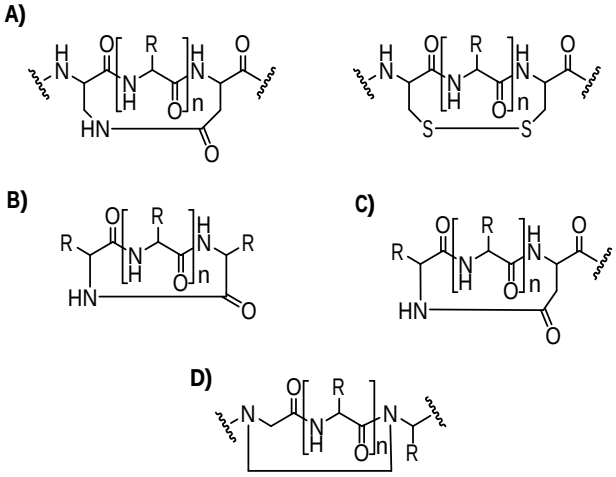

Scheme 1.10. Types of covalent cyclization. **A)** Cyclization involving two side chains. **B)** Cyclization involving two end termini. **C)** Cyclization involving side-chain to N-terminus (or C-terminus). **D)** Cyclization involving two backbone residues.

Among them, head-to-tail cyclised peptides are the most abundant and are found in a variety of biologically active natural products (Pedersen 2011), such as cyclosporin or gramicidin S which present a high antimicrobial activity (Scheme 1.11).

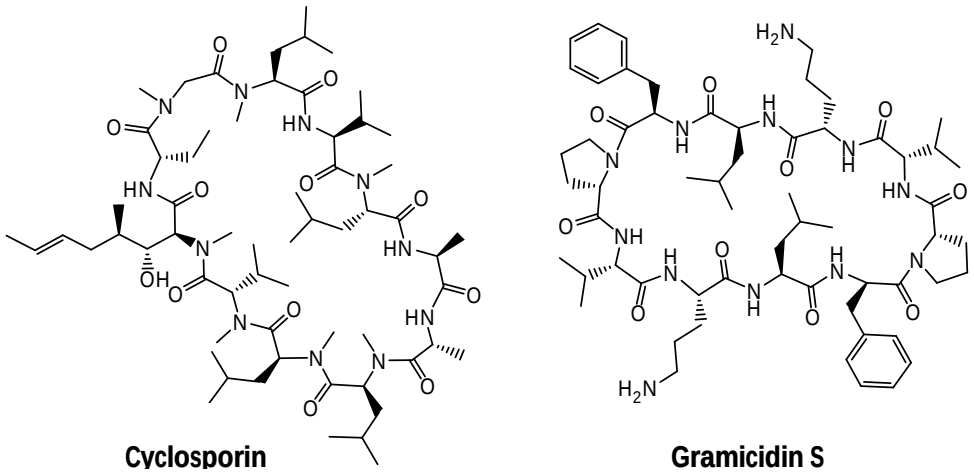

Cyclosporin **Gramicidin S**

Scheme 1.11. *Cyclic natural peptides.*

During the last years, the LIPPSO group has *de novo* designed and synthesized a family of head-to-tail cationic cyclic peptides of 4-10 residues. These cyclic peptides consisted of alternating cationic (Lys) and hydrophobic (Phe and Leu) amino acids with the general formula c(X_n-Y-X_m-Gln) where X is Lys or Leu and Y is L-Phe or D-Phe, m=n=1, or m=3 and n=0-5. A glutamic acid residue was introduced to facilitate the solid-phase cyclization step. These peptides were tested for antimicrobial activity against *E.*

amylovora, *P. syringae* and *X. vesicatoria,* and their cytotoxic effects were determined by measuring the hemolytic activity. Their stability towards protease degradation was also evaluated. The influence of cyclization, ring size, and replacement of L-Phe with D-Phe was studied. Results showed that linear peptides were inactive against the three tested bacteria and among the synthesized cyclic peptides, the most active sequence was the cyclodecapeptide BPC10L (c(KLKLKFKLKQ)). This peptide showed a minimum inhibitory concentration (MIC) of 6.2 to 2.5 µM against *P. syringae* and *X. vesicatoria* but did not show activity against *E. amylovora* and displayed a considerable hemolysis (81 % at 375 µM) (Monroc 2006a).

In order to improve the properties of **BPC10L**, a library of 56 cyclic decapeptides (library I) was prepared. An analysis of the most frequent residues at each position of the peptide sequence revealed that peptides with the general sequence c($X^1X^2X^3X^4$KFKKLQ), X being Lys or Leu, displayed the highest antibacterial activity. Thus, a second library (library II) was synthesized to check the influence on antibacterial and hemolytic activities of the residues at positions 1-4 by using a design of experiments (DOE). This library contained 16 cyclodecapeptides incorporating the substructure K^5FKKLQ^{10} and all possible combinations of Leu and Lys at positions 1-4. This library was screened for antibacterial activity against the aforementioned bacteria and also for hemolytic activity. Notably, peptides active against *E. amylovora* were identified and the best peptides displayed a low eukaryotic cytotoxicity at concentrations 30-120 times higher than the MIC. Peptides with the best biological properties were **BPC96**, **BPC98**, **BPC194** and **BPC198** which fulfilled the substitution rule found by DOE: $X^2 \neq X^3$ and X^4=Lys (Table 1.4). Among them, the most active analogue was **BPC194,** c(KKLKKFKKLQ), which displayed significant antibacterial activity and a low degree of hemolysis (17 % at 375 µM) (Monroc 2006b).

Thus, peptide **BPC194** can be considered as a good candidate for the development of effective antimicrobial agents in plant protection.

Table 1.4. *Antibacterial activity (MIC) and cytotoxicity of cyclopeptides de novo designed.*

Peptide	Sequence	MIC[a] (μM)			H (%)[c]
		Ps[b]	*Xv*[b]	*Ea*[b]	
BPC10L	c(KLKLKFKLKQ)	12.5-25	6.2-12.5	>100	84 ± 6.9
BPC88	c(KKLLKFKKLQ)	6.2-12.5	1.6-3.1	25-50	33 ± 3.3
BPC96	c(LKLKKFKKLQ)	6.2-12.5	3.1-6.2	12.5-25	24 ± 4.3
BPC98	c(LLKKKFKKLQ)	6.2-12.5	1.6-3.1	12.5-25	28 ± 2.4
BPC194	c(KKLKKFKKLQ)	3.1-6.2	3.1-6.2	6.2-12.5	17 ± 1.7
BPC198	c(KLKKKFKKLQ)	3.1-6.2	3.1-6.2	12.5-25	14 ± 1.4

[a]Minimum inhibitory concentration.

[b]*Ps*: *P. syringae*; *Xv*: *X. vesicatoria*; *Ea*: *E. amylovora.*

[c]Percent hemolysis at 375 μM plus confidence interval (α = 0.05).

1.4. New strategies for AMP synthesis

Based on these results, the LIPPSO has searched for new compound based on the structures of the lead peptides identified.

1.4.1. Peptidotriazoles

Another strategy that may be used to improve the biological profile of AMPs is the introduction in their sequence of nitrogen heterocycles which play an important role in biological systems. Among them, 1,2,3-triazoles have been shown to possess a number of desirable features in drug discovery. This ring is chemically stable to acidic and basic hydrolysis as well as to reductive and oxidative conditions, and it is relatively resistant to metabolic degradation (Tornøe 2004, Tron 2008, Scrima 2010). Moreover, 1,2,3-triazoles have a high dipole moment (about 5 D), which makes them resemble to the amide bond (around 3.5 D) (Scheme 1.12), being able to participate in hydrogen bonding, dipole-dipole and π-stacking interactions (Holub 2010). Consequently, this ring can interact with biological molecules acting as a powerful pharmacophore (Fan 1996, Tornøe 2004, Aufort 2008, Liu 2008, Tron 2008, Mamidyala 2010, Reck 2005, Wan 2006, Whiting 2006), and as a bioisoster of potentially labile functional groups (*e.g.,* esters, amides) (Moses 2007, Evans 2007; Holub 2010). For example triazoles are

present in commonly used antimicrobial agents such as fluconazole and its derivatives (Zhang 2011).

Scheme 1.12. *1,4-Disubstituted 1,2,3-triazoles share structural and electronic characteristics with amide bonds.*

1.4.1.1. Synthesis of 1,2,3-triazoles through a click reaction

The most versatile method for the synthesis of 1,2,3-triazoles is the Huisgen 1,3-dipolar cycloaddition reaction between an azide and an alkyne (Kobayashi 2002; Meldal 2008). This reaction is among the most important synthetic methods for the preparation of five-membered heterocycles (Kobayashi 2002), and is one of the most popular reactions within the click chemistry concept. Reactions defined as "click" require only benign reaction conditions, simple workups and purification procedures that can rapidly create molecular diversity through the use of reactive modular building blocks.

The first cycloadditions for the synthesis of 1,2,3-triazoles were performed in the absence of catalyst and resulted in a mixture of the 1,4- and the 1,5-regioisomers (Rostovtsev 2002) (Scheme 1.13).

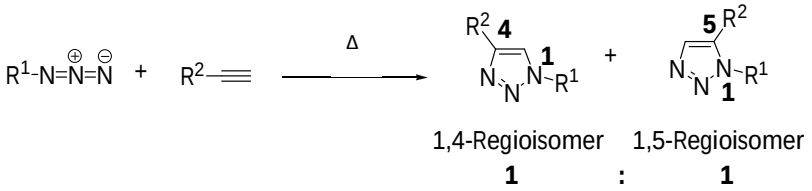

Scheme 1.13. *Uncatalyzed 1,3-dipolar cycloaddition to form a 1,2,3-triazole ring.*

Owing to this lack of regioselectivity, this approach was limited to those cases where one isomer was synthetically favoured over the other for electronic or steric/conformational reasons. An important advance in this field was the emergence of the copper-catalysed azide-alkyne cycloaddition, reported simultaneously and independently by the groups of Meldal and Sharpless. This discovery allowed the

synthesis of substituted 1,2,3-triazoles in mild conditions with total regioselective control leading to the 1,4-regioisomer in high yields (Tornøe 2002, Rostovtsev 2002).

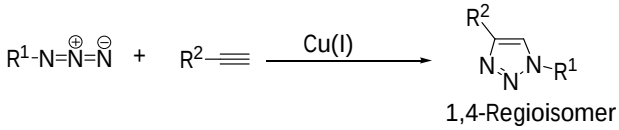

Scheme 1.14. *Copper-catalyzed 1,3-dipolar cycloaddition to form a 1,2,3-triazole ring.*

Despite the apparent simplicity of this reaction, its mechanism involves multiple reversible steps involving coordination complexes of copper(I) acetylides of varying nuclearity. This reaction goes through the catalytic cycle diagram shown in Scheme 1.15.

Hein *et al.* described the possible reaction pathways allowed for mononuclear copper(I) acetylides and organic azides by means of initial computational studies of this copper-catalyzed cycloaddition. Formation of copper(I) acetylide (**step a**) probably occurs through a π-alkyne copper complex intermediate where the π-coordination of alkyne to copper significantly acidifies the terminal hydrogen of the alkyne, which can be deprotonated resulting in the formation of a σ-acetylide. The azide is then activated by coordination to copper (**step b**) and its electrophilicity increases. In the next steps, the resulting complex rearranges into a 6-membered metallocycle, forming the first C-N bond (**step c**), and then into the copper-metallated triazole (**step d**). This copper-triazole complex eventually releases the free triazole and CuL_x by protonation or reaction with other electrophiles (**step e**). The authors also described that the introduction of a second copper(I) atom favorably influences the energetic profile of the reaction (Scheme 1.15B).

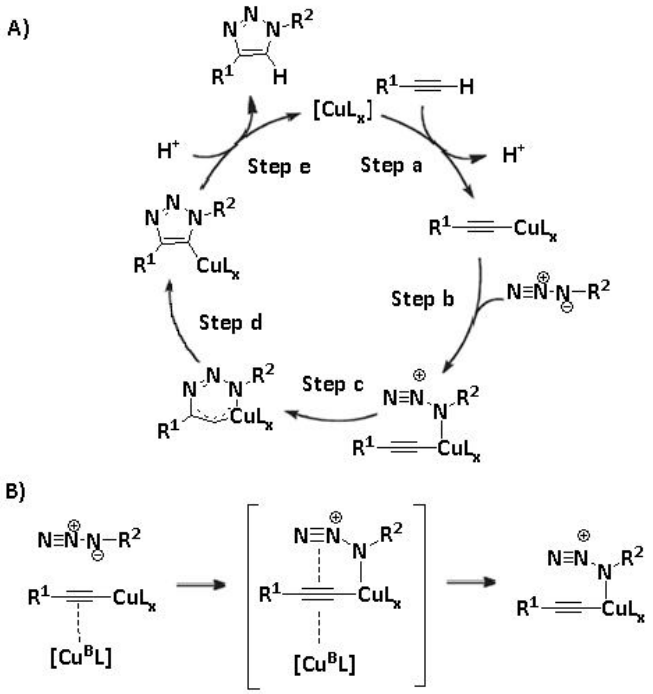

Scheme 1.15*. Proposed catalytic cycle for the copper-catalyzed azide-alkyne reaction.* ***A)*** *Early proposed catalytic cycle based on computational calculations.* ***B)*** *Introduction of a second copper(I) atom. Left: optimized structures for dinuclear Cu forms of the starting acetylide; Middle: transition state for the key C–N bond-forming step; Right: metallocycle.*

1.4.1.2. Synthesis of peptidotriazoles

Since this reaction is highly chemoselective, tolerates a variety of functionalities and is carried out under mild conditions with quantitative conversions, it is not surprising that it has been adapted to solid support, especially to obtain peptide derivatives (Sureshbabu 2010, Liu 2008). In particular, it has been reported its application to the solid-phase synthesis of β-turn mimics, protease inhibitors (Tornøe 2004, Tornøe 2002), cyclopeptide analogues (Liu 2008, Scrima 2010, Springer 2008, Cantel 2008, Jagasia 2009), assembled and scaffolded peptides (Franke 2005) or PEGylated lipopeptides (Jølck 2010). In these reports, the azide-alkyne cycloaddition is employed to introduce the 1,2,3-triazole unit in the peptide backbone or at the side-chain of an amino acid as a ligation technique for linking peptide fragments for macrocyclization or polymerization, or to obtain biologically active peptidotriazoles (Chakrabarty 2009, Wan 2006).

In the literature, the synthesis of a wide variety of both cyclic and linear peptidotriazoles has been described (Pedersen 2011). The triazole can be incorporated into an amino acid backbone or side-chain by reaction of suitable acetylene or azido substituted amino acid residues with an azide or alkyne, respectively, as depicted in Scheme 1.16. For instance, the synthesis of linear peptidotriazoles can involve different strategies, where the triazole ring can be introduced either into the peptide backbone **(A)** or onto the side-chain of an amino acid residue **(B)**. Cyclic peptides can be obtained following the strategies shown in **C)** which involve the formation of a triazole ring as a brigde between: the N- and C-teminus of the peptide, which is called "head-to-tail"; two backbone residues; or one amino acid side-chain and the N- or C-terminus of the peptide.

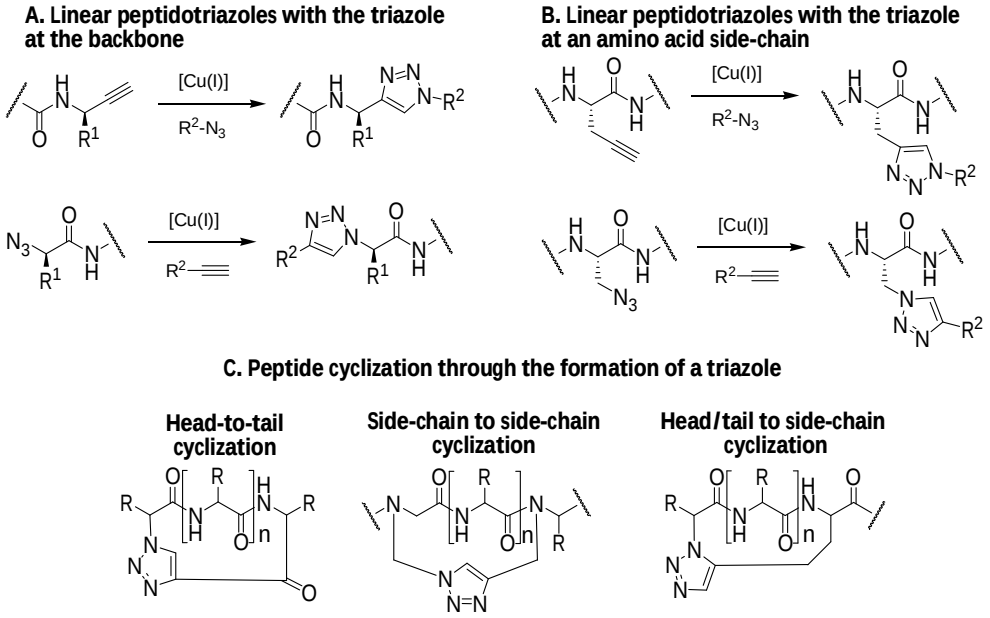

Scheme 1.16. *Synthesis of linear and cyclic peptidotriazoles.*

The same authors Pedersen and Abell (Pedersen 2011) described the synthesis in solution of linear peptidotriazoles with the appropriate geometry to adopt a β- turn according to molecular modeling. These peptidotriazoles were studied by NMR and FTIR to evaluate their potential as turn-inducing peptidomimetics (Scheme 1.17).

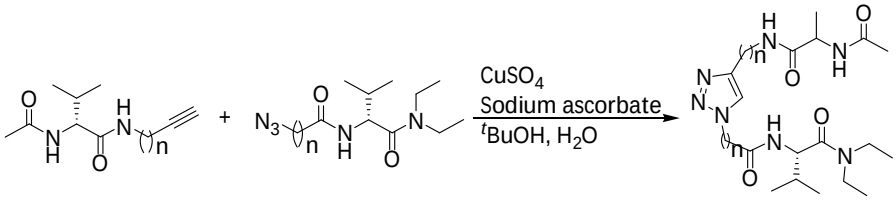

Scheme 1.17. *Synthesis of linear peptidomimetics.*

It has also been described the synthesis in solution of triazole-containing analogues of the naturally occurring tyrosinase inhibitor *cyclo*-[Pro-Val-Pro-Tyr] isolated from *Lactobacillus helveticus.* It has been shown that these analogues retained the enzyme inhibitory activity, demonstrating the effectiveness of a 1,4-connected 1,2,3-triazole as a *trans* peptide bond isostere (Bock 2007) (Scheme 1.18).

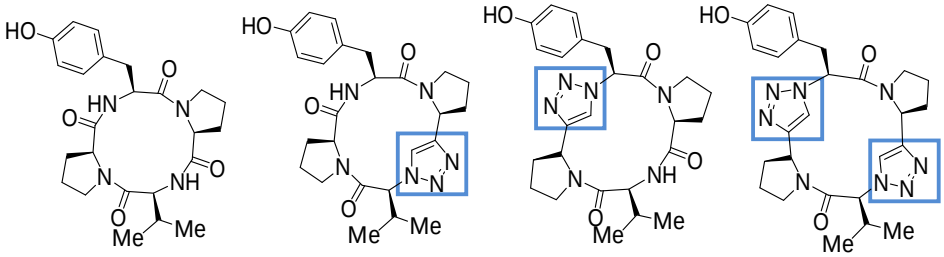

Scheme 1.18. *Structures of the natural peptide* cyclo-*[Pro-Val-Pro-Tyr] and its derivatives.*

In 2004, Meldal *et al.* synthesized in solid-phase a library of linear peptidotriazoles through azide-alkyne 1,3-dipolar cycloaddition to identify inhibitors of a recombinant *Leishmania mexicana* cysteine protease (Scheme 1.19) (Tornøe 2004).

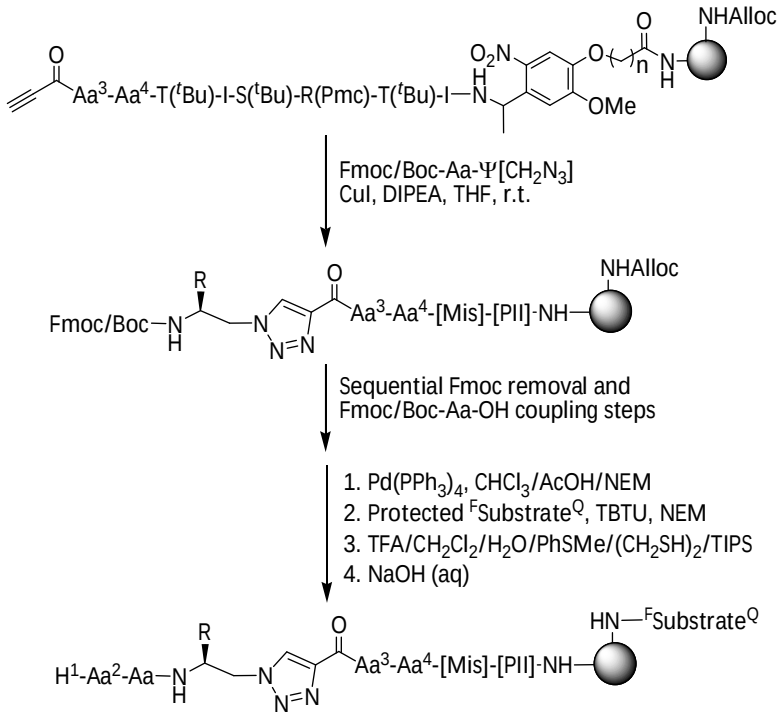

Scheme 1.19. *Synthesis of a library of peptidotriazoles, where protected* $^{F}Substrate^{Q}$ *corresponds to Boc-Y(*NO_2*)-E(*^{t}*Bu)-K(Boc)-F-R(Pmc)-R(Pmc)-G-K(Boc)-K(Abz-Boc)-G-OH (Tornøe 2004).*

Despite the vast number of techniques developed to cyclize small peptides, cyclization efficiency remains problematic in peptides that lack turn-promoting structures. In 2007, Turner *et al.* demonstrated the utility of click chemistry as a macrocyclization tool in the solid-phase synthesis of cyclic tetra-, penta-, hexa-, and heptapeptides. On-resin cyclization was completed at room temperature within 6 h, resulting predominantly in the corresponding monomer together with small amounts of cyclomultimer byproducts (Scheme 1.20) (Turner 2007).

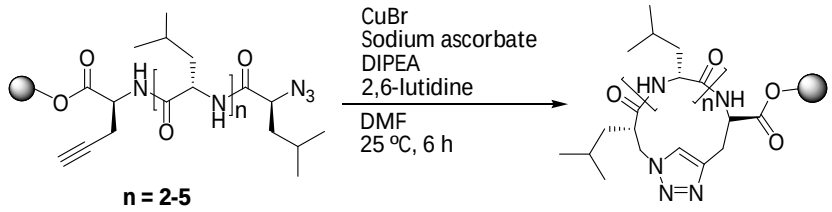

Scheme 1.20. *Click macrocyclization through the formation of a triazole ring.*

Following a similar strategy, in 2008, Liu *et al.* reported the synthesis of cyclic peptidotriazoles as potential ligands for integrins, a family of membrane adhesion proteins that play an important role in tumor-induced apoptosis (Scheme 1.21) (Liu 2008).

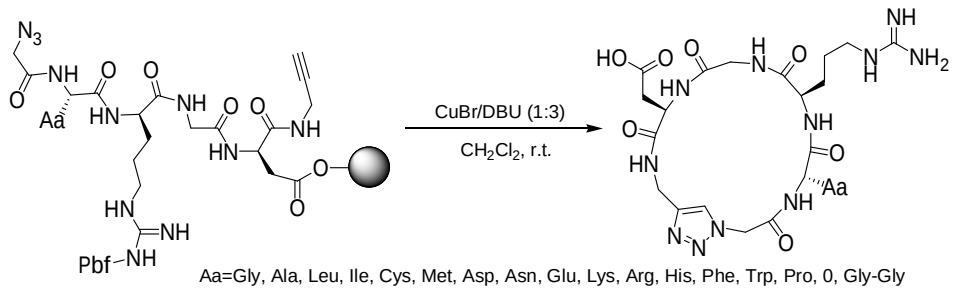

Scheme 1.21. *Synthesis of cyclo[-Arg-Gly-Asp- Ψ(triazole)-Gly-Aa].*

Although many peptides containing triazoles have been reported, so far peptidotriazoles active against plant pathogenic bacteria or fungi have not been described.

1.4.2. Multivalent macromolecules

Other approaches for designing AMPs are based on their mode of action. Several models have been proposed to account for the morphologic changes in the cell

membrane induced by AMPs, such us pore formation, lysis or peptide translocation into the cytoplasm (see section 1.2). Either model accounts for relatively high local density and synergy of monomeric peptides (Jenssen 2006, Ferre 2009, Pieters 2009).

It has been reported that an improved binding to microbial membranes and thus an improved antimicrobial activity can be achieved if several copies of AMPs are linked to form multimeric species, an effect known as multivalency (Sung 2006). It is proposed that these multivalent peptides interact easier with the membrane than the corresponding monomer, which means that the minimum concentration required might be reduced (Liu 2006, Arnusch 2007, Pieters 2009).

Nature often use multiple low affinity interactions to enhance the overall affinity and specificity of binding (Choi 2004). Inspired by nature's success, researchers nowadays often combine several low affinity ligands *e.g.* carbohydrates, peptides or proteins onto a single scaffold in order to create high affinity multivalent ligands as promising candidates for specific delivery of therapeutics or imaging probes (Martos 2008).

However, the synthesis of novel artificial proteins, such as peptide dendrimers or peptide/protein conjugates with branched structure is generally difficult to accomplish. The synthesis of these branched structures can be achieved by condensation of protected peptide segments. The limitations of this approach are the poor solubility of protected segments and the sluggish coupling rates (Shao 1995). These limitations could be overcome by using unprotected peptide segments as building blocks to form branched peptides. A key requirement in the ligation of unprotected peptides is chemoselectivity so that only the intended sites can react with each other in the presence of many side-chain functionalities (Shao 1995).

1.4.2.1. Chemoselective ligation

The development of techniques for chemoselective ligation of unprotected peptide segments has significantly broadened the field of synthetic peptide chemistry and chemoselective ligation reactions are now established tools for diverse applications in chemistry and biology (Lemieux 1998). They allow the selective formation of a covalent bond between highly complex biological molecules without the requirement of

protecting-group transformations. Several organic reactions have recently been identified that allow a "direct" formation of a chemoselective bond in the final product (Scheme 1.22) (Hackenberger 2008). This bond is constructed from two functional groups in the starting materials that do not show any cross-reactivity with other functional groups (Hoffman 2006). These reactions include native chemical ligation, the Staudinger reaction, cooper(I)-catalyzed azide-alkyne cycloaddition and oxime formation (Scheme 1.22).

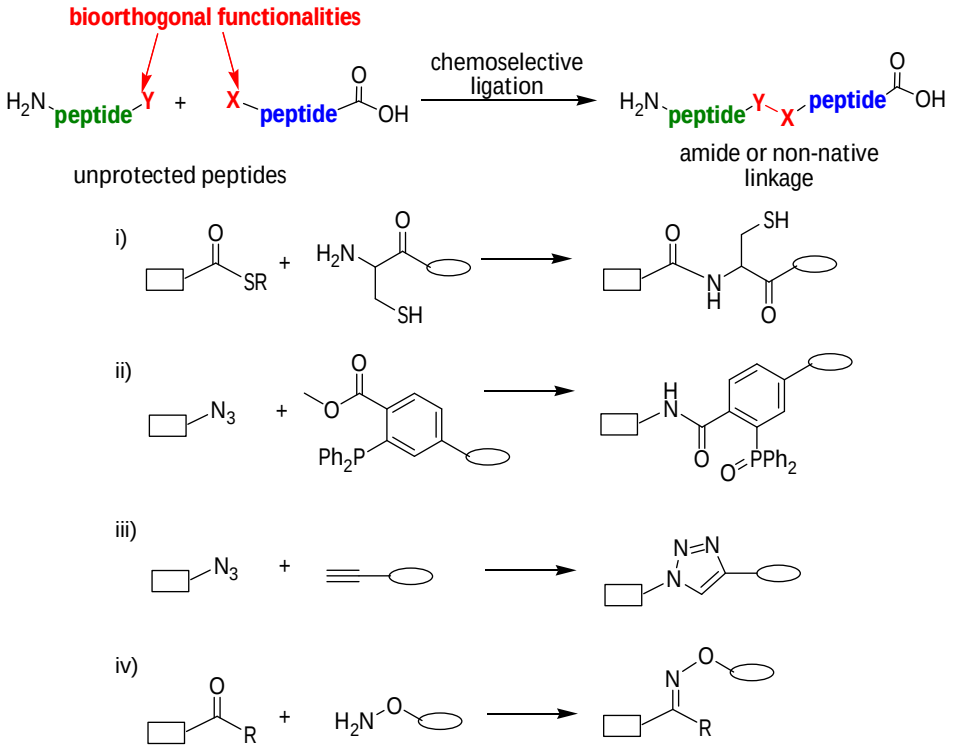

Scheme 1.22. *Chemoselective reactions for conjugation of biomolecules. i) Native chemical ligation between thioesters and cysteine residues. ii) Staudinger ligation of azides and triarylphosphines. iii) Cooper(I)-catalyzed cycloaddition of azides and alkynes to form triazoles. iv) Oxime formation between aldehydes/ketones and aminooxy groups.*

Currently, the most common ligation method is the "Native chemical ligation" which was first reported in 1994 by Dawson and Kent to facilitate the chemical synthesis of proteins from unprotected peptide fragments. This chemoselective reaction occurs spontaneously between a peptide with a C-terminal thioester and a peptide with an N-terminal cysteine residue under aqueous conditions at neutral pH (Scheme 1.22 i). Native chemical ligation has allowed the chemical synthesis of large proteins (by multistep ligation of several peptide fragments), the synthesis of proteins with

synthetic moieties such as fluorescent dyes and biotin tags, and the immobilization of peptides and proteins on surfaces (van Baal 2005). A limitation of Native chemical ligation is its intrinsic reliance on having a cysteine residue at the ligation juncture.

The Staudinger reaction was discovered almost a century ago by Nobel Prize laureate Herrmann Staudinger. Saxon and Bertozzi in 2000 introduced this reaction as a chemoselective ligation for compound conjugation because it allows the chemoselective formation of amide-linked products from azides and triaryl phosphines (Scheme 1.22 ii) (Saxon 2000). The reaction proceeds through the nucleophilic attack of a phosphine to an azide to give an aza-ylide intermediate, which is trapped in an intramolecular fashion by the methoxycarbonyl group to give an amide bond after hydrolysis (Lin 2005). Although the previously described methods for Staudinger ligation work well even in biological environments, a modification forming a native amide bond without leaving the unnatural phosphine oxide moiety in the product would be more attractive. In 2000, the groups of Bertozzi and Raines simultaneously introduced alternative ligation strategies (Nilsson 2000, Saxon 2000). Based on the same working principle as the nontraceless Staudinger ligation, the auxiliary phosphine reagent, a phosphinothioester, can be cleaved from the product after the ligation is completed, leaving a native amide bond. The traceless Staudinger ligation is of particular interest for ligation of peptide fragments as shown successfully by Wong et al. for the synthesis of glycopeptides in high yield (Liu 2006).

Azides can also participate in Huisgen-type [3+2] cycloadditions, such as the Cu(I)-catalyzed azide-alkyne cycloaddition reaction, for chemoselective ligation (Scheme 1.22 iii) (Rostovtsev 2002, Tornøe 2002). This reaction has been utilized as a conjugation strategy in the design and synthesis of complex biomimetic architectures in which the triazole linkage replaces and, in some cases, acts as a surrogate for peptide and phosphodiester bonds (Scheme 1.23). The reaction has found various applications in material and polymer science as well as in the specific labeling of biomolecules.

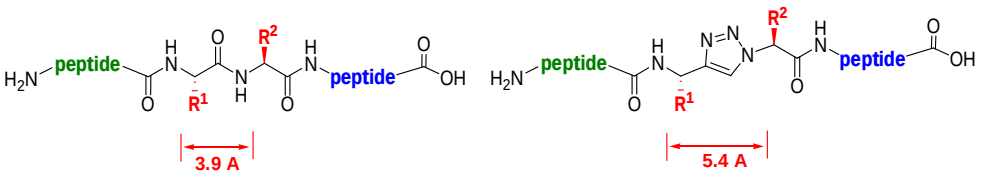

***Scheme 1.23**. Geometric comparison of a triazole bridge to a native amide bond.*

The two reaction partners involved in this reaction, azides and alkynes (Scheme 1.24), can be introduced into the peptide substrates by standard solid-phase peptide synthesis techniques. The cycloaddition yields exclusively the 1,4-disubstituted triazole (Scheme 1.24).

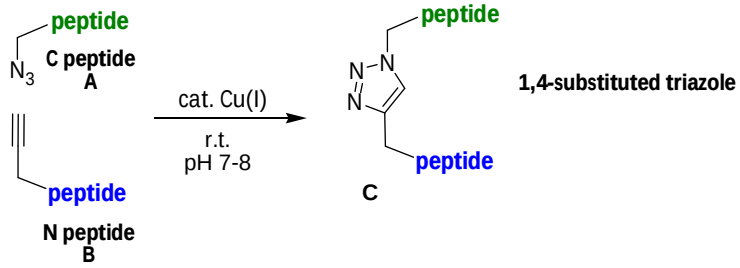

***Scheme 1.24.** Peptide ligation via the copper(I)-catalyzed formation of a 1,4-disubstituted triazole.*

In the literature, there are few examples on the formation of the triazole ring as a chemoselective ligation method, using unprotected functional groups. In 2008, Cantel and co-workers described an intramolecular side-chain to side-chain cyclization of linear peptides, using a copper-catalyzed azide-alkyne 1,3-dipolar Huisgen's cycloaddition. They attempted two different strategies, performing the cyclization either in solution, using the unprotected peptide (pathway A), or on solid-phase (pathway B) (Scheme 1.25). Only the former procedure afforded the desired product (Cantel 2008).

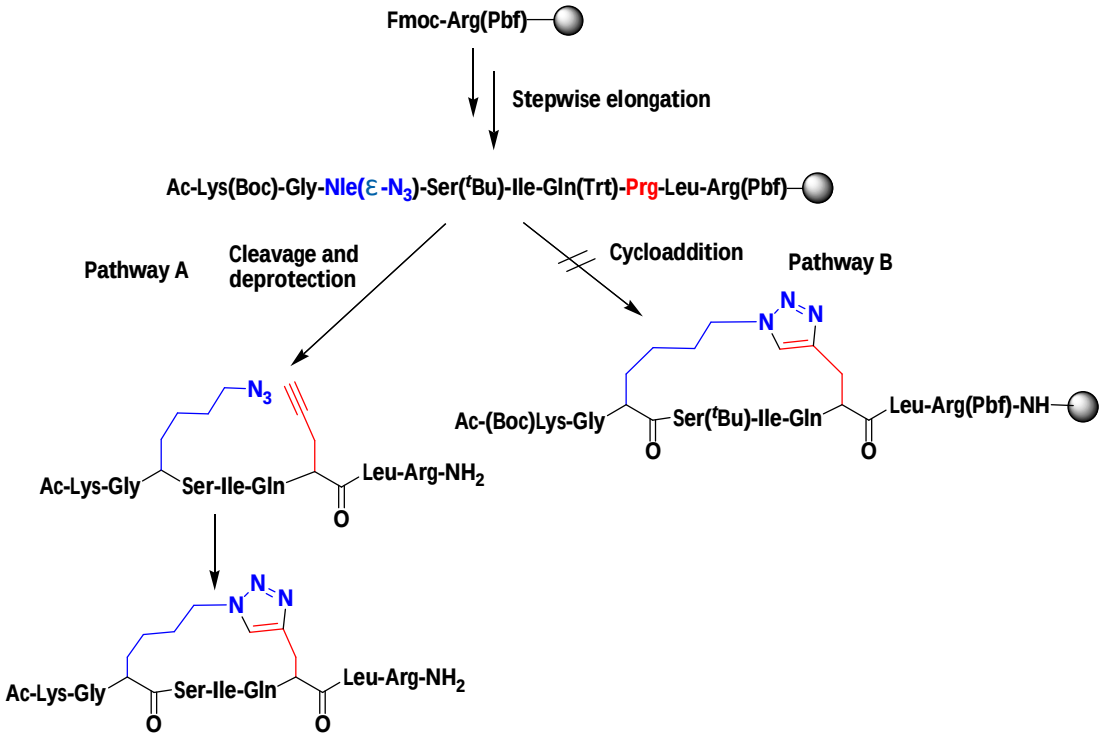

Scheme 1.25. *Strategies for the synthesis of a cyclic peptidotriazole.*

Haridas and co-workers described in 2011 the synthesis of unsymmetrical dendrimers by formation of a triazole ring. The synthesis involved the conjugation of two peptide sequences bearing lysine residues either protected with Boc or unprotected (Scheme 1.26) (Haridas 2011).

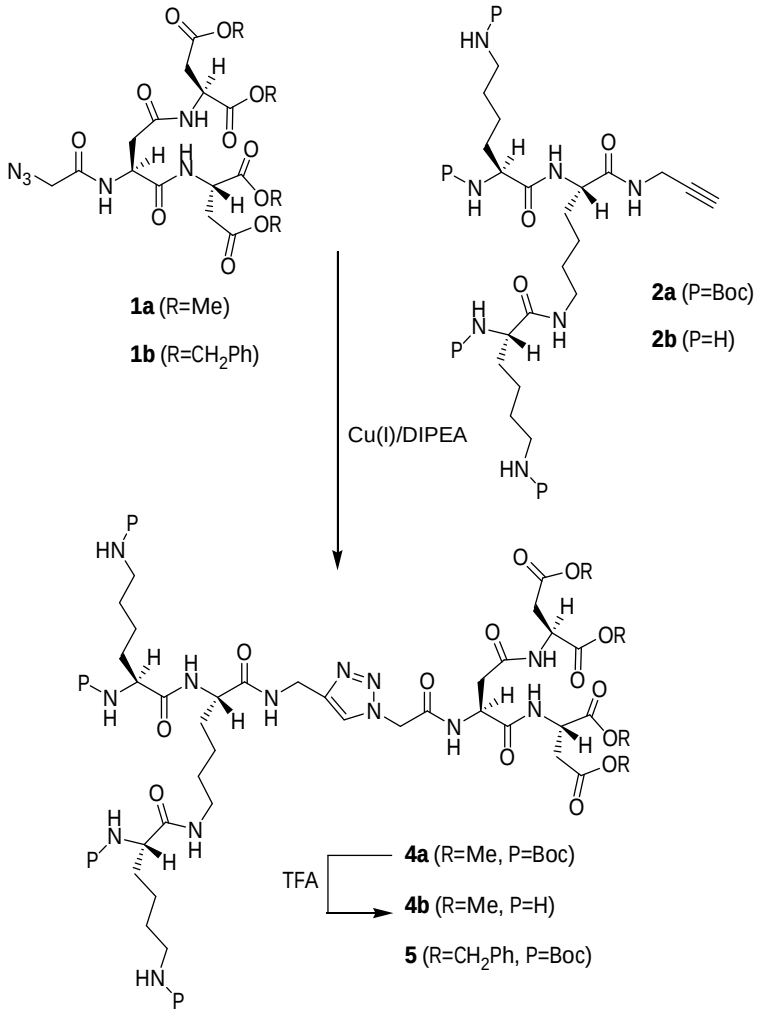

Scheme 1.26. *Synthesis of unsymmetrical dendrimers.*

Oxime and hydrazone ligations were first developed by Rose in 1994, in which aminooxy or hydrazine nucleophiles react with aldehydes or ketones. These ligations proceed via a common mechanism involving the nucleophilic attack of the amino group on a protonated carbonyl followed by a dehydration step (Scheme 1.22 iv). Due to the α-effect of the neighboring heteroatom, aminooxy derivatives are weak bases but reactive nucleophiles towards carbonyl groups (Hudson 1973). This reaction is especially favorable at an acidic pH range of 4–5.5 where basic side-chain nucleophiles are protonated. Furthermore, oximes formed are stable under neutral to mildly acidic conditions (Shao 1995).

The oximation reaction has proven to be very efficient for the synthesis of compounds such as: polypeptides, multimeric compounds for receptor targeting or vaccine design (Boturyn 2004), cyclic peptides (Roberts 2004), glycopeptides (Hang 2001), and

oligonucleotide-peptide conjugates (Zatsepin 2005). Some of these examples were described by Roberts and co-workers who established a general protocol for the synthesis of head-to-side chain cyclic oxime peptides (Scheme 1.27) (Roberts 2004).

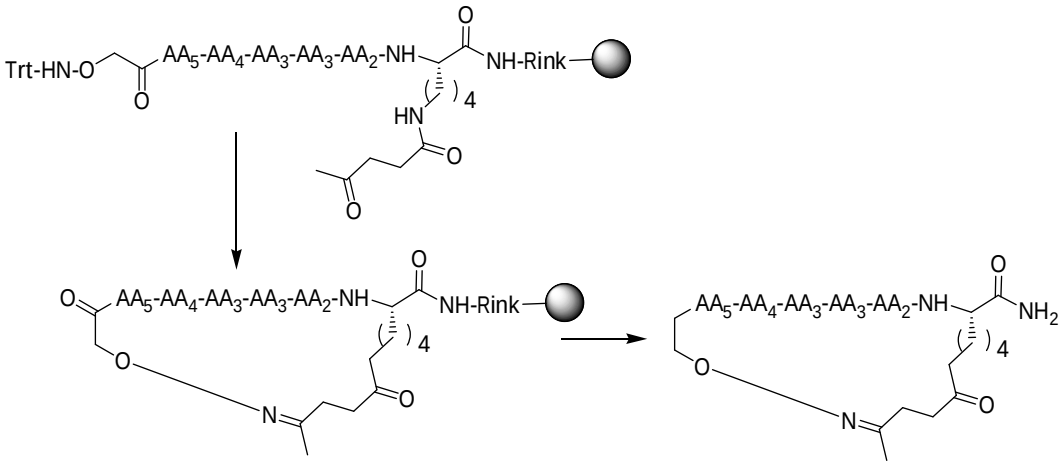

Scheme 1.27. *Synthesis of head-to-side chain cyclic oxime peptides.*

An example of the conjugation reaction of an oligonucleotide and a peptide through oxime ligation was described by Forget in 2001 (Scheme 1.28).

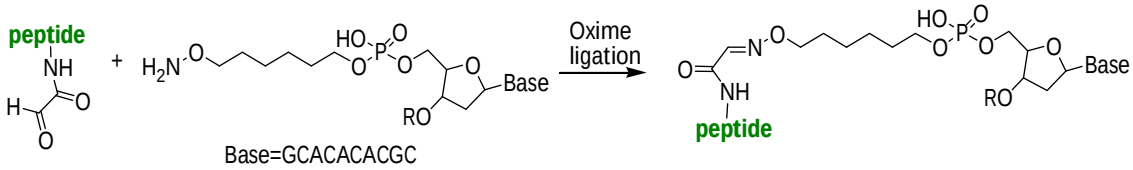

Scheme 1.28. *Conjugation reaction of an oxyamine-containing oligonucleotide and an aldehyde-containing peptide.*

1.4.2.2. Multivalent ligands

Most of the current approaches towards designing multivalent ligands are based on the attachment of monovalent ligands to multiple sites of generic backbones (Martos 2008). The enhancement on the activity of these multivalent ligands compared to the monovalent ligands varies widely ranging from zero to up to nine orders of magnitude. The valency, shape, orientation of ligands, flexibility and size of the template exert a significant influence on the binding and functional ability of these multivalent molecules (Choi 2004; Vadas 2007; Kiessling 2006).

To date, a wide variety of templates has been used in the design of multivalent molecules as shown in Scheme 1.29. These templates bear multiple chemically reactive sites for ligand attachment. Porphyrins, calixarenes and carbohydrates are examples of low molecular weight templates that possess a rigid core structure to which a few ligands can be conjugated (Fletcher 2005).

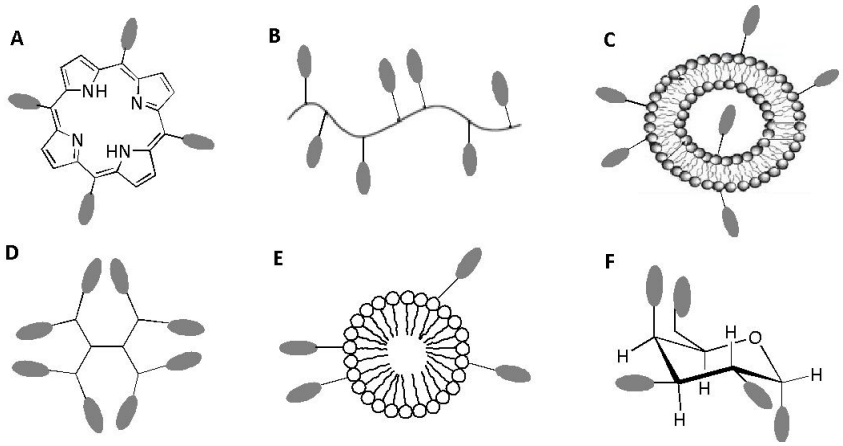

Scheme 1.29. *Synthetic templates used in the design of multivalent ligands* ***A)*** *Porphyrin,* ***B)*** *Linear polymers,* ***C)*** *Liposomes,* ***D)*** *Dendrimer,* ***E)*** *Micelles and* ***F)*** *Carbohydrates.*

Among the many different templates, carbohydrates stand out due to their inherent multifunctionality, relative rigidity of their ring forms, ease of regioselective chemical manipulations and access to stereoisomers of mono- and disaccharides (Hirschmann 1992, Hirschmann 1993, Brask 2000). During the 90s, it was described the use of monosaccharides as templates for the design of small nonpeptidyl peptidomimetics (Hirschmann 1992, Hirschmann 1993) and dipeptide isosteres (Roedern 1994), as well as for the attachment of Leu-enkephalin to a cyclodextrin derivative (Djedaïni-Pilard 1993). The large synthetic potential of carbohydrates as templates for the *de novo* design of protein models was later exploited by Jensen and co-workers. These authors described that carbohydrates can be used for the design and synthesis of new multivalent peptidomimetic and proteinomimetics as well as functionalized cyclodextrins (Jensen 2000, Jensen 2005). This novel class of chimeric protein models assembled on a carbohydrate template are named carbopeptides or carboproteins depending on the number of amino acids that they contain. This term was applied to

differentiate these novel chimeric compounds from the naturally occurring and synthetic glycopeptides and glycoproteins (Jensen 2000).

Due to the difficulties inherent in carbohydrate chemistry and the hydrolytic sensitivity of the glycosidic linkages, peptide chemists have been exploring methods for conjugating carbohydrates to peptide sequences with more metabolically stable linkages (Chittaboina 2005, Holub 2010). Among the several ways to covalently link a peptide to a carbohydrate Jensen and co-workers focused their attention on the oxime ligation, because this reaction is robust, fast, high yielding (Jensen 2002), extremely selective and compatible with unprotected side-chain functionalities with the exception of Cys (Kimmerlin 2005). In 2000, these authors first reported the chemoselective ligation of C-terminal peptide aldehydes to an aminooxy-functionalized methyl α-D-galactopyranoside (Gal*p*) template by oxime formation in solution (Scheme 1.30).

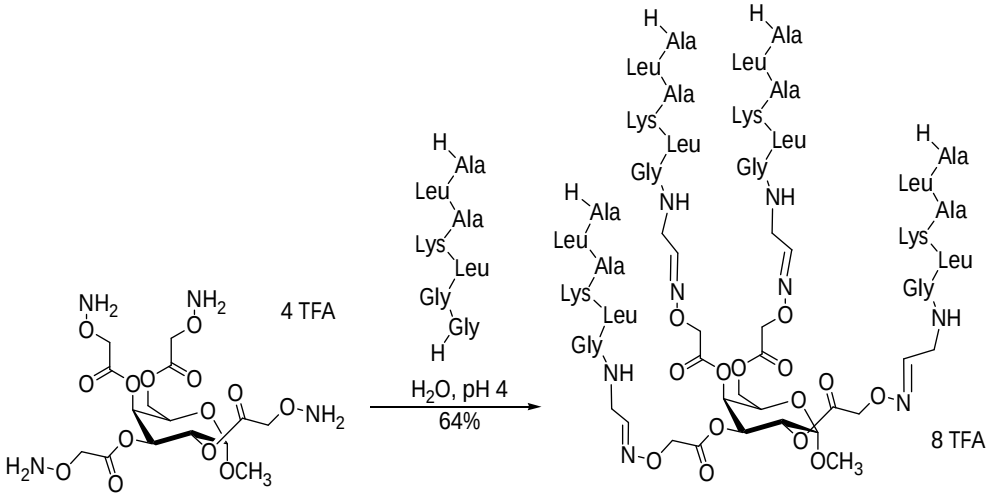

Scheme 1.30. *Preparation of a carbopeptide through the oxime ligation method.*

Afterwards, this group described and studied several carboproteins using the same or different carbohydrates such as methyl α-altropyranoside (Altp) or cyclo-dithioerythritol (cDTE) (Brask 2001, Jensen 2002, Jensen 2005, Tofteng 2007; Høiberg-Nielsen 2008).

1.5. Solid-phase peptide synthesis

Solid-phase synthesis is a process by which chemical transformations can be carried out on a solid support in order to prepare a wide range of synthetic compounds. This methodology was first developed by Bruce Merrifield in an effort to simplify the procedure for peptide synthesis (Merrifield 1963, Miranda 2000). Merrifield was awarded with the Nobel Prize in 1984 for this discovery.

Solid-phase chemistry offers many advantages over conventional synthesis in terms of efficiency as well as convenient work-up and purification procedures. Reagents can be used in excess to drive reactions to completion, following which the excess of reagents plus the reaction byproducts are readily removed by simple filtration and washing. Therefore, solvents with high boiling points, such as *N,N'*-dimethylformamide (DMF), dimethylsulfoxide (DMSO) or *N*-methylpyrrolidone (NMP), can be used without having to evaporate them. Furthermore, the simplicity of this process allows the automation of the synthesis (Kates 2000).

The solid-phase peptide synthesis is performed in the C → N direction; the carboxyl group of the amino acid to be incorporated reacts with the N^{α}-amino group of the peptidyl chain linked to the solid support. As shown in Scheme 1.31, the main steps for solid-phase peptide synthesis are: **(i)** attachment of the first amino acid, conveniently protected, to the solid support which usually includes a linker to facilitate the peptide release at the end the of synthesis; **(ii)** selective deprotection of the N^{α}-amino group of the first amino acid attached to the solid support; **(iii)** cycles of coupling and deprotection steps of the corresponding protected amino acids until the desired peptide sequence is achieved; **(iv)** deprotection and release of the peptide from the support to yield the final product.

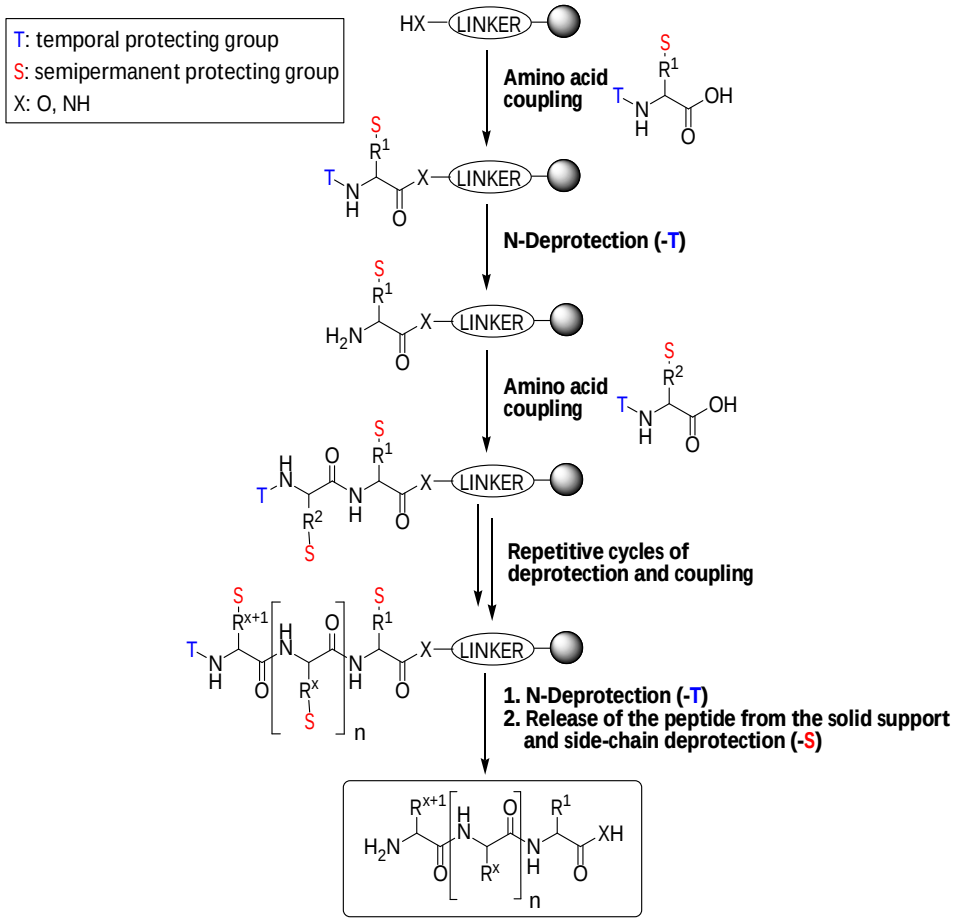

Scheme 1.31. *General strategy for solid-phase peptide synthesis.*

The success of solid-phase peptide synthesis requires the appropriate choice of the solid support, the linker, the coupling reagents and the protecting groups.

1.5.1. The solid support

The term solid support is commonly used to denote the matrix upon which peptide synthesis is performed. Certain physical and chemical propierties are required for a solid support to be useful for peptide synthesis. The support must be composed of particles of consistent and convenient shape and size, must be inert to all conditions used during the synthesis, must exhibit good mechanical stability, and must be completely insoluble in all solvents used. In addition, the support must contain functional groups so that a linker may be bound to it (Grant 1992).

Nowadays, two major families of supports are used for solid-phase peptide synthesis: polystyrene (PS), slightly cross-linked with divinylbenzene; and polyethylene glycol (PEG). Some representative examples are shown in Table 1.5.

Table 1.5. *Representative resins used in solid-phase peptide synthesis.*

Structure	Name
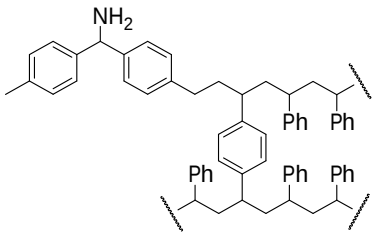	*p*-Methylbenzhydrylamine (**MBHA**)
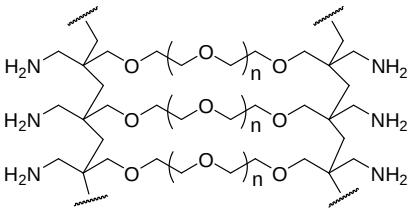	Aminomethyl ChemMatrix (**CM**)
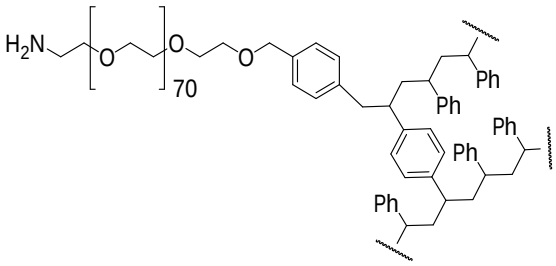	*o*-(2-Aminoethyl)polyethylene glycol (**TentaGel S NH_2**)

1.5.2. The linker

The linker is a bifunctional molecule which on the one hand is attached to the first amino acid through a bond labile to cleavage contidions and, on the other hand, is attached to the solid support through a bond that is stable throughout the synthesis (James 1999, Kates 2000).

There have been reported a variety of linkers that can be classified according to the cleavage conditions. The linkers used in this work, their respective cleavage conditions and the resulting C-terminus are shown in Table 1.6.

Table 1.6. *Linkers used in this work and cleavage conditions.*

Structure	Name	Cleavage conditions	Resulting C-terminus
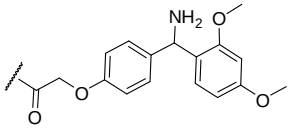	**Rink amide**	TFA	amide
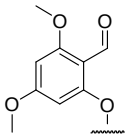	***o*-BAL**	TFA	aldehyde

1.5.3. Protecting groups

In order to avoid secondary reactions during the amino acid coupling steps, the use of protecting groups is essential for masking the functional groups which are not involved in the reaction. The main characteristics associated with a protecting group are: **(i)** it is easily introduced into the functional group; **(ii)** it is stable to a broad range of reaction conditions; and **(iii)** it is safely removed at the end of the synthetic process or when the functional group requires manipulation.

In solid phase peptide synthesis, there are at least two types of protecting groups: temporary, which protect the N^{α}-amino group and are removed before the attachment of an amino acid; and permanent, which are used to protect the side-chain functionality of trifunctional amino acids and are usually removed during the cleavage step (see Scheme 1.31). It is important that conditions for the removal of these two types of protecting groups are completely different in order to be able to remove them selectively.

The most common orthogonal strategy for peptide synthesis is the Fmoc/^{t}Bu, in which the Fmoc serves as protecting group for the N^{α}-amino of amino acids, and the *tert*-butyl (^{t}Bu) and its derivatives, such as *tert*-butyloxycarbonyl (Boc), are the protecting groups of the functional groups of the amino acid side-chains (Isidro-Llobet 2009). Some representative protecting groups are shown in Table 1.7.

Table 1.7. *Representative protecting groups and removal conditions.*

Structure	Name	Removal
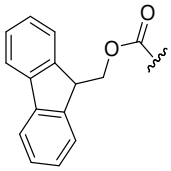	9- Fluorenylmethoxycarbonyl (**Fmoc**)	30 % Piperidine
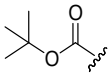	tert-Butyloxycarbonyl (**Boc**)	95 % TFA
	tert- Butyl (**^{t}Bu**)	95 % TFA
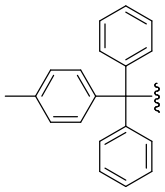	4-Methyltrityl (**Mtt**)	0.1 % TFA
	Allyl (**Al**)	$Pd(PPh_3)_4$

1.5.4. Coupling reagents

The formation of the amide bond between two amino acids does not occur spontaneously at room temperature and carboxylic acids must be activated at room temperature using coupling reagents. One of the most common type of reagents are benzotriazole derivatives, such as HBTU, HATU, HCTU or PyBOP and carbodiimides, such as DIPCDI and DCC (Scheme 1.32) (Valeurs 2009). However, derivatives containing a benzotriazole ring have been classified as explosives (Wehrstedt 2005) and can cause allergic reactions such as dermatitis or asthma. Recently, a new class of coupling reagents containing ethyl 2-cyano-2(hydroxyimino)acetate instead of the benzotriazole ring, such as COMU and PyOxim, have been reported to lead to high levels of efficiency and to be a safer alternative (Scheme 1.32) (El-Faham 2009, Subirós-Funosas 2009, El-Faham 2010).

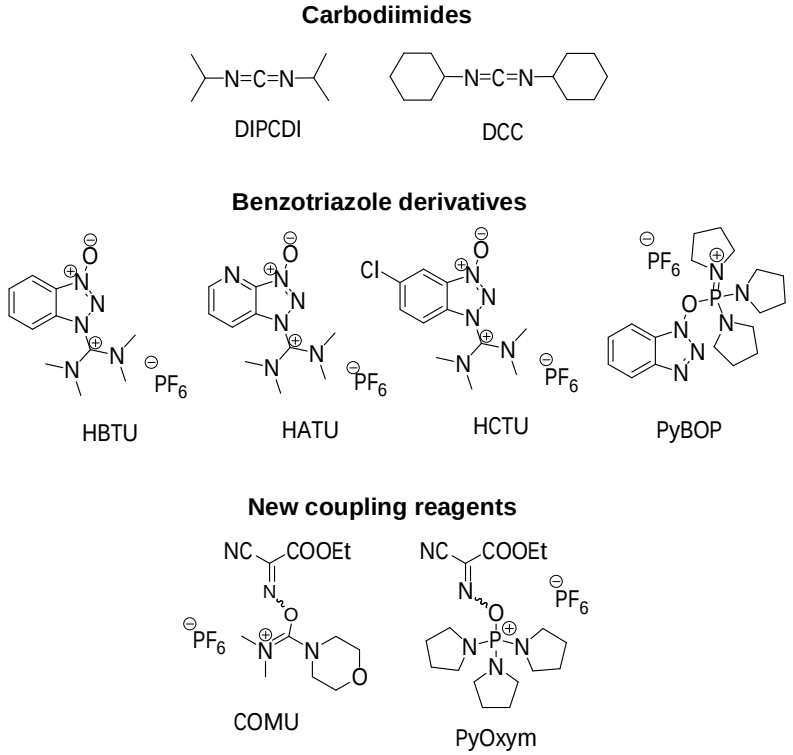

Scheme 1.32. *Representative coupling reagents.*

2. OBJECTIVES

The objective of this thesis was the synthesis of AMPs derived from **BP100** and **BPC194**. In particular, it was centered on:

1. The synthesis of **BP100** analogues by incorporating D-amino acids on their sequence and evaluation of the influence of their modification on the antimicrobial and hemolytic activities, and on the suceptibility to proteases.

2. The synthesis of **BP100** analogs by incorporating a 1,2,3-triazole ring onto the side chain of a selected residue of this sequence and evaluation of the influence of this modification on the antimicrobial, the antifungal and the hemolytic activities and the suceptibility to proteases.

3. The synthesis of multivalent peptides derived from **BPC194** and evaluation of the antimicrobial and hemolytic activities.

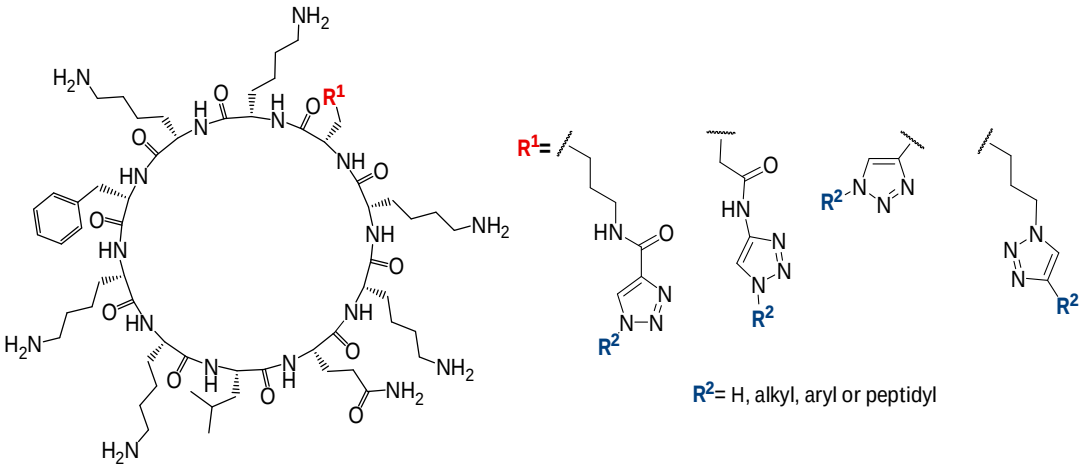

4. The synthesis of carbopeptides containing two or four units of **BP100** and **BP143** and evaluation of their antimicrobial and hemolytic activities.

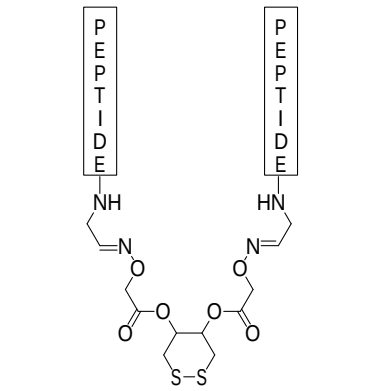

Carbopeptide
$(KKLFKKILKYLG)_2$-cDTE **cDTE(BP100)$_2$**
$(KKLfKKILKYLG)_2$-cDTE **cDTE(BP143)$_2$**

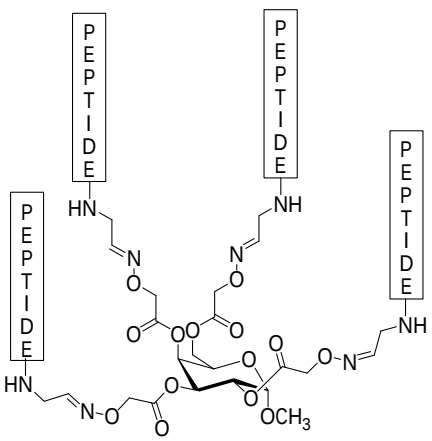

Carbopeptide
$(KKLFKKILKYLG)_4$-Gal*p* **Gal*p*(BP100)$_4$**

3. SYNTHESIS OF PEPTIDES DERIVED FROM BP100 CONTAINING D-AMINO ACIDS

In recent years, AMPs have been described to be effective against plant pathogens. There are several strategies to further improve the biological profile of peptides, one of which involves the introduction of D-amino acids in the sequence. Although this modification destabilizes the secondary structure, it maintains other structural properties such as the hydrophobicity, the side-chains and the peptide charge distribution. In addition, it leads to more stable, more active and, in some cases, less hemolytic sequences (Adessi 2002; Hong 1999).

Taking this as a basis, the main objective of this part of the PhD was to improve the biological profile of the antimicrobial peptide KKLFKKILKYL-NH_2 (**BP100**), one of the lead peptides previously identified in our group, by introducing D-amino acids in its sequence. Besides testing the influence on the activity of replacing all-L-amino acids, the influence of incorporating two or three D-amino acids at adjacent or non-consecutive positions, and four to ten D-amino acids in either the N- or the C-terminus was also investigated. Afterwards, for all the synthesized peptides, we studied their antibacterial activity against phytopathogenic and human bacteria, their hemolytic activity and the susceptibility to proteinase K degradation.

3.1. Design and synthesis of peptides

Based on **BP100** (KKLFKKILKYL-NH_2), a total of 20 sequences were designed, which contained Table 3.1:

- Two or three D-amino acids at consecutive and non-consecutive positions (**BP149** to **BP152** and **BP154**).
- Four to ten D-amino acids at the C-terminus (**BP155**-**BP161**).
- Four to ten D-amino acids at the N-terminus (**BP162**-**BP168**).
- All D-amino acids (**BP153**).

The synthesis was carried out manually by the solid-phase method using Fmoc-type chemistry with Boc side-chain protection for Lys and ^{t}Bu for Tyr (Scheme 3.1).

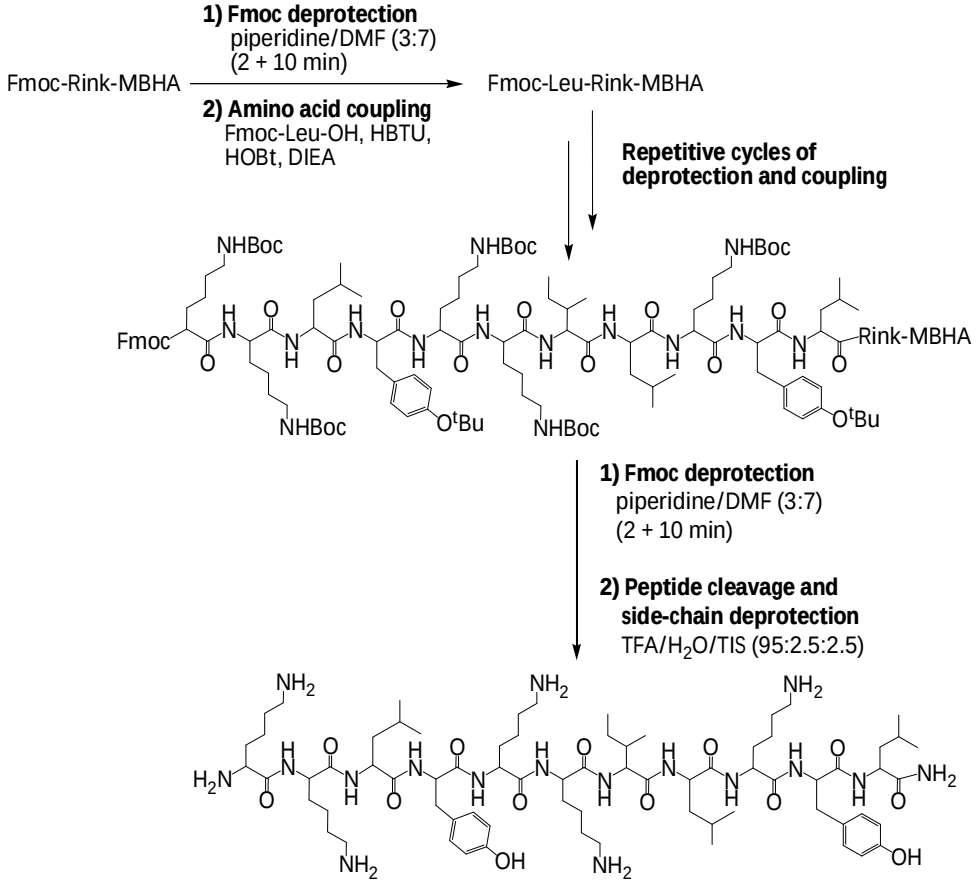

Scheme 3.1. *General strategy for the solid-phase peptide synthesis using a MBHA resin.*

Fmoc-Rink-MBHA resin (0.64 mmol/g) was used as solid support to obtain C-terminal peptide amides. Couplings of the Fmoc-amino acids were mediated by *O*-(benzotriazol-1-yl)-*N,N,N',N'*-tetramethyluronium hexafluorophosphate (HBTU) and 1-hydroxybenzotriazole (HOBt), as coupling reagents, and *N,N'*-diisopropylethylamine (DIPEA) as base in DMF for 1 h at room temperature, and they were monitored by the ninhydrin test. The Fmoc removal was performed by exposure of the peptidyl resin to a mixture of piperidine/DMF (3:7, 2+10 min).

Once the peptide chain was completed, the Fmoc group of the last amino acid was removed and peptides were cleaved from the resin with a solution of TFA/H_2O/Triisopropylsilane (TIS) (95:2.5:2.5) for 2 h. Water and TIS act as scavengers to capture the carbocation formed in this step to avoid secondary reactions. Following TFA evaporation and diethyl ether extraction, the crude peptides were dissolved in H_2O, lyophilized and analyzed by high-performance liquid chromatography (HPLC) (Table 3.1).

Table 3.1. *Sequences, retention times and purities on HPLC, and ESI-MS data.*

Peptide	Sequence[a]	t_R (min)	Purity[b] (%)	ESI-MS
BP149	KK**L**FKKIL**K**YL	6.21[c]	82	1443.0 $[M+Na]^+$
BP150	KKLFKKI**LK**YL	6.22[c]	81	1443.0 $[M+Na]^+$
BP151	KK**L**FK**K**IL**K**YL	6.20[c]	66	1443.0 $[M+Na]^+$
BP152	KKLFKK**ILK**YL	6.05[c]	71	711.5 $[M+2H]^{2+}$; 474.7 $[M+3H]^{3+}$
BP154	**KK**L**F**KKILKYL	6.25[c]	74	1443.0 $[M+Na]^+$
BP155	KKLFKKI**LKYL**	17.21[d]	64	1421.2 $[M+H]^+$
BP156	KKLFKK**ILKYL**	16.57[d]	55	1421.2 $[M+H]^+$
BP157	KKLFK**KILKYL**	16.28[d]	42 (98[f])	1443.0 $[M+Na]^+$; 1421.2 $[M+H]^+$
BP158	KKLF**KKILKYL**	6.23[c]	62	1420.9 $[M+H]^+$; 710.9 $[M+2H]^{2+}$
BP159	KKL**FKKILKYL**	6.28[c]	76	1421.3 $[M+H]^+$
BP160	KK**LFKKILKYL**	6.23[c]	80	1421.4 $[M+H]^+$
BP161	K**KLFKKILKYL**	6.37[c]	82	1421.4 $[M+H]^+$
BP162	**KKLF**KKILKYL	5.91[e]	76 (98[f])	1443.0 $[M+Na]^+$; 1421.0 $[M+H]^+$
BP163	**KKLFK**KILKYL	5.82[e]	48 (98[f])	1420.91 $[M+H]^+$; 711.0 $[M+2H]^{2+}$
BP164	**KKLFKK**ILKYL	5.90[e]	51 (98[f])	1442.9 $[M+Na]^+$; 1420.9 $[M+H]^+$
BP165	**KKLFKKI**LKYL	16.43[d]	58 (98[f])	1443.0 $[M+Na]^+$; 1421.0 $[M+H]^+$
BP166	**KKLFKKIL**KYL	6.03[c]	92	1443.0 $[M+Na]^+$; 1421.0 $[M+H]^+$
BP167	**KKLFKKILK**YL	6.06[c]	84	1443.0 $[M+Na]^+$; 1421.0 $[M+H]^+$
BP168	**KKLFKKILKY**L	15.88[d]	60 (95[f])	1443.0 $[M+Na]^+$; 1421.0 $[M+H]^+$
BP153	**KKLFKKILKYL**	6.18[c]	79	711.5 $[M+2H]^{2+}$; 474.7 $[M+3H]^{3+}$

[a]Underlined and bold amino acids are D-enantiomers. All peptides are C-terminal amides.
[b]Percentage determined by HPLC at 220 nm from the crude reaction mixture.
[c]HPLC analysis using method A (see Materials and Methods).
[d]HPLC analysis using method C (see Materials and Methods).
[e]HPLC analysis using method B (see Materials and Methods).
[f]Percentage determined by HPLC at 220 nm from the purified peptide.

As shown in Table 3.1 peptides were obtained in 42-92 % purity. Electrospray ionization mass spectrometry (ESI-MS) and matrix-assisted laser desorption ionization with time-of-flight analysis (MALDI-TOF) were used to confirm peptide identity.

Peptides with the highest percentage of purity (71-92 %) were **BP149**, **BP150**, **BP152**-**BP154**, **BP159**-**BP162**, **BP166** and **BP167**. Peptides **BP151**, **BP155**, **BP158** and **BP168**

were obtained in lower purity (60-66 %), while the lowest purity percentages (42-58 %) were observed for peptides **BP156**, **BP157** and **BP163**-**BP165**. The HPLC chromatogram of the latter showed two major peaks with similar retention times. Peptides **BP157**, **BP162**-**BP165** and **BP168** were purified by preparative HPLC and obtained in > 95 % purity.

Moreover, we analyzed by LC/MS the crude reaction mixture obtained in the synthesis of peptides **BP152**, **BP162**, **BP163** and **BP168**. As shown in Scheme 3.2, there was a major peak corresponding to the expected sequence together with minor peaks corresponding to incomplete sequences resulting from the deletion of one or two lysines. Taking into account that the ninhydrin test performed after each step was negative, we could assume that the last coupling and Fmoc removal steps were not successful.

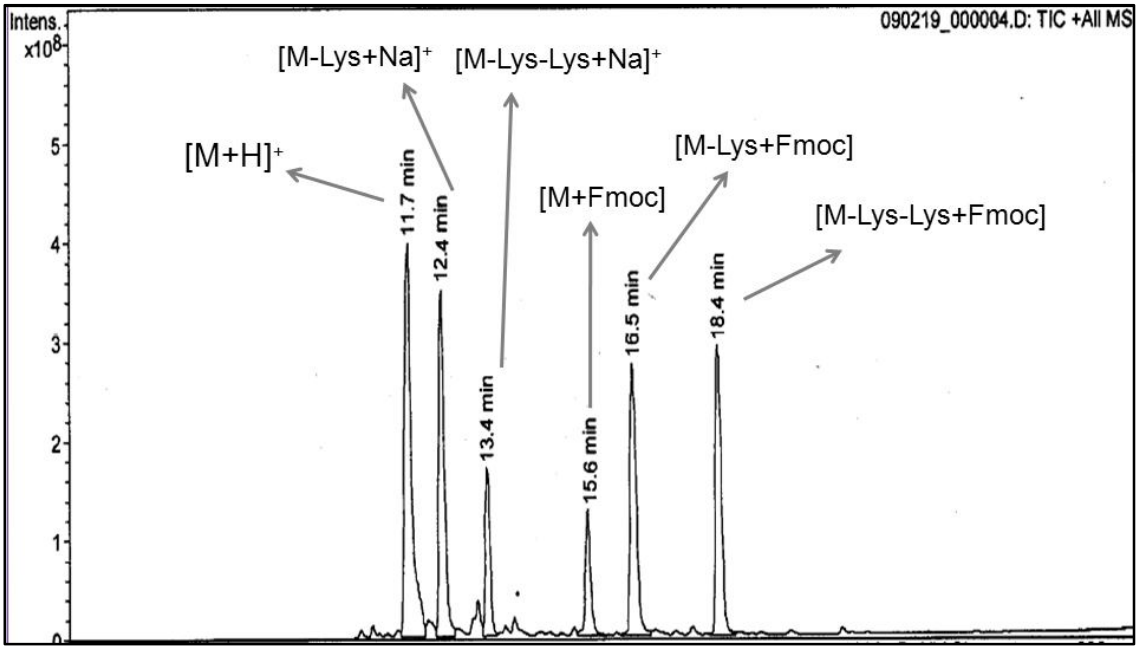

Scheme 3.2. *LC/MS of the reaction mixture of* ***BP163****.*

We next decided to study the use of an aminomethyl ChemMatrix (CM) resin as solid support. This resin has been described to be convenient for the synthesis of complex and long sequences that are difficult to prepare using polystyrene resins. Accordingly, **BP163** was prepared on an aminomethyl ChemMatrix resin (0.66 mmol/g). Until the ninth residue, couplings and Fmoc removal were carried out following the standard Fmoc/^{t}Bu strategy. Next coupling and deprotection steps were followed by HPLC. Best

conditions for the Fmoc removal of the ninth residue involved the treatment of the corresponding peptidyl resin with piperidine/DMF (3:7; 1 × 2 + 3 × 10 min), while the N-terminus deprotection of the tenth and eleventh residues required a (1 × 2 + 6 × 10 min) treatment. For the coupling of the tenth and eleventh residues, two and three treatments of the peptidyl resin with HOBt, HBTU and DIPEA for 24 h were necessary, respectively. This protocol led to **BP163** in 86 % HPLC purity which was higher than that obtained using the MBHA resin (48 %). This result pointed out that the ChemMatrix resin is a more convenient solid support than the MBHA resin for the synthesis of these undecapeptides.

3.2. Antibacterial activity assays

Peptides containing one or more D-amino acids were tested against plant and human pathogenic bacteria. The analogues incorporating one D-amino acid were synthesized in a previous work. However, their activity has been included in this thesis for a better discussion of the results.

3.2.1. Antibacterial activity against plant pathogenic bacteria

Peptides containing one or more than one D-amino acids were tested for *in vitro* growth inhibition of *E. amylovora*, *P. syringae* and *X. vesicatoria* at 0.62, 1.25, 2.5, 5.0 and 7.5 μM, and compared to **BP100** (Table 3.2 and 3.3, respectively). All these tests were performed by Dr. Esther Badosa of the Plant Pathology group at the University of Girona (UdG). The results are expressed as the minimum inhibitory concentration (MIC) which is the lowest peptide concentration for which there is no bacterial growth at the end of the experiment.

Table 3.2. *Antibacterial activity (MIC) of linear undecapeptides with one D-amino acid against three plant pathogenic bacteria.*

Peptide	Sequence[a]	MIC (μM)		
		X. vesicatoria	*P. syringae*	*E. amylovora*
BP100	KKLFKKILKYL	5-7.5	2.5-5	2.5-5
BP138	KKLFKKILK**Y**L	>7.5	>7.5	>7.5
BP139	KKLFKKILKY**L**	>7.5	>7.5	>7.5
BP140	KKLFKKIL**K**YL	>7.5	5-7.5	>7.5
BP141	KKLFKKI**L**KYL	>7.5	2.5-5	2.5-5
BP142	KKLF**K**KILKYL	>7.5	2.5-5	5-7.5
BP143	KKL**F**KKILKYL	5-7.5	2.5-5	2.5-5
BP144	KK**L**FKKILKYL	>7.5	2.5-5	>7.5
BP145	K**K**LFKKILKYL	5-7.5	2.5-5	2.5-5
BP146	KKLFK**K**ILKYL	>7.5	2.5-5	>7.5
BP147	**K**KLFKKILKYL	2.5-5	2.5-5	2.5-5
BP148	KKLFKK**I**LKYL	>7.5	>7.5	>7.5

[a]Underlined and bold amino acids are D-enantiomers. All peptides are C-terminal amides.

The antibacterial activity of the **BP100** isomers depended on the pathogen, the number of D-amino acids introduced and the residue that was replaced. Regarding the pathogen, in general, peptides did not display a clear pattern of activity. Among the 31 isomers studied, there were more peptides as active or more active than **BP100** against *P. syringae* and *X. vesicatoria* (21 and 18 sequences, respectively) than against *E. amylovora* (14 sequences). On the other hand, a differential susceptibility of bacteria to a given peptide was observed. This has been attributed to differences in the membrane components of the target microorganism, e.g. charge and lipid composition that would influence rates of binding of cationic peptides to the membranes (Huang 2000).

Table 3.3. *Antibacterial activity (MIC) of linear undecapeptides containing more than one D-amino acids against three plant pathogenic bacteria.*

Peptide	Sequence[a]	MIC (μM)		
		X. vesicatoria	***E. amylovora***	***P. syringae***
BP100	KKLFKKILKYL	5-7.5	2.5-5	2.5-5
BP149	KK**L**FKKIL**K**YL	>7.5	>7.5	>7.5
BP150	KKLFKKI**LK**YL	2.5-5	>7.5	>7.5
BP151	KK**L**FK**K**IL**K**YL	5-7.5	>7.5	5-7.5
BP152	KKLFKK**ILK**YL	5-7.5	>7.5	>7.5
BP154	**KK**L**F**KKILKYL	5-7.5	5-7.5	2.5-5
BP155	KKLFKKI**LKYL**	>7.5	>7.5	>7.5
BP156	KKLFKK**ILKYL**	5-7.5	>7.5	2.5-5
BP157	KKLFK**KILKYL**	1.25-2.5	1.25-2.5	2.5-5
BP158	KKLF**KKILKYL**	2.5-5	2.5-5	1.25-2.5
BP159	KKL**FKKILKYL**	2.5-5	2.5-5	1.25-2.5
BP160	KK**LFKKILKYL**	1.25-2.5	2.5-5	1.25-2.5
BP161	K**KLFKKILKYL**	1.25-2.5	1.25-2.5	1.25-2.5
BP162	**KKLF**KKILKYL	2.5-5	1.25-2.5	1.25-2.5
BP163	**KKLFK**KILKYL	5-7.5	2.5-5	>7.5
BP164	**KKLFKK**ILKYL	>7.5	>7.5	2.5-5
BP165	**KKLFKKI**LKYL	>7.5	>7.5	1.25-2.5
BP166	**KKLFKKIL**KYL	>7.5	>7.5	2.5-5
BP167	**KKLFKKILK**YL	2.5-5	2.5-5	2.5-5
BP168	**KKLFKKILKY**L	5-7.5	2.5-5	1.25-2.5
BP153	**KKLFKKILKYL**	0.6-1.2	1.2-2.5	1.2-2.5

[a]Underlined and bold amino acids are D-enantiomers. All peptides are C-terminal amides.

D-Diastereoisomers exhibited complicated activity patterns, and did not display a simple dependence on the polarity of the residue. However, general trends on the positions that influence the activity were observed. Analysis of the results previously obtained for single D-amino acid substitution reflected that replacement of residues I^7 (**BP148**), K^9 (**BP140**), Y^{10} (**BP138**), and L^{11} (**BP139**) decreased the antibacterial activity against the three pathogens, indicating that these amino acids are crucial for activity

and cannot be replaced. In contrast, residues F^4, K^2 and K^1 can be substituted, leading to peptides **BP143**, **BP145** and **BP147** (MIC of 2.5 to 7.5 μM), without weakening the activity against the three bacteria (Güell 2011) (Table 3.2). In the present study a similar tendency for peptides containing two and three D-amino acids was observed. Double- or triple-D-amino acid replacement led to peptides **BP149** (D-L^3,D-K^9), **BP150** (D-L^8,D-K^9), **BP151** (D-L^3,D-K^6,D-K^9) and **BP152** (D-I^7,D-L^8,D-K^9) which were less active than **BP100**, with the exception of **BP150** against *X. vesicatoria* (MIC of 2.5 to 5.0 μM). In contrast, the analogue **BP154** (D-K^1, D-K^2, D-F^4) had similar activity than **BP100** (MIC of 2.5 to 7.5 μM). Thus, sequences containing D-K^9 or D-I^7 and D-K^9 were less active than **BP100**, indicating that these amino acids are crucial for activity and cannot be replaced, whereas the presence of D-K^1, D-K^2 and D-F^4 did not influence the activity.

Introduction of D-amino acids at the N- or C-terminus resulted in distinctly improved activity. Peptides containing D-amino acids at the C-terminus (**BP155**-**BP161**) were more active and their activity increased with the number of D-amino acids, leading to peptides with MIC values of 1.2 to 5.0 μM. Peptides containing four (**BP155**) and five (**BP156**) D-amino acids were the less active, whereas the incorporation of six to nine D-amino acids resulted in peptides **BP157**-**BP160** displaying higher antibacterial activity than **BP100** against two pathogens (MIC of 1.2 to 5.0 μM). Accordingly, **BP161**, with ten D-amino acids, and the all-D isomer **BP153** were more active than the parent peptide against the three bacteria (MIC of 0.6 to 2.5 μM). When four to ten D-amino acids were incorporated at the N-terminus (**BP162**-**BP168**), a decrease of activity was generally observed. However, three sequences (**BP162**, **BP167**, and **BP168**) were more active than **BP100** with MIC values ranging from 1.2 to 7.5 μM. The all-D-amino acid isomer, **BP153**, was also analyzed and resulted to be the most active sequence.

3.2.2. Antibacterial activity against human pathogens

Peptides containing one or more than one D-amino acid were tested for *in vitro* growth inhibition of *E. coli*, S*. aureus, S. typhimurium* and *L. monocytogenes* at 6.25, 12.5, 25

and 50 μM, and compared to **BP100** (Table 3.4 and Table 3.5, respectively). All these tests were performed by Dr. Esther Badosa of the Plant Pathology group at the UdG.

As shown in Table 3.4 and Table 3.5 and, MIC values obtained for human bacteria were higher than those for the phytopathogenic bacteria. Similarly to phytopathogenic bacteria, antibacterial activity of the **BP100** isomers against the tested human bacteria depended on the pathogen, the number of D-amino acids introduced and the residue that was replaced.

Table 3.4. *Antibacterial activity (MIC) of linear undecapeptides containing one D-amino acid against four human bacteria.*

Peptide	Sequence[a]	MIC (μM)			
		E. coli	*S. aureus*	*S. typhimurium*	*L. monocytogenes*
BP100	KKLFKKILKYL	2.5-5	>20	5-10	>15
BP138	KKLFKKILK**Y**L	12.5-25	>20	>20	>20
BP139	KKLFKKILKY**L**	12.5-25	>50	12.5-25	>50
BP140	KKLFKKIL**K**YL	12.5-25	>50	25-50	>50
BP141	KKLFKKI**L**KYL	<6.2	>50	25-50	>50
BP142	KKLF**K**KILKYL	12.5-25	>50	25-50	>20
BP143	KKL**F**KKILKYL	<6.2	>50	<6.2	25-50
BP144	KK**L**FKKILKYL	12.5-25	>50	6.2-12.5	>50
BP145	K**K**LFKKILKYL	<6.2	>50	<6.2	12.5-25
BP146	KKLFK**K**ILKYL	12.5-25	25-50	6.2-12.5	>50
BP147	**K**KLFKKILKYL	<6.2	25-50	<6.2	25-50
BP148	KKLFKK**I**LKYL	12.5-25	>50	>50	>50

[a]Underlined and bold amino acids are D-enantiomers. All peptides are C-terminal amides.

Single D-amino acid replacement had a pronounced effect on the peptide activity. In agreement with the results obtained for phytopathogenic bacteria, the replacement of residues I^7 (**BP148**), K^9 (**BP140**), Y^{10} (**BP138**), and L^{11} (**BP139**) decreased the antibacterial activity. In this case a decrease of activity was also observed when the K^5 **BP142**) residue was substituted. On the contrary, residues F^4 (**BP143**), K^2 (**BP145**) and

K^1 (**BP147**) can be replaced without diminishing the peptide activity against the four pathogens. Regarding the pathogen, *E. coli* was the most sensitive to these peptides, 4 sequences displayed MIC < 6.25 μM and 7 sequences, MIC values of 12.5 to 25 μM. For *S. typhimurium,* 3 sequences displayed MIC < 6.25 μM, 2 sequences, MIC values of 6.25 to 12.5 μM and one sequence, MIC values of 12.5 to 25 μM. The bacteria *L. monocytogenes* and *S. aureus* were the least sensitive.

Among the 20 isomers containing more than one D-amino acid, 15 peptides were at least active against one pathogen with MIC < 25 μM. Similarly to peptides containing one D-amino acid, *E. coli* was the most sensitive to these peptides, 8 sequences displayed MIC < 6.25 μM and 3 sequences, MIC values of 6.25 to 12.5 μM. *S. typhimurium* was less sensitive with 3 sequences displaying MIC < 6.25 μM and 3 sequences, MIC values of 6.25 to 12.5 μM. The activity against *L. monocytogenes* and *S. aureus* increased compared to that observed for isomers **BP138**-**BP148**. For *L. monocytogenes,* sequences (**BP161** and **BP153**) with MIC < 12.5 μM were identified. In the case of *S. aureus*, **BP159** and **BP161** showed a MIC of 12.5 to 25 μM.

Double- or triple-D-amino acid replacement in general led to a decrease of activity. Consistently with the result obtained for isomers containing one D-amino acid, **BP154** (D-K^1, D-K^2, D-F^4) was the most active.

Similarly to phytopathogenic bacteria, when four to ten D-amino acids were incorporated at the N-terminus (**BP162**-**BP168**), a significant decrease of the activity was observed. Moreover, the activity of peptides incorporating four to ten D-amino acids at the C-terminus (**BP155**-**BP161**) generally increased with the number of D-residues. Peptide containing four D-amino acids (**BP155**) was the least active, whereas **BP161**, with ten D-amino acids, and the all-D isomer **BP153** were the peptides with the best profile of activity against the four human bacteria.

Table 3.5. *Antibacterial activity (MIC) of linear undecapeptides containing more than one D-amino acid against four human bacteria.*

Peptide	Sequence[a]	MIC (μM)			
		E. coli	*S. aureus*	*S. typhimurium*	*L. monocytogenes*
BP100	KKLFKKILKYL	2.5-5	> 20[b]	5-10	>15[b]
BP149	KK**L**FKKIL**K**YL	< 6.2[c]	> 50[b]	> 50	> 50[b]
BP150	KKLFKKI**LK**YL	6.2 - 12.5	> 50[b]	25 - 50	> 50[b]
BP151	KK**L**FK**K**IL**K**YL	6.2 - 12.5	> 50[b]	> 50	25 - 50
BP152	KKLFKK**ILK**YL	12.5 - 25	> 50[b]	25 - 50	25 - 50
BP154	**KK**L**F**KKILKYL	< 6.2[c]	> 50[b]	6.2 - 12.5	12.5 - 25
BP155	KKLFKKI**LKYL**	25 - 50	> 50[b]	> 50[b]	> 50[b]
BP156	KKLFKK**ILKYL**	< 6.2[c]	25 - 50	6.2 - 12.5	25 - 50
BP157	KKLFK**KILKYL**	6.2 - 12.5	> 50[b]	12.5 - 25	25 - 50
BP158	KKLF**KKILKYL**	< 6.2[c]	25 - 50	12.5 - 25	25 - 50
BP159	KKL**FKKILKYL**	< 6.2[c]	12.5 - 25	6.2 - 12.5	12.5 - 25
BP160	KK**LFKKILKYL**	< 6.2[c]	25 - 50	< 6.2[c]	12.5 - 25
BP161	K**KLFKKILKYL**	< 6.2[c]	12.5 - 25	< 6.2[c]	6.2 - 12.5
BP162	**KKLF**KKILKYL	> 50[b]	> 50[b]	> 50[b]	> 50[b]
BP163	**KKLFK**KILKYL	> 50[b]	> 50[b]	12.5 - 25	> 50[b]
BP164	**KKLFKK**ILKYL	> 50[b]	> 50[b]	> 50[b]	> 50[b]
BP165	**KKLFKKI**LKYL	> 50[b]	> 50[b]	12.5 - 25	> 50[b]
BP166	**KKLFKKIL**KYL	12.5 - 25	> 50[b]	25 - 50	12.5 - 25
BP167	**KKLFKKILK**YL	> 50[b]	> 50[b]	25 - 50	> 50[b]
BP168	**KKLFKKILKY**L	25 - 50	> 50[b]	> 50[b]	> 50[b]
BP153	**KKLFKKILKYL**	< 6.2[c]	25 - 50	< 6.2[c]	< 6.2[c]

[a]Underlined and bold amino acids are D-enantiomers. All peptides are C-terminal amides.
[b]Maximum concentration tested.
[c]Minimum concentration tested.

3.3. Hemolytic activity

Since the mechanism of action of AMPs consists on cell membrane disruption, toxicity to animal or plant cells (cytotoxicity) may be a problem. This cytotoxicity can be assessed with different animal or plant cell model systems, although erythrocytes most frequently used due to the easier comparison with existing reports (Badosa 2007; Bardají 2006; Monroc 2006). Thus, the toxicity of the peptides to eukaryotic cells was determined as the ability to lyse erythrocytes in comparison to melittin at peptide concentrations of 50, 150 and 250 μM (Table 3.7). All these tests were performed by Dr. Esther Badosa of the Plant Pathology group at the UdG. Results of the previously synthesized one D-amino acid analogues have also been included for comparison purpose (Table 3.6).

Table 3.6. *Cytotoxicity of linear undecapeptides containing one D-amino acid.*

Peptide	Sequence[a]	Hemolysis[b] (%)		
		50 μM	150 μM	250 μM
BP100	KKLFKKILKYL	3 ± 0.1	22 ± 2.8	54 ± 0.1
BP138	KKLFKKILK**Y**L	2 ± 0.5	11 ± 0.3	7 ± 0.1
BP139	KKLFKKILKY**L**	1 ± 0.4	4 ± 0.5	23 ± 0.9
BP140	KKLFKKIL**K**YL	1 ± 4	0 ± 0.1	0 ± 0
BP141	KKLFKKI**L**KYL	0 ± 0.4	0 ± 3	4 ± 0.3
BP142	KKLF**K**KILKYL	1 ± 2	0,3 ± 0.5	3 ± 0.6
BP143	KKL**F**KKILKYL	2 ± 31	2 ± 2	5 ± 0.8
BP144	KK**L**FKKILKYL	0,2 ± 0.2	2 ± 2	7 ± 0.4
BP145	K**K**LFKKILKYL	4 ± 0.2	27 ± 0.7	51 ± 0.5
BP146	KKLFK**K**ILKYL	4 ± 0.4	23 ± 2	53 ± 1.1
BP147	**K**KLFKKILKYL	8 ± 1	45 ± 0.1	71 ± 0.4
BP148	KKLFKK**I**LKYL	2 ± 0.4	11 ± 0.4	0 ± 0

[a]Underlined and bold amino acids are D-enantiomers. All peptides are C-terminal amides.
[b]Percent hemolysis at 50, 150 and 250 μM plus confidence interval (α = 0.05).

The analysis of the influence of a single D-amino acid replacement pointed out that there is not a clear pattern. However, substitution of residues L^3, F^4, K^5, I^7, L^8, K^9, and Y^{10} led to peptides with a low hemolytic activity (≤ 7 %). Replacement of the other

amino acids resulted in a slightly increase of the hemolysis (23-71 %). Notably, **BP143** which incorporates D-F^4 combined both high antibacterial activity (MIC of 2.5 to 7.5 μM) and low hemolysis (5 %). Thus, the hemolytic activity of **BP100** isomers depended on the residue that was replaced, but followed a different pattern than the one for antibacterial activity (Güell 2011) (Table 3.6).

Table 3.7. *Cytotoxicity of linear undecapeptides containing more than one D-amino acid.*

Peptide	Sequence[a]	Hemolysis[b] (%)		
		50 μM	150 μM	250 μM
BP100	KKLFKKILKYL	3 ± 0.1	22 ± 2.8	54 ± 0.1
BP149	KK**L**FKKIL**K**YL	0 ± 0.2	0 ± 0.2	0 ± 0.1
BP150	KKLFKKI**LK**YL	0 ± 0.2	0 ± 0.4	1 ± 0.1
BP151	KK**L**FK**K**IL**K**YL	0 ± 0	1 ± 0.2	1 ± 0.3
BP152	KKLFKK**ILK**YL	0 ± 0.6	3 ± 0.6	5 ± 1.6
BP154	**KK**L**F**KKILKYL	1 ± 0.5	3 ± 0.4	41 ± 6.2
BP155	KKLFKKI**LKYL**	2 ± 2.6	2 ± 1.0	3 ± 0.1
BP156	KKLFKK**ILKYL**	7 ± 4	26 ± 1.2	49 ± 1.2
BP157	KKLFK**KILKYL**	0 ± 1	0 ± 0.7	3 ± 1.0
BP158	KKLF**KKILKYL**	1 ± 0.5	9 ± 0.5	28 ± 2.1
BP159	KKL**FKKILKYL**	4 ± 0.5	27 ± 4.5	58 ± 5.7
BP160	KK**LFKKILKYL**	11 ± 0.6	35 ± 1.0	65 ± 1.9
BP161	K**KLFKKILKYL**	18 ± 1	47 ± 1	66 ± 2.9
BP162	**KKLF**KKILKYL	0 ± 0.3	4 ± 1.8	17 ± 0.7
BP163	**KKLFK**KILKYL	0 ± 0.5	2 ± 0.5	8 ± 5.0
BP164	**KKLFKK**ILKYL	0 ± 0.1	0 ± 0.5	0 ± 0.7
BP165	**KKLFKKI**LKYL	0 ± 0.3	1 ± 0.5	6 ± 0.2
BP166	**KKLFKKIL**KYL	0 ± 0.9	0 ± 0	1 ± 0.2
BP167	**KKLFKKILK**YL	2 ± 0.9	6 ± 2.3	21 ± 7.4
BP168	**KKLFKKILKY**L	0 ± 0	1 ± 1.2	3 ± 2.7
BP153	**KKLFKKILKYL**	1 ± 0.4	11 ± 2.5	50 ± 2.1

[a]Underlined and bold amino acids are D-enantiomers. All peptides are C-terminal amides.
[b]Percent hemolysis at 50, 150 and 250 μM plus confidence interval (α = 0.05).

For peptides containing more than one D-amino acid, eleven out of 20 isomers displayed less than 10 % hemolysis at 250 μM. Accordingly to the results of single D-amino acid analogues, when two or three residues were replaced with the corresponding enantiomer, the resulting peptides **BP149**-**BP152** displayed low hemolytic activity (≤5 %). In contrast, **BP154** containing D-K^1, D-K^2 and D-F^4 showed a higher cytotoxicity (41 %). Hemolysis of peptides incorporating from four to ten D-amino acids at the N- or at the C-terminus did not depend on the number of D-amino acids incorporated. However, the former were less hemolytic (0-21 %) while the latter showed significant hemolysis (28-66 %) except for **BP155** and **BP157** which had a percentage of hemolysis of 3 %. Moreover, even though attempts to use enantiomeric peptides solely composed of D-amino acids have been made to enhance peptide cell selectivity (Matsuzaki 2009), in the present study the all-D-peptide **BP153** was as cytotoxic as **BP100**.

3.4. Susceptibility to protease degradation

Protease digestion stability is a desired property in AMPs to assure a reasonable half-life of the molecules in the plant environment. Proteases from epiphytic microorganisms or intrinsic to the plant in internal tissues may degrade AMPs (Ali 2000; Cavallarin 1998). In this PhD thesis, the susceptibility to proteolysis of peptides **BP149**-**BP168** (Table 3.9) was studied by exposure to proteinase K, a cocktail of proteases of bacterial origin with a broad selectivity. Results were compared to those previously obtained for **BP138**-**BP148** (Table 3.8) for which it would appear that in general residues in the C-terminal part of the peptide are more critical for stability. The degradation of peptides **BP149**-**BP155** and **BP157**-**BP161** was monitored by reverse-phase HPLC over time. As expected, replacement of amino acids for the corresponding enantiomer in **BP100** had a strong influence in susceptibility to protease digestion, being all peptides more stable than **BP100**. Single D-amino acid replacement led to 5 sequences displaying a degradation below 20 % after 1 h of incubation. The least stable peptides were **BP138** (D-Y^{10}), **BP142** (D-K^5), **BP144** (D-L^3), **BP145** (D-K^2), **BP146** (D-K^6) and **BP147** (D-K^1) with 24 to 61 % degradation (Table 3.8).

Table 3.8. *Stability against protease degradation of linear undecapeptides containing one D-amino acid.*

Peptide	Sequence[a]	Digestion[b] (%)
BP100	KKLFKKILKYL	75
BP138	KKLFKKILK**Y**L	53
BP139	KKLFKKILKY**L**	6
BP140	KKLFKKIL**K**YL	1
BP141	KKLFKKI**L**KYL	1
BP142	KKLF**K**KILKYL	35
BP143	KKL**F**KKILKYL	18
BP144	KK**L**FKKILKYL	50
BP145	K**K**LFKKILKYL	61
BP146	KKLFK**K**ILKYL	24
BP147	**K**KLFKKILKYL	47
BP148	KKLFKK**I**LKYL	0

[a]Underlined and bold amino acids are D-enantiomers. All peptides are C-terminal amides.
[b]Percentage of degraded peptide calculated by HPLC.

For peptides containing more than one D-amino acid, all sequences displayed a degradation below 15 %, except for **BP154** (D-K[1], D-K[2], D-F[4]) which showed a 37 % degradation after 1 h incubation. The degradation of peptides **BP156** and **BP162**-**BP168** could not be monitored by HPLC and was analyzed by MALDI-TOF. They were detected after 1 h incubation with protease, which was indicative that these peptides were not completely degraded (Table 3.9).

Table 3.9. *Stability against protease degradation of linear undecapeptides containing more than one D-amino acid.*

Peptide	Sequence[a]	Digestion[b] (%)
BP100	KKLFKKILKYL	75
BP149	KK**L**FKKIL**K**YL	6
BP150	KKLFKKI**LK**YL	0
BP151	KK**L**FK**K**IL**K**YL	0
BP152	KKLFKK**ILK**YL	1
BP154	**KK**L**F**KKILKYL	37
BP155	KKLFKKI**LKYL**	6
BP156	KKLFKK**ILKYL**	-[c]
BP157	KKLFK**KILKYL**	0
BP158	KKLF**KKILKYL**	0
BP159	KKL**FKKILKYL**	12
BP160	KK**LFKKILKYL**	0
BP161	K**KLFKKILKYL**	1
BP162	**KKLF**KKILKYL	-[c]
BP163	**KKLFK**KILKYL	-[c]
BP164	**KKLFKK**ILKYL	-[c]
BP165	**KKLFKKI**LKYL	-[c]
BP166	**KKLFKKIL**KYL	-[c]
BP167	**KKLFKKILK**YL	-[c]
BP168	**KKLFKKILKY**L	-[c]
BP153	**KKLFKKILKYL**	6

[a]Underlined and bold amino acids are D-enantiomers. All peptides are C-terminal amides.
[b]Percentage of degraded peptide calculated by HPLC.
[c]Degradation was monitored by MALDI-TOF and peptide was detected after 1 h.

Peptides with an optimal balance between antibacterial and hemolytic activities were **BP153** and **BP161** with MIC values ranging from 3.1 to 50 μM, and hemolytic percentages of 50-66 % at 250 μM, concentration considerably higher than the MIC. Thus, the present study demonstrates how the activity against plant pathogenic and

human bacteria of a linear undecapeptide can be improved through D-amino acid substitution.

3.5. *Ex vivo* infection assays and whole-plant assays

Several D-diastereomeric peptides displayed a good *in vitro* activity profile, however their high production cost imposes severe limitations to their application as plant protection products. Therefore, in the course of this thesis, isomers containing a single D-amino acid substitution were evaluated in plant material. In particular, the activity of peptides **BP138**-**BP147** that contain one D-amino acid was compared to that of the parent peptide **BP100** in a detached plant organ assay using a preventative application. Moreover, a non-treated control and a reference treatment with streptomycin (strep) were used (Scheme 3.3).

The disease intensity in the nontreated controls for the three plant-pathogenic bacteria was high and ranged from 65 to 95 % (necrosis progressed around the wound with mean diameter >3 mm). For the three pathogens in the two experiments performed, streptomycin-treated wounds were not infected or infections remained at the site of inoculation. More peptides were found to be active against *P. syringae* and *E. amylovora* on pear leaves or fruits than against *X. vesicatoria* on pepper leaves. This finding is in agreement with the results of *in vitro* activity. Also, it was confirmed a considerable specificity of the peptides for the pathogen-host system, in comparison to streptomycin that was consistently effective in the three pathosystems used. In pepper leaves inoculated with *X. vesicatoria*, peptide **BP145** resulted to be the best peptide, being effective in both experiments and as effective as streptomycin in the assay 1. In pear leaves inoculated with *P. syringae*, peptide **BP146** had a statistically significant effect in both experiments. In immature pear fruits inoculated with *E. amylovora*, peptides **BP100**, **BP144**, **BP146** and **BP147** were effective in both assays.

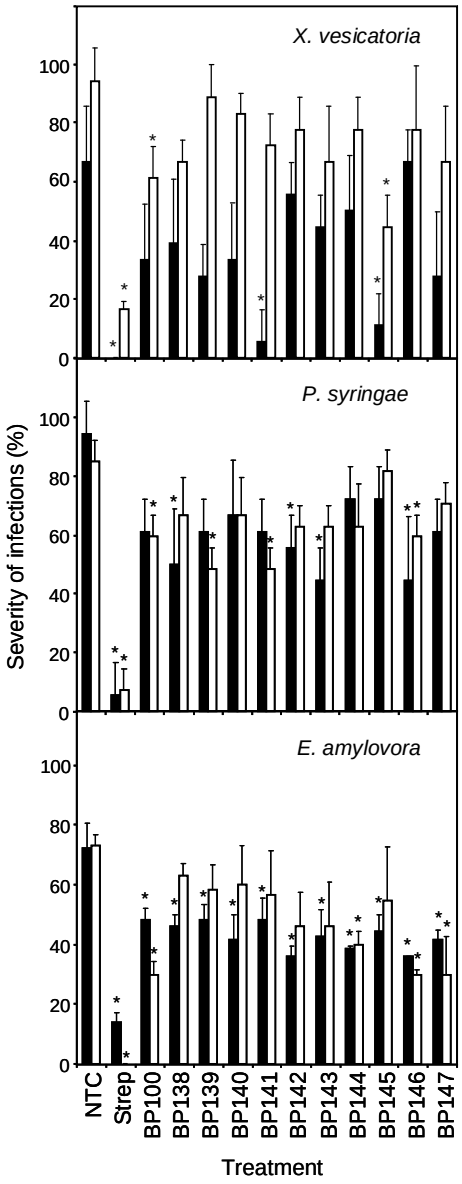

Scheme 3.3. *Effect of the preventative application of linear undecapeptides to control infections in detached pear (P. syringae) and pepper (X. vesicatoria) leaves and in immature pear fruits (E. amylovora). Two independent experiments, assay 1 (black bars) and assay 2 (white bars), were performed. A non-treated control (NTC) and a reference treatment with streptomycin (strep) were used. The confidence interval for the mean is indicated on the top of the bars. An asterisk over a bar indicates significant differences compared to the non-treated control for a given experiment according to Tukey's test (P < 0.05).*

Moreover, peptides **BP143** and **BP145** were selected to evaluate their activity in whole pear (*E. amylovora* and *P. syringae*) and pepper (*X. vesicatoria*) plant assays (Scheme 3.4). The activity was compared to those of **BP100** and streptomycin.

Streptomycin controlled the disease caused by the three pathogens in the two experiments performed (Scheme 3.4). Peptide **BP100** did not differ from streptomycin in the two experiments against *E. amylovora* on pear and in one experiment against *X. vesicatoria* on pepper. Peptide **BP145** was as effective as **BP100** in the three pathosystems *in planta.* These results clearly suggest that subtle changes in the structure of AMPs affect not only the *in vitro* antibacterial and hemolytic activities and protease degradation susceptibility, but also other biological properties like *in planta* activity. Peptide **BP143** was more effective than **BP100** in one experiment against *X.*

vesicatoria on pepper and in one experiment against *P. syringae* on pear and did not differ significantly against *E. amylovora* on pear. Interestingly, peptide **BP143** was as effective as streptomycin in all three pathosystems. Antibiotics like streptomycin, tetracycline, and kasugamycin are used in certain countries to control plant bacterial diseases at doses that are only slightly lower than those used for this antimicrobial peptide in the present study (McManus 2002; Vidaver 2002; Agrios 2005).

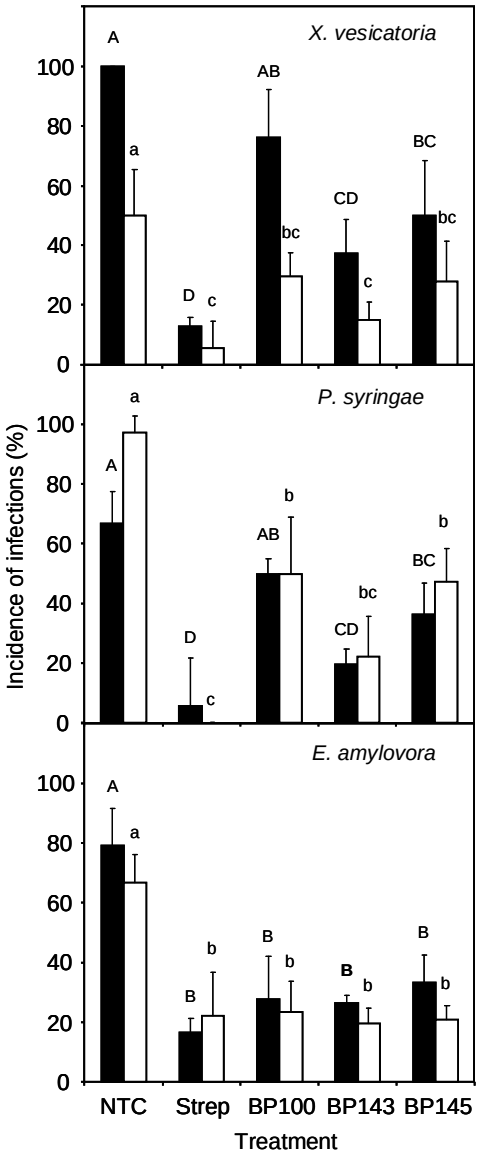

Scheme 3.4. *Effect of the preventative application of linear undecapeptides to control bacterial blight of pepper (X. vesicatoria), bacterial blight of pear (P. syringae), and fire blight of pear (E. amylovora) under controlled greenhouse conditions. Two independent experiments, assay 1 (black bars) and assay 2 (white bars), were performed. A non-treated control (NTC) and a reference treatment with streptomycin (Strep) were used. The confidence interval for the mean is indicated on the top of the bars. Letters over the bars indicates significant differences for assay 1 (capital letters) and assay 2 (small letters) comparing to the non-treated control according to Tukey's test (P≤0.05).*

This study shows that screening based on *in vitro* and *ex vivo* procedures can deliver effective compounds to control plant infections in model plant pathogenic bacteria. The fact that peptide **BP143** showed an efficacy *in planta* comparable to the reference antibiotic streptomycin against the three plant bacterial diseases, confirms the potential of antimicrobial peptides as plant protection products.

4. SYNTHESIS OF PEPTIDOTRIAZOLES DERIVED FROM BP100

This chapter includes the synthesis of linear peptidotriazoles derived from **BP100** (KKLFKKILKYL-NH_2). The 1,2,3-triazole ring was selected because it has been shown to be a crucial motif in biologically active compounds. Moreover, the synthesis of 1,2,3-triazole can be conveninently achieved by a copper(I)-catalyzed azide-alkyne cycloaddition, which are mild conditions that have been successfully adapted to solid support. Although many peptides containing triazoles have been reported, so far peptidotriazoles active against plant pathogenic bacteria or fungi have not been described. The linear peptidotriazoles synthesized in this PhD were screened for their in vitro growth inhibition of bacterial and fungal phytopathogens, their cytotoxic effects on eukaryotic cells and their proteolytic susceptibility.

4.1. Design of the peptidotriazoles

In order to investigate the influence of the 1,2,3-triazole ring on the biological activity of the parent peptide **BP100** (KKLFKKILKYL-NH_2), a total of 13 sequences (Table 4.1) were designed based on its structure by:

- Modifying each Lys residue with an unsubstituted triazole or with a triazole bearing a 2-aminohexanoic acid (Ahx) (**BP238-BP247**).
- Replacing the benzene ring of the Phe residue at position 4 by an unsubstituted triazole (**BP248**) or by a triazole substituted with a 2-aminohexanoic acid (Ahx) (**BP249**) or with a benzyl group (**BP250**).

Table 4.1. *Structure of the peptidotriazoles* ***BP238-BP250****.*

Peptide	Sequence
BP238	**X_a**KLFKKILKYL-NH_2
BP239	**X_b**KLFKKILKYL-NH_2
BP240	K**X_a**LFKKILKYL-NH_2
BP241	K**X_b**LFKKILKYL-NH_2
BP242	KKLF**X_a**KILKYL-NH_2
BP243	KKLF**X_b**KILKYL-NH_2
BP244	KKLFK**X_a**ILKYL-NH_2
BP245	KKLFK**X_b**ILKYL-NH_2
BP246	KKLFKKIL**X_a**YL-NH_2
BP247	KKLFKKIL**X_b**YL-NH_2
BP248	KKL**X_c**KKILKYL-NH_2
BP249	KKL**X_d**KKILKYL-NH_2
BP250	KKL**X_e**KKILKYL-NH_2

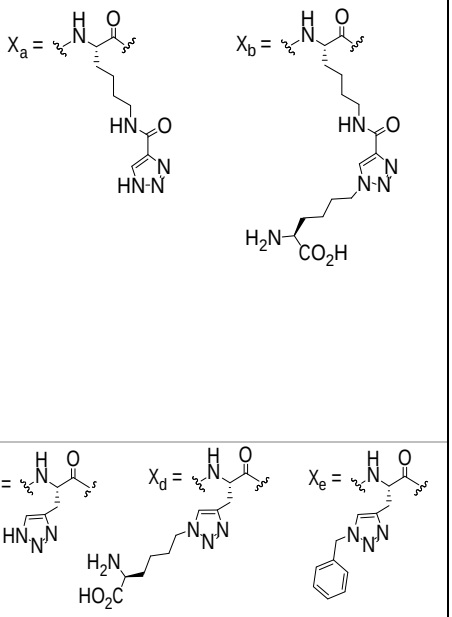

4.2. Solid-phase synthesis of the peptidotriazoles

The synthesis of the peptidotriazoles **BP238-BP247** would involve the preparation of the corresponding alkynyl peptidyl resin **1** and its subsequent reaction with NaN_3 or Boc-Ahx(N_3)-OH (Scheme 4.1). The alkynyl peptidyl resins would be prepared by selective acylation of the corresponding Lys residue with propiolic acid. This residue would be introduced with its ε-amino group protected with a methyltrityl (Mtt) group to be selectively deprotected.

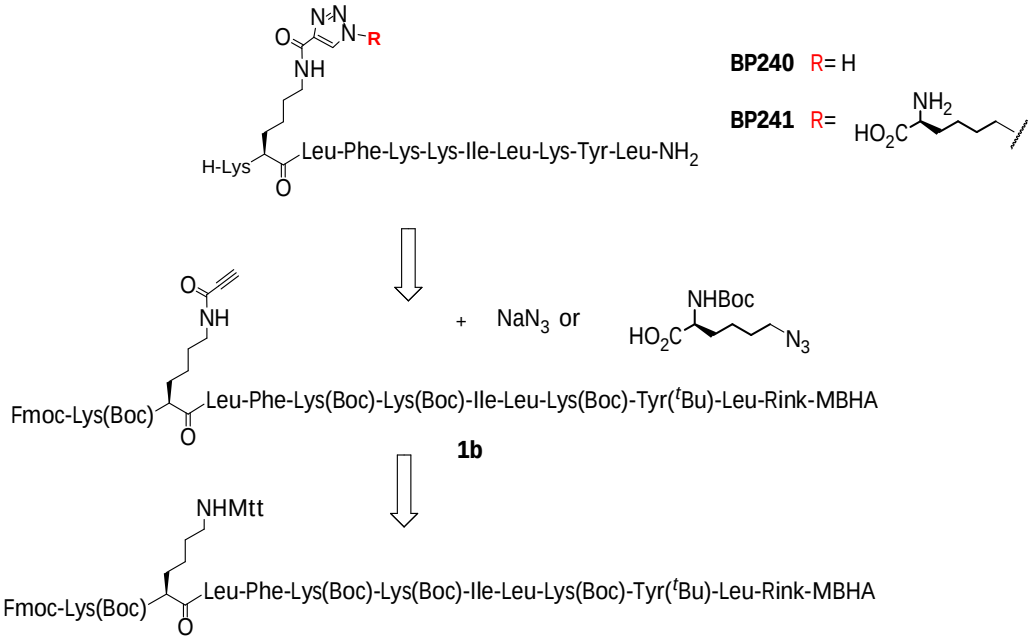

Scheme 4.1. *Retrosynthesis for the preparation of* ***BP238-BP247****, exemplified for* ***BP240*** *and* ***BP241****.*

Peptidotriazoles **BP248-BP250** could be prepared following a similar strategy. In this case, the alkynyl peptidyl resin **2** would be obtained by incorporating a propargylglycine residue at position 4. The 1,2,3-triazole ring would be formed by cycloaddition with NaN_3, Boc-Ahx(N_3)-OH or BnN_3 (Scheme 4.2).

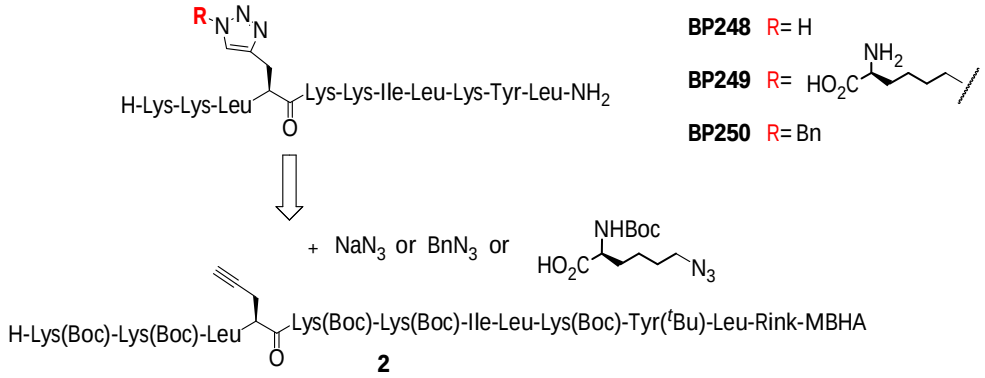

Scheme 4.2. *Retrosynthetic scheme for the preparation of* ***BP248-BP250****.*

4.2.1. Synthesis of the alkynyl peptidyl resins

The alkynyl peptidyl resins **1a-e**, containing an alkynyl moiety at a Lys side-chain and required for the preparation of peptidotriazoles **BP238-BP247**, respectively, were

synthesized starting from a Fmoc-Rink-MBHA resin following a Fmoc-type chemistry (Table 4.2 and Scheme 4.3). The amino acids used were Fmoc-Leu-OH, Fmoc-Phe-OH, Fmoc-Ile-OH, Fmoc-Tyr(^{t}Bu)-OH, Fmoc-Lys(Boc)-OH or Fmoc-Lys(Mtt)-OH. The latter was incorporated at the position that would be modified with a triazole ring. Couplings of the Fmoc-amino acids (4 equiv) were mediated by Oxyma pure (4 equiv) and DIPCDI (4 equiv) in DMF for 1 h, and monitored by the ninhydrin test. The Fmoc group was removed by treating the resin with a mixture of piperidine/DMF (3:7; 2 + 10 min). Washings were performed with DMF (6 × 1 min) and CH_2Cl_2 (6 × 1 min). Peptide elongation was carried out by repeated cycles of Fmoc group removal, couplings and washings.

Once chain assembly was completed, peptidyl resins containing an Mtt-protected Lys were treated with 1 % TFA in CH_2Cl_2 upon which the solution became yellow. Each mixture was stirred for 10 min and the resins were then washed with CH_2Cl_2 (2 × 1 min), MeOH (2 × 1 min) and CH_2Cl_2 (2 × 1 min). TFA treatment and washes were repeated until the solution remained colorless. Then, the N^{ε}-amino group was acylated with propiolic acid under the standard coupling conditions resulting in resins **1a-e** (Scheme 4.3).

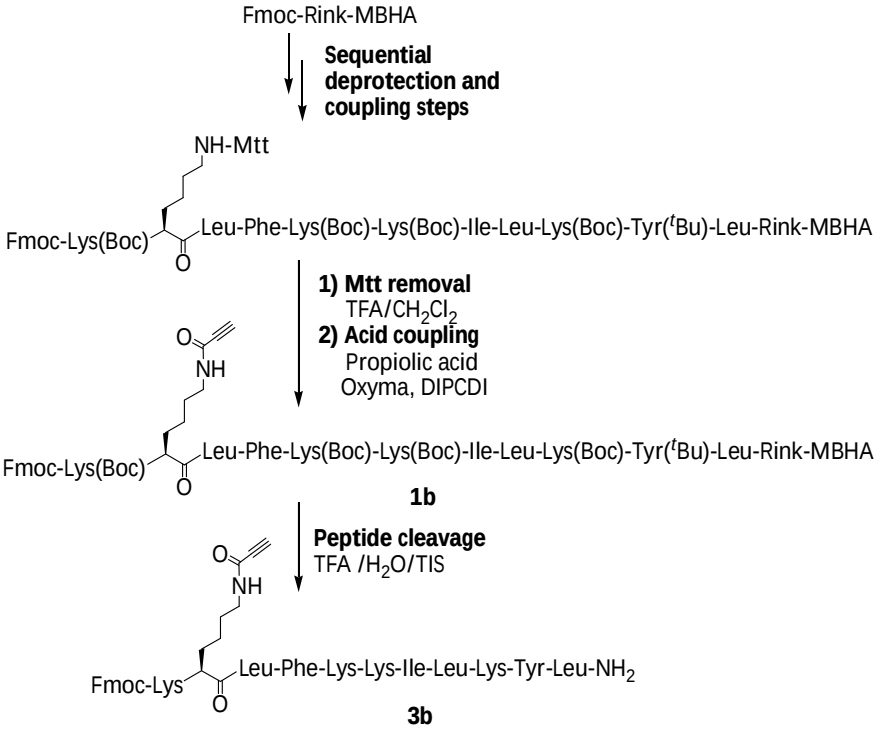

Scheme 4.3. *Synthesis of alkynyl resins* ***1a-e****, exemplified for* ***1b.***

Once the synthesis was performed, an aliquot of the resins **1a-e** was treated with TFA/H_2O/TIS (95:2.5:2.5) for 2 h and the resulting crude was analyzed by HPLC and mass spectrometry. As shown in Table 4.2, peptides **3a-e** were obtained in 77-84 % purity.

Table 4.2. *Sequences, retention times and purities on HPLC, and MS data of alkynyl peptides* ***3a-e.***

Resin	Peptide	Sequence[a]	t_R (min)[b]	Purity[c] (%)	ESI-MS
1a	**3a**	Fmoc-**X_a**KLFKKILKYL	8.32	79	1695.8 $[M+H]^+$
1b	**3b**	Fmoc-K**X_a**LFKKILKYL	7.93	77	1695.8 $[M+H]^+$
1c	**3c**	Fmoc-KKLF**X_a**KILKYL	8.10	80	1695.8 $[M+H]^+$
1d	**3d**	Fmoc-KKLFK**X_a**ILKYL	8.37	84	1695.8 $[M+H]^+$
1e	**3e**	Fmoc-KKLFKKIL**X_a**YL	7.79	80	1695.8 $[M+H]^+$

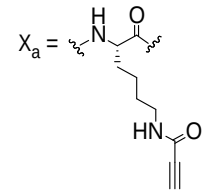

[a]All peptides are C-terminal amides.
[b]HPLC retention time using method A (see Materials and Methods).
[c]Percentage determined by HPLC at 220 nm from the crude reaction mixture.

The preparation of the alkynyl resin **2**, incorporating a propargylglycine at position 4 and required for the synthesis of **BP248-BP250**, was achieved following a strategy similar to that described above. An aliquot of resin **2** was cleaved affording peptide **4** in 80 % purity (t_R= 7.56 min, 1592.1 $[M+H]^+$) (Scheme 4.4).

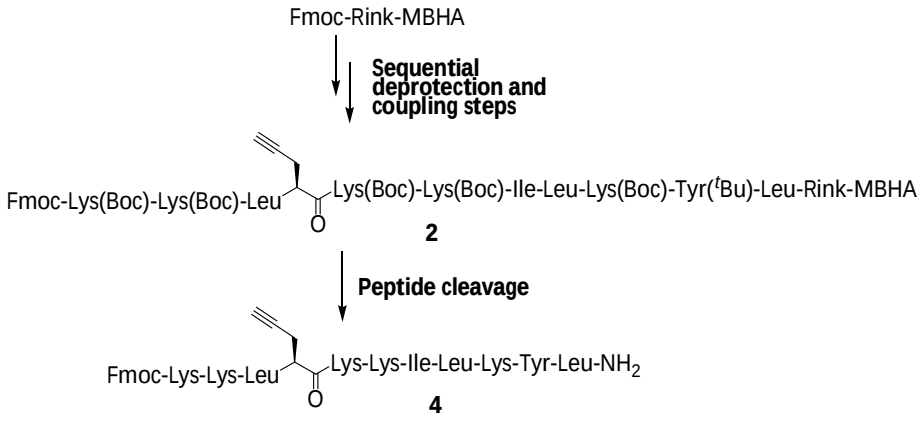

Scheme 4.4. *Synthesis of the alkynyl resin* ***2****.*

4.2.2. Synthesis of peptidotriazoles

Peptidotriazoles **BP238-BP247** were prepared by treating the corresponding alkynyl peptidyl resin **1a-e** with NaN_3 or Boc-Ahx(N_3)-OH (5 equiv) in presence of ascorbic acid (5 equiv) and CuI (5 equiv) in piperidine/DMF (2:8), standard conditions for the synthesis of a triazole ring. First, the reaction mixture was stirred for 5 h at room temperature. The resulting resins were washed with sodium *N,N*-diethyldithiocarbamate in order to remove residual divalent copper (Rijkers 2002), cleaved with TFA/H_2O/TIS (95:2.5:2.5), and crudes were analyzed by HPLC and mass spectrometry. These conditions led to the formation of the expected triazole ring and also to the Fmoc group removal, but the reaction was not completed (Scheme 4.5). Therefore, the reaction was carried out under the same conditions, but by stirring the reaction mixture overnight at room temperature. In this case, the desired peptidotriazoles were obtained in 71-92 % purity (Table 4.3).

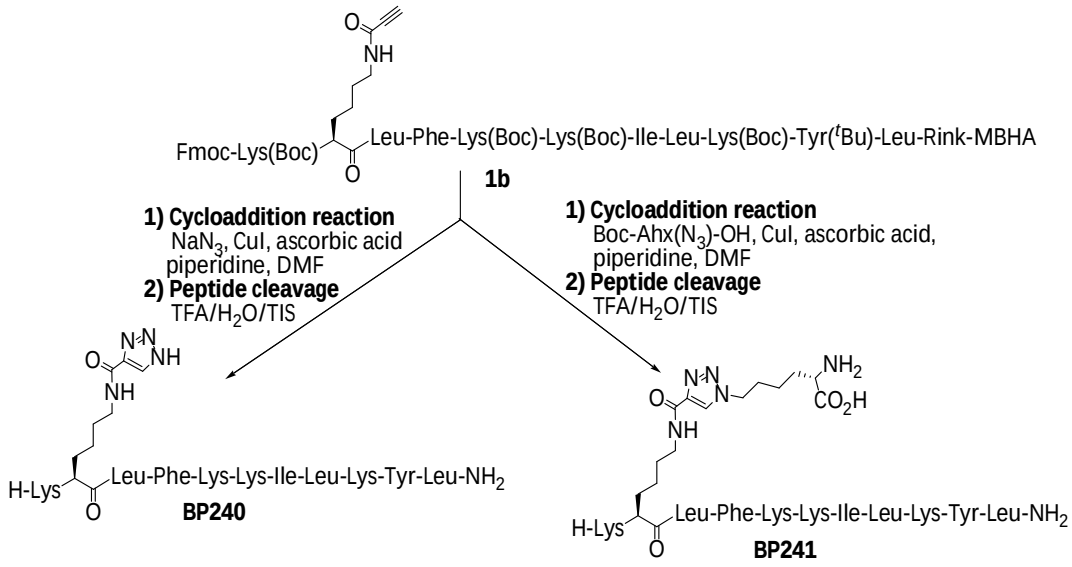

Scheme 4.5. *General strategy for the synthesis of peptidotriazoles* ***BP238-BP247****, exemplified for* ***BP240*** *and* ***BP241****.*

Table 4.3. *Sequences, retention times and purities on HPLC, and HRMS data of peptides* ***BP238-BP247****.*

Peptide	Sequence[a]	t_R (min)[b]	Purity (%)[c]	HRMS
BP238	**X_a**KLFKKILKYL	17.70	84	506.0014 $[M+3H]^{3+}$, 758.4946 $[M+2H]^{2+}$
BP239	**X_b**KLFKKILKYL	17.33	73	549.0280 $[M+3H]^{3+}$, 823.0338 $[M+2H]^{2+}$
BP240	K**X_a**LFKKILKYL	17.94	84	506.0008 $[M+3H]^{3+}$, 758.4940 $[M+2H]^{2+}$
BP241	K**X_b**LFKKILKYL	17.67	82	549.0295 $[M+3H]^{3+}$, 823.0358 $[M+2H]^{2+}$
BP242	KKLF**X_a**KILKYL	17.85	79	506.0025 $[M+3H]^{3+}$
BP243	KKLF**X_b**KILKYL	17.48	92	549.0300 $[M+3H]^{3+}$, 823.0352 $[M+2H]^{2+}$
BP244	KKLFK**X_a**ILKYL	17.85	84	506.0015 $[M+3H]^{3+}$
BP245	KKLFK**X_b**ILKYL	17.43	81	549.0288 $[M+3H]^{3+}$
BP246	KKLFKKIL**X_a**YL	17.51	72	506.0034 $[M+3H]^{3+}$, 758.4979 $[M+2H]^{2+}$
BP247	KKLFKKIL**X_b**YL	17.16	71	549.0289 $[M+3H]^{3+}$, 823.0373 $[M+2H]^{2+}$

[a]All peptides are C-terminal amides.
[b]HPLC retention time using method D (see Materials and Methods).
[c]Percentage determined by HPLC at 220 nm from the crude reaction mixture.

Similarly, peptidotriazoles **BP248-BP250** were obtained from the alkynyl resin **2** by treatment with NaN_3, Boc-Ahx(N_3)-OH and BnN_3, respectively, under stirring overnight at room temperature (Scheme 4.6). After cleavage, peptidotriazoles were obtained in 65-91 % purity (Table 4.4).

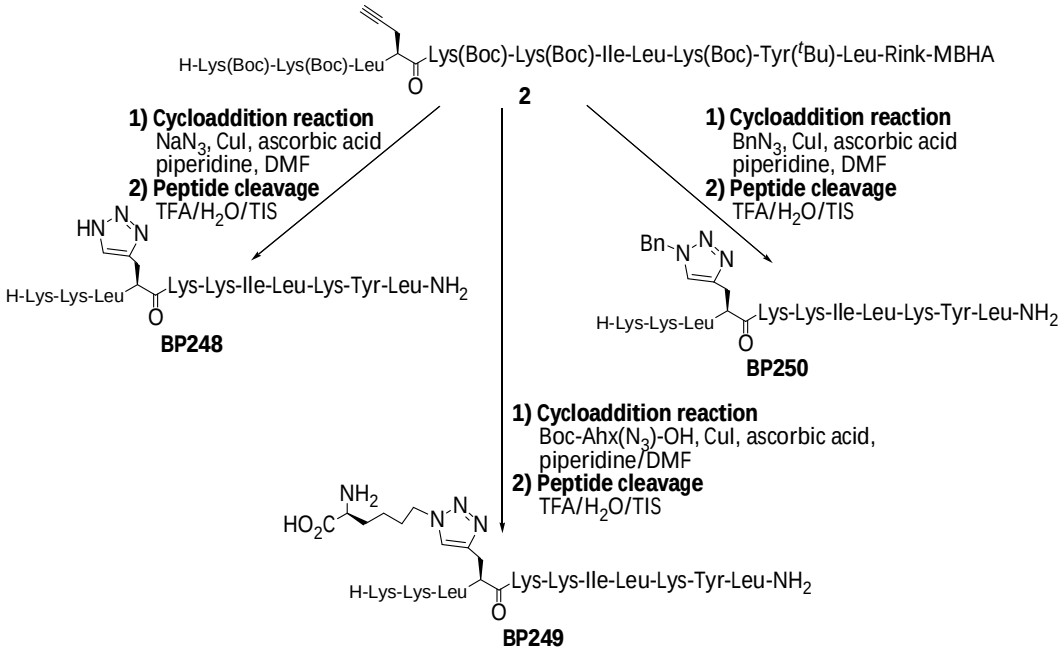

Scheme 4.6. *Synthesis of peptidotriazoles* ***BP248-BP250****.*

Table 4.4. *Sequences, retention times and purities on HPLC, and HRMS data of peptides* ***BP248-BP250****.*

Peptide	Sequence[a]	t_R (min)[c]	Purity (%)[d]	HRMS
BP248	KKL**X$_c$**KKILKYL 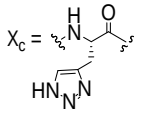	15.82	76	471.3279 $[M+3H]^{3+}$, 706.4847 $[M+2H]^{2+}$
BP249	KKL**X$_d$**KKILKYL 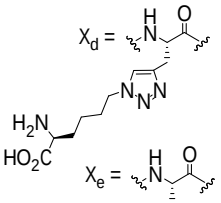	15.69	65	514.3538 $[M+3H]^{3+}$, 771.0215 $[M+2H]^{2+}$
BP250	KKL**X$_e$**KKILKYL 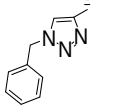	16.91	91	376.2594 $[M+3H]^{4+}$, 501.3431 $[M+2H]^{3+}$

[a]All peptides are C-terminal amides.
[b]HPLC retention time using method D (see Materials and Methods).
[c]Percentage determined by HPLC at 220 nm from the crude reaction mixture.

4.3. Antibacterial activity against plant pathogenic bacteria

Peptidotriazoles were tested for *in vitro* growth inhibition of *E. amylovora*, *P. syringae* and *X. vesicatoria* at 1.6, 3.1, 6.2, 12.5, 25, and 50 μM (Table 4.5). All these tests were performed by Dr. Esther Badosa of the Plant Pathology group at the UdG. To facilitate the discussion, peptidotriazoles (**BP238-BP250**) have been denoted as Lys^n(CO-Tr), Lys^n(CO-Tr-Ahx), Ala^4(Tr), Ala^4(Tr-Ahx) or Ala^4(Tr-Bn), where *n* is the position of the Lys residue that bears the triazole ring, Tr stands for an unsubstituted triazole, Tr-Ahx corresponds to a triazole substituted with a 2-aminohexanoic acid, and Tr-Bn is a triazole substituted with a benzyl group.

The evaluation of the antibacterial activity showed that, in general, peptidotriazoles **BP238-BP250** incorporating a triazole onto a side-chain of a Phe or a Lys were considerably active. They exhibited similar activity to the parent peptide, with eleven out of thirteen sequences displaying MIC <12.5 μM against the three pathogens. A different susceptibility of bacteria to the two sets of peptidotriazoles **BP238-BP247** and **BP248-BP250** was observed. This differential susceptibility of bacteria to a given

peptide has been attributed to differences in the membrane components of the target microorganism, e.g. charge and lipid composition, that would influence rates of binding of peptides to the membrane (Huang 2000).

Peptidotriazoles **BP238-BP247** incorporating a Lys residue modified with a triazole exhibited higher activity against *X. vesicatoria* and *E. amylovora* than against *P. syringae*. Nine out of ten sequences displayed MIC values ranging from 1.6 to 6.2 μM against *X. vesicatoria*, **BP245** being the most active sequence. This peptide incorporated a triazole bearing an Ahx moiety at residue 6 (Lys^6(CO-Tr-Ahx)) (MIC of 1.6-3.1 μM), and showed a higher activity than **BP100** (MIC of 3.1-6.2 μM). **BP247** (Lys^9(CO-Tr-Ahx)) was the least active against this pathogen with a MIC of 6.2-12.5 μM. Against *E. amylovora,* seven peptides displayed MIC values ranging from 1.6 to 6.2 μM, **BP246** (Lys^9(CO-Tr)) and **BP247** (Lys^9(CO-Tr-Ahx)) being more active than **BP100** (MIC of 1.6-3.1 vs 3.1-6.2 μM). **BP240** (Lys^2(CO-Tr)), **BP241** (Lys^2(CO-Tr-Ahx)) and **BP242** (Lys^5(CO-Tr)) showed the lowest activity (MIC of 6.2-12.5 μM). Three peptides, **BP243** (Lys^5(CO-Tr-Ahx)), **BP244** (Lys^6(CO-Tr)) and **BP247** (Lys^9(CO-Tr-Ahx)), exhibited MIC values ranging from 3.1-6.2 μM against *P. syringae*, and were as active as **BP100**.

Analysis of these results suggested that the introduction of a substituent in the triazole ring did not significantly influence the antibacterial activity. In fact, the sequences bearing an unsubstituted triazole displayed MIC values similar to that of the corresponding counterpart bearing a triazole substituted with an Ahx moiety. However, the more sensitive positions to the introduction of the substituent were Lys^5, Lys^6 and Lys^9 resulting in peptides **BP243**, **BP245** and **BP247** with higher activity than the unsubstituted analogue, **BP242**, **BP244** and **BP246**. Moreover, the activity of all these derivatives did not differ from that of the parent sequence **BP100**, suggesting that the triazole ring does not modify the peptide hydrophilicity.

Peptidotriazoles **BP248-BP250**, bearing a triazole instead of a benzene ring at the Phe^4 residue in **BP100**, displayed a higher activity against *P. syringae* (MIC of 1.6-25 μM) than against the other two pathogens (MIC of 3.1- >50 μM). **BP250** (Ala^4(Tr-Bn)) was the most active of these three sequences (MIC of 1.6-12.5 μM), being more active than **BP100** against *P. syringae* (MIC of 1.6-3.1 vs 3.1-6.2 μM). **BP248** (Ala^4(Tr)) showed a

slightly lower activity (MIC of 3.1-25 μM) as compared to **BP250** and was as active as **BP100** against *P. syringae* (MIC of 3.1-6.2 μM). The analogue incorporating an Ahx moiety substituent at the triazole ring, **BP249** (Ala^4(Tr-Ahx)), was the least active with MIC values ranging from 12.5 to >50 μM. These results pointed out that the hydrophobicity at this position is crucial because the most active analogue had the benzyl group as a triazole ring substituent, while when the ring its unsubstituted or it is substituted with a more polar group the activity decreases.

Table 4.5. *Antibacterial activity (MIC) of the linear peptidotriazoles.*

Peptide	Sequence[a]	Notation[b]	MIC (μM)		
			X. vesicatoria	*E. amylovora*	*P. syringae*
BP100	KKLFKKILKYL	-	3.1-6.2	3.1-6.2	3.1-6.2
BP238	**X$_a$**KLFKKILKYL	Lys^1(CO-Tr)	3.1-6.2	3.1-6.2	6.2-12.5
BP239	**X$_b$**KLFKKILKYL	Lys^1(CO-Tr-Ahx)	3.1-6.2	3.1-6.2	6.2-12.5
BP240	K**X$_a$**LFKKILKYL	Lys^2(CO-Tr)	3.1-6.2	6.2-12.5	6.2-12.5
BP241	K**X$_b$**LFKKILKYL	Lys^2(CO-Tr-Ahx)	3.1-6.2	6.2-12.5	6.2-12.5
BP242	KKLF**X$_a$**KILKYL	Lys^5(CO-Tr)	3.1-6.2	6.2-12.5	6.2-12.5
BP243	KKLF**X$_b$**KILKYL	Lys^5(CO-Tr-Ahx)	3.1-6.2	3.1-6.2	3.1-6.2
BP244	KKLFK**X$_a$**ILKYL	Lys^6(CO-Tr)	3.1-6.2	3.1-6.2	3.1-6.2
BP245	KKLFK**X$_b$**ILKYL	Lys^6(CO-Tr-Ahx)	1.6-3.1	3.1-6.2	6.2-12.5
BP246	KKLFKKIL**X$_a$**YL	Lys^9(CO-Tr)	3.1-6.2	1.6-3.1	6.2-12.5
BP247	KKLFKKIL**X$_b$**YL	Lys^9(CO-Tr-Ahx)	6.2-12.5	1.6-3.1	3.1-6.2
BP248	KKL**X$_c$**KKILKYL	Ala^4(Tr)	6.2-12.5	12.5-25	3.1-6.2
BP249	KKL**X$_d$**KKILKYL	Ala^4(Tr-Ahx)	25-50	>50	12.5-25
BP250	KKL**X$_e$**KKILKYL	Ala^4(Tr-Bn)	6.2-12.5	3.1-6.2	1.6-3.1

[a]All peptides are C-terminal amides.

[b]The notation defines the variation at the X position indicated as superscript. For peptides **BP238**-**BP250** the side-chain substituent of the Lys or the Ala residue is in parenthesis being: Tr, unsubstituted triazole; Tr-Ahx, triazole bearing a 2-aminohexanoic acid; Tr-Bn, triazole bearing a benzyl group.

4.4. Antifungal activity

The antifungal activity of the peptidotriazoles was screened *in vitro* against *P. expansum* and *F. oxysporum* at 6.2, 12.5, 25 and 50 μM (Table 4.6). All these tests were performed by Dr. Esther Badosa of the Plant Pathology group at the UdG.

Table 4.6. *Antifungal activity (MIC) of the linear peptidotriazoles.*

Peptide	Sequence[a]	Notation[b]	MIC (μM)	
			P. expansum	*F. oxysporum*
BP100	KKLFKKILKYL	-	25-50	<6.2
BP238	**X_a**KLFKKILKYL	Lys^1(CO-Tr)	25-50	<6.2
BP239	**X_b**KLFKKILKYL	Lys^1(CO-Tr-Ahx)	25-50	<6.2
BP240	K**X_a**LFKKILKYL	Lys^2(CO-Tr)	25-50	<6.2
BP241	K**X_b**LFKKILKYL	Lys^2(CO-Tr-Ahx)	25-50	<6.2
BP242	KKLF**X_a**KILKYL	Lys^5(CO-Tr)	25-50	6.2-12.5
BP243	KKLF**X_b**KILKYL	Lys^5(CO-Tr-Ahx)	25-50	<6.2
BP244	KKLFK**X_a**ILKYL	Lys^6(CO-Tr)	25-50	<6.2
BP245	KKLFK**X_b**ILKYL	Lys^6(CO-Tr-Ahx)	25-50	<6.2
BP246	KKLFKKIL**X_a**YL	Lys^9(CO-Tr)	>50	6.2-12.5
BP247	KKLFKKIL**X_b**YL	Lys^9(CO-Tr-Ahx)	>50	6.2-12.5
BP248	KKL**X_c**KKILKYL	Ala^4(Tr)	>50	6.2-12.5
BP249	KKL**X_d**KKILKYL	Ala^4(Tr-Ahx)	>50	6.2-12.5
BP250	KKL**X_e**KKILKYL	Ala^4(Tr-Bn)	>50	6.2-12.5

[a]All peptides are C-terminal amides.

[b]The notation defines the variation at the X position indicated as superscript. For peptides **BP238**-**BP250** the side-chain substituent of the Lys or the Ala residue is in parenthesis being: Tr, unsubstituted triazole; Tr-Ahx, triazole bearing a 2-aminohexanoic acid; Tr-Bn, triazole bearing a benzyl group.

The antifungal activity of the peptidotriazoles correlated with that previously reported for structurally related undecapeptides, which showed that *F. oxysporum* was more susceptible than *P. expansum* to these compounds (Badosa 2009). For the latter, only eight sequences showed MIC values ranging from 25 to 50 μM while for *F. oxysporum* seven sequences displayed MIC values < 6.2 μM and six sequences with MICs within 6.2 and 12.5 μM.

Peptidotriazoles **BP238-BP247**, bearing a triazole at a Lys side chain, were more active than those including a triazole ring at position 4 (**BP248-BP250**), being the best derivatives as active as **BP100**. Moreover, the incorporation of a substituent in the triazole ring did not influence the antifungal activity.

4.5. Hemolytic activity

The toxicity to eukaryotic cells of peptidotriazoles was determined as the ability to lyse erythrocytes in comparison to melittin. Percent hemolysis at 50 and 150 μM is shown in Table 4.7. All these tests were performed by Dr. Esther Badosa of the Plant Pathology group at the UdG.

Peptidotriazole cytotoxicity was also strongly influenced by the amino acid (Lys or Phe) that was modified with a triazole as well as by the absence or presence of a substituent in this heterocyclic ring. In general, peptidotriazoles resulting from the modification of the Phe^4 were less hemolytic than those obtained from the incorporation of a triazole at a Lys side chain. For the former (**BP248-BP250**), the replacement of the benzene ring by a triazole, either substituted or unsubstituted, rendered sequences with a lower hydrophobic character than that of **BP100**, being not hemolytic even at 150 μM.

For the derivatives incorporating a triazole at a Lys side-chain (**BP238-BP247**), the least hemolytic sequences were those bearing an Ahx substituent (**BP239**, **BP241**, **BP243**, **BP245**, and **BP247**) (1-21 % at 50 μM). In this case, the presence of this substituent also decreases the hydrophobic character of the triazole moiety. However, these sequences were more hemolytic than **BP100** suggesting that the triazole ring confers a higher hydrophobic character than the free ε-amino group of a Lys. These results are in good agreement with previous studies on AMPs reporting that an increase of the peptide hydrophobicity is related to an increase in the cytotoxicity (Blondelle 2000; Oh 2000).

Table 4.7. *Cytotoxicity of linear peptidotriazoles.*

Peptide	Sequence[a]	Notation[b]	Hemolysis[c] (%)		
			50 µM	150 µM	250 µM
BP100	KKLFKKILKYL	-	3 ± 0.1	22 ± 2.8	54 ± 0.1
BP238	**X_a**KLFKKILKYL	Lys^1(CO-Tr)	23 ± 2.6	43 ± 4.0	54 ± 15
BP239	**X_b**KLFKKILKYL	Lys^1(CO-Tr-Ahx)	14 ± 1.2	30 ± 1.2	42 ± 0.3
BP240	K**X_a**LFKKILKYL	Lys^2(CO-Tr)	34 ± 2.1	57 ± 1.2	25 ± 5
BP241	K**X_b**LFKKILKYL	Lys^2(CO-Tr-Ahx)	1 ± 1	6 ± 1.2	39 ± 0.6
BP242	KKLF**X_a**KILKYL	Lys^5(CO-Tr)	39 ± 2.9	62 ± 5.5	73 ± 0.3
BP243	KKLF**X_b**KILKYL	Lys^5(CO-Tr-Ahx)	10 ± 1.5	22 ± 4.7	34 ± 4
BP244	KKLFK**X_a**ILKYL	Lys^6(CO-Tr)	37 ± 0.9	73 ± 2.0	71 ± 5
BP245	KKLFK**X_b**ILKYL	Lys^6(CO-Tr-Ahx)	21 ± 0.5	54 ± 1.2	78 ± 4
BP246	KKLFKKIL**X_a**YL	Lys^9(CO-Tr)	48 ± 1.3	75 ± 4.7	75 ± 1
BP247	KKLFKKIL**X_b**YL	Lys^9(CO-Tr-Ahx)	20 ± 0.7	38 ± 3.4	49 ± 2
BP248	KKL**X_c**KKILKYL	Ala^4(Tr)	1 ± 0.1	1.3 ± 0.2	0.4 ± 0.2
BP249	KKL**X_d**KKILKYL	Ala^4(Tr-Ahx)	0 ± 0.2	0 ± 0.7	0 ± 0.3
BP250	KKL**X_e**KKILKYL	Ala^4(Tr-Bn)	0 ± 0.1	0 ± 0.5	2 ± 0.7

[a]All peptides are C-terminal amides.

[b]The notation defines the variation at the X position indicated as superscript. For peptides **BP238**-**BP250** the side-chain substituent of the Lys or the Ala residue is in parenthesis being: Tr, unsubstituted triazole; Tr-Ahx, triazole bearing a 2-aminohexanoic acid; Tr-Bn, triazole bearing a benzyl group.

[c]Percent hemolysis at 50, 150 and 250 µM plus confidence interval ($\alpha = 0.05$).

Peptides with an optimal balance between antibacterial and hemolytic activities were **BP238**, **BP239**, **BP243**, **BP245**, **BP247**, and **BP250**. Among them, **BP238**, **BP239**, **BP243**, and **BP245** also showed high antifungal activity (Table 4.8).

Table 4.8. *Summary table of the peptide with an optimal biological balance.*

Peptide	MIC (μM)					Hemolysis[a]
	Xv	*Ea*	*Ps*	*Pe*	*Fo*	(%)
BP100	3.1-6.2	3.1-6.2	3.1-6.2	25-50	<6.2	54 ±0.1
BP238	3.1-6.2	3.1-6.2	6.2-12.5	25-50	<6.2	54 ±15
BP239	3.1-6.2	3.1-6.2	6.2-12.5	25-50	<6.2	42 ±0.3
BP243	3.1-6.2	3.1-6.2	3.1-6.2	25-50	<6.2	34 ±4
BP245	1.6-3.1	3.1-6.2	6.2-12.5	25-50	<6.2	78 ±4
BP247	6.2-12.5	1.6-3.1	3.1-6.2	>50	6.2-12.5	49 ±2
BP250	6.2-12.5	3.1-6.2	1.6-3.1	>50	6.2-12.5	2 ±0.7

[b]*Xv, Xanthomonas vesicatoria; Ea, Erwinia amylovora; Pss, Pseudomonas syringae; Pe, Penicillium expansum; Fo, Fusarium oxysporum*.

[a]Percent hemolysis at 250 μM plus confidence interval (α = 0.05).

4.6. Susceptibility to protease degradation

The susceptibility of the peptides to proteolysis was studied by exposure to proteinase K and degradation was monitored by HPLC over time (Table 4.9). The modification of Lys^5 and Lys^6 with an unsubstituted or substituted triazole as well as the incorporation of a triazole substituted with an Ahx moiety at Lys^9 afforded the least stable peptidotriazoles (**BP242-BP245** and **BP247**). **BP240** (Lys^2(CO-Tr)), **BP241** (Lys^2(CO-Tr-Ahx)), **BP246** (Lys^9(CO-Tr)), and **BP250** (Ala^4(Tr-Bn)) displayed higher stability than B**P100** (55-64 % degradation). The rest of sequences **BP238** (Lys^1(CO-Tr)), **BP239** (Lys^1(CO-Tr-Ahx)), **BP248** (Ala^4(Tr)), **BP249** (Ala^4(Tr-Ahx)) showed similar protease susceptibility than that of the parent peptide **BP100**, after 1 h incubation only 70-79 % degradation was observed. Peptidotriazoles with a good biological profile, **BP238**, **BP239**, and **BP250**, also showed good stability towards protease degradation. Especially noteworthy is **BP250** that is active against the three bacteria, not hemolytic and more stable to proteases than **BP100**.

Table 4.9. *Stability against protease degradation of linear peptidotriazoles.*

Peptide	Sequence[a]	Notation[b]	Digestion[c] (%)
BP100	KKLFKKILKYL	-	75
BP238	**X_a**KLFKKILKYL	Lys^1(CO-Tr)	79
BP239	**X_b**KLFKKILKYL	Lys^1(CO-Tr-Ahx)	73
BP240	K**X_a**LFKKILKYL	Lys^2(CO-Tr)	64
BP241	K**X_b**LFKKILKYL	Lys^2(CO-Tr-Ahx)	59
BP242	KKLF**X_a**KILKYL	Lys^5(CO-Tr)	91
BP243	KKLF**X_b**KILKYL	Lys^5(CO-Tr-Ahx)	100
BP244	KKLFK**X_a**ILKYL	Lys^6(CO-Tr)	93
BP245	KKLFK**X_b**ILKYL	Lys^6(CO-Tr-Ahx)	97
BP246	KKLFKKIL**X_a**YL	Lys^9(CO-Tr)	55
BP247	KKLFKKIL**X_b**YL	Lys^9(CO-Tr-Ahx)	91
BP248	KKL**X_c**KKILKYL	Ala^4(Tr)	79
BP249	KKL**X_d**KKILKYL	Ala^4(Tr-Ahx)	70
BP250	KKL**X_e**KKILKYL	Ala^4(Tr-Bn)	62

[a]All peptides are C-terminal amides.
[b]The notation defines the variation at the X position indicated as superscript. For peptides **BP238**-**BP250** the side-chain substituent of the Lys or the Ala residue is in parenthesis being: Tr, unsubstituted triazole; Tr-Ahx, triazole bearing a 2-aminohexanoic acid; Tr-Bn, triazole bearing a benzyl group.
[c]Percentage of degraded peptide calculated by HPLC.

4.7. Cytotoxicity of peptidotriazoles against tobacco leaves

In this study, we further examined the toxicity of all peptidotriazoles to tobacco leaves (Makovitzki 2007). This toxicity was assessed by infiltrating 100 μL of a 25 and 50 μM solution of each compound into the mesophylls of the leaves using a syringe without a needle (Figure 4.1). Control infiltrations with water (negative control) or the nonspecific and nonselective peptide mellitin (positive control) at the same molar concentration were performed. Three infiltrations were performed for each peptide at each concentration. The appearance of symptoms on the leaves was followed for 48 h after infiltration. After this period, a brown necrotic area was observed for melittin positive control, which severely damaged the leaf mesophyll tissues. In contrast, no

necrosis could be detected in the mesophylls of the leaves that were infiltrated with the peptidotriazoles, thus, these compounds did not induce any phytotoxicity. Two representative examples, **BP242** and **BP238**, are shown in Figure 4.1.

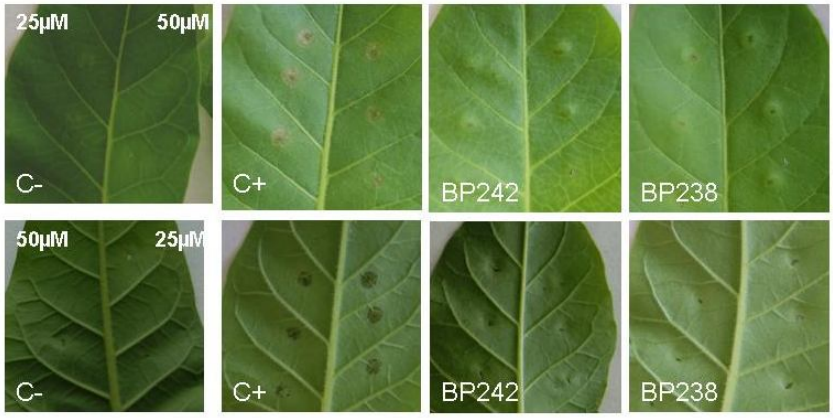

Figure 4.1. *Evaluation of cytotoxicity on tobacco leaves.*

In summary, we have designed and synthesized **BP100** analogues containing a triazole ring. The introduction of this moiety at a Lys or a Phe side chain has led to the identification of sequences active against *X. vesicatoria*, *E. amylovora*, *P. syringae*, and *F. oxysporum* with low hemolytic activity, high stability to protease digestion and no phytotoxicity, being good candidates to design new antimicrobial agents.

5. STUDIES FOR THE SYNTHESIS OF MULTIVALENT PEPTIDES DERIVED FROM BPC194

Multivalent peptides have been reported to be more active than the corresponding monomers due to the synergy of monomeric units (Liu 2006). Based on this, we envisioned that the biological activity of the antimicrobial lead cyclic peptide **BPC194** (Figure 5.1) could be enhanced by the preparation of multivalent derivatives.

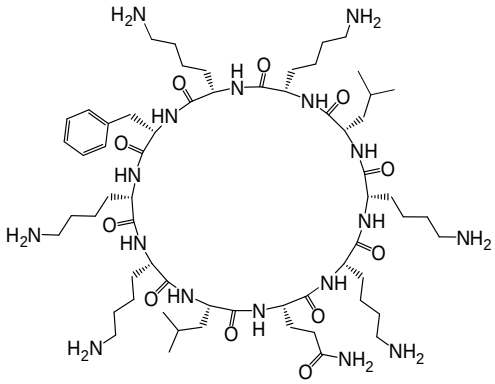

Figure 5.1. *Structure of peptide* ***BPC194****.*

One strategy to prepare multivalent derivatives of **BPC194** would involve the linkage of peptide units through a 1,2,3-triazole ring. In particular, in this work we studied the synthesis of **BPC194** analogues incorporating a 1,2,3-triazole ring at the side-chain of a selected residue (Figure 5.2). This approach would serve as a model system for the synthesis of multivalent peptides. Afterwards, for the synthesized cyclic peptidotriazoles, we studied the antibacterial activity against phytopathogenic and human bacteria and biocontrol agents, and the hemolytic activity.

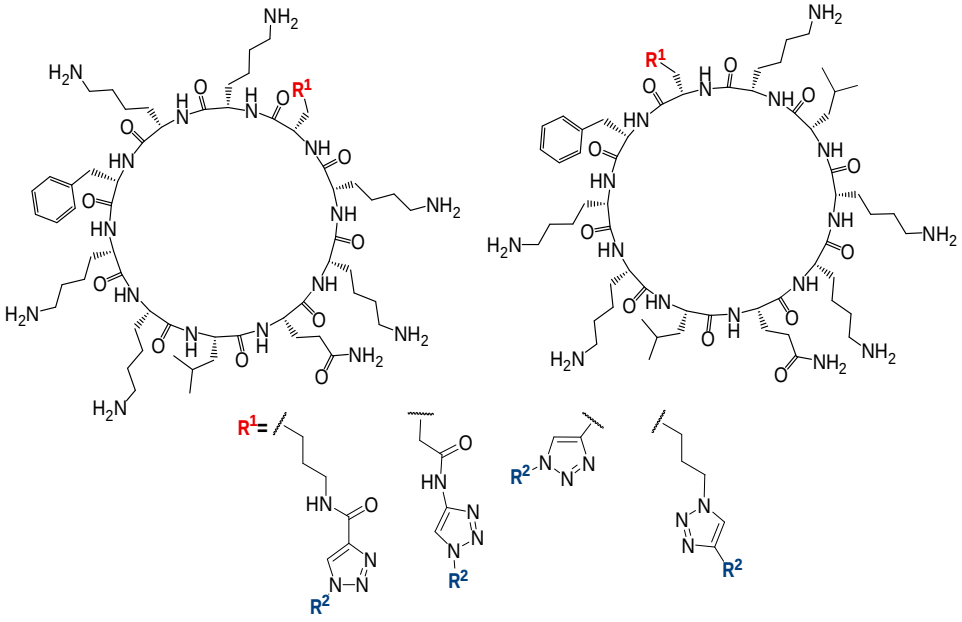

R^2= H, alkyl, aryl or peptidyl

Figure 5.2. *Structure of* ***BPC194*** *derivatives.*

5.1. Design and retrosynthetic analysis

Cyclic peptidotriazoles were designed based on the structure of **BPC194** c(Lys[1]-Lys-Leu[3]-Lys-Lys[5]-Phe-Lys[7]-Lys-Leu[9]-Gln) by replacing Leu[3] or Lys[5] for residues incorporating a triazole at the side-chain. The synthesis of the cyclic peptidotriazoles was planned following two different strategies. In the first strategy (A), the cycloaddition reaction would be carried out between a resin-bound alkyne and an azide in solution (Scheme 5.1). In the second strategy (B), the formation of the triazole would involve the reaction of a resin-bound azide and an alkyne in solution (Scheme 5.2). The retrosynthetic analysis of cyclic peptidotriazoles incorporating a triazole ring at the side-chain of the residue at position 3 is depicted in Scheme 5.1 and 5.2. A similar retrosynthesis could be drawn for cyclic peptidotriazoles bearing a triazole at the residue of position 5.

According to strategy A, the alkynyl peptidyl resins that we planned to prepare contained:

- A propargylglycine at position 3 (**resin 5**) or at position 5 (**resin 6**) (Scheme 5.1A).
- A Gln($CH_2C\equiv CH$) residue at position 3 (**resin 7**) (Scheme 5.1B).
- A Lys(COC$\equiv$CH) residue at position 3 (**resin 8**) or at position 5 (**resin 9**) (Scheme 5.1C).

According to strategy B, the azido peptidyl resins that we planned to prepare contained Nle(ε-N_3) at position 3 (resin **10**) or at position 5 (resin **11**) (Scheme 5.2).

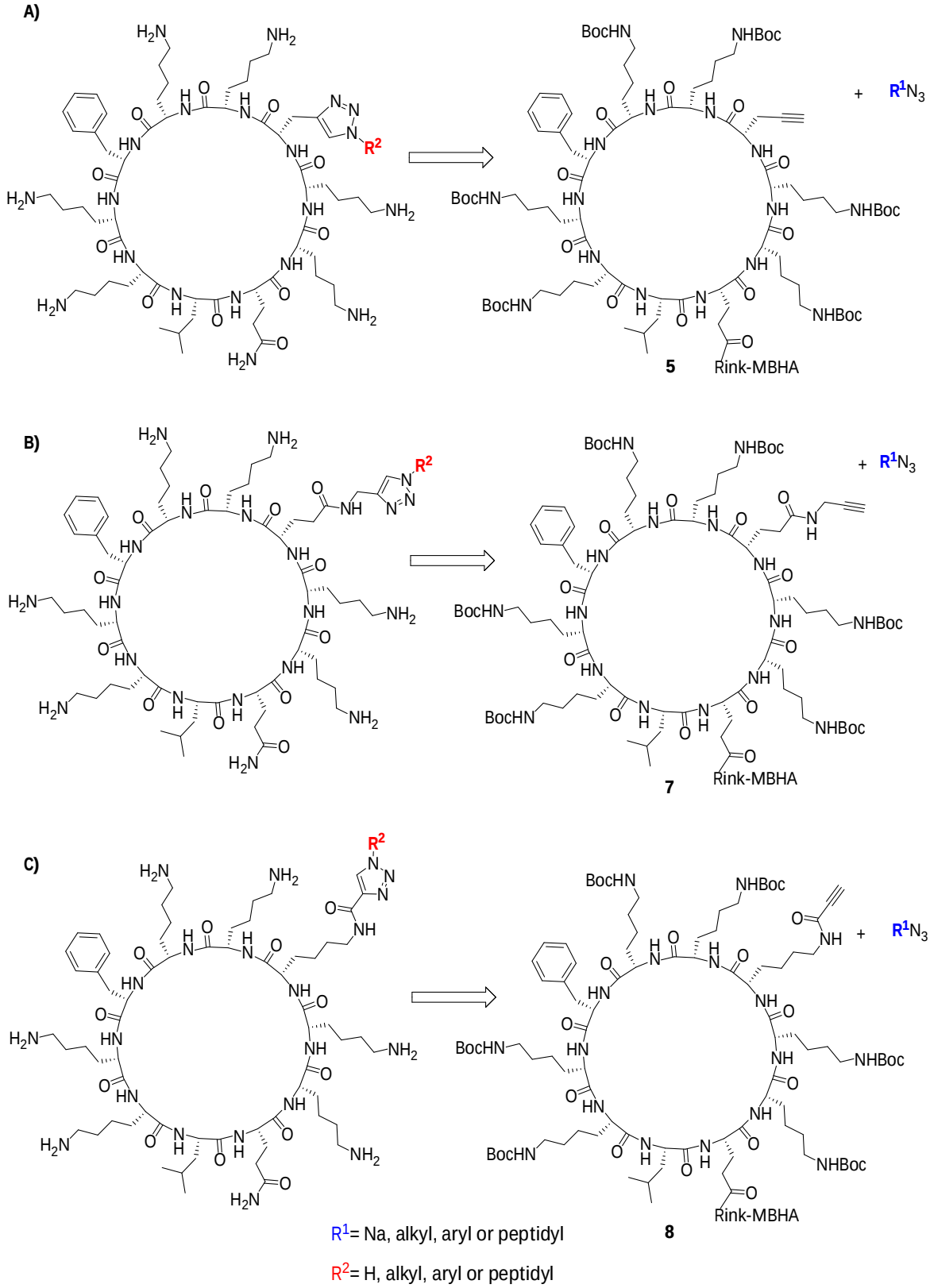

Scheme 5.1. *Retrosynthesis of cyclic peptidotriazoles from an alkynyl peptidyl resin (**strategy A**).*

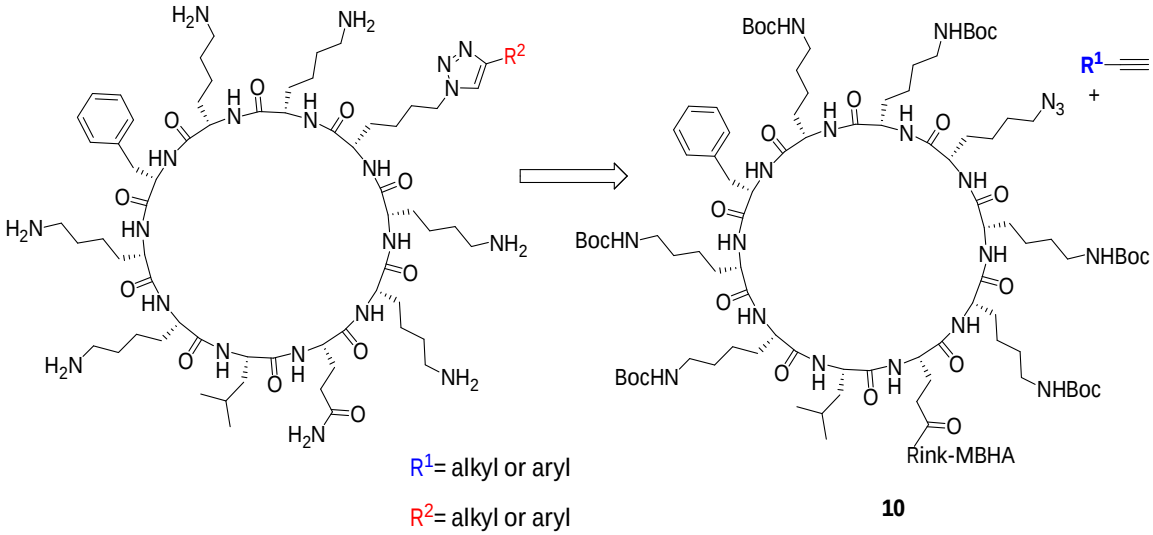

Scheme 5.2. *Retrosynthesis of cyclic peptidotriazoles from an azido peptidyl resin (**strategy B**).*

5.2. Synthesis of alkynyl and azido cyclic peptidyl resins

The general strategy for the solid-phase synthesis of the alkynyl and azido cyclic peptidyl resins involved the preparation of a linear peptidyl sequence followed by head-to-tail cyclization (Scheme 5.3). A three dimensional orthogonal Fmoc/Boc/Al strategy was used. First, Fmoc-Glu-OAl was coupled to a Rink-MBHA resin through its side-chain carboxylic group. The linear sequence was then elongated by sequential Fmoc removal and coupling steps. Fmoc removal was accomplished by treatments with piperidine/DMF (3:7). Couplings of the Fmoc-amino acids (4 equiv) were mediated by Oxyma pure (4 equiv) and DIPCDI (4 equiv) in DMF for 1 h. Once the protected linear sequence was completed, the allyl group was removed by treatment with $Pd(PPh_3)_4$ in $CHCl_3$/NMM/AcOH (3:2:1) for 3 h. Following Fmoc removal, cyclization was performed using PyOxim (5 equiv), Oxyma (5 equiv) and DIEA (10 equiv) in NMP for 24 h.

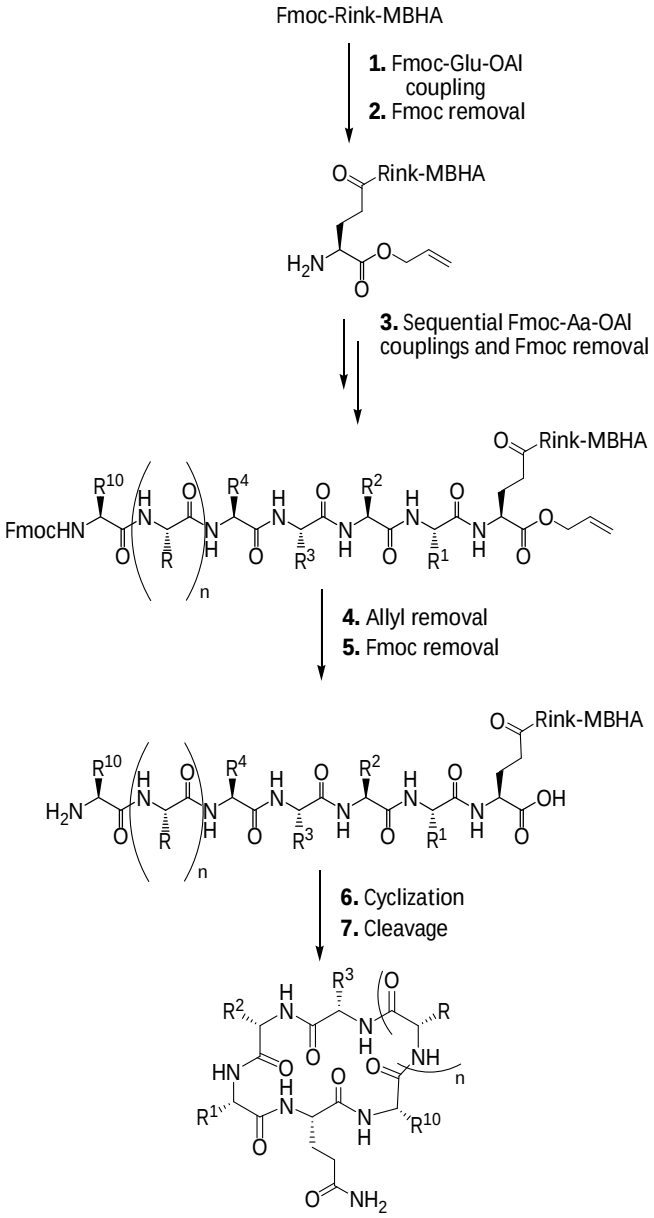

Scheme 5.3. *General strategy for the solid-phase synthesis of cyclic decapeptides.*

5.2.1. Synthesis of alkynyl cyclic peptidyl resins 5-9 (strategy A)

The synthesis of alkynyl peptidyl resins **5**-**9** (Scheme 5.1) followed the general strategy described above. For the resins **5** and **6**, the assembly of the linear peptidyl resin would required the use of Fmoc-Prg-OH at positions 3 and 5, respectively (Scheme 5.4). For resin **7** or Fmoc-Gln($CH_2C\equiv CH$)-OH was needed as alkynyl-functionalized residue (Scheme 5.5). Fmoc-Gln($CH_2C\equiv CH$)-OH is not commercially available but could be easily prepared from Fmoc-Glu-O^{t}Bu. Moveover, since the synthetic strategy of the cyclic peptides involves the allyl group removal in presence of the alkynyl function, we

decided to study the stability of this functional group under the conditions for the allyl cleavage.

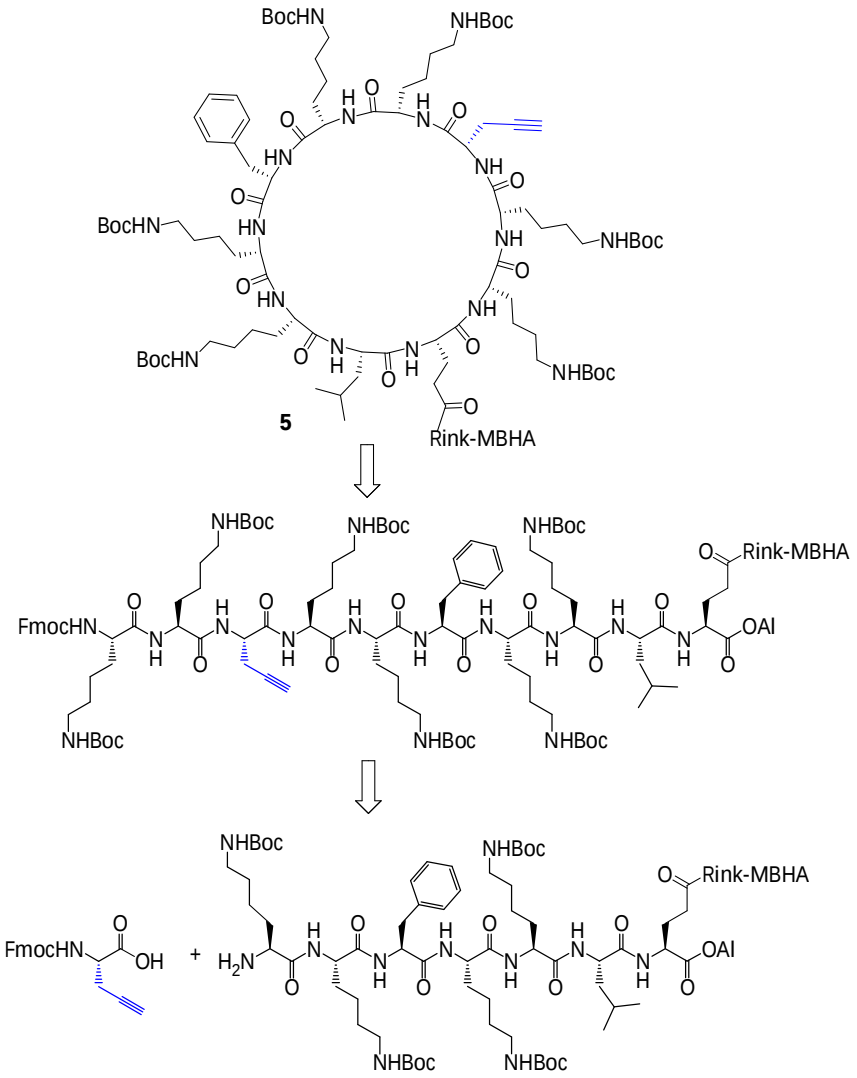

Scheme 5.4. *Retrosynthesis of the alkynyl peptidyl resins* ***5*** *and* ***6****, exemplified for* ***5****.*

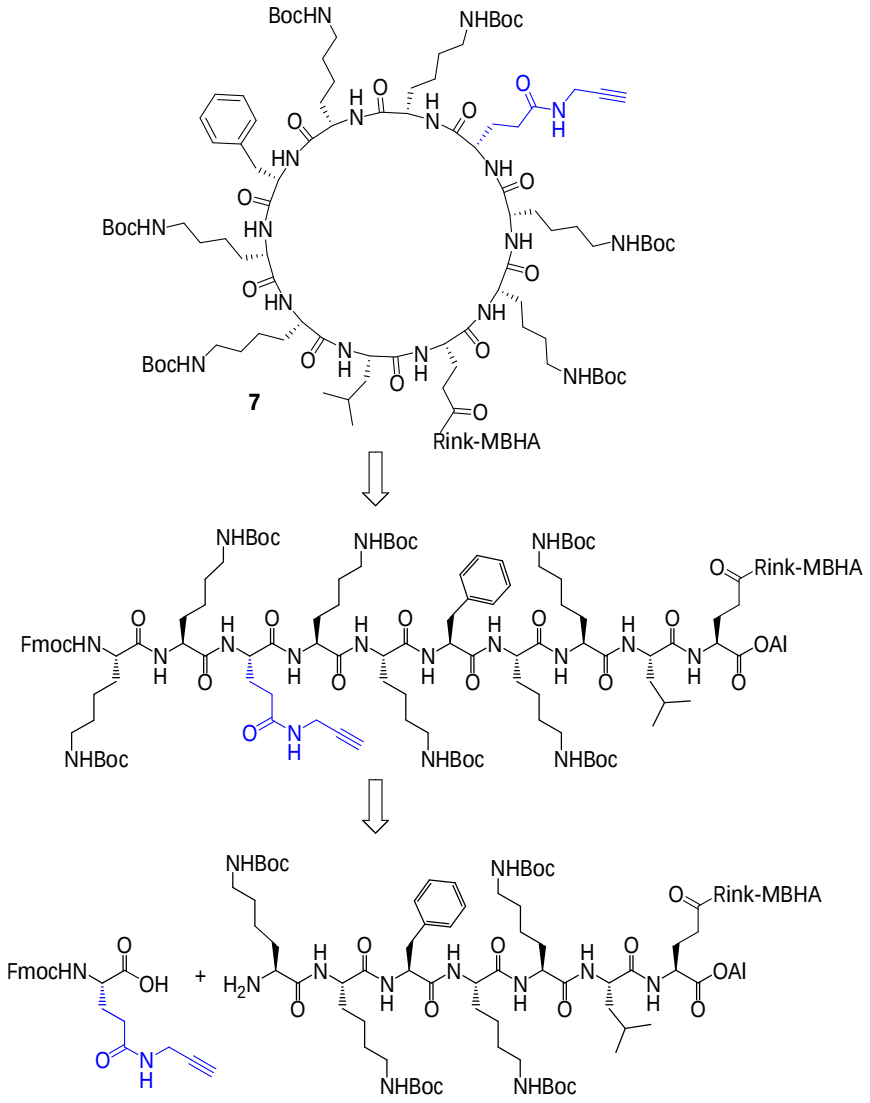

Scheme 5.5. *Retrosynthesis of the alkynyl peptidyl resin* ***7****.*

The synthesis of the alkynyl peptidyl resin **8** involved the preparation of the cyclic peptidyl resin **12** followed by coupling of the propiolic acid (Scheme 5.6). A similar strategy could be applied for resin **9**, containing the alkynyl-modified residue at position 5.

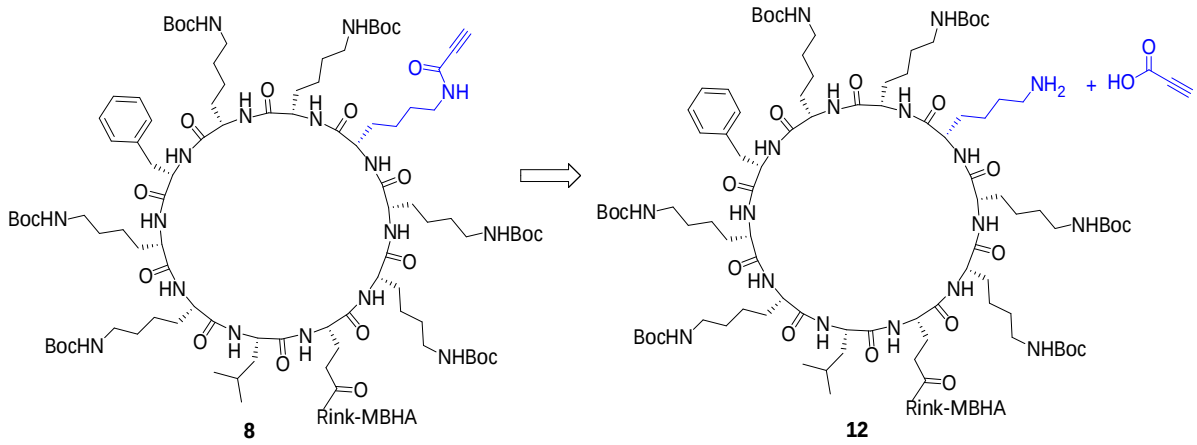

Scheme 5.6. *Retrosynthesis of the alkynyl peptidyl resin* ***8****.*

5.2.1.1. Synthesis of Fmoc-Gln($CH_2C\equiv CH$)-OH

Fmoc-Gln($CH_2C\equiv CH$)-OH was prepared from the commercially available Fmoc-Glu-O^{t}Bu by reaction with propargylamine followed by carboxylic acid deprotection. For the first reaction, different conditions were tested (Table 5.1). First, Fmoc-Glu-O^{t}Bu was treated with propargylamine using ethyl-(*N,N'*-dimethylamino)propylcarbodiimide (EDC) and HOBt as coupling reagents, DIPEA as base in dry tetrahydrofuran (THF) yielding Fmoc-Gln($CH_2C\equiv CH$)-OH in 52 % yield. To improve this result, we decided to test the reaction in the absence of HOBt or using Oxyma as additive (Table 5.1). The best result was obtained using the latter additive, affording Fmoc-Gln($CH_2C\equiv CH$)-O^{t}Bu as a yellow oil in 98 % yield. This compound was characterized by IR, ^{1}H-NMR, ^{13}C-NMR, HSQC edited, HPLC and ESI.

Table 5.1. *Conditions tested for the preparation of Fmoc-Gln($CH_2C\equiv CH$)-O^{t}Bu.*

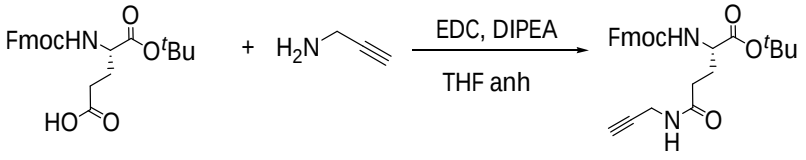

Entry	EDC (equiv)	HOBt (equiv)	Oxyma (equiv)	DIPEA (equiv)	t (h)	Yield (%)
1	1.2	1.0	-	1.97	17	52
2	1.2	-	-	1.97	46[a]	30
3	1.2	-	1.0	1.97	48[b]	98

[a]After 24 h, additional EDC (1.0 equiv) and DIPEA (1.0 equiv) were added.
[b]After 24 h, additional EDC (1.0 equiv), Oxyma (1 equiv) and DIPEA (1.0 equiv) were added.

Next, the ^{t}Bu group was removed by treating Fmoc-Gln($CH_2C\equiv CH$)-O^{t}Bu with TFA/CH_2Cl_2 (1:1) under stirring for 2 h at room temperature (Scheme 5.7). Fmoc-Gln($CH_2C\equiv CH$)-OH was obtained as a white powder in 58 % yield and was characterized by IR, ^{1}H-NMR, ^{13}C-NMR, HSQC edited, HPLC, ESI and HRMS.

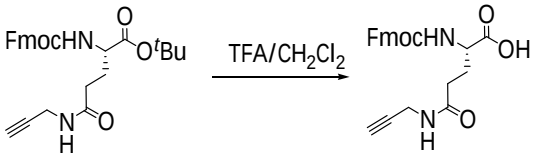

Scheme 5.7. *Synthesis of Fmoc-Gln($CH_2C\equiv CH$)-OH.*

5.2.1.2. Preliminary studies: Removal of the allyl group in presence of an alkynyl function

It has been described that alkynyl groups are stable under a wide variety of reaction conditions (Holub 2010). However, we decided to study the stability of an alkynyl moiety under the conditions of allyl removal. With this aim, alkynyl peptidyl resins **13-16** of 3 or 4 amino acids length were designed as model systems. A propargylglycine or a Gln($CH_2C\equiv CH$) residue was incorporated at positions 1 or 2 of the sequence in order to check the influence of the alkynyl position during the allyl removal (Figure 5.3).

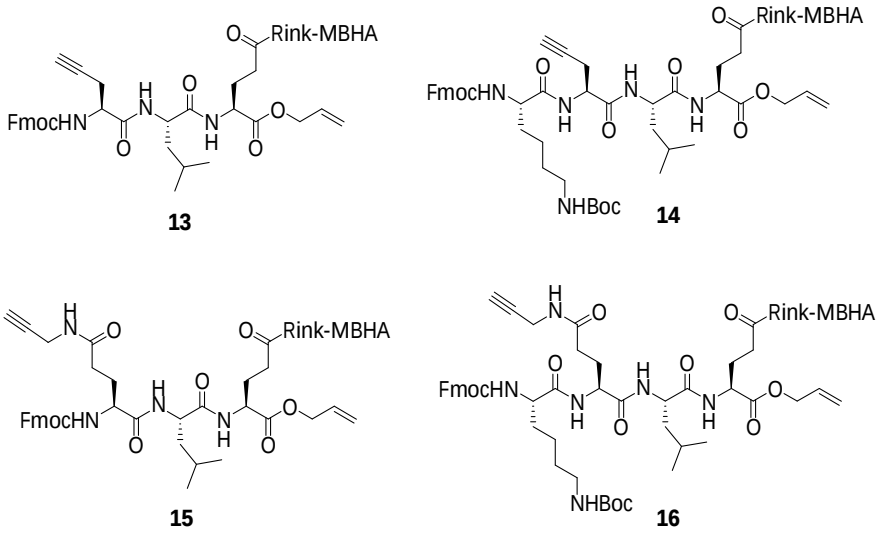

Figure 5.3. *Structures of peptidyl resins* ***13-16.***

The synthesis of peptidyl resins **13-16** was carried out manually using the standard solid-phase Fmoc/Boc/Al strategy, as depicted in Scheme 5.8 for peptidyl resins **13** and **15**. Fmoc-Prg-OH and Fmoc-Gln($CH_2C\equiv CH$)-OH were used as alkynyl-functionalized amino acids. An aliquot of the final peptidyl resins was cleaved by treatment with TFA/H_2O/TIS (95:2.5:2.5), affording the expected peptides in moderate to good purities.

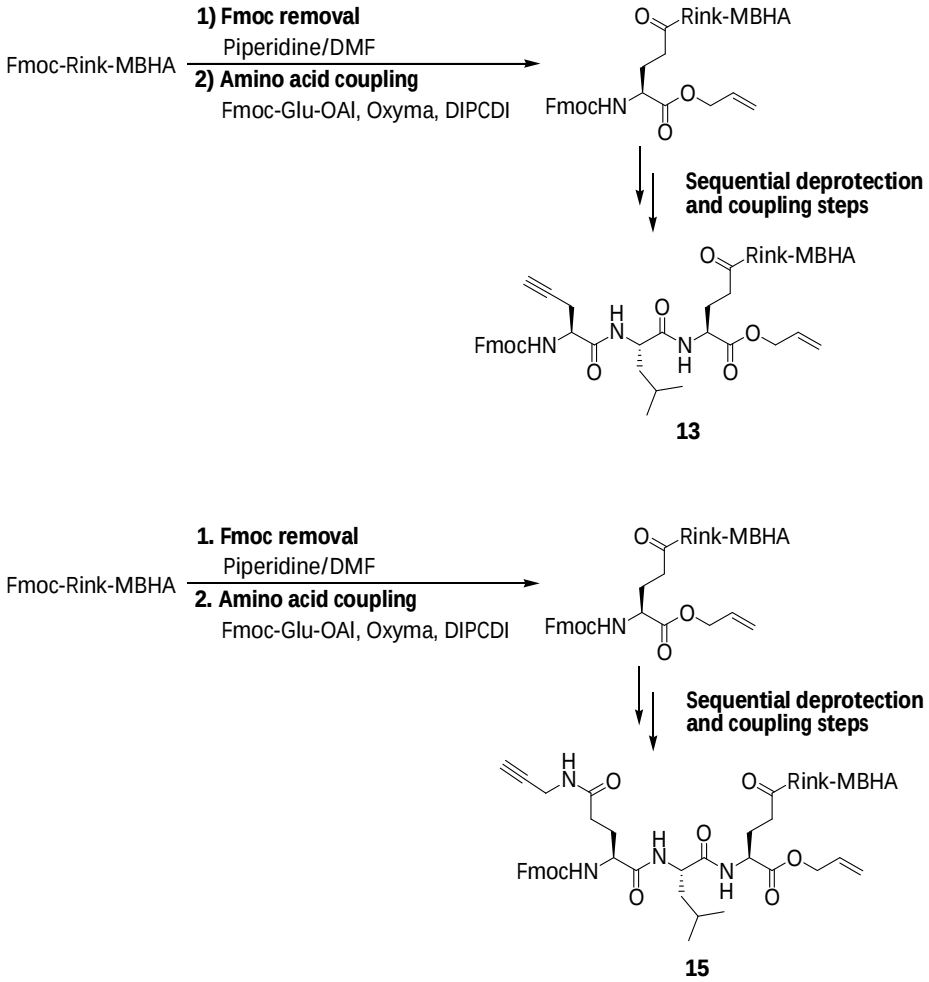

Scheme 5.8. *General scheme for the synthesis of peptidyl resins **13**-**16**, exemplified for **13** and **15**.*

Once the chain assembly was completed, each of the alkynyl resins **13**-**16** was treated with $Pd(PPh_3)_4$ and $CHCl_3$/AcOH/NMM (3:2:1) under stirring for 3 h at room temperature in order to remove the allyl protecting group (Scheme 5.9). An aliquot of the resulting resins **17**-**20** was cleaved but, unfortunately, we could not detect the expected peptides in the crude reaction mixtures by ESI-MS.

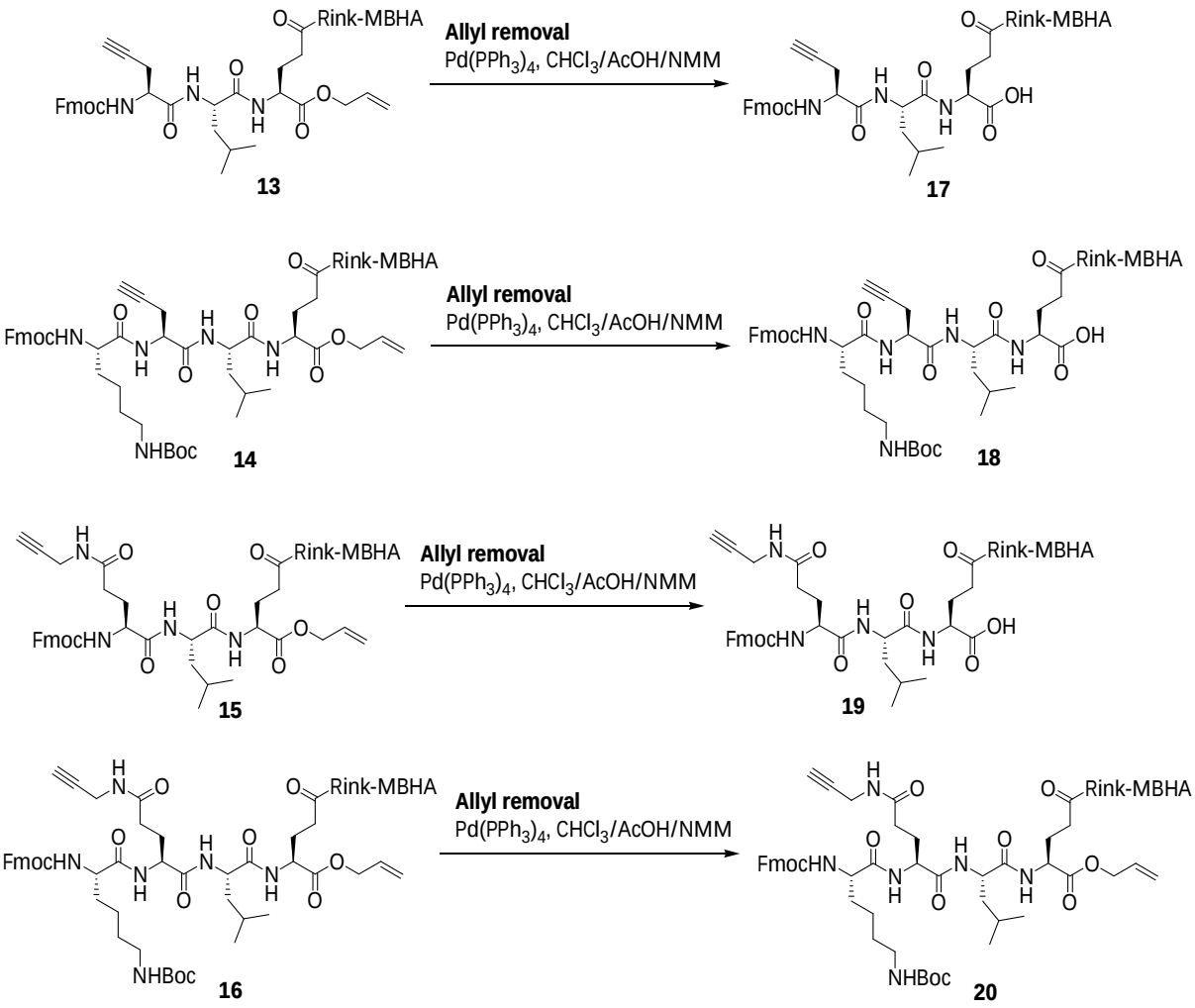

Scheme 5.9. *Removal of the allyl group of* ***13-16****.*

Despite these results, we decided to subject the alkynyl resins **17-20** to the cycloaddition reaction with BnN_3, CuI and ascorbic acid in piperidine/DMF for 5 h (Scheme 5.10). After cleavage with TFA/H_2O/TIS (95:2.5:2.5) the crude reaction mixtures were analyzed by HPLC and mass spectrometry. As shown in Table 5.2 peptidotriazoles **BP286**-**BP289** were obtained in 70-86 % purity. This result indicates that the alkynyl moiety is stable to the conditions of allyl group removal.

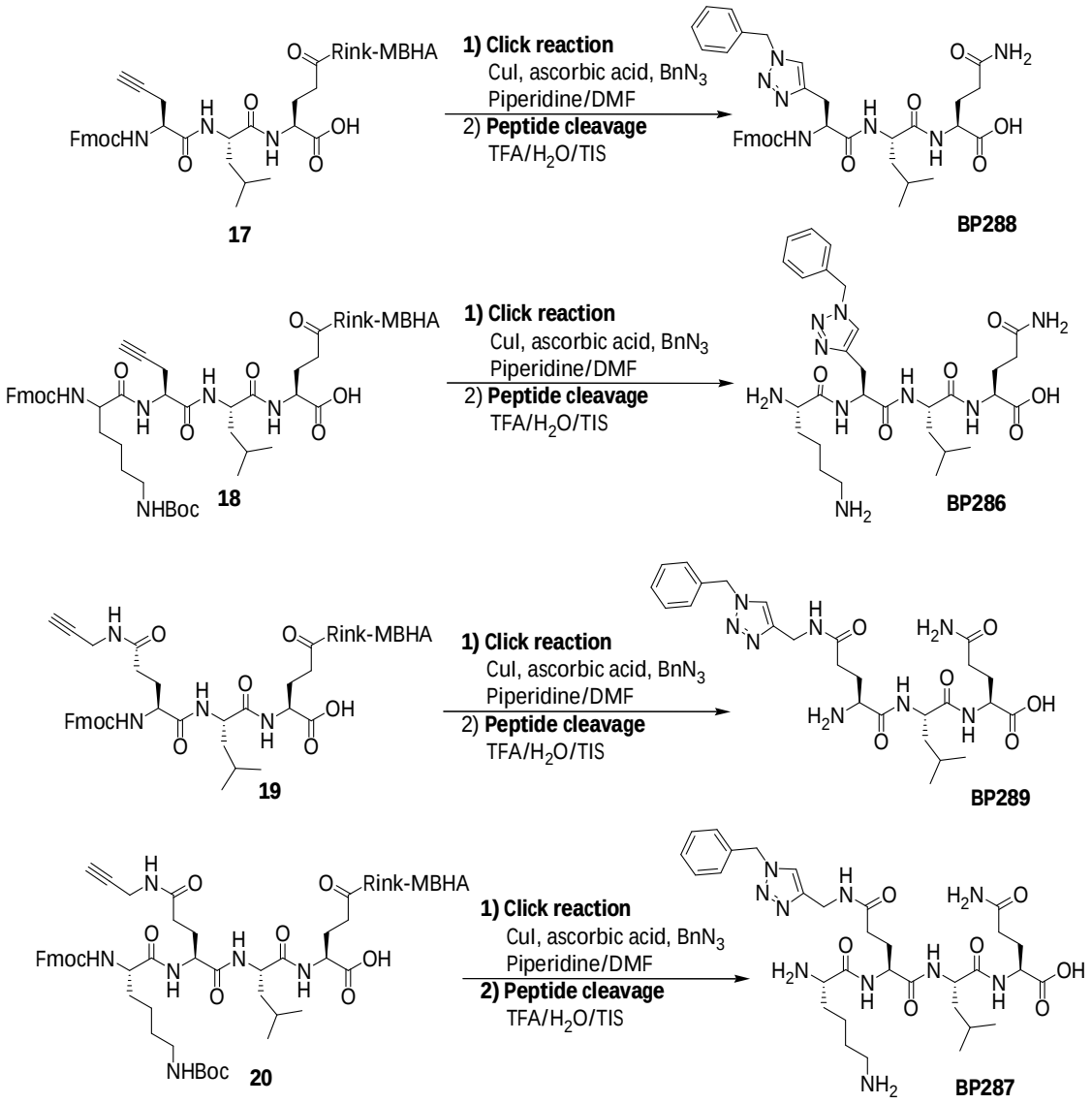

Scheme 5.10. *Cycloaddition reaction of* ***17-20*** *with* BnN_3.

Table 5.2. *Retention times and purities on HPLC, and MS data of* ***BP286-BP289****.*

Peptide	t_R (min)[a]	Purity[b] (%)	ESI-MS
BP288	16.09	70	687.4 $[M+H]^+$
BP286	15.71	85	616.4 $[M+H]^+$
BP289	16.88	76	659.3 $[M+H]^+$
BP287	16.23	86	488.2 $[M+H]^+$

[a]HPLC retention time using method D (see Materials and Methods).

[b]Percentage determined by HPLC at 220 nm from the crude reaction mixture.

5.2.1.3. Synthesis of the alkynyl peptidyl resins 5-7

The alkynyl peptidyl resin **5**, containing a propargylglycine at position 3, was synthesized manually using the standard Fmoc/^{t}Bu/Al strategy (Scheme 5.11). Fmoc-Rink-MBHA resin, with a low loading (0.3 mmol/g), was used as solid support to avoid cyclodimerization during the cyclization step. The alkynyl amino acid Fmoc-Prg-OH was incorporated as part of the standard stepwise synthesis. The cyclization was carried out by treating the resin with Oxyma, PyOxim and DIPEA under stirring for 24 h.

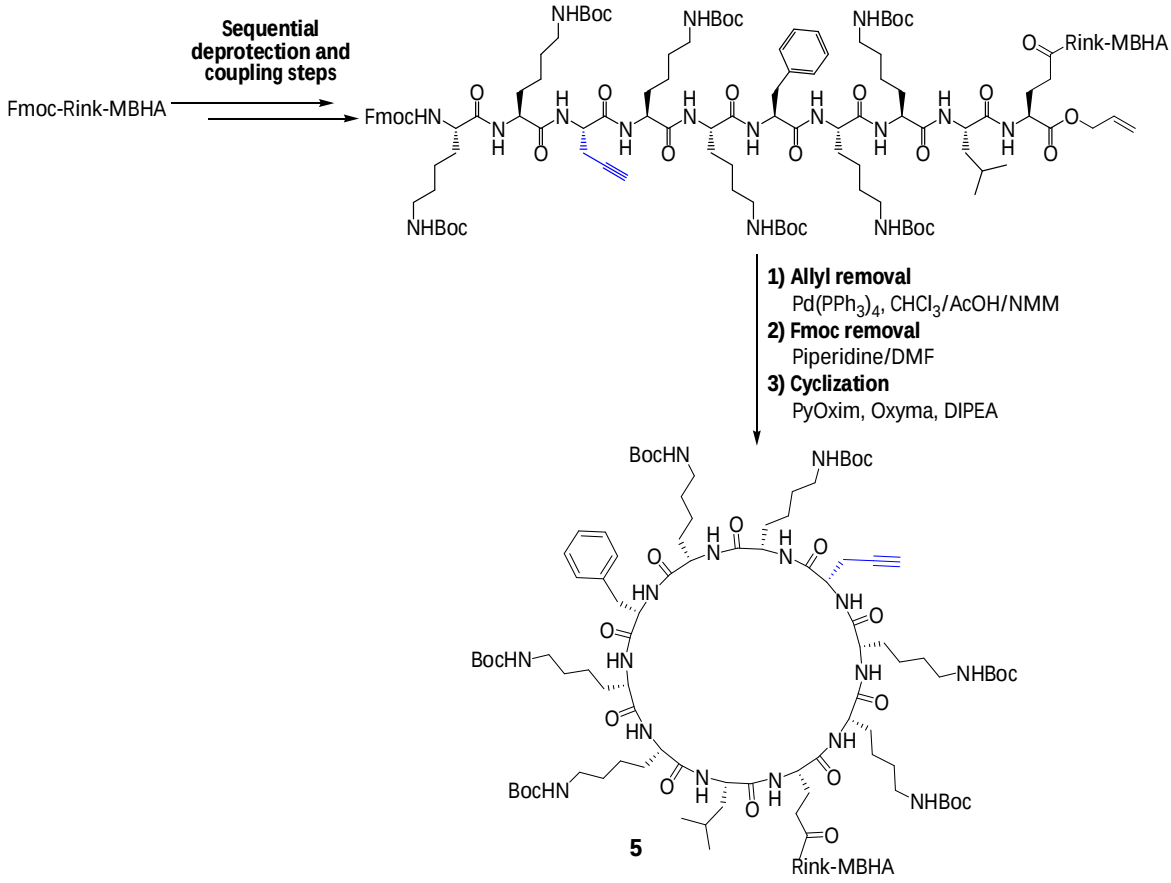

Scheme 5.11. *Synthesis of alkynyl resin* ***5.***

An aliquot of the resin **5** was cleaved with TFA/H_2O/TIS (95:2.5:2.5), affording peptide **BPC466** which was analyzed by HPLC (96 % purity) and mass spectrometry (Scheme 5.12).

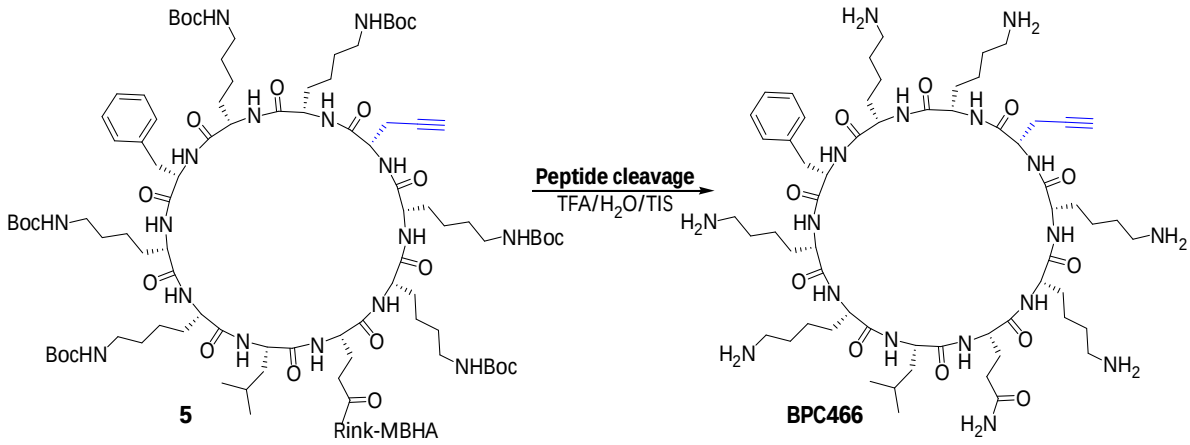

Scheme 5.12. *Synthesis of* ***BPC466****.*

This strategy was extended to the synthesis of the alkynyl resin **6** incorporating a propargylglycine residue at position 5. Cleavage of an aliquot of **6** afforded **BPC574** in 92 % purity (Scheme 5.13).

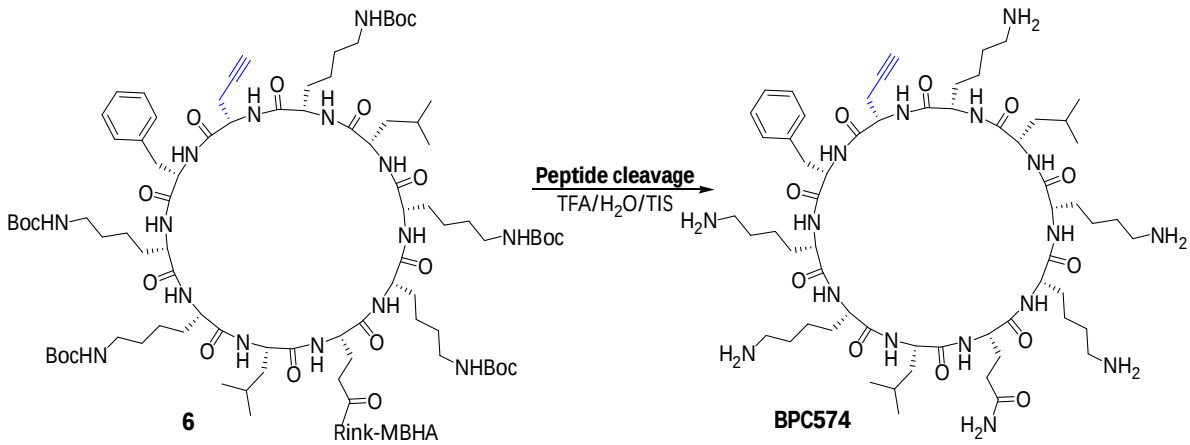

Scheme 5.13. *Cleavage of alkynyl resin* ***6*** *and obtention of* ***BPC574.***

Similarly, the alkynyl resin **7,** incorporating Gln($CH_2C\equiv CH$) at position 3, was prepared using the previously prepared alkynyl-functionalized amino acid Fmoc-Gln($CH_2C\equiv CH$)-OH (Scheme 5.14). After acidolytic cleavage of an aliquot of the resulting resin **7**, **BPC580** was obtained in 99 % purity (Scheme 5.15).

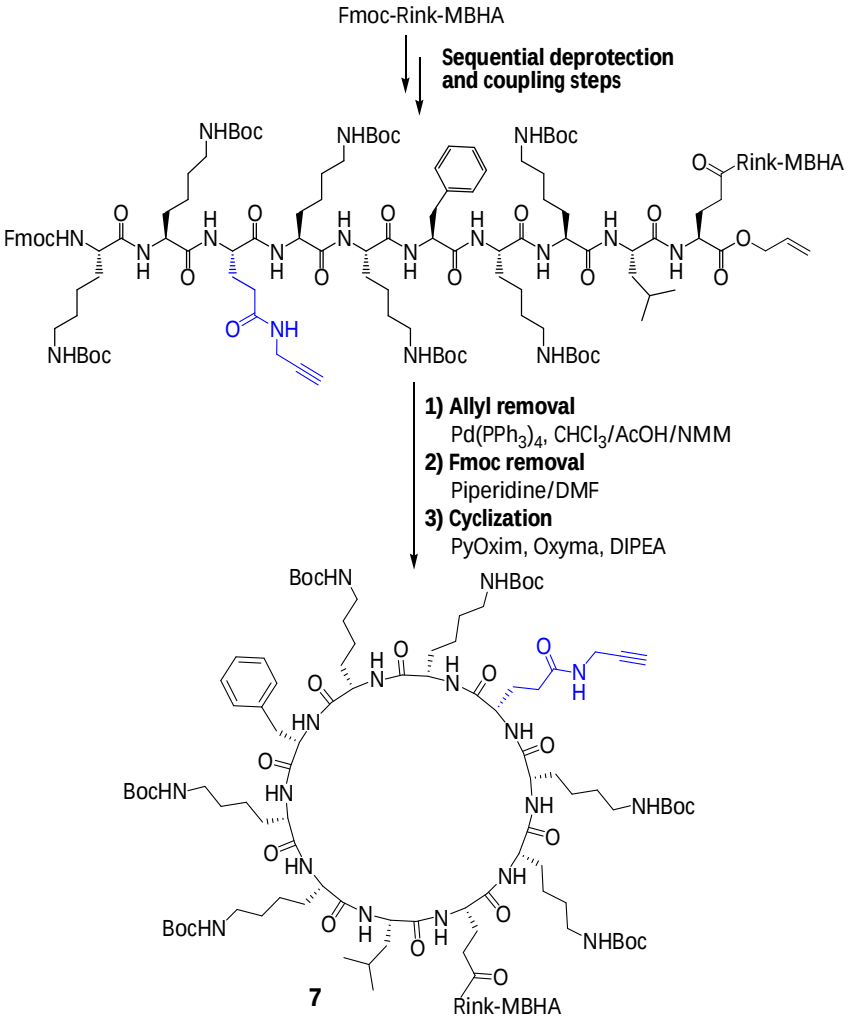

Scheme 5.14. *Synthesis of the alkynyl resin* ***7.***

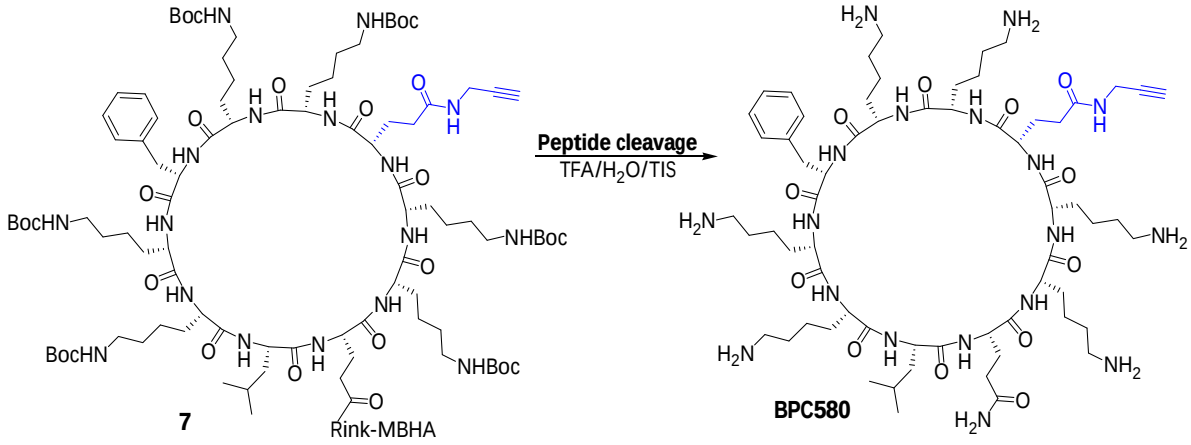

Scheme 5.15. *Cleavage of alkynyl resin* ***7*** *and obtention of* ***BPC580****.*

5.2.1.4. Synthesis of alkynyl peptidyl resins 8 and 9

The synthesis of the alkynyl peptidyl resins **8** and **9**, incorporating a lysine residue at positions 3 and 5, with the side-chain derivatized with a propioloyl group required the preparation of cyclic peptidyl resins with the lysine residue at these positions protected with a group that could be selectively removed. We chose the Mtt group because it is highly acid labile, enabling its selective removal without compromising the resin anchorage and the other side-chain protecting groups. Thus, for the synthesis of the alkynyl peptidyl resin **8**, we prepared the cyclic peptidyl resin **21** (Scheme 5.16). The cleavage of an aliquot of **21** yielded the desired cyclic peptide c(Lys-Lys-Lys-Lys-Lys-Phe-Lys-Lys-Leu-Gln) **22** (Figure 5.4) in 91 % purity.

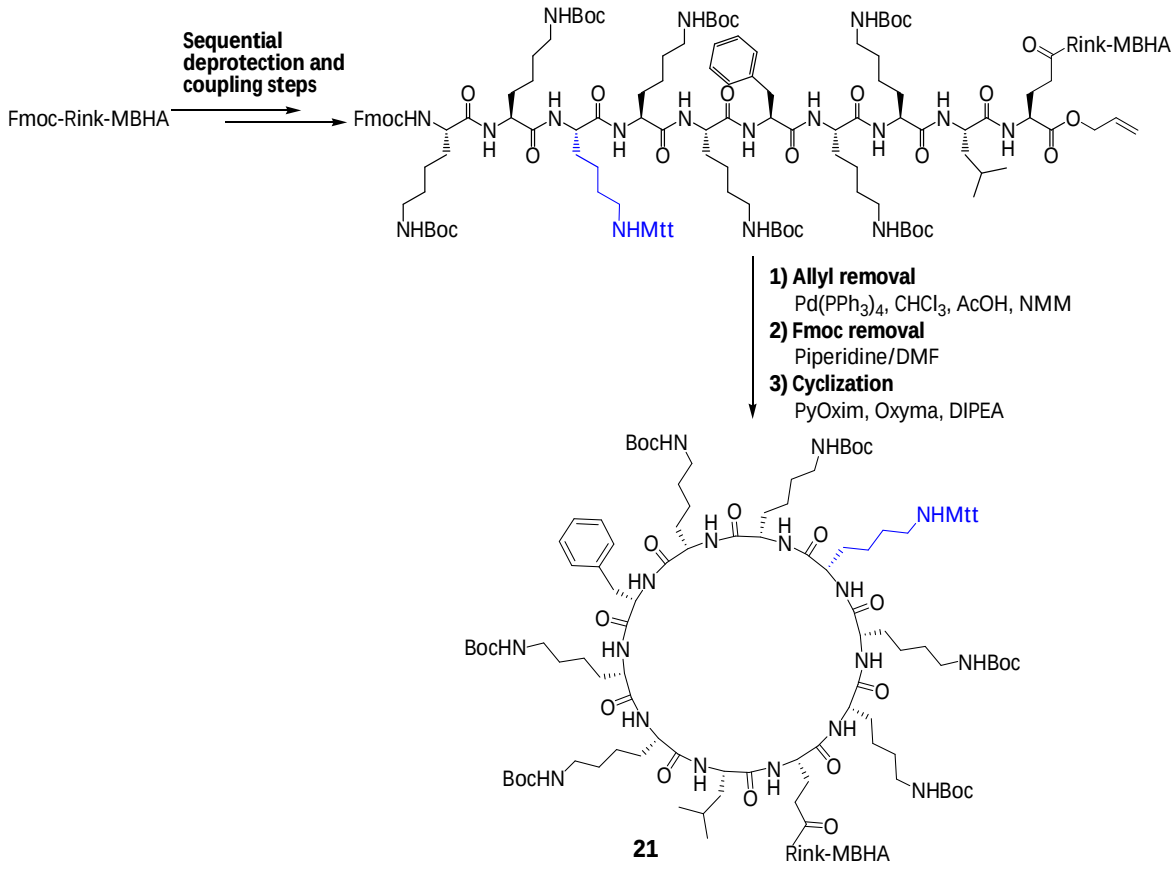

Scheme 5.16. *Synthesis of the alkynyl resin* ***21.***

Next, the resin **21** was treated using the conditions described by Cantel and co-workers for Mtt removal: 1 % TFA in CH_2Cl_2 under stirring for 3 min at room temperature (Cantel 2008). Then, the resin was washed with CH_2Cl_2, MeOH and CH_2Cl_2. The progress of the reaction was followed by the disappearance of the yellow color

produced by the release of the Mtt cation. The process was repeated 8 times until the solution remained colorless. This reaction was carried out using the minimum amount of solvent, because the removal of the Mtt cations is a slow process and multiple treatments with small volumes of acidic solutions are more effective than a single treatment with a large volume of this solution (Li 2002). Following Mtt removal, the N^{ε}-amino group was acylated with propiolic acid under the standard coupling conditions (Scheme 5.17). The resulting resin was cleaved and the crude mixture was analyzed by ESI-MS. A minor peak at *m/z* 1337.7 corresponding to the expected product **BPC468** was observed together with a a major peak at *m/z* 1285.7 corresponding to **22** (Figure 5.4). This result indicated that the Mtt group was not completely removed.

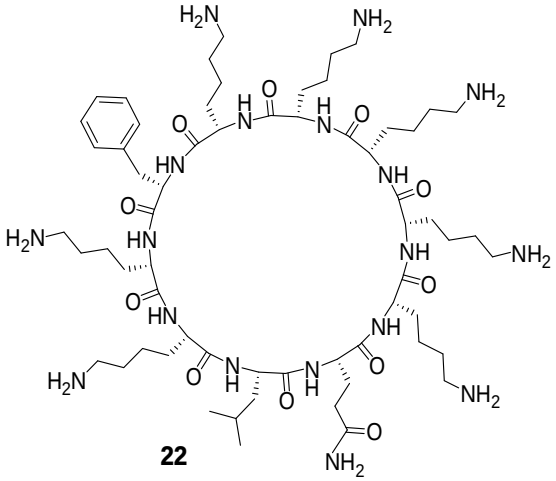

Figure 5.4. *Cyclic peptide 22*

Taking into account these results, we decided to perform the Mtt cleavage using the above conditions but for longer reaction times, 5 or 10 min at room temperature. After acylation with propiolic acid and cleavage, mass spectrometry analysis of the crude reaction mixtures indicated that prolonged reaction times also led to the removal of one or two Boc groups. Thus, when the Mtt group removal was carried out for 10 min, **BPC468** was obtained together with diacylated (*m/z* 1390.7) and triacylated (*m/z* 1441.6) peptides. By contrast, the reaction performed for 5 min yielded **BPC468** in 99 % HPLC purity and only traces of diacetylated and triacetylated peptides were detected by ESI-MS.

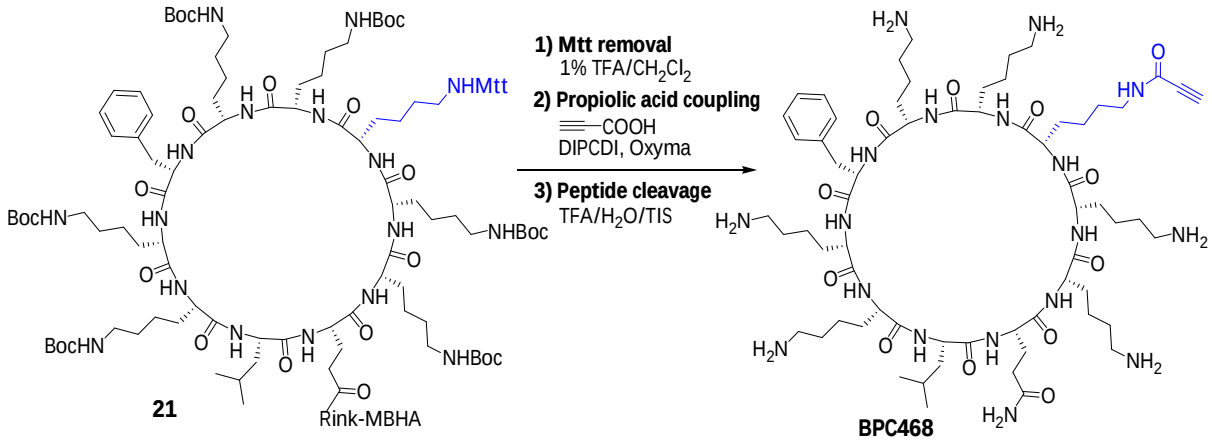

Scheme 5.17. *Synthesis of peptide* ***BCP468****.*

The alkynyl resin **23** incorporating the acylated lysine at position 5 was prepared following a similar strategy. Cleavage of an aliquot of **23** afforded **BPC578** in 97 % purity (Scheme 5.18).

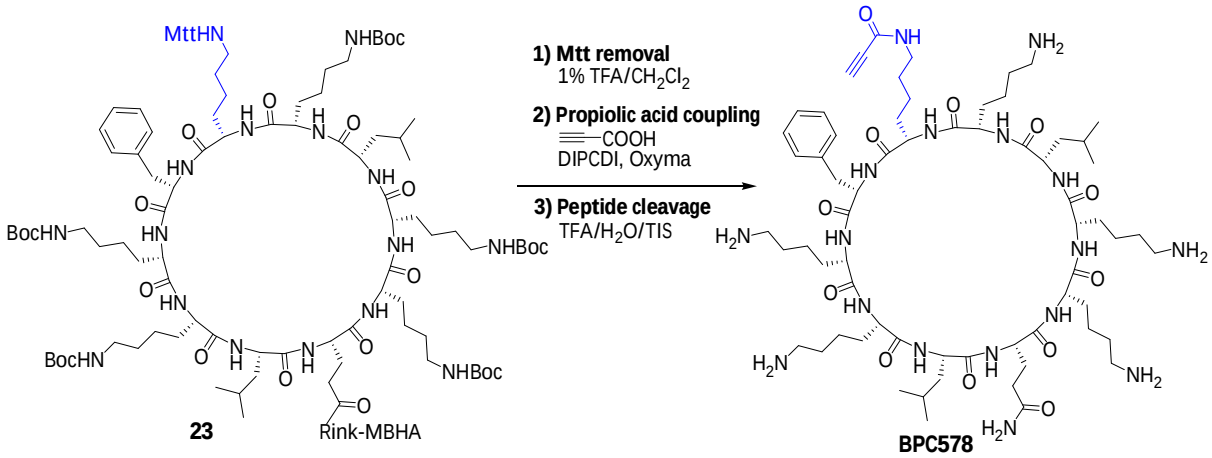

Scheme 5.18. *Cleavage of resin* ***9*** *and obtention of* ***BPC578****.*

5.2.2. Synthesis of azido cyclic peptidyl resins (strategy B)

In order to prepare the azidopeptidyl resins **10** and **11**, incorporating Nle(ε-N_3) at positions 3 and 5, respectively, we planned two strategies. The first strategy involved the solid-phase azidation of the corresponding lysine residue. In the second strategy, the azido-functionalized amino acid Fmoc-Nle(ε-N_3)-OH was incorporated as part of the stepwise on-resin peptide assembly (Scheme 5.19).

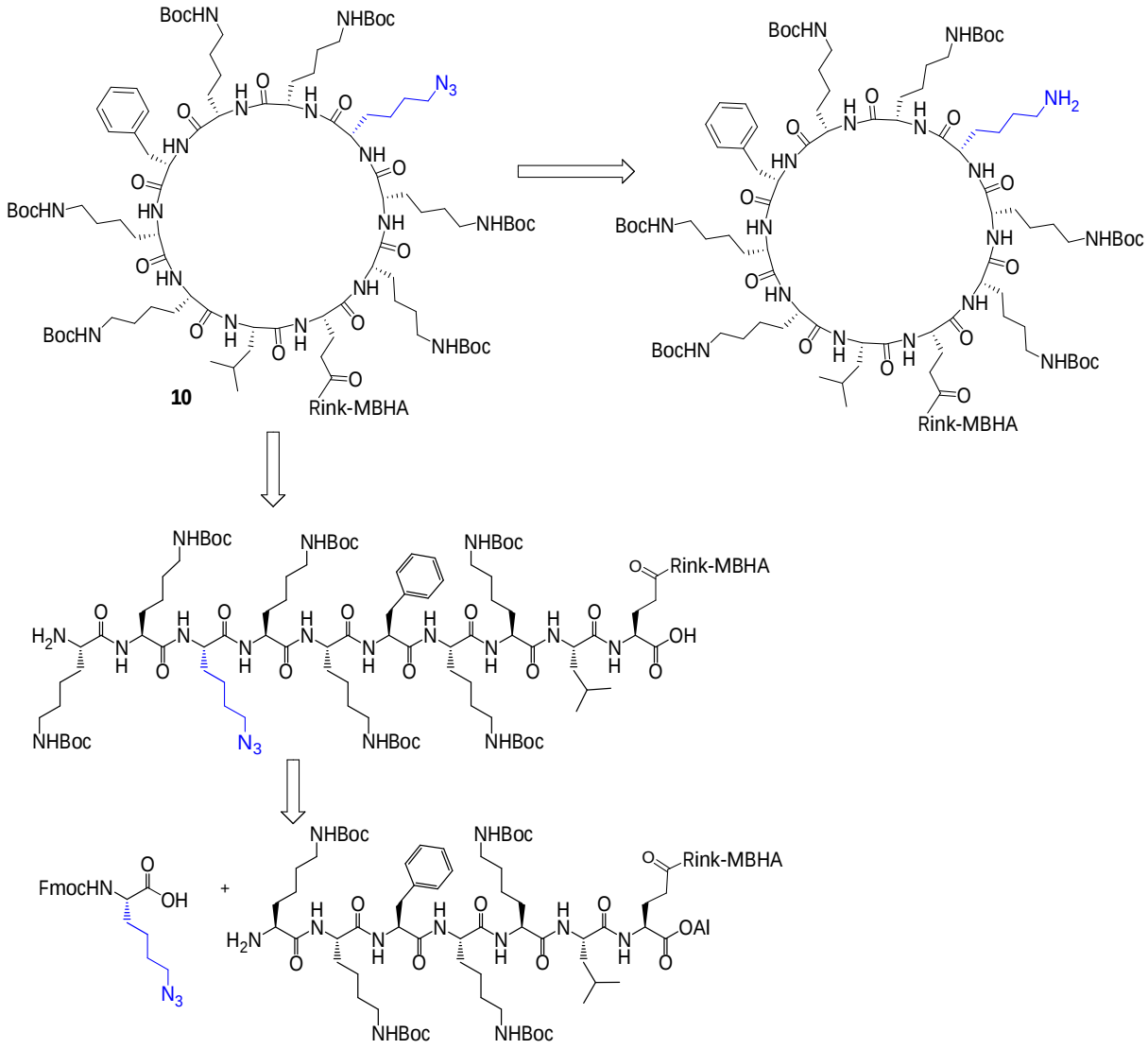

Scheme 5.19. *Retrosynthetic analysis for the azido peptidyl resin* ***10*** *and* ***11,*** *exemplified for* ***10****.*

5.2.2.1. Solid-phase azidation of a lysine residue

The solid-phase azidation of a lysine residue was first studied using **BP252** as model system (Figure 5.5).

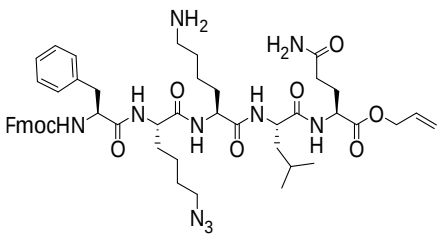

Figure 5.5. *Structure of the azido peptide* ***BP252****.*

With this purpose, we prepared the peptidyl resin **24** incorporating the lysine residue to be azidated as Fmoc-Lys(Mtt)-OH (Scheme 5.20). Once chain assembly was completed, **24** was treated with 1 % TFA in CH_2Cl_2 for 5 min in order to remove the Mtt protecting group. The solution became yellow instantaneously. TFA treatment and washes were repeated until the solution remained colorless.

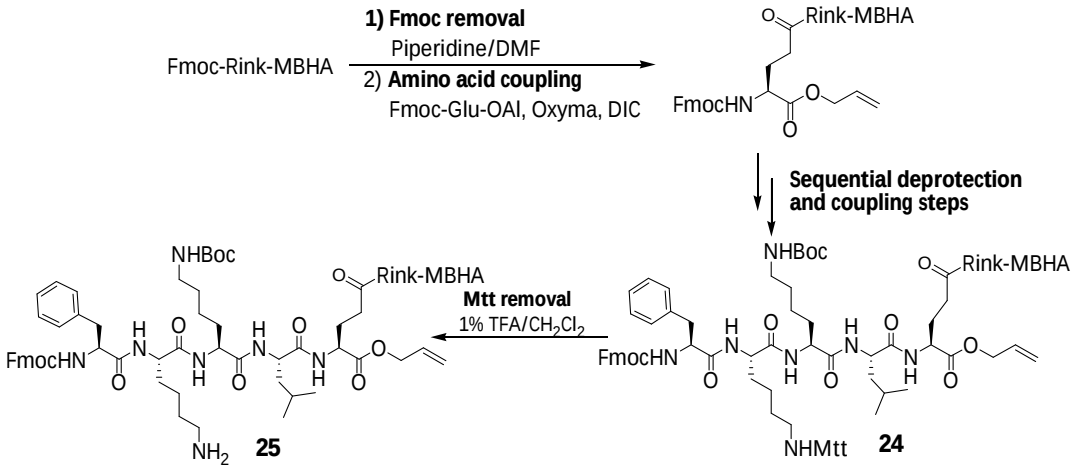

Scheme 5.20. *Synthesis of peptidyl resin* ***25.***

Then, we proceeded to study the azidation of resin **25** using conditions previously described in the literature (Rijkers 2002; Oyelere 2006; Cantel 2008) (Scheme 5.21). First, we prepared a solution of triflyl azide (TfN_3) in CH_2Cl_2 from NaN_3 and Tf_2O. The resin **25** was then treated with this solution, and the addition of K_2CO_3, $CuSO_4 \cdot 5H_2O$, MeOH and H_2O was evaluated (Table 5.3).

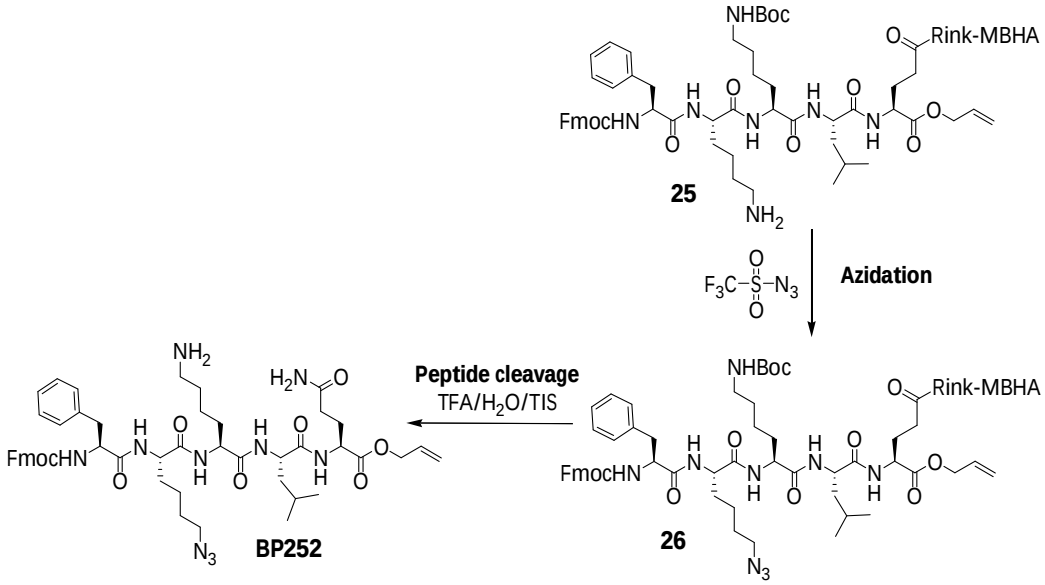

Scheme 5.21. *Azidation of a lysine residue on solid-phase.*

In each experiment, resin **25** was subjected to the corresponding conditions for two treatments of 18 h. The final resin **26** was cleaved and the crude product was analyzed by HPLC and ESI-MS. Conditions described in entries 1 and 3 in Table 5.3, afforded the expected azidopeptide **BP252** (Figure 5.5) in 94 % purity. Conditions of entry 2 led to the recovery of the starting material.

Table 5.3. *Conditions tested for the azidation of* ***25****.*

Entry	K_2CO_3 (equiv)	$CuSO_4 \cdot 5H_2O$ (equiv)	MeOH (equiv)	H_2O (equiv)	Time (h)	Purity (%)
1	0.4	0.1	11	-	2 × 18	94
2	-	0.1	8	-	2 × 18	-
3	-	0.1	-	8	2 × 18	94

Best conditions where then applied to longer linear peptides (10 amino acids lenght) and placing the lysine moiety to be azidated at different positions of the sequence. The peptidyl resin 27, incorporating the lysine residue at position 7, was prepared. Azidation was assayed using the previous conditions (Table 5.3 entries 1 and 3). In this case, despite subjecting the resin to three treatments of 18 h, the reaction was still incomplete. Taking as basis conditions of entry 1 in Table 5.4, which gave the best conversion percentage, we increased the equivalents of $CuSO_4 \cdot 5H_2O$ (Table 5.4, entry 3). Rijkers described that if the length of the peptide sequence increases the concentration of $CuSO_4 \cdot 5H_2O$ has to be increased due to copper complexation (Rijkers 2002). Unfortunately, these conditions did not improve the results, leading to azido peptide **27** in 43 % conversion.

Table 5.4. *Conditions tested for the azidation of* ***27.***

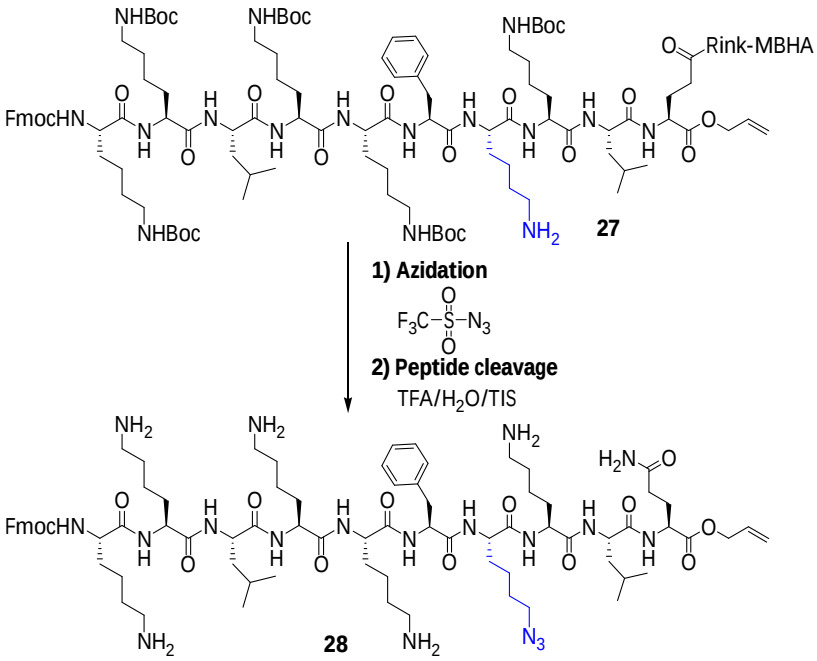

Entry	K_2CO_3 (equiv)	$CuSO_4 \cdot 5H_2O$ (equiv)	MeOH (equiv)	H_2O (equiv)	Time (h)	Conversion (%)
1	0.4	0.1	11	-	3 × 18[a]	41
2	-	0.1	-	8	3 × 18[a]	19
3	0.4	0.5	11	-	3 × 18[a]	43

[a]Ninhydrin test was still positive.

Similarly, we tested the azidation of the peptidyl resin **29**, incorporating the lysine residue to be azidated at position 3 (Table 5.5). We assayed the same reaction conditions as for resin **27**. In this case, after three treatments of 18 h, the reaction was still incomplete, affording azido peptide **30** in 58 % conversion (Table 5.5).

Table 5.5. *Conditions tested for solid-phase azidation of* ***29.***

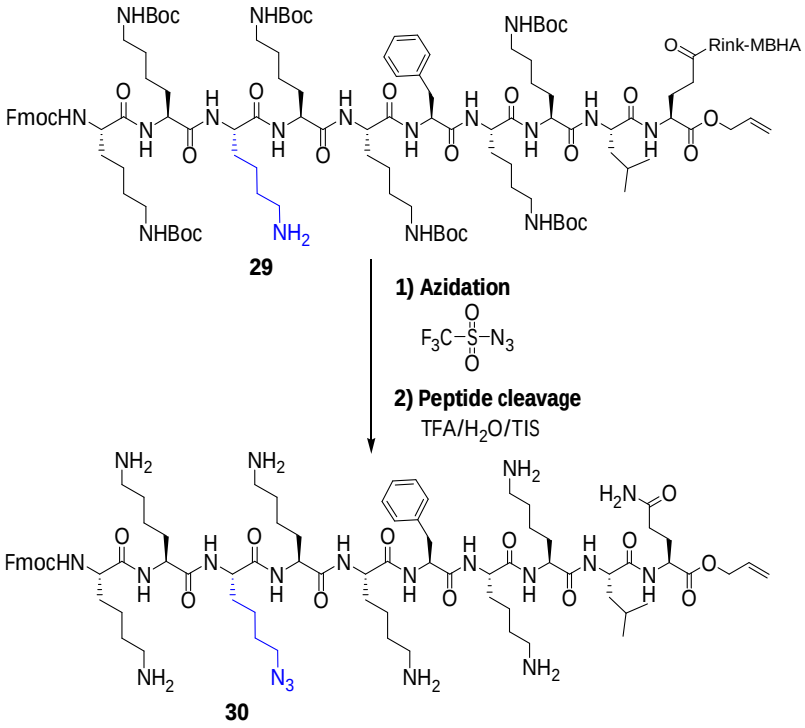

Test	K_2CO_3 (equiv)	$CuSO_4 \cdot 5H_2O$ (equiv)	MeOH (equiv)	H_2O (equiv)	Time (h)	Conversion (%)
1	0.4	0.1	11	-	3 × 18[a]	27
3	-	0.1	-	8	3 × 18[a]	42
4	0.4	0.5	11	-	3 × 18[a]	58

[a]Ninhydrin test was still positive.

5.2.3. Synthesis of azido peptidyl resins 10 and 11 using Fmoc-Nle(ε-N_3)-OH

Since the solid-phase azidation of a lysine residue required long reaction times and did not afford the desired product in good purity for long peptide sequences, we decided to synthesize Fmoc-Nle(ε-N_3)-OH in solution and then incorporate it in the sequence.

Following the terms described by Chevalier-Isaad, we studied the preparation of Fmoc-Nle(ε-N_3)-OH from commercially available Boc-Lys-OH by azidation of the ε-amino group and replacement of the Boc group by an Fmoc (Scheme 5.22).

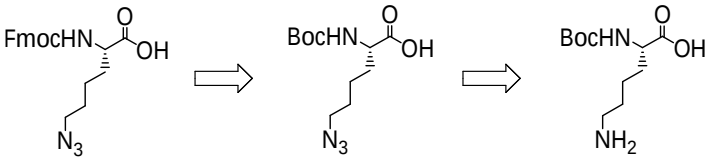

Scheme 5.22. *Retrosynthetic scheme for the preparation of Fmoc-Nle(ε-N_3)-OH.*

The azidation of Boc-Lys-OH was performed by dissolving it in H_2O and MeOH in presence of K_2CO_3 and $CuSO_4 \cdot 5H_2O$, followed by treatment with a solution of TfN_3 in CH_2Cl_2, previously prepared, under pressure at room temperature overnight (Scheme 5.23) (Chevalier-Isaad 2008). Several tests increasing the reaction time (from 18 h to 3 days) were performed in order to improve the reaction conversion; unfortunately, yields obtained in this reaction did not improve (Scheme 5.23).

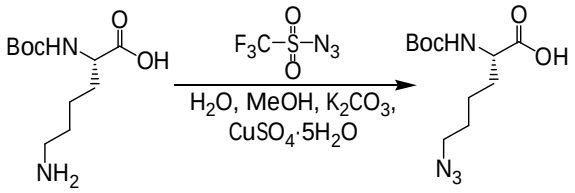

Scheme 5.23. *Azidation of Boc-Nle(ε-N_3)-OH.*

Alternatively, we decided to study the synthesis of Fmoc-Nle(ε-N_3)-OH by azidation of Fmoc-Lys-OH. This amino acid was obtained by Boc removal of commercially available Fmoc-Lys(Boc)-OH by treatment with TFA/CH_2Cl_2 (1:1) for 2 h at room temperature. Fmoc-Lys-OH was obtained as a white powder in 95 % yield (Scheme 5.24). Afterwards, we proceeded to perform the azidation of Fmoc-Lys-OH. K_2CO_3 is generally used in this reaction as base (Lundquist 2001; Rijkers 2002), but the Fmoc group is not stable under these conditions. To avoid the Fmoc cleavage, $NaHCO_3$ was used (Katayama 2008). Thus, Fmoc–Lys–OH, $NaHCO_3$ and $CuSO_4 \cdot 5H_2O$ were dissolved in distilled H_2O and MeOH. Thereafter, TfN_3 in CH_2Cl_2 was added. The mixture was stirred under pressure overnight at room temperature and the reaction was followed by HPLC. The crude product was digested with pentane to give Fmoc-Nle(ε-N_3)-OH as a white powder in 94 % yield (Scheme 5.24).

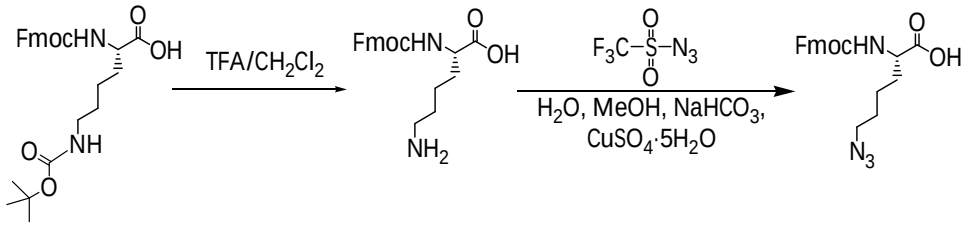

Scheme 5.24. *Synthesis of Fmoc-Nle(ε-N_3)-OH.*

With this amino acid in hand, we prepared the azido peptidyl resin **10**, containing the azido group at position 3, following the standard Fmoc/^{t}Bu/Al strategy previously described. The azido amino acid Fmoc-Nle(ε-N_3)-OH was incorporated as part of the stepwise synthesis (Scheme 5.25).

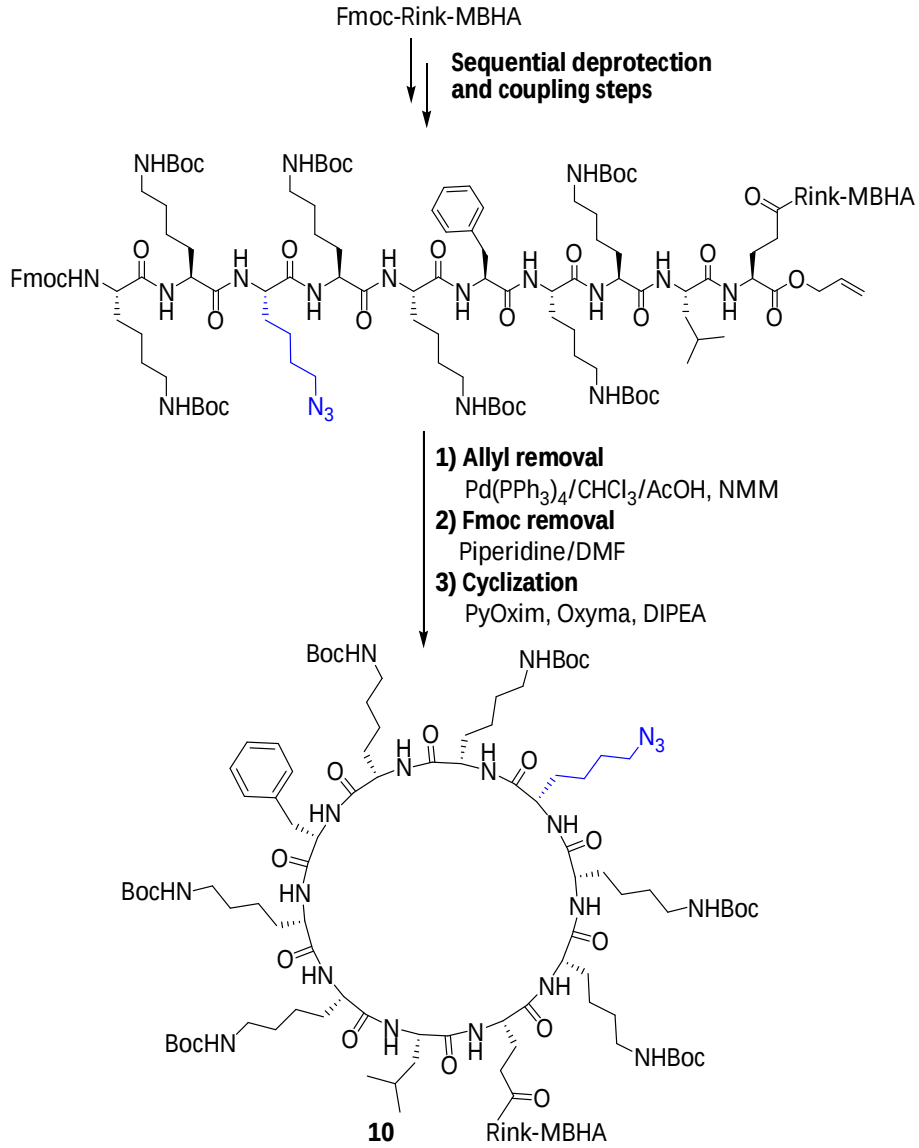

Scheme 5.25*. Synthesis of the azido peptidyl resin* ***10.***

Once the synthesis was completed, an aliquot of the resin **10** was cleaved with TFA/H_2O/TIS (95:2.5:2.5) and the crude product was analyzed by HPLC and ESI-MS. **BPC464** was obtained in 94 % purity (Scheme 5.26).

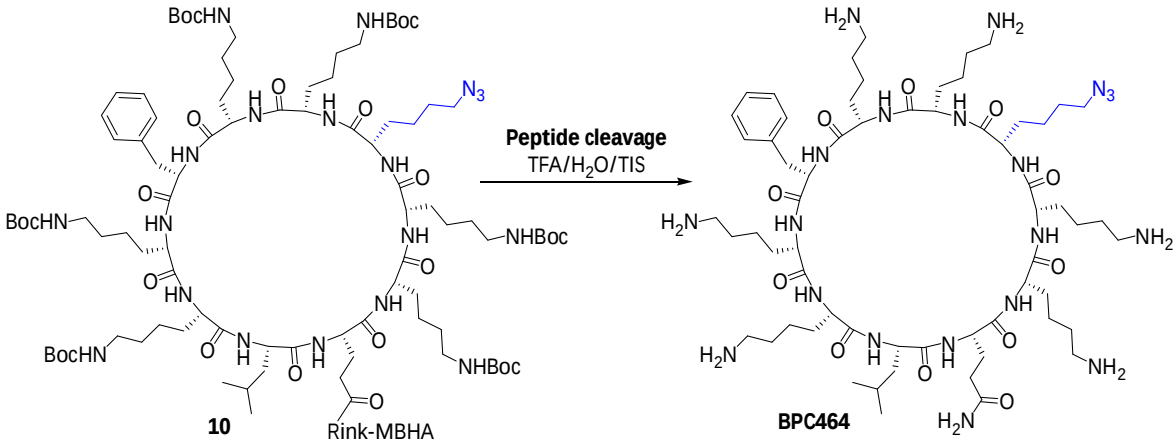

Scheme 5.26. *Cleavage of resin **10** and obtention of **BPC464.***

The above methodology was extended to the synthesis of the azido peptidyl resin **11** incorporating the azido group at position 5 (Scheme 5.27). Once the synthesis was completed, an aliquot of the resin was cleaved with TFA/H_2O/TIS (95:2.5:2.5) and the crude product was analyzed by HPLC and ESI-MS. **BPC576** was obtained in 94 % purity.

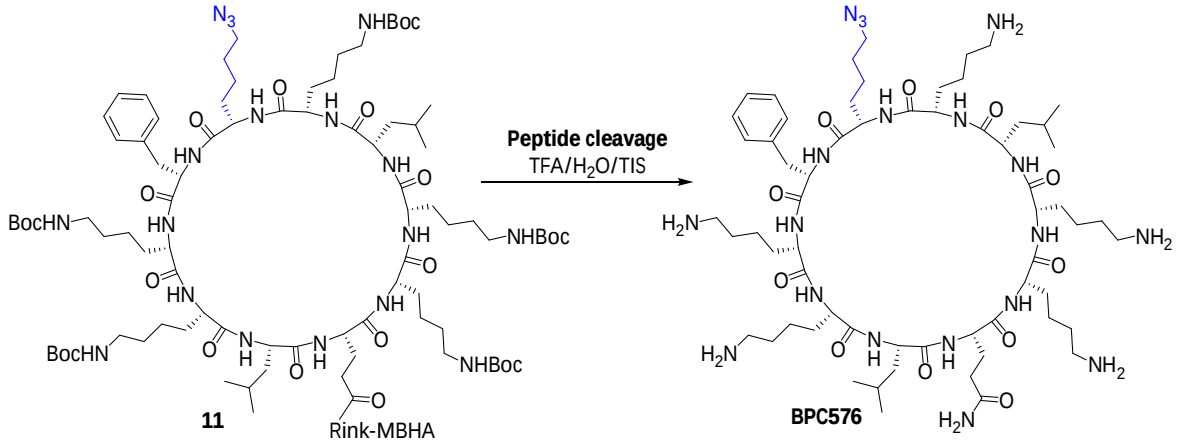

Scheme 5.27. *Cleavage of resin **11** and obtention of **BPC576.***

5.3. Synthesis of cyclic peptidotriazoles

Once the synthesis of the cyclic alkynyl and azido peptidyl resins was performed, we proceeded to carry out the synthesis of the corresponding cyclic peptidotriazoles.

5.3.1. Synthesis of cyclic peptidotriazoles from alkynyl peptidyl resins

5.3.1.1. Synthesis of cyclic peptidotriazoles from resins 5 and 6

The alkynyl peptidyl resin **5**, containing a propargylglycine at position 3, was treated with the azides included in Table 5.6 in presence of ascorbic acid and CuI in piperidine/DMF (2:8), as previously described for the synthesis of linear peptidotriazoles. The reaction mixture was stirred for 5 h at room temperature. In the case of NaN_3, two treatments of 10 h were required to lead the reaction to completion. Cyclic peptidotriazoles were individually cleaved from the resin with TFA/H_2O/TIS (95:2.5:2.5) and analyzed by HPLC and ESI-MS. These compounds, containing a triazolylalanine were obtained in excellent purities (90-96 %).

Table 5.6. *Synthesis of cyclic peptidotriazoles from alkynyl resin* ***5****.*

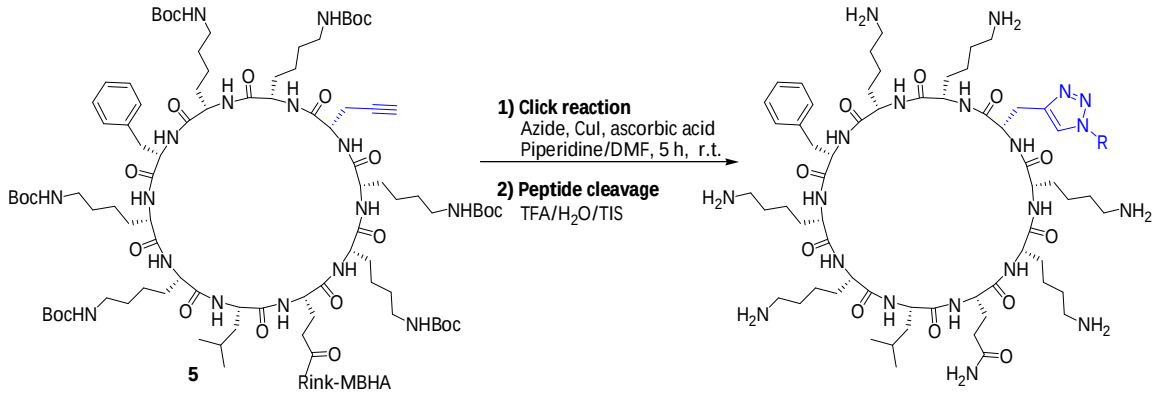

Azide	Peptidotriazole	Notation[a]	R	Purity[c] (%)
NaN_3[b]	**BPC456**	Ala(Tr)	H	96
BnN_3	**BPC458**	Ala(Tr-Bn)	Bn	94
***p*-Azidoaniline**	**BPC518**	Ala(Tr-C_6H_4-NH_2)	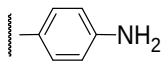	95
Boc-Nle(ε-N_3)-OH	**BPC460**	Ala(Tr-Ahx)	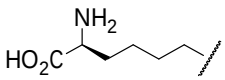	90
***p*-Azidotoluene**	**BPC540**	Ala(Tr-C_6H_4-Me)	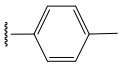	99
***p*-Azidoanisole**	**BPC542**	Ala(Tr-C_6H_4-OMe)	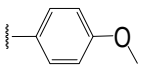	96
Azidobenzene	**BPC544**	Ala(Tr-Ph)		92

[a]The notation defines the amino acid modified with a triazole ring. Tr stands for the triazole.

[b]Reaction time: 2 x 10 h

[c]Percentage determined by HPLC at 220 nm from the crude reaction mixture.

The alkynyl peptidyl resin **6**, containing a propargylglycine at position 5, was treated with the azides included in Table 5.7 following the procedure described above. After 5 h of reaction, cleavage of the final resins afforded the corresponding peptidotriazoles, incorporating a triazolylalanine, in good to excellent purities (77-99 %).

Table 5.7. *Synthesis of cyclic peptidotriazoles from the alkynyl resin* ***6****.*

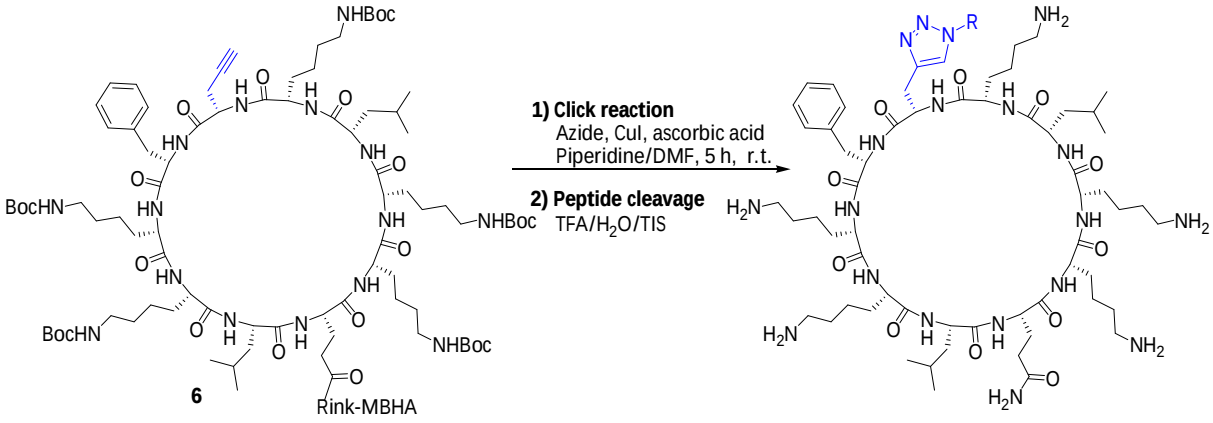

Azide	Peptidotriazole	Notation[a]	R	Purity[b] (%)
BnN_3	**BPC510**	Ala(Tr-Bn)	Bn	77
***p*-Azidoaniline**	**BPC514**	Ala(Tr-C_6H_4-NH_2)	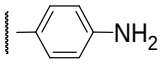	90
Boc-Nle(ε-N_3)-OH	**BPC512**	Ala(Tr-Ahx)	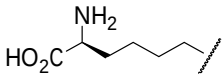	95
***p*-Azidotoluene**	**BPC564**	Ala(Tr-C_6H_4-Me)	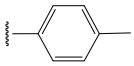	88
***p*-Azidoanisole**	**BPC566**	Ala(Tr-C_6H_4-OMe)	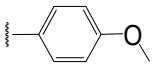	80
Azidobenzene	**BPC568**	Ala(Tr-Ph)		78

[a]The notation defines the amino acid modified with a triazole ring. Tr stands for the triazole.

[b]Percentage determined by HPLC at 220 nm from the crude reaction mixture.

5.3.1.2. Synthesis of cyclic peptidotriazoles from resin 7

The above methodology was extended to the synthesis of peptidotriazoles starting from the alkynyl peptidyl resin **7**, containing a Gln($CH_2C\equiv CH$) residue at position 3. In

this case, the click reaction was performed with NaN_3, BnN_3 and Boc-Nle(ε-N_3)-OH (Table 5.8). After 5 h, cyclic peptidotriazoles **BPC520** and **BPC522** were obtained in excellent purities, 98 and 94 %, respectively. The reaction with NaN_3 required two treatments of 10 h to afford **BPC532** in 98 % purity.

Table 5.8. *Synthesis of cyclic peptidotriazoles derived from alkynyl resin* ***7****.*

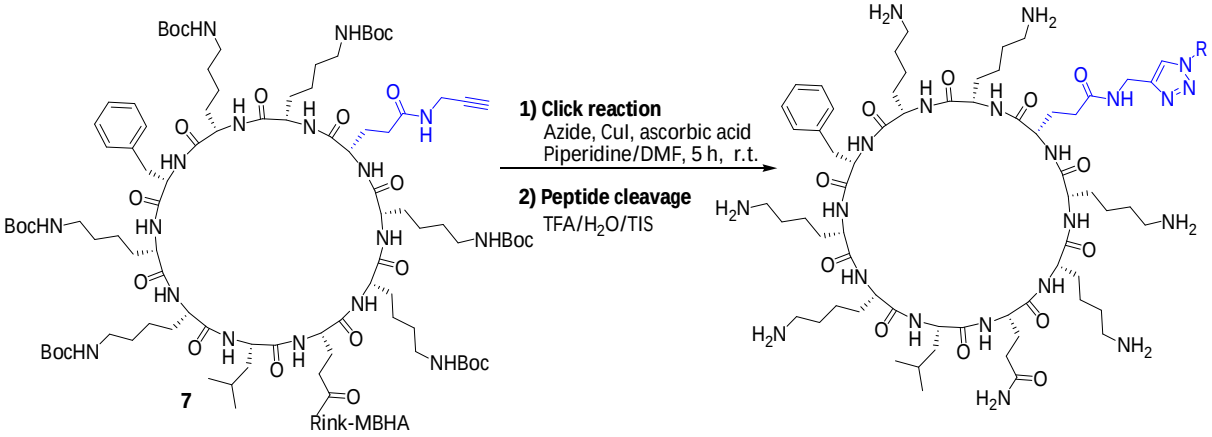

Azide	Peptide	Notation[a]	R	Purity[c] (%)
NaN_3[b]	**BPC532**	Gln(CH_2-Tr)	H	98
BnN_3	**BPC520**	Gln(CH_2-Tr-Bn)	Bn	98
Boc-Nle(ε-N_3)-OH	**BPC522**	Gln(CH_2-Tr-Ahx)	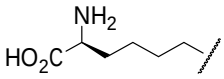	94

[a]The notation defines the amino acid modified with a triazole ring. Tr stands for the triazole.

[b]Reaction time: 2 x 10 h

[c]Percentage determined by HPLC at 220 nm from the crude reaction mixture.

5.3.1.3. Synthesis of cyclic peptidotriazoles from resins 8 and 9

Alkynyl peptidyl resins **8** and **9** (Scheme 5.1), containing a Lys(COC≡CH) at position 3 and 5, respectively, were reacted with NaN_3, BnN_3 and Boc-Nle(ε-N_3)-OH (Table 5.9 and 5.10). After 5 h, cyclic peptidotriazoles were obtained in good HPLC purities (75-86 %). Mass spectrometry showed a peak corresponding to the unmodified cyclic peptide **22** (Figure 5.4) or to **BPC194** (Figure 5.1) which revealed that during the synthesis the Mtt group was not completely removed preventing the acylation of the corresponding lysine residue with propiolic acid.

Table 5.9. *Synthesis of cyclic peptidotriazoles derived from the alkynyl resin* ***8****.*

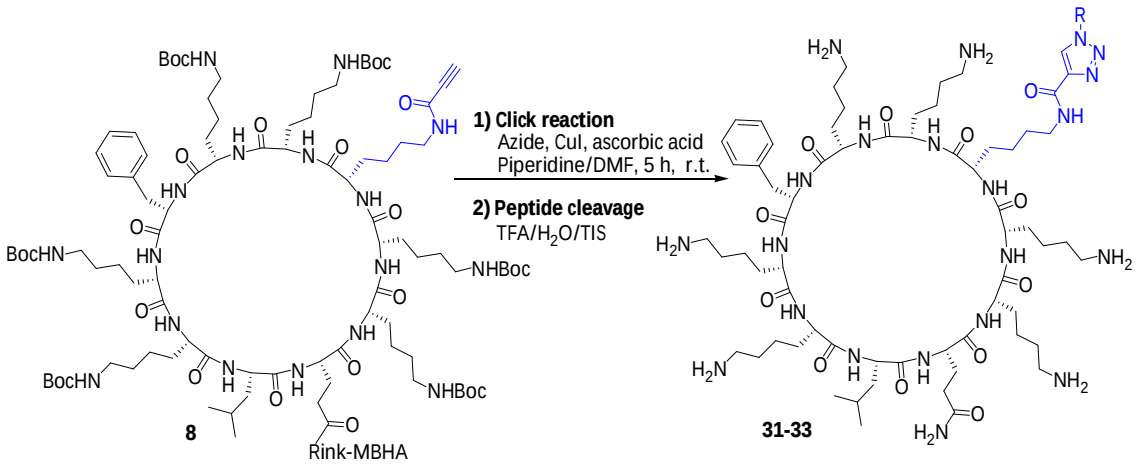

Azide	Peptidotriazole	Notation[a]	R	Purity[b] (%)
NaN_3	**31**	Lys(CO-Tr)	H	75
BnN_3	**32**	Lys(CO-Tr-Bn)	Bn	82
Boc-Nle(ε-N_3)-OH	**33**	Lys(CO-Tr-Ahx)	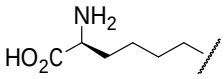	86

[a]The notation defines the amino acid modified with a triazole ring. Tr stands for the triazole.

[b]Percentage determined by HPLC at 220 nm from the crude reaction mixture.

Table 5.10. *Synthesis of cyclic peptidotriazoles derived from the alkynyl resin* ***9****.*

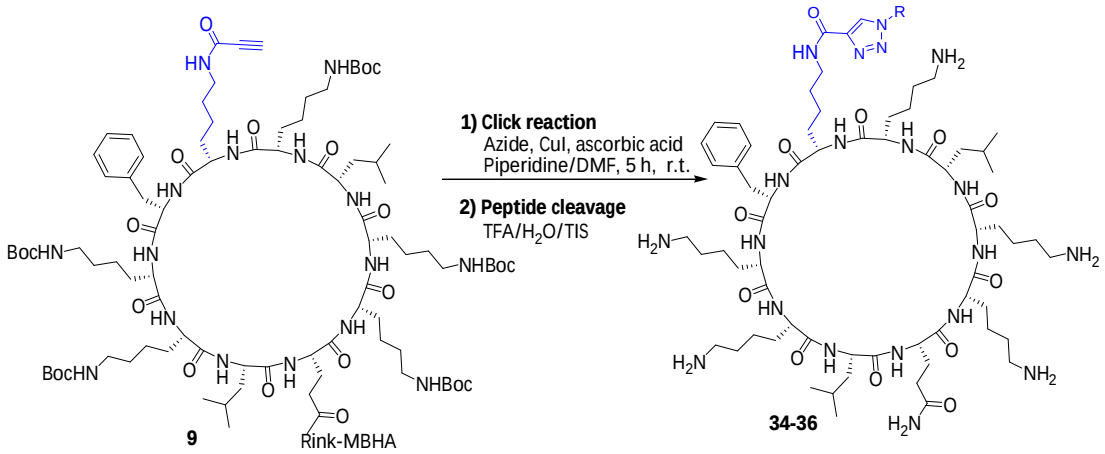

Azide	Peptidotriazole	Notation[a]	R	Purity[b] (%)
NaN_3	**34**	Lys(CO-Tr)	H	76
BnN_3	**35**	Lys(CO-Tr-Bn)	Bn	86
Boc-Nle(ε-N_3)-OH	**36**	Lys(CO-Tr-Ahx)	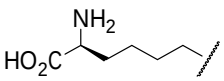	83

[a]The notation defines the amino acid modified with a triazole ring. Tr stands for the triazole.

[b]Percentage determined by HPLC at 220 nm from the crude reaction mixture.

5.3.2. Synthesis of cyclic peptidotriazoles from azido peptidyl resins 10 and 11

We first attempted the click reaction between the linear azido peptidyl resin **26** and several alkynes (Table 5.11). Thus, **26** was treated with the corresponding alkyne (5 equiv) in presence of ascorbic acid (5 equiv) and CuI (5 equiv) in piperidine/DMF (2:8) for 5 h at room temperature. After cleavage, peptidotriazoles **BP253** and **BP254** were obtained in excellent purities (96 and 99 %, respectively). In contrast, in the crude mixtures resulting from the reaction of **26** with propiolic acid and ethyl propiolate, the corresponding expected peptidotriazoles were not observed (Table 5.11).

Table 5.11. *Synthesis of peptidotriazoles derived from the azidopeptidyl resin* ***26****.*

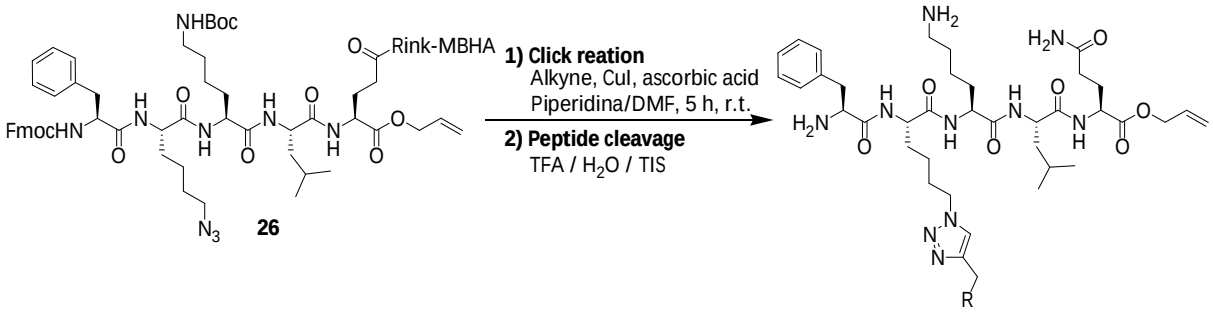

Alkyne	Peptide	R	Purity[a] (%)
1-Heptyne	**BP253**	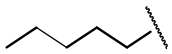	96
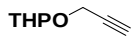	**BP254**		99
Propiolic acid	-		-
Ethyl propiolate	-	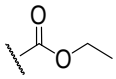	-

[a]Percentage determined by HPLC at 220 nm from the crude reaction mixture.

With these results in hand, we proceeded to synthesize peptidotriazoles derived from the cyclic azido peptidyl resins **10** and **11** containing the Nle(ε-N_3) at positions 3 and 5, respectively. The alkynes that were used are depicted in Table 5.12 and 5.13. The corresponding cyclic peptidotriazoles were obtained in good to excellent purities (76-99 %).

Table 5.12. *Synthesis of cyclic peptidotriazoles from the azido peptidyl resin* ***10****.*

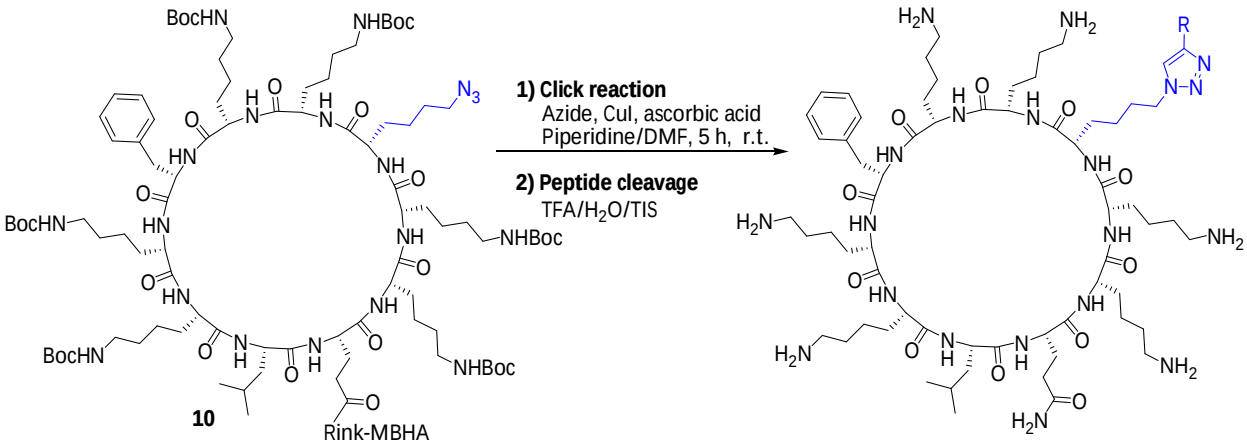

Alkyne	Peptide	Notation[a]	R	Purity[c] (%)
1-Heptyne[b]	**BPC470**	Lys(Tr-C_5H_{11})	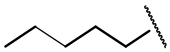	99
Phenylacetylene	**BPC516**	Lys(Tr-Ph)		97
***p*-Ethynylaniline**	**BPC538**	Lys(Tr-C_6H_4-NH_2)	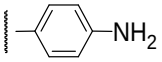	95
***p*-Ethynyltoluene**	**BPC548**	Lys(Tr-C_6H_4-Me)	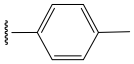	95
***p*-Ethynylanisole**	**BPC550**	Lys(Tr-C_6H_4-OMe)	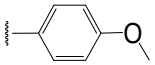	86
***p*-Ethynylpentylbenzene**	**BPC546**	Lys(Tr-C_6H_4-C_5H_{11})	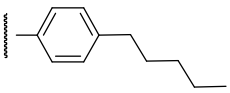	81
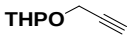	**BPC552**	Lys(Tr-CH_2-OH)		90

[a]The notation defines the amino acid modified with a triazole ring. Tr stands for the triazole.

[b]Reaction time: 1 x 5 + 2 x 8 h

[c]Percentage determined by HPLC at 220 nm from the crude reaction mixture.

Peptidotriazoles derived either from an azido or alkynyl peptidyl resin were obtained in similar purities. In general, better purities were observed when the click reaction was performed at the residue at position 3.

Table 5.13. *Synthesis of cyclic peptidotriazoles from the azido peptidyl resin* ***11****.*

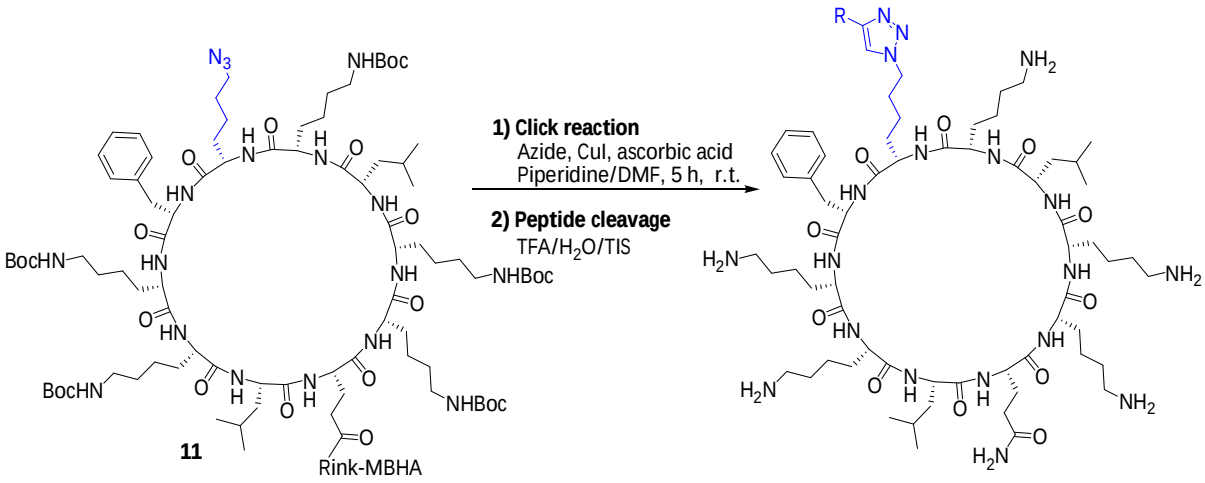

Alkyne	Peptide	Notation[a]	R	Purity[b] (%)
1-Heptyne	**BPC570**	Lys(Tr-C_5H_{11})	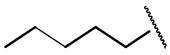	94
Phenylacetylene	**BPC562**	Lys(Tr-Ph)		90
***p*-Ethynylaniline**	**BPC572**	Lys(Tr-C_6H_4-NH_2)	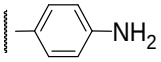	90
***p*-Ethynyltoluene**	**BPC556**	Lys(Tr-C_6H_4-Me)	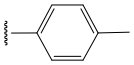	85
***p*-Ethynylanisole**	**BPC558**	Lys(Tr-C_6H_4-OMe)	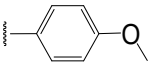	95
***p*-Ethynylpentylbenzene**	**BPC554**	Lys(Tr-C_6H_4-C_5H_{11})	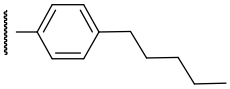	76
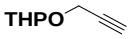	**BPC560**	Lys(Tr-CH_2-OH)		96

[a]The notation defines the amino acid modified with a triazole ring. Tr stands for the triazole.

[b]Percentage determined by HPLC at 220 nm from the crude reaction mixture.

5.4. Synthesis of conjugated peptidotriazoles

5.4.1. Conjugation under standard conditions

Once we had optimized the reaction conditions for the synthesis of cyclic peptides containing a triazole ring, we decided to apply these conditions to the synthesis of conjugated peptidotriazoles by linking the cyclic alkynyl peptidyl resin **5** to an

azidopeptide unit through a triazole ring. This resin was selected because it was easy to prepare and provided peptidotriazoles in good purities.

First, we performed the click reaction between resin **5** and the linear azidopentapeptide **BP252** (Figure 5.5) (5 equiv). We carried out the reaction using the previously described conditions but under stirring for 7 h (Scheme 5.28). The conjugated peptide **BPC472** was cleaved from the resin with TFA/H_2O/TIS (95:2.5:2.5) and analyzed by HPLC and mass spectrometry, being obtained in 98 % purity.

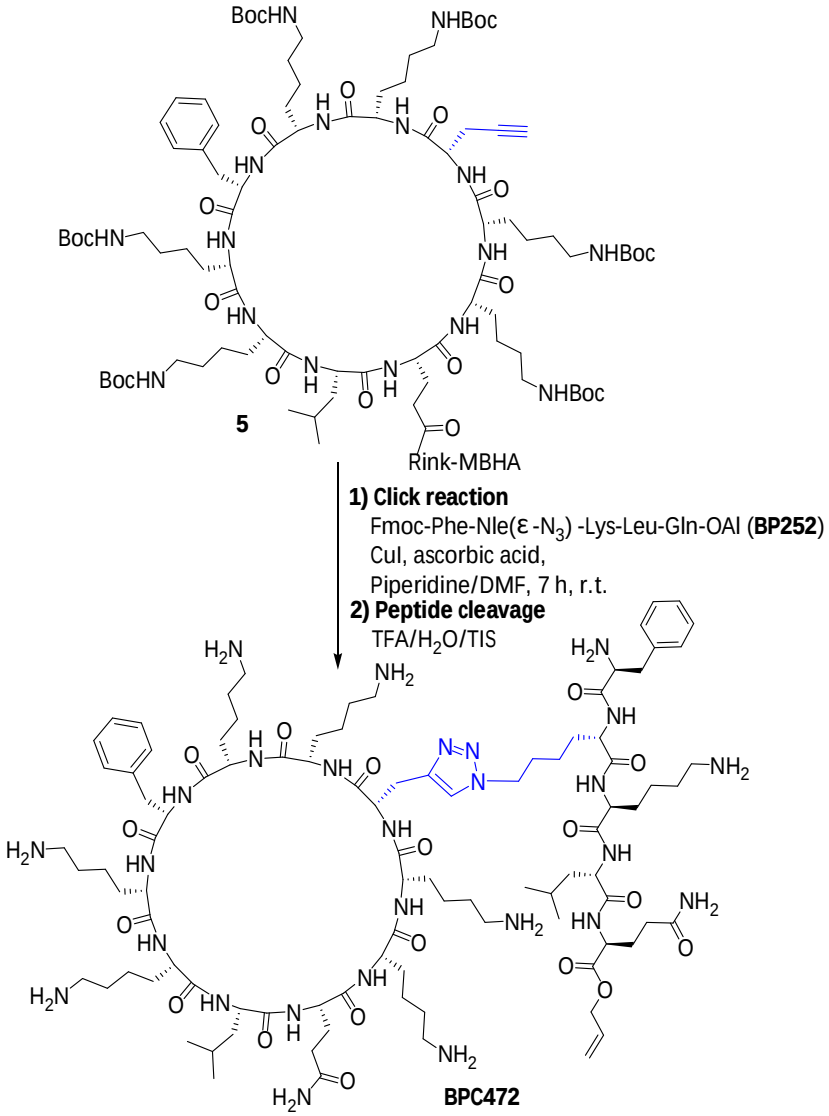

Scheme 5.28. *Synthesis of the conjugated peptide* ***BPC472****.*

With these results in hand, and considering that the goal of this chapter was to synthesize a multivalent peptide, we studied the conjugation of the alkynyl resin **5** with

the linear azido undecapeptide **BP304** (Figure 5.6) and the cyclic azidopeptide **BPC464** (Figure 5.6).

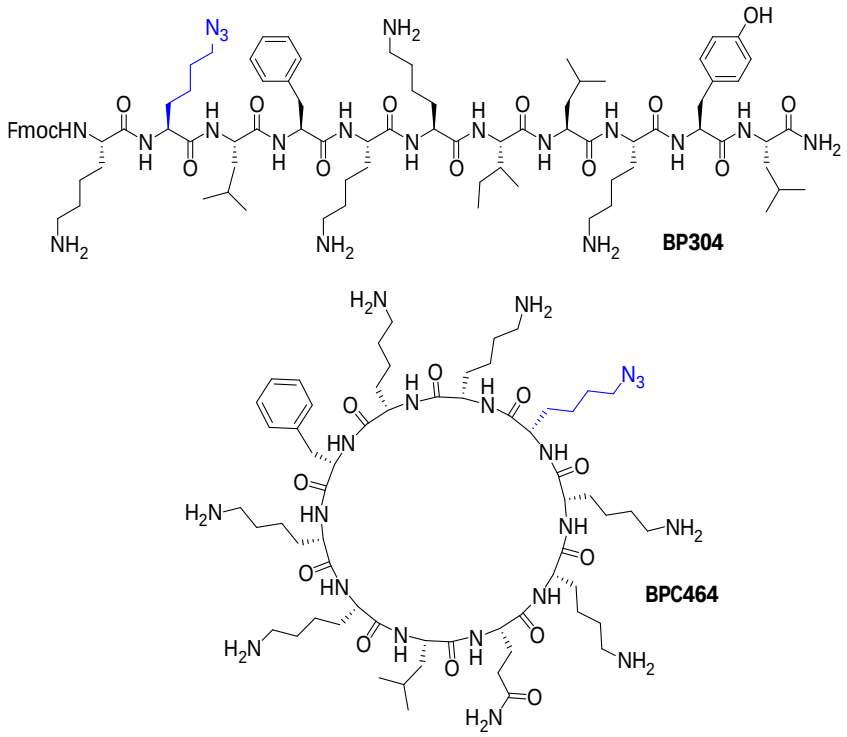

Figure 5.6. *Structures of the linear azidopeptide* ***BP304*** *and the cyclic azidopeptide* ***BPC464****.*

BP304 derives from the lead antimicrobial peptide **BP100** but it contains a Nle(ε-N_3) at position 2. This peptide was synthesized using the general Fmoc/^{t}Bu strategy. The azido moiety was introduced as Fmoc-Nle(ε-N_3)-OH during the on-resin peptide synthesis (Scheme 5.29). The resin was cleaved with TFA/H_2O/TIS (95:2.5:2.5) and the crude mixture was analyzed by HPLC and mass spectrometry. **BP304** was obtained in 82 % HPLC purity.

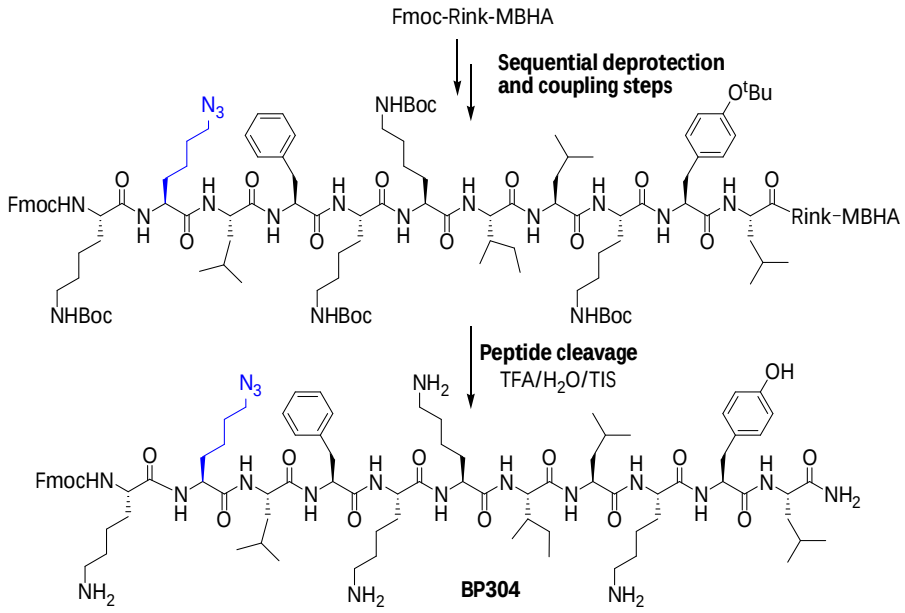

Scheme 5.29. *Synthesis of azidopeptide* ***BP304****.*

We then attempted the click reaction between the alkynyl resin **5** and **BP304** using the conditions for the synthesis of **BPC472** (Scheme 5.30). After cleavage, HPLC and mass spectrometry analysis only showed the presence of the starting cyclic peptide **BPC466.**

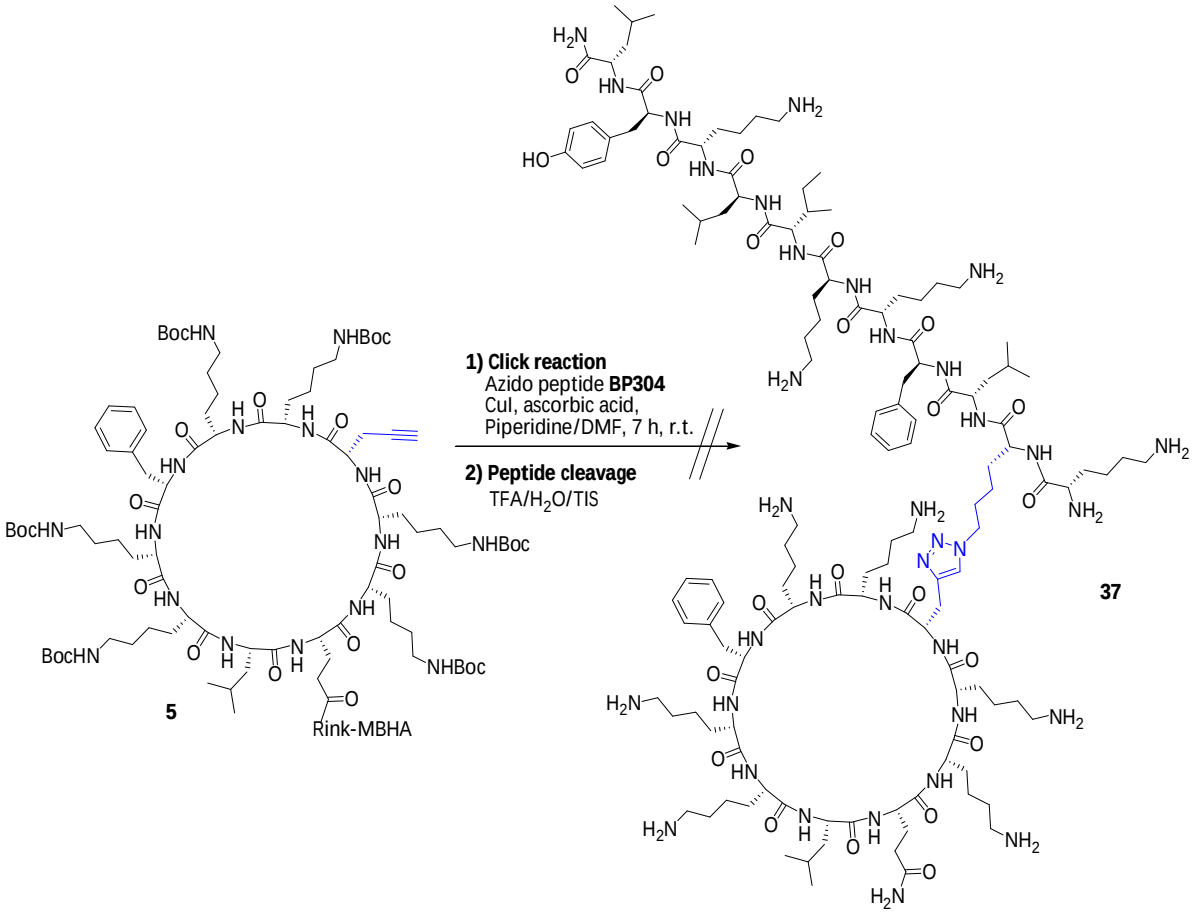

Scheme 5.30. *Attempt to synthesize the conjugated peptide* ***37****.*

Similarly, resin **5** was treated with the cyclic azidopeptide **BPC464** (Scheme 5.31). Unfortunately, this reaction did not afford the desired multivalent peptide **38**. After cleavage, HPLC and mass spectrometry analysis only showed the presence of the starting cyclic peptide **BPC466**.

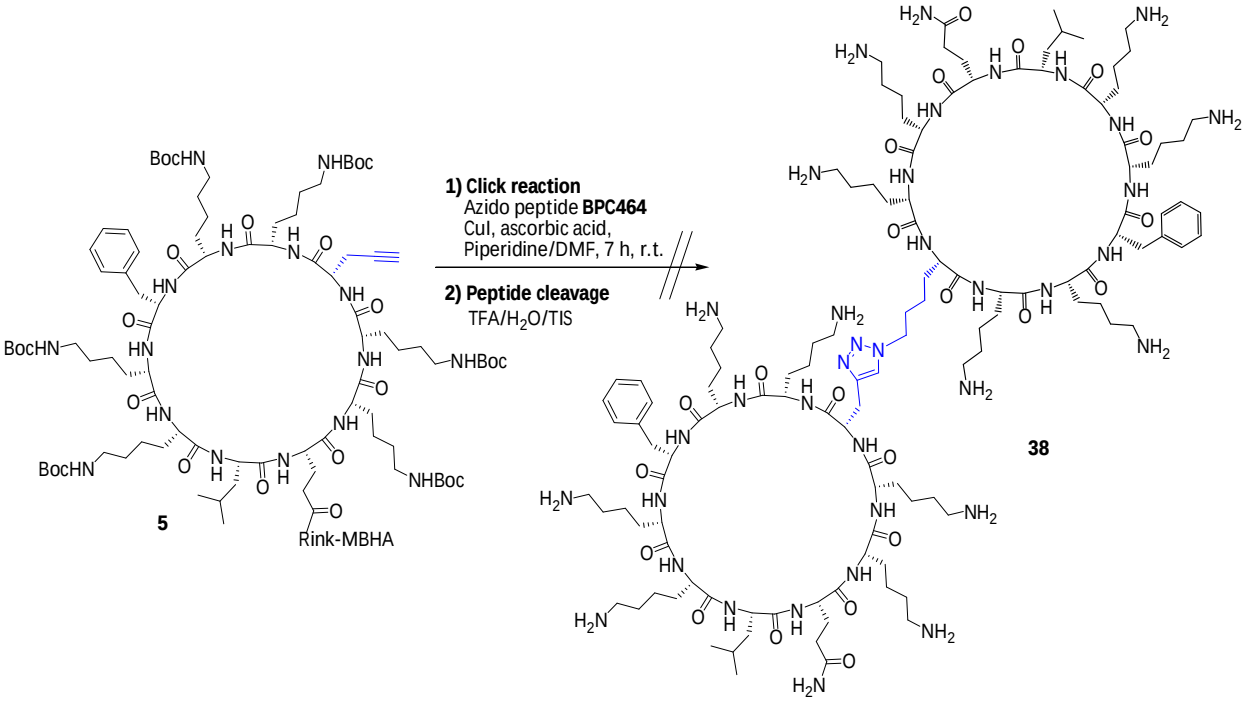

Scheme 5.31. *Attempt to synthesize the multivalent peptide* ***38.***

5.4.2. Conjugation under microwave irradiation

Since the synthesis of the conjugated peptides **37** and **38** failed, we thought that microwaves could promote the conjugation of the peptidyl units. The microwave-assisted organic synthesis is a relatively new technique, the use of which has experienced significant growth in recent years both in academic and industry fields (Appukkuttan 2008). Recently, it has been shown that microwave irradiation can be applied to many types of organic transformations and offers several advantages. The microwave irradiation accelerates reactions and increases the yield and purity of the final products. This reduction in the reaction time is explained by the heating process. Microwave irradiation produces efficient internal heating resulting from the interaction of microwaves with solvents, reagents and catalysts present in the reaction mixture. Since the reactors used for these reactions are usually made of transparent

materials to microwaves, such as quarts or Teflon, this type of irradiation causes an increase in temperature on the entire volume simultaneously (Kappe 2004).

We first assayed the reaction of the alkynyl resin **5** with BnN_3 in presence of CuI and ascorbic acid in piperidine/DMF under microwave irradiation at 80 °C for 30 min, using BnN_3 as azide (Scheme 5.32). After this time, the resin was treated with TFA/H_2O/TIS for 2 h and the resulting crude was analyzed by HPLC and mass spectrometry. Peptidotriazole **BPC458** was obtained in 99 % purity. Comparing this result with the one obtained at room temperature, we observed that microwaves reduced the reaction time from 5 h to 30 min giving the final product in similar purity.

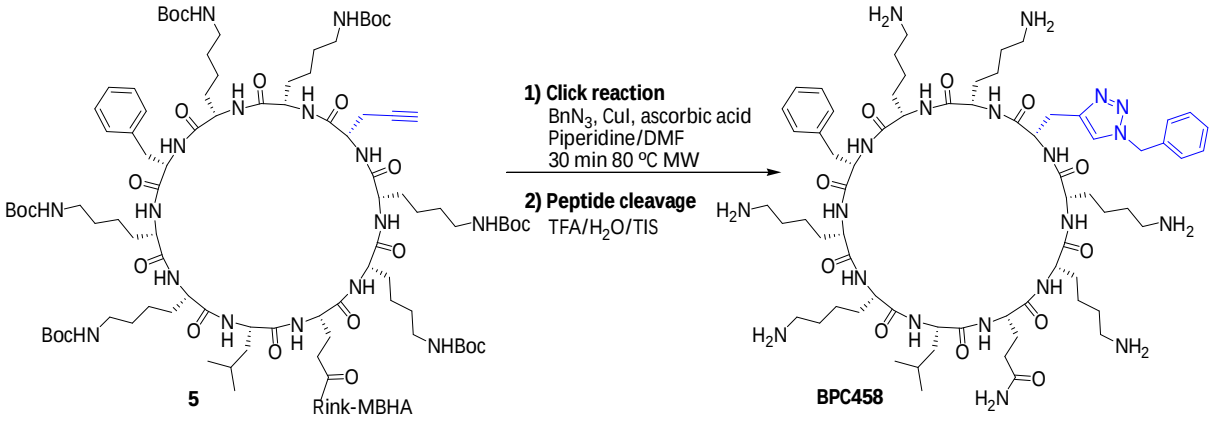

Scheme 5.32. *Synthesis of* ***BPC458*** *under microwave irradiation.*

Thus, the click reaction for the formation of the conjugated peptide **BPC472** was also conducted under microwave irradiation at 80 °C for 30 min (Scheme 5.33). After the experiment, acydolytic cleavage of the resin afforded **BPC472** in 99 % purity, being this result similar to that obtained at room temperature.

The synthesis of the multivalent peptide **38** under microwave irradiation is in progress.

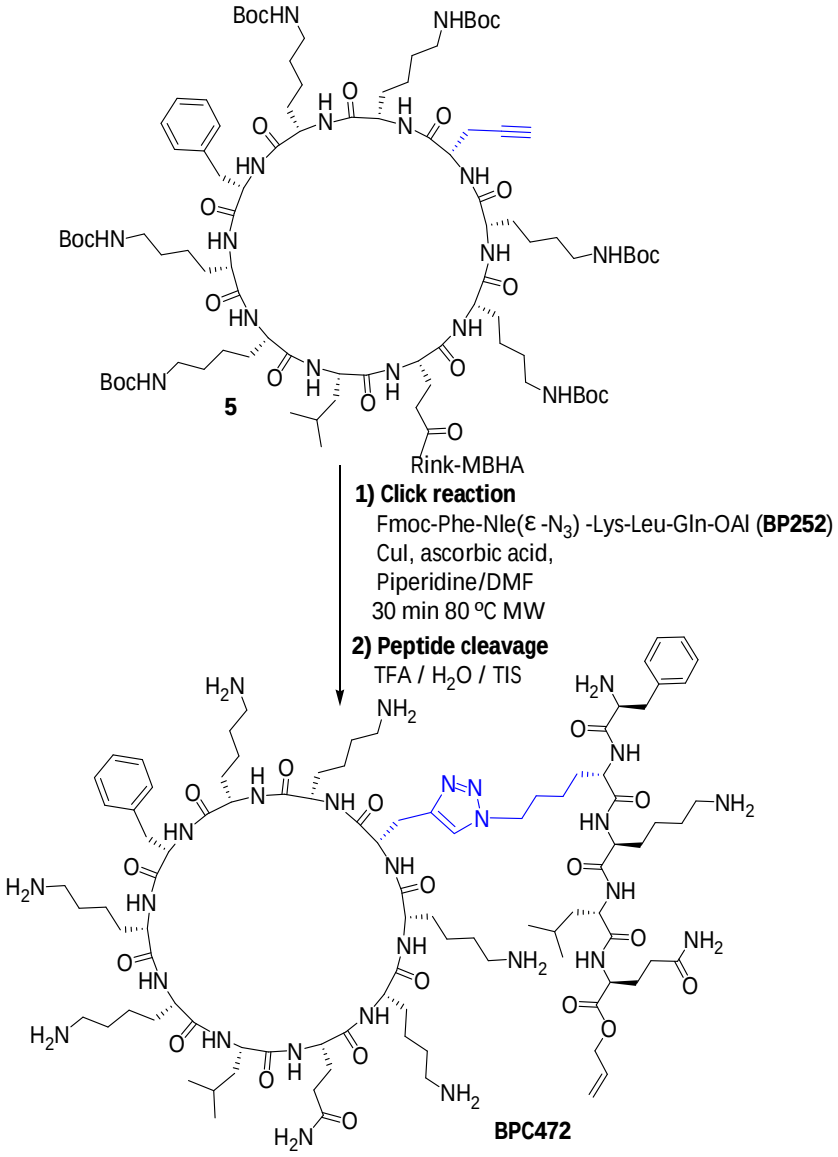

***Scheme 5.33**. Synthesis of **BPC472** under microwave irradiation.*

5.5. Antibacterial activity assays

Peptidotriazoles were tested for *in vitro* growth inhibition of: **(i)** the plant pathogenic bacteria *E. amylovora*, *P. syringae* and *X. vesicatoria* at 3.1, 6.2, 12.5, 25 and 50 μM; **(ii)** the human pathogenic bacteria *E. coli* and *S. aureus* at 6.2, 12.5, 25 and 50 μM; **(iii)** the biocontrol agents *L. mesenteroides* and *B. subtilis* at 6.2, 12.5, 25 and 50 μM. The results were compared to those obtained for **BPC194** (Figure 5.1) and for the corresponding parent peptide **BPC466** (Scheme 5.12), **BPC574** (Scheme 5.13), **BPC464**

(Scheme 5.26) or **BPC576** (Scheme 5.27). All these tests were performed by Dr. Esther Badosa of the Plant Pathology group at the UdG.

5.5.1. Cyclic peptidotriazoles bearing a triazolylalanine or a triazolyl-modified glutamine

We evaluated the antibacterial activity of the cyclic peptidotriazoles containing a triazolylalanine residue and we compared it to that of **BPC466** (Scheme 5.12) and **BPC574** (Scheme 5.13), bearing a propargylglycine. The antibacterial activity of cyclic peptidotriazoles incorporating a triazolyl-modified glutamine was also analyzed.

The evaluation of the antibacterial activity of **BPC466** and of the corresponding cyclic peptidotriazoles bearing a triazolylalanine at position 3 (Table 5.6) showed that, in general, these compounds were considerably active against the plant pathogenic bacteria *P. syringae* and *X. vesicatoria* (Table 5.14). They exhibited similar activity than the parent peptide **BPC194** (Figure 5.1), with seven out of nine sequences displaying MIC <12.5 μM against these two pathogens. *E. amylovora* was the least sensitive bacteria to these peptides, with five sequences exhibiting MIC values of 25 to 50 μM. Regarding these plant pathogenic bacteria, the introduction of the triazole ring did not significantly influence the antibacterial activity compared to **BPC466**, except for **BPC460** (Ala(Tr-Ahx)) which activity decreased dramatically. This decrease may be attributed to the presence of two highly polar groups (NH_2 and OH) in the triazole ring substituent. Moreover, the conjugated peptidotriazole **BPC472** (Scheme 5.33**)** resulted to be only active against *X. vesicatoria* (MIC= 3.1-6.2 μM).

Against human bacteria, MIC values were higher than those obtained for phytopathogenic bacteria (Table 5.14). In this case, most sequences exhibited MIC values >50 μM and only three out of nine sequences displayed a MIC of 25 to 50 μM against *E. coli*.

These peptides also exhibited low activity against the biocontrol agents *L. mesenteroides* and *B. subtilis*. The latter was more sensitive with six sequences displaying MIC values of 25 to 50 μM.

Table 5.14. *Antimicrobial activity (MIC) of* ***BPC466*** *and cyclic peptidotriazoles bearing a triazolylalanine at position 3.*

Peptide	Sequence	Notation[a]	MIC (μM)						
			Xv[b]	*Ea*[b]	*Ps*[b]	*Ec*[b]	*Sa*[b]	*Lm*[b]	*Bs*[b]
BPC194	c(KKLKKFKKLQ)	-	3.1-6.2	6.2-12.5	3.1-6.2	12.5-25	>50	>50	>50
BPC466	c(KK**Prg**KKFKKLQ)	-	<3.1	25-50	3.1-6.2	>50	>50	>50	25-50
BPC456	c(KK**X**KKFKKLQ)	Ala(Tr)	6.2-12.5	>50	6.2-12.5	>50	>50	>50	>50
BPC458	c(KK**X**KKFKKLQ)	Ala(Tr-Bn)	6.2-12.5	>50	6.2-12.5	>50	>50	>50	25-50
BPC518	c(KK**X**KKFKKLQ)	Ala(Tr-C_6H_4-NH_2)	3.1-6.2	25-50	12.5-25	>50	>50	>50	25-50
BPC460	c(KK**X**KKFKKLQ)	Ala(Tr-Ahx)	25-50	>50	>50	>50	>50	>50	>50
BPC540	c(KK**X**KKFKKLQ)	Ala(Tr-C_6H_4-Me)	6.2-12.5	25-50	3.1-6.2	25-50	>50	>50	25-50
BPC542	c(KK**X**KKFKKLQ)	Ala(Tr-C_6H_4-OMe)	3.1-6.2	25-50	3.1-6.2	25-50	>50	>50	25-50
BPC544	c(KK**X**KKFKKLQ)	Ala(Tr-Ph)	3.1-6.2	25-50	3.1-6.2	25-50	>50	>50	25-50
BPC472	c(KK**X**KKFKKLQ)	Ala(Tr-BP252)	3.1-6.2	>50	>50	>50	>50	>50	>50

[a]The notation defines the amino acid modified with a triazole ring. Tr stands for the triazole.

[b]*Xv, Xanthomonas vesicatoria; Ea, Erwinia amylovora; Ps, Pseudomonas syringae; Ec, Escherichia coli; Sa, Staphylococcus aureus; Lm, Leuconostoc mesenteroides; Bs, Bacillus subtilis*.

The antibacterial activity against plant pathogenic bacteria of **BPC574** (Scheme 5.13) and the corresponding cyclic peptidotriazoles bearing a triazolylalanine at position 5 (Table 5.7) followed a similar pattern than that observed for derivatives modified at position 3 (Table 5.15). *E. amylovora* was the least sensitive pathogen. However, three sequences displayed MIC values of 12.5 to 25 μM against this pathogen. *X. vesicatoria* was the most sensitive with six out of seven sequences diplaying MIC <6.2 μM. Similarly to derivatives bearing a triazolylalanine at position 3, the introduction of a triazole at position 5 did not significantly influence the activity. In this case, **BP512** (Ala(Tr-Ahx)) was not active against *E. amylovora* and *P. syringae*.

Analysis of the antibacterial activity against human bacteria showed that these derivatives were less active than against the phytopathogenic bacteria *P. syringae and X. vesicatoria* (Table 5.15). Interestingly, unlike peptidotriazoles with a triazolylalanine at position 3, these analogues were active against *E. coli,* with five out of seven sequences as active as **BPC194** (MIC= 12.5-25 μM).

In general, these cyclic peptidotriazoles were not active against the biocontrol agents *L. mesenteroides* and *B. subtilits* (Table 5.15). The lowest MIC (12.5-25 μM) was obtained for **BPC510** against *B. subtilis*.

Table 5.15. *Antimicrobial activity (MIC) of* ***BPC574*** *and cyclic peptidotriazoles bearing a triazolylalanine at position 5.*

Peptide	Sequence	Notation[a]	MIC (μM)						
			Xv[b]	*Ea*[b]	*Ps*[b]	*Ec*[b]	*Sa*[b]	*Lm*[b]	*Bs*[b]
BPC194	c(KKLKKFKKLQ)	-	3.1-6.2	6.2-12.5	3.1-6.2	12.5-25	>50	>50	>50
BPC574	c(KKLK**Prg**FKKLQ)	-	3.1-6.2	12.5-25	6.2-12.5	25-50	>50	>50	>50
BPC510	c(KKLK**X**FKKLQ)	Ala(Tr-Bn)	3.1-6.2	12.5-25	12.5-25	12.5-25	>50	>50	12.5-25
BPC514	c(KKLK**X**FKKLQ)	Ala(Tr-C_6H_4-NH_2)	<3.1	25-50	12.5-25	12.5-25	>50	>50	25-50
BPC512	c(KKLK**X**FKKLQ)	Ala(Tr-Ahx)	<3.1	>50	25-50	12.5-25	>50	>50	>50
BPC564	c(KKLK**X**FKKLQ)	Ala(Tr-C_6H_4-Me)	3.1-6.2	25-50	6.2-12.5	12.5-25	>50	>50	25-50
BPC566	c(KKLK**X**FKKLQ)	Ala(Tr-C_6H_4-OMe)	6.2-12.5	25-50	6.2-12.5	25-50	>50	>50	25-50
BPC568	c(KKLK**X**FKKLQ)	Ala(Tr-Ph)	3.1-6.2	12.5-25	3.1-6.2	12.5-25	>50	>50	25-50

[a]The notation defines the amino acid modified with a triazole ring. Tr stands for the triazole.

[b]*Xv, Xanthomonas vesicatoria; Ea, Erwinia amylovora; Ps, Pseudomonas syringae; Ec, Escherichia coli; Sa, Staphylococcus aureus; Lm, Leuconostoc mesenteroides; Bs, Bacillus subtilis.*

The antibacterial activity of the peptidotriazoles incorporating a triazolyl-modified glutamine is shown in Table 5.16. In contrast to previous results, **BPC522** (Gln(CH_2-Tr-Ahx)) resulted to be the most active sequence against the three pathogens, displaying a higher activity than **BPC194** against *X. vesicatoria* (MIC <3.1 μM). Peptidotriazoles **BPC532** (Gln(CH_2-Tr)) and **BPC520** (Gln(CH_2-Tr-Bn)) were considerably active against *P. syringae* and *X. vesicatoria.* These cyclic peptidotriazoles were not active against the tested human and biocontrol bacteria. **BPC522** (Gln(Tr-Ahx)) was the only active sequence against the *E.* coli, being as active as the parent peptide **BPC194** (MIC= 12.5-25 μM).

Since the activity of all these cyclic peptidotriazoles is considerably higher against phytopathogenic bacteria than against the biocontrol agents, they can be considered as good candidates for plant protection.

Table 5.16. *Antimicrobial activity (MIC) of cyclic peptidotriazoles bearing a triazolyl-modified glutamine.*

Peptide	Sequence	Notation[a]	MIC (μM)						
			Xv[b]	*Ea*[b]	*Ps*[b]	*Ec*[b]	*Sa*[b]	*Lm*[b]	*Bs*[b]
BPC194	c(KKLKKFKKLQ)	-	3.1-6.2	6.2-12.5	3.1-6.2	12.5-25	>50	>50	>50
BPC532	c(KK**X**KKFKKLQ)	Gln(CH_2-Tr)	12.5-25	>50	6.2-12.5	>50	>50	>50	>50
BPC520	c(KK**X**KKFKKLQ)	Gln(CH_2-Tr-Bn)	3.1-6.2	>50	12.5-25	>50	>50	>50	25-50
BPC522	c(KK**X**KKFKKLQ)	Gln(CH_2-Tr-Ahx)	<3.1	6.2-12.5	6.2-12.5	12.5-25	>50	>50	25-50

[a]The notation defines the amino acid modified with a triazole ring. Tr stands for the triazole.

[b]*Xv, Xanthomonas vesicatoria; Ea, Erwinia amylovora; Ps, Pseudomonas syringae; Ec, Escherichia coli; Sa, Staphylococcus aureus; Lm, Leuconostoc mesenteroides; Bs, Bacillus subtilis*.

5.5.2. Cyclic peptidotriazoles bearing a triazolyllysine

The antibacterial activity of peptidotriazoles containing a triazolyllysine at positions 3 or 5 of the sequence, and of the azido cyclic peptides **BPC464** (Scheme 5.26) and **BPC576** (Scheme 5.27) was analyzed also against phytopathogenic, human and biocontrol bacteria.

The evaluation of the antibacterial activity of **BPC464** (Nle(ε-N_3)) and cyclic peptidotriazoles incorporating a triazolyllysine at position 3 showed that, in general, these peptides were considerably active against the plant pathogenic bacteria *X. vesicatoria* and *P. syringae* (Table 5.17). All sequences exhibited similar activity than the parent peptide **BPC194** displaying MIC <12.5 μM against these two pathogens. Thus, the presence of either an azido moiety or a triazole ring at this position did not affect the antibacterial activity. In contrast, these functional groups decreased the antibacterial activity against *E. amylovora*, and only three sequences exhibited MICs values of 12.5 to 25 μM.

Among the human pathogens, *E. coli* was more sensitive than *S. aureus* with 5 out of 9 sequences exhibiting MIC values of 12.5 to 25 μM, being as active as **BCP194**. Concerning the tested biocontrol agents, *B. subtilis* was more sensitive than *L. mesenteroides* with 4 sequences displaying MICs of 25 to 50 μM.

Table 5.17. *Antimicrobial activity (MIC) of* ***BPC464*** *and cyclic peptidotriazoles bearing a triazolyllysine at position 3.*

Peptide	Sequence	Notation[a]	MIC (μM)						
			Xv[b]	*Ea*[b]	*Ps*[b]	*Ec*[b]	*Sa*[b]	*Lm*[b]	*Bs*[b]
BPC194	c(KKLKKFKKLQ)	-	3.1-6.2	6.2-12.5	3.1-6.2	12.5-25	>50	>50	>50
BPC464	c(KK**K(N_3)**KKFKKLQ)	-	<3.1	25-50	6.25-12.5	12.5-25	>50	>50	>50
BPC470	c(KK**X**KKFKKLQ)	Lys(Tr-C_5H_{11})	3.1-6.2	12.5-25	<3.1	12.5-25	>50	>50	25-50
BPC516	c(KK**X**KKFKKLQ)	Lys(Tr-Ph)	3.1-6.2	25-50	6.2-12.5	>50	>50	>50	25-50
BPC538	c(KK**X**KKFKKLQ)	Lys(Tr-C_6H_4-NH_2)	6.2-12.5	25-50	3.1-6.2	25-50	>50	>50	>50
BPC548	c(KK**X**KKFKKLQ)	Lys(Tr-C_6H_4-Me)	3.1-6.2	12.5-25	3.1-6.2	12.5-25	>50	>50	25-50
BPC550	c(KK**X**KKFKKLQ)	Lys(Tr-C_6H_4-OMe)	3.1-6.2	12.5-25	3.1-6.2	12.5-25	>50	>50	>50
BPC546	c(KK**X**KKFKKLQ)	Lys(Tr-C_6H_4-C_5H_{11})	6.2-12.5	>50	6.2-12.5	12.5-25	>50	>50	25-50
BPC552	c(KK**X**KKFKKLQ)	Lys(Tr-CH_2-OH)	3.1-6.2	25-50	6.2-12.5	>50	>50	>50	>50

[a]The notation defines the amino acid modified with a triazole ring. Tr stands for the triazole

[b]*Xv, Xanthomonas vesicatoria; Ea, Erwinia amylovora; Pss, Pseudomonas. Syringae; Ec, Escherichia coli; Sa, Staphylococcus aureus; Lm, Leuconostoc mesenteroides; Bs, Bacillus subtilis*.

The activity of analogues incorporating an azide or a triazolyllysine at position 5 was slightly better than that observed for those bearing these modifications at position 3 against phytopathogenic bacteria (Table 5.18). The most sensitive plant pathogenic bacteria was *X. vesicatoria* with three sequences being more active than the parent peptide **BPC194** (MIC <3.1 μM) and five out of eight sequences displaying the same activity than **BPC194** (MIC 3.1-6.2 μM). Although *E. amylovora* was the least sensitive bacteria, two sequences displayed similar activity than **BPC194** (MIC 5.2-12.5 μM). Thus, the presence of the triazole ring in these sequences did not influence the antibacterial activity. Moreover, triazole substituents did not cause major differences on the activity.

Analysis of the results obtained against human bacteria revealed that the introduction of either an azido moiety or a triazole ring did not influence the antibacterial activity. All peptides were as active as **BPC194** against *E. coli* (MIC= 12.5-25 μM). These peptidotriazoles displayed low activity against the biocontrol agents. Only **BPC562** showed MIC of 12.5 to 25 μM against *B. subtilis*.

All these peptidotriazoles can be considered good candidates for plant protection because their activity is higher against the plant pathogenic bacteria than against the biocontrol agents.

Table 5.18. *Antimicrobial activity (MIC) of* ***BPC576*** *and cyclic peptidotriazoles bearing a triazolyllysine at position 5.*

Peptide	Sequence	Notation[a]	MIC (μM)						
			Xv[b]	*Ea*[b]	*Ps*[b]	*Ec*[b]	*Sa*[b]	*Lm*[b]	*Bs*[b]
BPC194	c(KKLKKFKKLQ)	-	3.1-6.2	6.2-12.5	3.1-6.2	12.5-25	>50	>50	>50
BPC576	c(KKLK**K(N_3)**FKKLQ)	-	3.1-6.2	12.5-25	3.1-6.2	12.5-25	>50	>50	>50
BPC570	c(KKLK**X**FKKLQ)	Lys(Tr-C_5H_{11})	<3.1	6.2-12.5	6.2-12.5	12.5-25	>50	>50	25-50
BPC562	c(KKLK**X**FKKLQ)	Lys(Tr-Ph)	3.1-6.2	12.5-25	3.1-6.2	12.5-25	>50	>50	12.5-25
BPC572	c(KKLK**X**FKKLQ)	Lys(Tr-C_6H_4-NH_2)	3.1-6.2	25-50	6.2-12.5	12.5-25	>50	>50	25-50
BPC556	c(KKLK**X**FKKLQ)	Lys(Tr-C_6H_4-Me)	<3.1	6.2-12.5	6.2-12.5	12.5-25	>50	>50	25-50
BPC558	c(KKLK**X**FKKLQ)	Lys(Tr-C_6H_4-OMe)	3.1-6.2	12.5-25	6.2-12.5	12.5-25	>50	>50	25-50
BPC554	c(KKLK**X**FKKLQ)	Lys(Tr-C_6H_4-C_5H_{11})	3.1-6.2	12.5-25	6.2-12.5	12.5-25	>50	>50	25-50
BPC560	c(KKLK**X**FKKLQ)	Lys(Tr-CH_2-OH)	<3.1	12.5-25	3.1-6.2	12.5-25	>50	>50	25-50

[a]The notation defines the amino acid modified with a triazole ring. Tr stands for the triazole.

[b]*Xv, Xanthomonas vesicatoria; Ea, Erwinia amylovora; Ps, Pseudomonas. Syringae; Ec, Escherichia coli; Sa, Staphylococcus aureus; Lm, Leuconostoc mesenteroides; Bs, Bacillus subtilis.*

5.6. Hemolytic activity

The toxicity to eukaryotic cells of the cyclic peptidotriazoles was determined as the ability to lyse erythrocytes in comparison to melittin. Percent hemolysis at 150, 250 and 375 μM was tested. All these tests were performed by Dr. Esther Badosa of the Plant Pathology group at the UdG.

5.6.1. Cyclic peptidotriazoles bearing a triazolylalanine or a triazolyl-modified glutamine

We evaluated the hemolytic activity of the alkynyl peptides **BPC466** and **BPC574** and of the corresponding cyclic peptidotriazoles bearing a triazolylalanine at position 3 or 5. Moreover, we evaluated the hemolytic activity of peptidotriazoles **BPC532**, **BPC520** and **BPC522** containing a triazolyl-modified glutamine at position 3.

The analysis of the influence of the presence of a propargylglycine or of a triazolylalanine at position 3 pointed out that these modifications significantly decreased the hemolytic activity (Table 5.19). All peptides showed ≤6 % hemolysis at 375 μM.

Table 5.19. *Cytotoxicity of* ***BPC466*** *and of cyclic peptidotriazoles bearing a triazolylalanine at position 3.*

Peptide	Sequence	Notation[a]	Hemolysis[b] (%)		
			150 µM	250 µM	375 µM
BPC194	c(KKLKKFKKLQ)	-	7 ± 0.6	9 ± 0.6	17 ± 1.7
BPC466	c(KK**Prg**KKFKKLQ)	-	1 ± 0.5	1 ± 0.5	1 ± 0.06
BPC456	c(KK**X**KKFKKLQ)	Ala(Tr)	0 ± 1	3 ± 0.3	6 ± 0.5
BPC458	c(KK**X**KKFKKLQ)	Ala(Tr-Bn)	2 ± 0.3	3 ± 0.5	5 ± 0.2
BPC518	c(KK**X**KKFKKLQ)	Ala(Tr-C_6H_4-NH_2)	1 ± 0.07	1 ± 0.07	1 ± 0.1
BPC460	c(KK**X**KKFKKLQ)	Ala(Tr-Ahx)	0 ± 0.3	0 ± 0.3	0 ± 0.1
BPC540	c(KK**X**KKFKKLQ)	Ala(Tr-C_6H_4-Me)	2 ± 0.5	4 ± 0.4	6 ± 1.0
BPC542	c(KK**X**KKFKKLQ)	Ala(Tr-C_6H_4-OMe)	1 ± 0.6	2 ± 0.2	4 ± 0.4
BPC544	c(KK**X**KKFKKLQ)	Ala(Tr-Ph)	1 ± 0.4	1 ± 0.3	2 ± 0.4
BPC472	c(KK**X**KKFKKLQ)	Ala(Tr)	2 ± 0.3	3 ± 0.4	6 ± 0.3

[a]The notation defines the amino acid modified with a triazole ring. Tr stands for the triazole

[b]Percent hemolysis at 50, 150 and 250 µM plus confidence interval (α = 0.05).

The incorporation of a propargylglicine or a triazolylalanine at position 5 resulted in peptidotriazoles with increased hemolytic activity than the analogue containing these modifications at position 3 (Table 5.20). These cyclic peptides displayed a percentage of hemolysis between 23 and 60 % at 375 µM, except for **BP574** and **BPC512** (Ala(Tr-Ahx)) which showed the lowest hemolysis (9 and 3 % at 375 µM, respectively).

Table 5.20. *Cytotoxicity of* ***BPC574*** *and of cyclic peptidotriazoles bearing a triazolylalanine at position 5.*

Peptide	Sequence	Notation[a]	Hemolysis[b] (%)		
			150 µM	250 µM	375 µM
BPC194	c(KKLKKFKKLQ)	-	7 ± 0.6	9 ± 0.6	17 ± 1.7
BPC574	c(KKLK**Prg**FKKLQ)	-	2 ± 0.1	5 ± 0.5	9 ± 0.5
BPC510	c(KKLK**X**FKKLQ)	Ala(Tr-Bn)	32 ± 2	35 ± 3	40 ± 4
BPC514	c(KKLK**X**FKKLQ)	Ala(Tr-C_6H_4-NH_2)	16 ± 0.9	19 ± 0.8	23 ± 1.7
BPC512	c(KKLK**X**FKKLQ)	Ala(Tr-Ahx)	2 ± 0.07	2 ± 0.2	3 ± 0.4
BPC564	c(KKLK**X**FKKLQ)	Ala(Tr-C_6H_4-Me)	38 ± 0.4	54 ± 3	60 ± 2
BPC566	c(KKLK**X**FKKLQ)	Ala(Tr-C_6H_4-OMe)	28 ± 6	32 ± 2	50 ± 5
BPC568	c(KKLK**X**FKKLQ)	Ala(Tr-Ph)	32 ± 0.6	45 ± 5	53 ± 5

[a]The notation defines the amino acid modified with a triazole ring. Tr stands for the triazole.

[b]Percent hemolysis at 50, 150 and 250 µM plus confidence interval (α = 0.05).

BPC532 and **BPC520**, containing a triazolyl-modified glutamine at position 3, were slightly less hemolytic than **BPC194** (≤4 % at 375 µM) (Table 5.21). The analogue incorporating a triazole substituted with an Ahx residue displayed a high percent hemolysis.

Table 5.21. *Cytotoxicity of cyclic peptidotriazoles bearing a triazolyl-modified glutamine.*

Peptide	Sequence	Notation[a]	Hemolysis[b] (%)		
			150 µM	250 µM	375 µM
BPC194	c(KKLKKFKKLQ)	-	7 ± 0.6	9 ± 0.6	17 ± 1.7
BPC532	c(KK**X**KKFKKLQ)	Gln(CH_2-Tr)	2 ± 0.05	3 ± 0.3	4 ± 0.4
BPC520	c(KK**X**KKFKKLQ)	Gln(CH_2-Tr-Bn)	2 ± 0.1	1 ± 0.1	2 ± 0.2
BPC522	c(KK**X**KKFKKLQ)	Gln(CH_2-Tr-Ahx)	78 ± 0.2	87 ± 0.2	100 ± 6

[a]The notation defines the amino acid modified with a triazole ring. Tr stands for the triazole.

[b]Percent hemolysis at 50, 150 and 250 µM plus confidence interval (α = 0.05).

5.6.2. Cyclic peptidotriazoles bearing a triazolyllysine

Among the derivatives containing an azido moiety or a triazolyllysine at position 3, **BPC464**, **BPC516** (Lys(Tr-Ph)), **BPC538** (Lys(Tr-C_6H_4-NH_2)) and **BPC552** (Lys(Tr-CH_2-OH)) displayed lower hemolysis than **BPC194** (1-8 % vs. 17 % at 375 μM). The rest of sequences resulted to have similar hemolysis than **BPC194**, 18-26 % at 375 μM, except for **BPC546** (Lys(Tr-C_6H_4-C_5H_{11})) which showed a 45 % hemolysis (Table 5.22).

Table 5.22. *Cytotoxicity of **BPC464** and of cyclic peptidotriazoles bearing a triazolyllysine at position 3.*

Peptide	Sequence	Notation[a]	Hemolysis[b] (%)		
			150 μM	250 μM	375 μM
BPC194	c(KKLKKFKKLQ)	-	7 ± 0.6	9 ± 0.6	17 ± 1.7
BPC464	c(KK**K(N_3)**KKFKKLQ)	-	4 ± 0.2	4 ± 0.1	5 ± 0.8
BPC470	c(KK**X**KKFKKLQ)	Lys(Tr-C_5H_{11})	10 ± 1	13 ± 11	18 ± 11
BPC516	c(KK**X**KKFKKLQ)	Lys(Tr-Ph)	5 ± 0.2	6 ± 0.4	8 ± 0.1
BPC538	c(KK**X**KKFKKLQ)	Lys(Tr-C_6H_4-NH_2)	1 ± 0.8	1 ± 0.4	2 ± 0.4
BPC548	c(KK**X**KKFKKLQ)	Lys(Tr-C_6H_4-Me)	12 ± 0.3	24 ± 1	26 ± 4
BPC550	c(KK**X**KKFKKLQ)	Lys(Tr-C_6H_4-OMe)	7 ± 0.8	10 ± 0.8	19 ± 5
BPC546	c(KK**X**KKFKKLQ)	Lys(Tr-C_6H_4-C_5H_{11})	32 ± 8	33 ± 1	45 ± 12
BPC552	c(KK**X**KKFKKLQ)	Lys(Tr-CH_2-OH)	1 ± 0.2	1 ± 0.5	1 ± 1

[a]The notation defines the amino acid modified with a triazole ring. Tr stands for the triazole.

[b]Percent hemolysis at 50, 150 and 250 μM plus confidence interval (α = 0.05).

The incorporation of an azido moiety or a triazolyllysine at position 5 resulted in analogues more hemolytic than those modified at position 3 (Table 5.23). The least hemolytic peptides were **BPC576**, **BPC572** (Lys(Tr-C_6H_4-NH_2)) and **BCP560** (Lys(Tr-CH_2-OH)) incorporating a triazole ring substituted with a polar group, displaying similar hemolytic activity than **BPC194** (15-25 % at 375 μM).

Table 5.23. *Cytotoxicity of* ***BPC576*** *and of cyclic peptidotriazoles bearing a triazolyllysine at position 5.*

Peptide	Sequence	Notation[a]	Hemolysis[b] (%)		
			150 µM	250 µM	375 µM
BPC194	c(KKLKKFKKLQ)	-	7 ± 0.6	9 ± 0.6	17 ± 1.7
BPC576	c(KKLK**K(N_3)**FKKLQ)	-	9 ± 0.8	14 ± 1	15 ± 0.9
BPC570	c(KKLK**X**FKKLQ)	Lys(Tr-C_5H_{11})	70 ± 5	83 ± 4	88 ± 0.3
BPC562	c(KKLK**X**FKKLQ)	Lys(Tr-Ph)	42 ± 5	51 ± 3	58 ± 1
BPC572	c(KKLK**X**FKKLQ)	Lys(Tr-C_6H_4-NH_2)	8 ± 0.2	13 ±0.2	25 ± 5
BPC556	c(KKLK**X**FKKLQ)	Lys(Tr-C_6H_4-Me)	56 ± 1	79 ± 12	72 ± 5
BPC558	c(KKLK**X**FKKLQ)	Lys(Tr-C_6H_4-OMe)	54 ± 4	76 ± 8	90 ± 8
BPC554	c(KKLK**X**FKKLQ)	Lys(Tr-C_6H_4-C_5H_{11})	61 ± 11	68 ± 6	80 ± 5
BPC560	c(KKLK**X**FKKLQ)	Lys(Tr-CH_2-OH)	8 ± 2	12 ± 1	20 ± 0.7

[a]The notation defines the amino acid modified with a triazole ring. Tr stands for the triazole.

[b]Percent hemolysis at 50, 150 and 250 µM plus confidence interval (α = 0.05).

These results are in good agreement with previous studies reporting that an increase of peptide hydrophobicity is related to an increase of the hemolysis (Blondelle 2000; Oh 2000). Peptidotriazoles resulting from the substitution of an apolar residue, such as leucine, at position 3 of **BPC194** by a triazolyl-modified amino acid were less hemolytic than these resulting from the substitution of a polar lysine residue at position 5. Among those peptidotriazoles, the ones bearing a polar substituent at the triazole ring were the least hemolytic.

In summary, we have designed and synthesized **BPC194** analogues containing a triazole ring. The introduction of the triazole ring provided sequences active against the plant or human pathogenic bacteria *X. vesicatoria, E. amylovora*, *P. syringae* and *E. coli*, displaying low antimicrobial activity against biocontrol bacteria and low hemolytic activity, being good candidates to design new antimicrobial agents.

6. SYNTHESIS OF CARBOPEPTIDES

Multivalent peptides have been reported to be more active than the corresponding monomers due to the synergy of monomeric units (Liu 2006; Arnusch 2007). Multivalent peptides can be easily obtained by the synthesis of carbopeptides and carboproteins bearing several copies of a peptide or a protein tethered in a carbohydrate template. Recently, Jensen and co-workers have developed an efficient strategy for the synthesis of carboproteins, in which C-terminal peptide aldehydes are ligated by oxime bond formation to tetra-aminooxyacetyl functionalized monosaccharide templates (Brask 2000; Brask 2001; Tofteng 2007).

Based on this, the aim of this part of this thesis was to evaluate if the assembly of several antimicrobial peptide sequences on a carbohydrate template could provide carbopeptides with improved biological properties. For this purpose, we planned to prepare carbopeptides with four and two units of the lead antimicrobial peptides **BP100** and **BP143** attached to a sugar template using the carbopeptide technology (Figure 6.1). **BP100** (KKLFKKILKYL-NH_2) displayed antibacterial activity with MIC within 2.5-7.5 μM against plant pathogenic bacteria and also showed low hemolysis (22 % at 150 μM). **BP143** (KKLfKKILKYL-NH_2), which is a D-isomer of **BP100**, resulted to be equally active, significantly less hemolytic (2 % at 150 μM) and more stable to protease degradation than **BP100**. The carbohydrates used in this study were the cyclo-dithioerythritol (cDTE) and the α-D-galactopyranoside (Gal*p*) (Figure 6.1).

The resulting carbopeptides were screened for their antibacterial activity against phytopathogenic and human bacteria, and for their hemolytic activity.

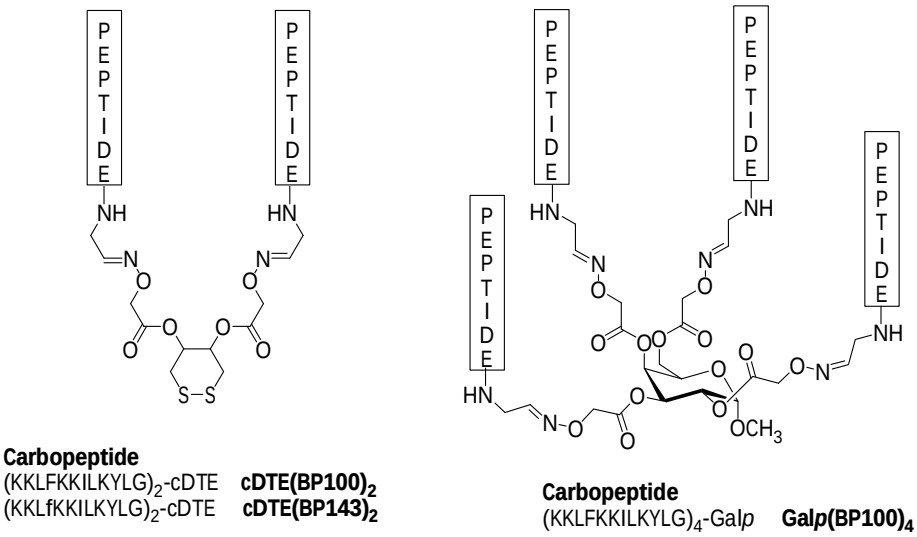

Figure 6.1. *Carbopeptides containing two and four units of peptide.*

6.1. Synthesis of carbopeptides Gal*p*(BP100)$_4$, cDTE(BP100)$_2$ and cDTE(BP143)$_2$

Carbopeptides **Gal*p*(BP100)$_4$**, **cDTE(BP100)$_2$** and **cDTE(BP143)$_2$** were designed and synthesized by linking two or four copies of **BP100** and **BP143** on a cDTE or a Galp template. The strategy for the synthesis of these multivalent structures consisted on the attachment of C-terminal peptide aldehydes derived from **BP100** or **BP143** on multi-aminoxyacetyl functionalized monosaccharide templates **39** and **40** through an oxime ligation reaction (Scheme 6.1). Oxime ligation (Rose 1994) was chosen as the key reaction to combine the carbohydrate and the peptide because this reaction is robust, fast and high yielding (Jensen 2002) (see section 1.4.2.1). Moreover, oximes are stable under neutral to mildly acidic conditions (Shao 1995).

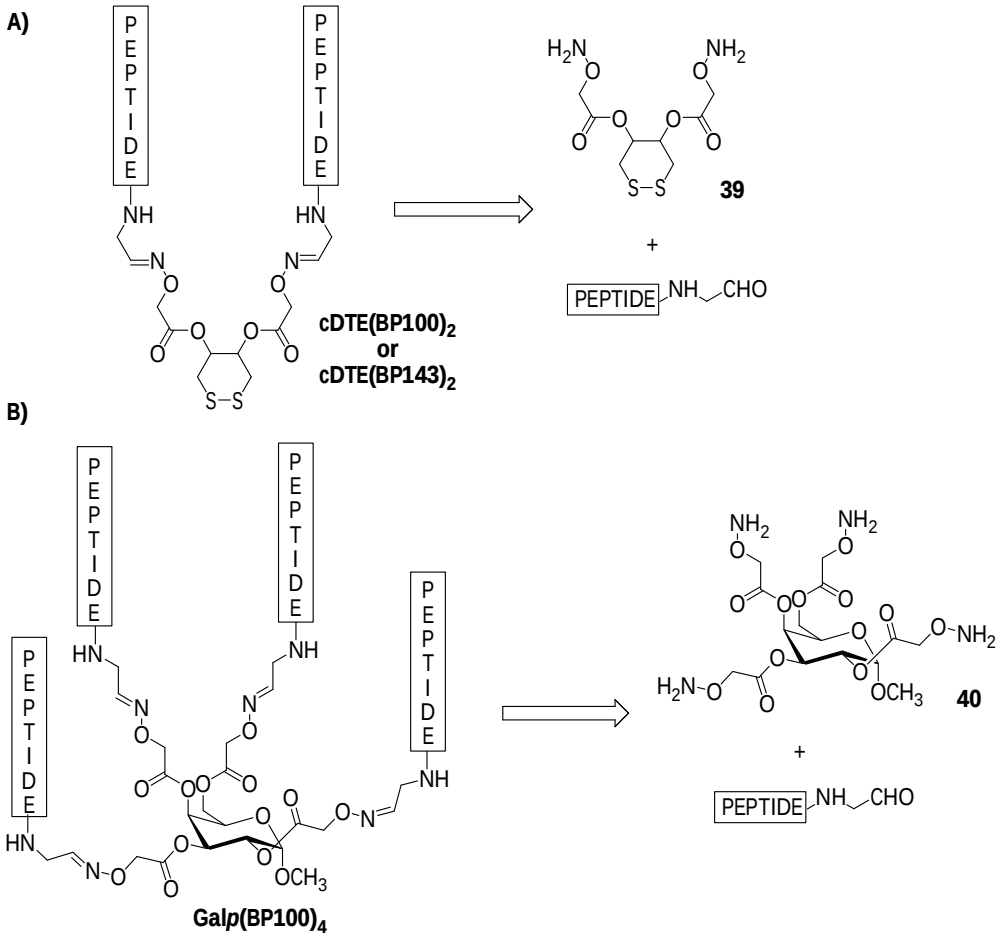

Scheme 6.1. *Retrosynthetic scheme for the preparation of carbopeptides.*

6.1.1. Synthesis of the carbohydrate templates 39 and 40

The carbohydrate templates 4,5-di-*O*-Aoa-cDTE (**39**) and methyl 2,3,4,6-tetra-*O*-Aoa-α-D-Gal*p* (**40**) and were prepared following the methodology previously described in the group of Jensen and co-workers (Figure 6.2) (Brask 2000). In this work, we only needed to perform the synthesis of **39**.

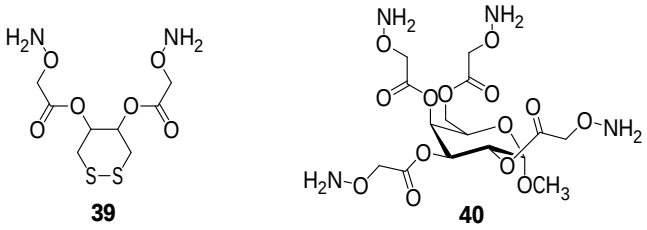

Figure 6.2. *Carbohydrates 4,5-di-*O*-Aoa-cDTE (**39**) and methyl 2,3,4,6-tetra-*O*-Aoa-α-D-Gal*p* (**40**).*

The carbohydrate template **39** was prepared by per-*O*-acylation of cDTE with di-Boc-aminoxyacetic acid (Boc_2-Aoa-OH). The di-Boc protection was necessary to completely remove the nucleophilicity of the nitrogen (Jensen 2002). The Boc-protected aminoxy template **41** was analysed and purified by analytical and preparative HPLC and its structure was confirmed by HPLC, ESI-MS and ^{1}H-NMR. **41** was obtained in 70 % yield (Scheme 6.2). Then, the Boc groups of **41** were removed by treatment with TFA/CH_2Cl_2 (1:1).

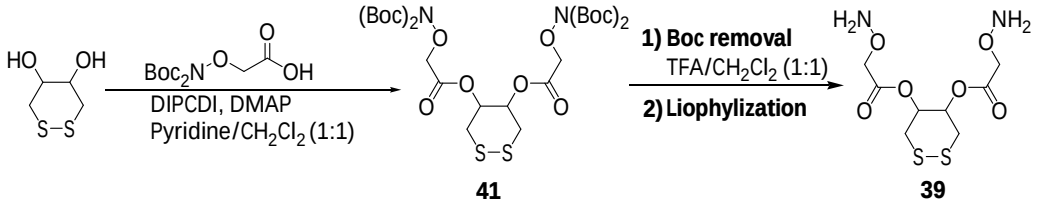

Scheme 6.2. *Preparation of 4,5-di-*O*-Aoa-cDTE (**39**).*

6.1.2. Synthesis of the peptide aldehydes 42 and 43

The C-terminal linear peptide aldehydes derived from **BP100** and **BP143** were synthesized manually by an assisted-microwave irradiation procedure and using a peptide synthesizer. A general Fmoc-strategy was followed using a backbone amide linker (BAL) attached to an amino functionalized TentaGel (TG) resin (Scheme 6.3). This linker incorporates an aldehyde function and allows the linkage to the solid support of amines as well as the synthesis of C-terminal modified peptides. A C-terminal glycinal residue masked as an acetal was anchored to the solid support by reductive amination in the presence of $NaBH_3CN$ at 60 ºC under microwave irradiation. The newly formed secondary amine was then acylated with Fmoc-Leu-OH by treatment with DIPCDI and DCE at 60 ºC under microwave irradiation. The peptide chain was assembled by subsequent Fmoc removal and coupling steps.

Once the chain assembly was completed, the final resin was treated with TFA/H_2O (95:5), which released the peptide from the support, removed the side-chain protecting groups and also hydrolyzed the acetal to an aldehyde. The use of silanes was avoided because aldehydes are likely to be reduced by silanes under acidic conditions (Tofteng 2007). The peptide aldehydes **42** and **43** were analyzed and

purified by HPLC and their structure was confirmed by ESI-MS. Both peptides were obtained in 99 % purity after purification.

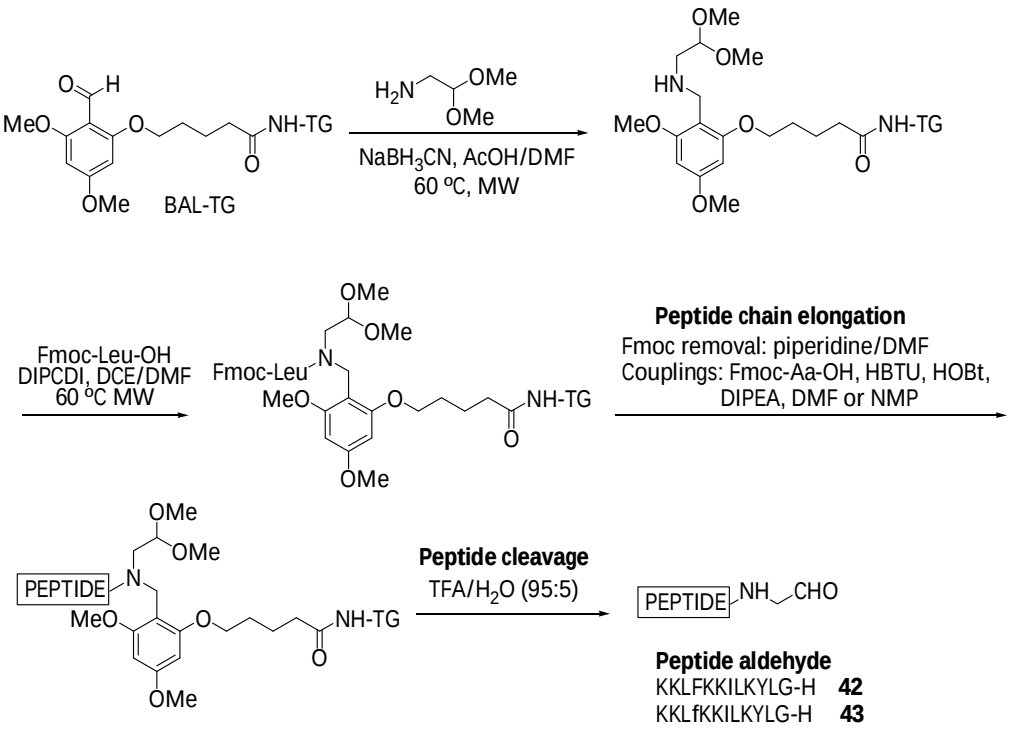

Scheme 6.3. *Synthesis of the peptide aldehydes* ***42*** *and* ***43****.*

6.1.3. Ligation of carbohydrate templates with peptide aldehydes

Carbopeptides **Gal*p*(BP100)$_4$**, **cDTE(BP100)$_2$** and **cDTE(BP143)$_2$** were synthesized by chemoselective oxime ligation between the aminoxy group of the templates **39** and **40**, and the C-terminal aldehyde group of the peptides **42** and **43**.

First of all, and taking into account previous results, we decided to explore the use of aniline in the oxime ligation reaction using carbohydrate **40** and 2-hydroxy-4 methoxybenzaldehyde (Table 6.1). Recently, Dirksen et al. explored the use of aniline as a nucleophilic catalyst for oxime ligations. Rate enhancements of up to three orders of magnitude were achieved enabling reactions to be performed even at low concentrations and neutral pH (Dirksen 2006). Thus, the benzaldehyde and **40** were dissolved in 1:1 solution (1 mL) of ACN and acetate buffer (0.1 M, pH 4.76) without aniline or containing aniline (100 mM).

Table 6.1. *Assays for the oxime ligation reaction of* ***40*** *with a benzaldehyde derivative.*

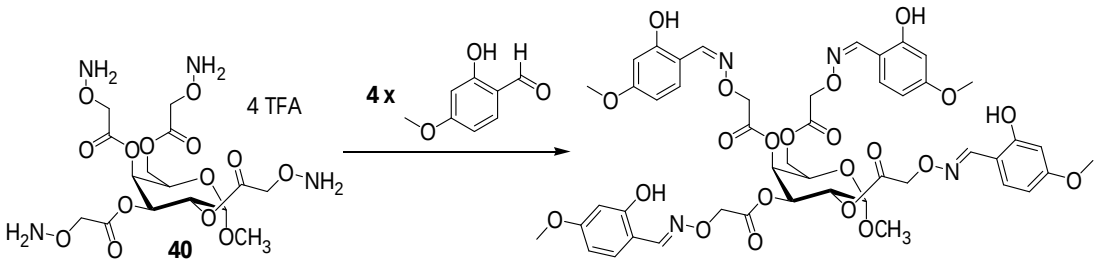

Entry	40 (equiv)	Aldehyde (equiv)	ACN:Buffer[a]	Aniline	Volume (mL)	Time (h)
1	1	5	1:1	-	1	5
2	1	5	1:1	100 mM	1	1.5

[a]Acetate buffer (0.1 M, pH 4.76)

Considering that the reaction time when using aniline was three times shorter and the crude mixture was obtained in a higher purity (Table 6.1, entry 2), the synthesis of carbopeptides were performed using these conditions. However, when these conditions were applied for the synthesis of carbopeptide **Galp(BP100)$_4$** by oxime ligation of peptide **42** with carbohydrate **40**, although increasing the reaction time, the peak of the desired product could not be detected by mass spectrometry (Table 6.2, entries 1 and 2). The synthesis was also assayed without aniline, but the expected product was not observed (Table 6.2, entry 3).

Liophylization of the scaffold after Boc cleavage improved the results either in the presence or in the absence of aniline (Table 6.2, entries 4 and 5). In both cases, the desired carbopeptide was observed but could not be quantified. Thus, we repeated the reaction by adding more peptide after 2 or 3 h (Table 6.2, entries 6 and 7). The best reaction conditions were those described in entry 8, in which more peptide was added dissolved in acetate buffer containing aniline after 2 h. These conditions involved a shorter reaction time than conditions in entry 6 (18 h) and let to a higher purity than that obtained in entry 7. Carbopeptide **Gal*p*(BP100)$_4$** was analyzed and purified by HPLC and its structure was confirmed by ESI-MS, being obtained in 64 % purity.

Table 6.2. *Tests for the preparation of the carbopeptide* ***Galp(BP100)$_4$****.*

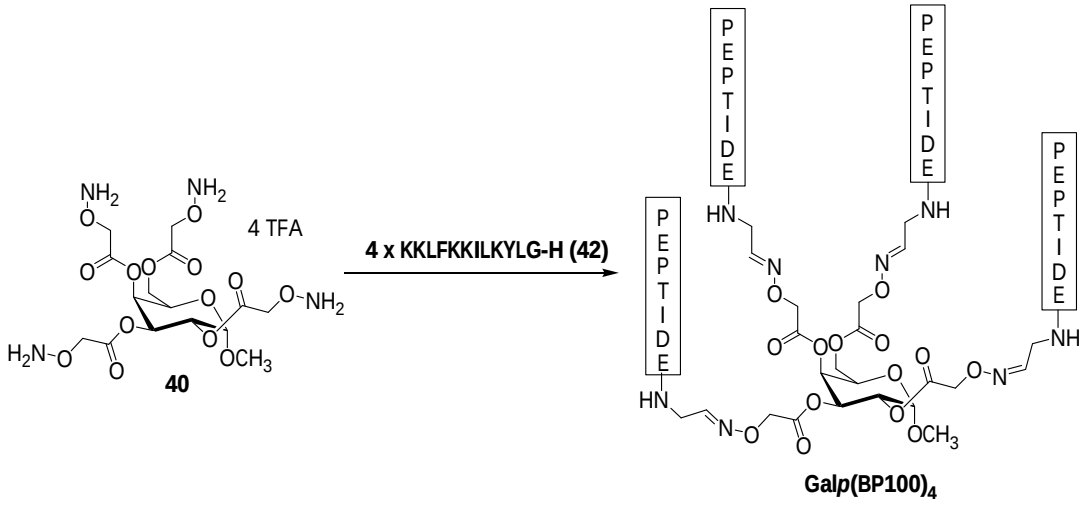

Entry	Template 31 (equiv)	Peptide aldehyde 34 (equiv)	ACN:Buffer[a]	Aniline	Volume (mL)	Time (h)
1	1	1.25	1:1	100 mM	1	48[b]
2	1	1.5	1:9	100 mM	1	18[b]
3	1	1.25	1:1	-	1.2	2[b]
4[c]	1	1.25	1:1	-	1.2	5
5[c]	1	1.25	1:1	100 mM	1.2	5
6[c]	1	1.25	1:1	100 mM	1.2	18[d]
7[c]	1	1.25	1:1	-	1.2	5[e]
8[c]	1	1.25	1:1	-	1.2	5[f]

[a]Acetate buffer (0.1 M, pH 4.76)
[b]No desired product was observed.
[c]The scaffold was liophylized before the ligation.
[d]More peptide was added after 3 h.
[e]More peptide was added after 2 h.
[f]More peptide dissolved in acetate buffer containing aniline was added after 2 h.

The synthesis of carbopeptide **cDTE(BP100)$_2$** was achieved by oxime ligation of carbohydrate **39** with the peptide aldehyde **42** using the conditions described above in Table 6.1, entry 2 (Scheme 6.4). In this case, liophylization of the template did not improve the results. The reaction was followed by HPLC being completed after 3 h. The crude mixture was purified to give **cDTE(BP100)$_2$** in 98 % purity and 42 % yield. The structure was analyzed by HPLC and confirmed by ESI-MS.

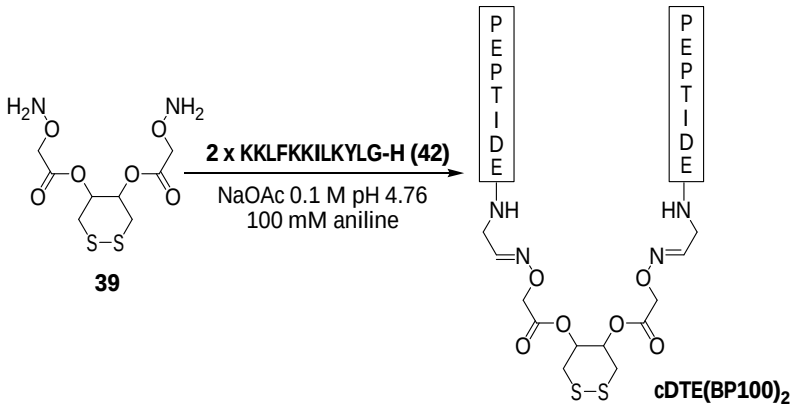

Scheme 6.4. *Synthesis of the carbopeptide* ***cDTE(BP100)$_2$***.

This methodology was extended to the synthesis of carbopeptide **cDTE(BP143)$_2$** containing the peptide aldehyde **43** derived from **BP143** with one D-amino acid in the sequence. The reaction was followed by HPLC being completed after 3 h. The crude mixture was purified to give **cDTE(BP143)$_2$** in 98 % purity and 62 % yield. The structure was analyzed by HPLC and confirmed by ESI-MS.

6.2. Antimicrobial activity

6.2.1. Antimicrobial activity against plant pathogenic bacteria

Carbopeptides were tested for *in vitro* growth inhibition of *E. amylovora*, *P. syringae* and *X. vesicatoria* at 0.6, 1.2, 2.5, 5, 7.5, and 10 μM (Table 6.3). All these tests were performed by Dr. Esther Badosa of the Plant Pathology group at the UdG.

When comparing the MIC values of **BP100** and **BP143** with its corresponding multimeric structures, it should be taken into account that the latter contain multiple copies of the same peptide. Furthermore, whereas **BP100** and **BP143** have a C-terminal amide, carbopeptides **Gal*p*(BP100)$_4$, cDTE(BP100)$_2$** and **cDTE(BP143)$_2$** have a C-terminal glycinal oxime, hence these carbopeptides contain a substituted C-terminal amide. For **cDTE(BP100)$_2$** and **cDTE(BP143)$_2$** we should thus expect at least a two-fold decreased MIC and for **Gal*p*(BP100)$_4$** a four-fold decrease, when the MIC values are given based on concentration, rather than on the concentration of peptide chains. If there is a multimeric effect, the MIC value should be decreased further. **Gal*p*(BP100)$_4$** displayed MIC values from four- to eight-fold lower than the parent peptide. For

cDTE(BP100)$_2$ an increase of the activity was also observed, being two- to eight-fold more active than **BP100**. By contrast, **cDTE(BP143)$_2$** exhibited the same activity than **BP143**. Therefore, for these antimicrobial peptides the multimeric effect depended on the sequence.

Table 6.3. *Antibacterial activity (MIC) of carbopeptides against plant pathogenic bacteria.*

Peptide	MIC (μM)		
	E. amylovora	***X. vesicatoria***	***P. syringae***
BP100	7.5-10	5-7.5	5-7.5
Gal*p*(BP100)$_4$	1.2-2.5	0.6-1.2	0.6-1.2
cDTE(BP100)$_2$	2.5-5	0.6-1.2	1.2-2.5
BP143	2.5-5	5-7.5	2.5-5
cDTE(BP143)$_2$	2.5-5	2.5-5	2.5-5

6.2.2. Antimicrobial activity against human pathogens

Carbopeptides were tested for *in vitro* growth inhibition of *E. coli*, *S. aureus, S. typhimurium* and *L. monocytogenes* at 1.2, 2.5, 5, 7.5, 10 and 20 μM, and compared to the parent peptide (**BP100** or **BP143**) (Table 6.4). All these tests were performed by Dr. Esther Badosa of the Plant Pathology group at the UdG. As shown in Table 6.4, MIC values obtained for human bacteria were higher than those for the phytopathogenic bacteria. Carbopeptides were considerably active against the four pathogens, improving the antimicrobial activity of the parent peptides against at least three bacteria. However, two- to four-fold decrease of MIC was not generally observed.

Regarding the pathogen, *E. coli* was the most sensitive to these carbopeptides displaying MIC values of 1.2 to 2.5 μM. The bacterium *S. aureus* was the least sensitive, only the cDTE derivatives showed MICs of 10 to 20 μM, being more active than the parent peptide.

Table 6.4. *Antibacterial activity (MIC) of carbopeptides against human bacteria.*

Peptide	MIC (μM)			
	E. coli	***S. aureus***	***L. monocytogenes***	***S. typhimurium***
BP100	2.5-5	>20	>10	5-10
Gal*p*(BP100)$_4$	1.2-2.5	>20	5-7.5	2.5-5
cDTE(BP100)$_2$	2.5-5	10-20	5-7.5	2.5-5
BP143	10-20	>20	>20	5-7.5
cDTE(BP143)$_2$	1.2-2.5	10-20	7.5-10	2.5-5

6.3. Hemolytic activity

The toxicity to eukaryotic cells of carbopeptides was determined as the ability to lyse erythrocytes in comparison to melittin. Percent hemolysis at 12.5, 25, 50, 150 and 250 μM is shown in Table 6.5. All these tests were performed by Dr. Esther Badosa of the Plant Pathology group at the UdG. As shown in Table 6.5, all carbopeptides were highly hemolytic compared to the parent peptide.

Table 6.5. *Cytotoxicity of carbopeptides.*

Peptide	Hemolysis[a] (%)				
	12.5 μM	**25 μM**	**50 μM**	**150 μM**	**250 μM**
BP100	ND[b]	ND	3 ± 0.1	22 ± 2.8	54±0.1
Gal*p*(BP100)$_4$	94 ± 6.7	100 ± 6.6	100 ± 18.8	100 ± 18.8	100 ± 1.1
cDTE(BP100)$_2$	76 ± 3.0	97 ± 1.6	100 ± 4.1	99 ± 5.2	-
BP143	ND	ND	2 ± 2.8	22 ± 2.8	43 ± 1.8
cDTE(BP143)$_2$	69 ± 4.8	99 ± 1.8	96 ± 0.9	92 ± 7.2	99 ± 2.6

[a]Percent hemolysis at 12.5, 25, 50, 150 and 250 μM plus confidence interval (α = 0.05).

[b]ND: not determined.

7. CONCLUSIONS

- We have synthesized antimicrobial peptides derived from **BP100** containing D-amino acids with moderate to good purities. Moreover, we have described a method for the synthesis of difficult sequences using a ChemMatrix resin obtaining a peptide in a good purity percentage.

- Peptides active against all the studied pathogens have been identified, displaying a better activity against phytopathogenic than human bacteria and also a low hemolysis percentage (45 % hemolysis at 150 μM). Some of these sequences were more active than **BP100** and less hemolytic. Besides, these peptides were less prone to protease degradation than **BP100**.

- **BP143** containing one D-amino acid showed an efficacy *in planta* comparable to streptomycin and higher than that of the parent peptide **BP100**.

- We have prepared in solid-phase 13 antimicrobial peptides derived from **BP100** containing a 1,2,3-triazole ring onto an amino acid side-chain. The synthesis of this ring involved the reaction between an alkynyl resin and an azide. All peptidotriazoles were obtained in moderate to good purities.

- We have identified linear peptidotriazoles active against the studied phytopathogenic bacteria and fungi. Some of these peptidotriazoles had a low hemolytic activity. Besides, four sequences displayed higher stability than **BP100**. Interestingly, **BP250** was active against the three bacteria, not hemolytic and more estable to proteases than the parent peptide.

- We have prepared cyclic peptidotriazoles based on the structure of **BPC194** containing a triazolyl alanine, a triazolyl-modified glutamine or a tryazolyl lysine at positions 3 or 5. The synthesis was achieved via a cycloaddition reaction either between an alkynyl peptidyl resin and an azide in solution or between an azidopeptidyl resin and an alkyne in solution. Both strategies afforded the cyclic peptidotriazoles in good purities.

- We have synthesized a conjugated peptidotriazole in excellent purity by linking a cyclic alkynyl peptidyl resin and an azidopentapeptide. The use of microwave irradiation reduced the reaction time from 7 h to 30 min.

- We have identified cyclic peptidotriazoles with high activity against *X. vesicatoria*, *P. syringae*, *E. amylovora* and *E. coli*, and low hemolysis. In addition, these compounds were not active against the biocontrol agents *L. mesenteroides* and *B. subtilis*. Therefore, these sequences can be considered as good candidates for plant protection. It has been observed that the introduction of a triazole moiety in **BPC194** did not significantly influence the antibacterial activity. Peptidotriazoles resulting from the substitution of an apolar residue of **BPC194** by a triazolyl-modified amin acid were less hemolytic than those resulting from the substitution of a polar residue. Among these peptidotriazoles, the ones bearing a polar substituent at the triazole ring were the least hemolytic.

- We have designed and synthesized carbopeptides containing two or four units of the lead antimicrobial peptides **BP100** and **BP143** attached to the carbohydrate template cDTE or Gal*p*. The oxime ligation reaction between peptides and the carbohydrate template required the use of aniline as nucleophilic catalyst. Carbopeptides**, cDTE(BP143)$_2$** and were obtained in moderate yields and good purities. These carbopeptides were active against phytopathogenic and human bacteria but highly hemolytic. For **Gal*p*(BP100)$_4$** and **cDTE(BP100)$_2$** a multimeric effect was observed against the plant pathogens.

8. EXPERIMENTAL SECTION

8.1. Material and Methods

8.1.1. Ninhydrin or Kaiser test

The ninhydrin test is a qualitative colour test to detect the presence or absence of free primary amino groups, constituting a useful indication about the completeness of the amino acid coupling in solid-phase peptide synthesis. The test is based on the reaction of ninhydrin with free primary amines causing the oxidative deamination of the α-amino function which gives an intensive dark blue colour, Ruhemann's purple (Kaiser et al., 1970) (Scheme 8.1).

The ninhydrin test kit contains three solutions:

Solution A: ninhydrin (500 mg) in absolute ethanol (10 mL).

Solution B: phenol (100 mg) in absolute ethanol (25 mL).

Solution C: 1mM NaCN (1 mL) in of pyridine (49 mL).

A few resin beads from the reaction vessel are transferred into a small test tube and 3 drops of each solution of the test kit are added. Next, the suspension is mixed well and heated at 100 ºC for 3 min. The resin beads and the solution turn dark blue when free primary amines are present. The colour of the resin beads doesn't change and the solution stays yellow when no free primary amines are present.

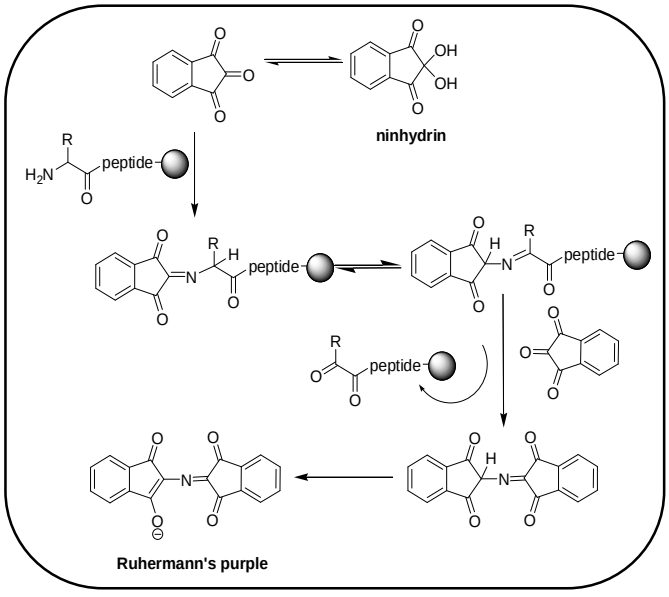

Scheme 8.1. *The nynhidrin test reaction.*

8.1.2. High performance liquid chromatography (HPLC)

8.1.2.1. Analytical HPLC

The equipment used were an Agilent Technologies 1200 Series apparatus and a Summit Dionex instrument. Flow rate used was of 1 mL/min and solvent A was 0.1 % aqueous TFA and solvent B was 0.1 % TFA in ACN. Detection was performed at 220 nm. Purity was estimated with the integrated area under peaks.

Samples were analyzed using different procedures:

- Method A:
  - Column: C_{18}-Kromasil 100 (40×4.6 mm, 3.5 μm particle size).
  - Gradient: 2-100 % B over 7 min.
- Method B:
  - Column: C_{18}-Kromasil 100 (40×4.6 mm, 3.5 μm particle size).
  - Gradient: 2-100 % B over 6 min.
- Method C:
  - Column: C_{18}-Kromasil 100 (250×4.6 mm, 3.5 μm particle size).
  - Gradient: 2-100 % B over 28 min.
- Method D:
  - Column: C_{18}-Ultrabase 100 (250×4.6 mm, 3.5 μm particle size).
  - Gradient: 2-100 % B over 28 min.

8.1.2.2. Preparative HPLC

The equipment used was an Agilent Tecnologies 1200 Series equipped with a Diode Array detector an autosampler and an automatic collector. Purification was carried out with a C_{18} 0D52 Ultrabase column (7.8×250 mm, 5 μm particle size) and a flow rate of 3 mL/min. The following linear gradients of 0.1 % aqueous TFA (solvent A) and 0.1 % TFA in ACN (solvent B) were run:

- Method E: 2-100 % B over 28 min.
- Method F: 2-30 % B over 6 min and 30-58 % B over 23 min.
- Method G: 2-45 % B over 5 min and 45-100 % B over 17 min.
- Method H: 58-100 % B over 2 min.

Other eqquipment used was a Dionex UltiMate 3000 Quaternary Micro LC System equipped with a Standard Thermostatted Column Compartment (TCC), a Diode Array detector, an autosampler and an automatic collector. The following protocols were employed:

- Method I:
  - Column: Phenomenex Gemini-NX 5u C_{18} 110 Axia (100×21.2 mm, 5 μm particle size).
  - Gradient: 5-60 % B over 8 min and 60-100 % B over 27 min.
  - Temperature: room temperature.
  - Flow: 10 mL/min.
- Method J:
  - Column: Phenomenex Gemini-NX 5u C_{18} 110 Axia (100×21.2 mm, 5 μm particle size).
  - Gradient: 5-55 % B over 24min and 55-100 % B over 11 min.
  - Temperature: room temperature.
  - Flow: 10 mL/min.
- Method K:
  - Column: Phenomenex Gemini-NX 5u C_{18} 110 Axia (100×21.2 mm, 5 μm particle size).
  - Gradient: 5-50 % B over 24 min, 50-95 % B over 11 min and 95-100 % B over 2 min.
  - Temperature: 42ºC.
  - Flow: 10 mL/min.
- Method L:
  - Column: FeF Chemicals C_4 250 Å (20x250mm, 5 μm particle size).
  - Gradient: 5-95 % B over 28 min.
  - Temperature: 42ºC.
  - Flow: 15 mL/min.

8.1.3. Analytical thin layer chromatography (TLC)

Precoated TLC plates of silica gel 60 E_{254} (Merck) were used. The spots on the TLC plates were visualized with UV/visible light (254 nm) and/or stained with a solution of $KMnO_4$ (1.5 g/100 mL H_2O).

8.1.4. Mass spectrometry

8.1.4.1. Electrospray ionization-mass spectrometry (ESI/MS)

Mass spectra were acquired using a low-resolution mass spectrometer from Serveis Tècnics de Recerca (STR) at the University of Girona. It consisted of a Navigator quadrupole, an aqua system analyzer, a source of atmospheric pressure chemical ionization (APCI), a ThermoQuest electrospray (ESI) with a positive/negative ionization mode and a Thermo Separation Products binary pump P2000. This mass spectrometer analyzes in a mass range of *m/z* = 2 to *m/z* = 1600. Samples were introduced by direct injection through an automatic injector with a 20 μL loop and the mobile phase flow (0.3 mL/min) was provided by the above mentioned binary pump. The mobile phase was a gradient of 2-100 % ACN over 10 minutes.

Other ESI-MS analyses were recorded on an Esquire 6000 ESI ion Trap LC/MS (Bruker Daltonics) equipped with an electrospray ion source at the University of Saragossa. The instrument was operated either in the positive ESI(+) or negative ESI(-) ion mode and samples (5 μL) were introduced into the mass spectrometer ion source directly through a HPLC autosampler. The mobile phase flow (100 μL/min of 20 % ACN) was delivered by 1100 Series HPLC pump (Agilent).

8.1.4.2. High resolution mass spectrometry (HRMS)

Analyses were performed under conditions of ESI on a Bruker MicroToe-Q instrument using a hybrid quadrupole time-of-flight mass spectrometer (University of Zaragoza). Samples were introduced into the mass spectrometer ion source directly through a 1100 Series Agilent HPLC autosampler and were externally calibrated using sodium formiate. The instrument was operated either in the positive ESI(+) or negative ESI(-) ion mode.

8.1.4.3. Matrix-assisted laser desorption/ionization time-of-flight (MALDI-TOF)

Bruker Daltonics Ultraflex apparatus consisting of a linear ion analyzer, a nitrogen laser and an electrostatic ion reflector was used.

8.1.4.4. Liquid chromatography coupled to mass spectrometry (LC/MS)

Some analyses were performed on a LC/MS system consisting of an Agilent Tecnologies 1200 Series HPLC coupled to an ion trap Esquire 6000 (Daltonics Bruker) equipped with an electrospray ion source. Analyses were carried out using a C_{18} Kromasil reverse-phase column (250×4.6 mm, 3.5 µm particle size). A flow rate of 1 mL/min and a gradient of 2-100 % B over 28 min were used (solvent A was 0.015 % HCOOH in H_2O and solvent B was 0.015 % HCOOH in ACN). The instrument was operated in the positive ESI(+) ion mode and nitrogen was employed as both drying and nebulizing gas. Detection was performed at 220 nm.

Other analyses were performed on a LC/MS system consisting of a Dionex UltiMate 3000 Quaternary Micro LC System equipped with a Standard Thermostatted Column Compartment (TCC), a Diode Array detector, an automatic sampler and an ESI/MS MSQ Plus mass spectrometer (Thermo). Analyses were carried out using a flow rate of 1 mL/min, a temperature of 42°C, 0.1 % HCOOH in H_2O as solvent A and 0.1 % HCOOH in ACN as solvent B. The instrument was operated in the positive ESI(+) and the detection was performed at 215 nm.

- Method M:
  - Column: C_{18} Phenomenex Gemini 110 Å (4.6×50 mm, 3 µm particle size).
  - Gradient: 5-80 % B over 5 min and 80-100 % B over 5 min.
- Method N:
  - Column: C_4Phenomenex Jupiter 300 Å (4.6 × 150 mm, 5 µm particle size).
  - Gradient: 5-20 % B over 2 min, 20-40 % B over 8 min and 40-100 % B over 2 min.

8.1.5. Infrared spectroscopy (IR)

Spectra were recorded on a Mattson-Galaxy Satellite FT-IR using a MKII Golden Gate single reflection ATR system (Spacec) as a sampling accessory. Absorption and position were registered in cm^{-1}.

8.1.6. Nuclear Magnetic Resonance (NMR)

NMR spectra were measured at the Serveis Tècnics de Recerca of the University of Girona using a Bruker DPX400 Avance (9.40T) ^{1}H (400 MHz) and ^{13}C (100 MHz) spectrometer equipped with a BBI probe and a temperature control unit (BCU Xtreme). $CDCl_3$, DMSO-d_6 and CD3OD-d_4 were used as deuterated solvents. Chemical shifts were reported as δ values (ppm) directly referenced to the solvent signal. Coupling constants (*J*) were given in Herz (Hz).

8.1.7. Automated synthesizer

Some peptides were prepared on a fully automated Syro II peptide synthesizer (MultiSynTech).

8.1.8. Microwave-assisted synthesis

The microwave-assisted synthesis was carried out using a Discover S-Class Corporation microwave apparatus that consists of a continuous power delivery system equipped with a selectable power output from 0 to 300 watts. Time, temperature and power of the experiments were controlled with the Synergy software. This microwave apparatus has a temperature control system that uses a non-contact, infrared sensor to measure the temperature at the bottom of the vessel.

8.1.9. Synthesis of $Pd(PPh_3)_4$

$$2\ PdCl_2 + 8\ PPh_3 + NH_2NH_2{\cdot}H_2O \xrightarrow{DMF} 2\ Pd(PPh_3)_4 + 4\ NH_2NH_2{\cdot}HCl + N_2 + 5\ H_2O$$

A mixture of $PdCl_2$ (2.3 g, 13.0 mmol) and PPh_3 (13.6 g, 52 mmol) in DMF (150 mL) was stirred at 130 °C under N_2 until the solid was dissolved. After that, upon cooling, the mixture was stirred at room temperature for 15 min. Next, hydrazine hydrate (1.6 g, 32

mmol) was added and the resulting mixture was cooled to 0 °C. The resulting yellow precipitate was filtered and washed with both degassed absolute EtOH and dry diethyl ether, affording palladium (0) $Pd(PPh_3)_4$ (12.7 g, 85 % yield) (Coulson 1990).

mp: 119-120 °C. **mp (lit)**: 116 °C (Coulson 1990).

IR (neat) ν (cm^{-1}): 3052, 1475, 1430, 1082, 1025, 998, 740, 690.

8.2. General method for solid-phase peptide synthesis

Couplings of the Fmoc-amino acids (4 equiv) were carried out manually in polypropylene syringes equipped with a polyethylene filter using different reaction conditions:

- Conditions A: HBTU (3.8 equiv), HOBt (4 equiv) and DIPEA (7.8 equiv) in DMF under stirring for 1 h at room temperature.
- Conditions B: Oxyma pure (4 equiv) and DIPCDI (4 equiv) in DMF under stirring for 1 h at room temperature.

The completion of the reactions was monitored by the Kaiser test. Peptide elongation was performed by repeated cycles of Fmoc group removal, coupling and washings. Fmoc group was removed by treating the resin with a mixture of piperidine/DMF (3:7; 2 + 10 min). Washings were performed with DMF (6×1 min) and CH_2Cl_2 (6×1 min). After the fifth coupling, NMP was used instead of DMF. The resulting peptides were cleaved from the resin with TFA/TIS/H_2O (95:2.5:2.5) for 2 h at room temperature. Following TFA evaporation and diethyl ether extraction, the crude peptides were dissolved in H_2O, lyophilized, tested for purity with HPLC and characterized by ESI/MS or MALDI.

8.3. Syntesis of linear peptides containing d-amino acids

The required amount of Fmoc-Rink-MBHA resin (0.64 mmol/g) was swollen with CH_2Cl_2 (1×20 min) and with DMF (1×20 min). Couplings of the Fmoc-amino acids were mediated by conditions A (Section 8.2).

8.3.1. H-Lys-Lys-D-Leu-Phe-Lys-Lys-Ile-Leu-D-Lys-Tyr-Leu-NH_2 (BP149)

This peptide was synthesized following the procedure described above incorporating a D-amino acid at positions 3 and 9 of the sequence. After cleavage, BP149 was obtained in 82 % purity.

HPLC (λ=220 nm): 6.21 min [Method A]; ***ESI/MS (m/z)***: 1443.0 $[M+ Na]^+$.

8.3.2. H-Lys-Lys-Leu-Phe-Lys-Lys-Ile-D-Leu-D-Lys-Tyr-Leu-NH_2 (BP150)

This peptide was synthesized following the procedure described above incorporating a D-amino acid at positions 8 and 9 of the sequence. After cleavage, BP150 was obtained in 81 % purity.

HPLC (λ=220 nm): 6.22 min [Method A]; ***ESI/MS (m/z)***: 1443.0 $[M+ Na]^+$.

8.3.3. H-Lys-Lys-D-Leu-Phe-D-Lys-Lys-Ile-Leu-D-Lys-Tyr-Leu-NH_2 (BP151)

This peptide was synthesized following the procedure described above incorporating a D-amino acid at positions 3, 5 and 9 of the sequence. After cleavage, BP151 was obtained in 66 % purity.

HPLC (λ=220 nm): 6.20 min [Method A]; ***ESI/MS (m/z)***: 1443.0 $[M+ Na]^+$.

8.3.4. H-Lys-Lys-Leu-Phe-Lys-Lys-D-Ile-D-Leu-D-Lys-Tyr-Leu-NH_2 (BP152)

This peptide was synthesized following the procedure described above incorporating a D-amino acid at positions 7, 8 and 9 of the sequence. After cleavage, BP152 was obtained in 71 % purity.

HPLC (λ=220 nm): 6.05 min [Method A]; ***ESI/MS (m/z)***: 474.7 $[M+3H]^{3+}$, 711.5 $[M+4H]^{4+}$.

8.3.5. H-D-Lys-D-Lys-D-Leu-D-Phe-D-Lys-D-Lys-D-Ile-D-Leu-D-Lys-D-Tyr-D-Leu-NH_2 (BP153)

This peptide was synthesized following the procedure described above using only D-amino acids. After cleavage, BP153 was obtained in 79 % purity.

HPLC (λ=220 nm): 6.18 min [Method A]; ***ESI/MS (m/z)***: 474.7 $[M+3H]^{3+}$, 711.5 $[M+4H]^{4+}$.

8.3.6. H-D-Lys-D-Lys-Leu-D-Phe-Lys-Lys-Ile-Leu-Lys-Tyr-Leu-NH_2 (BP154)

This peptide was synthesized following the procedure described above incorporating a D-amino acid at positions 1, 2 and 4 of the sequence. After cleavage, BP154 was obtained in 74 % purity.

HPLC (λ=220 nm): 6.25 min [Method A]; ***ESI/MS (m/z)***: 1443.0 $[M+ Na]^+$.

8.3.7. H-Lys-Lys-Leu-Phe-Lys-Lys-Ile-D-Leu-D-Lys-D-Tyr-D-Leu-NH_2 (BP155)

This peptide was synthesized following the procedure described above incorporating a D-amino acid at positions 8 to 11 of the sequence. After cleavage, BP155 was obtained in 64 % purity.

HPLC (λ=220 nm): 17.21 min [Method C]; ***ESI/MS (m/z)***: 1421.2 $[M+ H]^+$.

8.3.8. H-Lys-Lys-Leu-Phe-Lys-Lys-D-Ile-D-Leu-D-Lys-D-Tyr-D-Leu-NH_2 (BP156)

This peptide was synthesized following the procedure described above incorporating a D-amino acid at positions 7 to 11 of the sequence. After cleavage, BP156 was obtained in 55 % purity.

HPLC (λ=220 nm): 16.57 min [Method C]; ***ESI/MS (m/z)***: 1421.2 $[M+ H]^+$.

8.3.9. H-Lys-Lys-Leu-Phe-Lys-D-Lys-D-Ile-D-Leu-D-Lys-D-Tyr-D-Leu-NH_2 (BP157)

This peptide was synthesized following the procedure described above incorporating a D-amino acid at positions 6 to 11 of the sequence. After cleavage, BP157 was obtained in 42 % purity and was purified using method F (x % purity).

HPLC (λ=220 nm): 16.28 min. [Method C]; ***ESI/MS (m/z)***: 474.4 $[M+3H]^{3+}$, 711.0 $[M+2H]^{2+}$, 1421.2 $[M+ H]^+$, 1443.0 $[M+ Na]^+$.

8.3.10. H-Lys-Lys-Leu-Phe-D-Lys-D-Lys-D-Ile-D-Leu-D-Lys-D-Tyr-D-Leu-NH_2 (BP158)

This peptide was synthesized following the procedure described above incorporating a D-amino acid at positions 5 to 11 of the sequence. After cleavage, BP158 was obtained in 62 % purity.

HPLC (λ=220 nm): 6.23 min [Method A]; ***ESI/MS (m/z)***: 474.0 $[M+3H]^{3+}$, 710.95 $[M+2H]^{2+}$, 1420.91 $[M+ H]^{+}$.

8.3.11. H-Lys-Lys-Leu-D-Phe-D-Lys-D-Lys-D-Ile-D-Leu-D-Lys-D-Tyr-D-Leu-NH_2 (BP159)

This peptide was synthesized following the procedure described above incorporating a D-amino acid at positions 4 to 11 of the sequence. After cleavage, BP159 was obtained in 76 % purity.

HPLC (λ=220 nm): 6.28 min [Method A]; ***ESI/MS (m/z)***: 1421.3 $[M+ H]^{+}$.

8.3.12. H-Lys-Lys-D-Leu-D-Phe-D-Lys-D-Lys-D-Ile-D-Leu-D-Lys-D-Tyr-D-Leu-NH_2 (BP160)

This peptide was synthesized following the procedure described above incorporating a D-amino acid at positions 3 to 11 of the sequence. After cleavage, BP160 was obtained in 80 % purity.

HPLC (λ=220 nm): 6.23 min [Method A]; ***ESI/MS (m/z)***: 1421.4 $[M+ H]^{+}$.

8.3.13. H-Lys-D-Lys-D-Leu-D-Phe-D-Lys-D-Lys-D-Ile-D-Leu-D-Lys-D-Tyr-D-Leu-NH_2 (BP161)

This peptide was synthesized following the procedure described above incorporating a D-amino acid at positions 2 to 11 of the sequence. After cleavage, BP161 was obtained in 82 % purity.

HPLC (λ=220 nm): 6.37 min [Method A]; ***ESI/MS (m/z)***: 1421.4 $[M+ H]^{+}$.

8.3.14. H-D-Lys-D-Lys-D-Leu-D-Phe-Lys-Lys-Ile-Leu-Lys-Tyr-Leu-NH_2 (BP162)

This peptide was synthesized following the procedure described above incorporating a D-amino acid at positions 1 to 4 of the sequence. After cleavage, BP162 was obtained in 76 % purity and was purified using method E (99 % purity).

HPLC (λ=220 nm): 5.91 min [Method B]; ***ESI/MS (m/z)***: 474.4 $[M+3H]^{3+}$, 711.0 $[M+2H]^{2+}$, 1421.0 $[M+ H]^{+}$, 1443.0 $[M+ Na]^{+}$.

8.3.15. H-D-Lys-D-Lys-D-Leu-D-Phe-D-Lys-Lys-Ile-Leu-Lys-Tyr-Leu-NH_2 (BP163)

This peptide was synthesized following the procedure described above incorporating a D-amino acid at positions 1 to 5 of the sequence. After cleavage, BP163 was obtained in 48 % purity and was purified using method G (99 % purity).

HPLC (λ=220 nm): 5.82 min [Method B]; ***ESI/MS (m/z)***: 474.3 $[M+3H]^{3+}$, 711.0 $[M+2H]^{2+}$, 1420.9 $[M+ H]^{+}$.

Alternatively, BP163 was prepared using a ChemMatrix resin following the methodology described in section 8.2 (conditions A) until the ninth residue. The deprotection of the ninth residue was performed by treatment with piperidine/DMF (3:7; 1×2 + 3×10 min). Fmoc removal of the tenth and eleventh residues required a (1×2 + 6×10) min treatment. For the coupling of the tenth and eleventh residues, two and three treatments of 24 h were necessary, respectively. This protocol led to BP163 in 86 % HPLC purity.

8.3.16. H-D-Lys-D-Lys-D-Leu-D-Phe-D-Lys-D-Lys-Ile-Leu-Lys-Tyr-Leu-NH_2 (BP164)

This peptide was synthesized following the procedure described above incorporating a D-amino acid at positions 1 to 6 of the sequence. After cleavage, BP164 was obtained in 51 % purity and was purified using method E (98 % purity).

HPLC (λ=220 nm): 5.90 min [Method B]; ***ESI/MS (m/z)***: 474.4 $[M+3H]^{3+}$, 711.0 $[M+2H]^{2+}$, 1420.9 $[M+ H]^{+}$, 1442.9 $[M+ Na]^{+}$.

8.3.17. H-D-Lys-D-Lys-D-Leu-D-Phe-D-Lys-D-Lys-D-Ile-Leu-Lys-Tyr-Leu-NH_2 (BP165)

This peptide was synthesized following the procedure described above incorporating a D-amino acid at positions 1 to 7 of the sequence. After cleavage, BP165 was obtained in 58 % purity and was purified using method H (99 % purity).

HPLC (λ=220 nm): 16.42 min [Method C]; ***ESI/MS (m/z)***: 474.6 $[M+3H]^{3+}$, 711.0 $[M+2H]^{2+}$, 1421.0 $[M+ H]^{+}$, 1443.0 $[M+ Na]^{+}$.

8.3.18. H-D-Lys-D-Lys-D-Leu-D-Phe-D-Lys-D-Lys-D-Ile-D-Leu-Lys-Tyr-Leu-NH_2 (BP166)

This peptide was synthesized following the procedure described above incorporating a D-amino acid at positions 1 to 8 of the sequence. After cleavage, BP166 was obtained in 92 % purity.

HPLC (λ=220 nm): 6.03 min [Method A]; ***ESI/MS (m/z)***: 474.3 $[M+3H]^{3+}$, 711.0 $[M+2H]^{2+}$, 1421.0 $[M+ H]^{+}$, 1443.0 $[M+ Na]^{+}$.

8.3.19. H-D-Lys-D-Lys-D-Leu-D-Phe-D-Lys-D-Lys-D-Ile-D-Leu-D-Lys-Tyr-Leu-NH_2 (BP167)

This peptide was synthesized following the procedure described above incorporating a D-amino acid at positions 1 to 9 of the sequence. After cleavage, BP167 was obtained in 84 % purity.

HPLC (λ=220 nm): 6.06 min [Method A]; ***ESI/MS (m/z)***: 474.3 $[M+3H]^{3+}$, 711.5 $[M+2H]^{2+}$, 1443.0 $[M+Na]^{+}$; 1421.0 $[M+H]^{+}$.

8.3.20. H-D-Lys-D-Lys-D-Leu-D-Phe-D-Lys-D-Lys-D-Ile-D-Leu-D-Lys-D-Tyr-Leu-NH_2 (BP168)

This peptide was synthesized following the procedure described above incorporating a D-amino acid at positions 1 to 9 of the sequence. After cleavage, BP168 was obtained in 60 % purity and was purified using method E (99 % purity).

HPLC (λ=220 nm): 15.88 min [Method C]; ***ESI/MS (m/z)***: 474.4 $[M+3H]^{3+}$, 711.0 $[M+2H]^{2+}$, 1421.0 $[M+H]^{+}$, 1443.0 $[M+Na]^{+}$.

8.4. Synthesis of linear peptidotriazoles

The required amount of Fmoc-Rink-MBHA resin (0.54 mmol/g) was swollen with CH_2Cl_2 (1×20 min) and DMF (1×20 min).

8.4.1. Synthesis of linear alkynyl peptides

Peptidyl resins containing an Mtt-protected lysine or a propargylglycine were prepared following the general procedure described above (Conditions B, section 8.2). Once chain assembly was completed, peptidyl resins containing an N^{ε}-Mtt-protected lysine were treated with 1 % TFA in CH_2Cl_2 upon which the solution became yellow. Each mixture was stirred for 10 min and the resins were then washed with CH_2Cl_2 (2×1 min), MeOH (2×1 min) and CH_2Cl_2 (2×1 min). The TFA treatment and the washes were repeated until the solution remained colorless. Then, the N^{ε}-amino group was acylated with propiolic acid under the coupling conditions B.

8.4.1.1. Fmoc-Lys(COC≡CH)-Lys(Boc)-Leu-Phe-Lys(Boc)-Lys(Boc)-Ile-Leu-Lys(Boc)-Tyr(^{t}Bu)-Leu-Rink-MBHA (1a)

This alkynyl resin was synthesized following the procedure described above from the resin Fmoc-Lys(CO-C≡CH)-Lys(Boc)-Leu-Phe-Lys(Boc)-Lys(Boc)-Ile-Leu-Lys(Boc)-Tyr(^{t}Bu)-Leu-Rink-MBHA. An aliquot of the alkynyl resin was cleaved and the respective Fmoc-Lys(CO-C≡CH)-Lys-Leu-Phe-Lys-Lys-Ile-Leu-Lys-Tyr-Leu-NH_2 (**3a**) was obtained in 79 % purity.

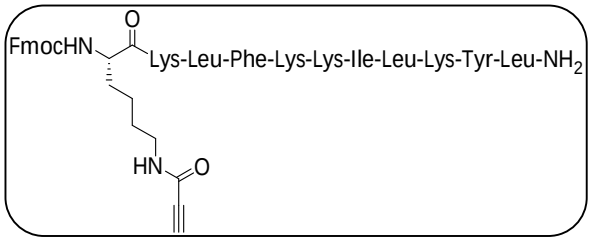

HPLC (λ=220 nm): 8.32 min [Method A]. ***ESI/MS (m/z)***: 1695.8 $[M+H]^{+}$.

8.4.1.2. H-Lys-Lys(COC≡CH)-Leu-Phe-Lys-Lys-Ile-Leu-Lys-Tyr-Leu-NH_2 (1b)

This alkynyl resin was synthesized following the procedure described above from the resin Fmoc-Lys(Boc)-Lys(CO-C≡CH)-Leu-Phe-Lys(Boc)-Lys(Boc)-Ile-Leu-Lys(Boc)-

Tyr(^{t}Bu)-Leu-Rink-MBHA. An aliquot of the alkynyl resin was cleaved and the respective H-Lys-Lys(CO-C≡CH)-Leu-Phe-Lys-Lys-Ile-Leu-Lys-Tyr-Leu-NH_2 (**3b**) was obtained in 77 % purity.

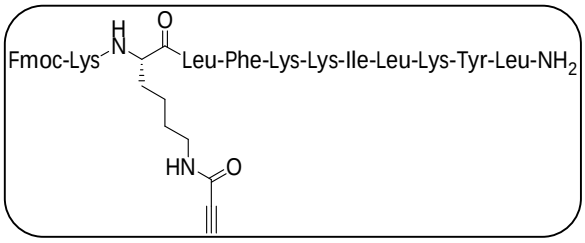

HPLC (λ=220 nm): 7.93 min [Method A]. ***ESI/MS (m/z)***: 848.6 $[M+2H]^{2+}$, 1695.8 $[M+H]^+$.

8.4.1.3. Fmoc-Lys(Boc)-Lys(Boc)-Leu-Phe-Lys(CO-C≡CH)-Lys(Boc)-Ile-Leu-Lys(Boc)-Tyr(^{t}Bu)-Leu-Rink-MBHA (1c)

This alkynyl resin was synthesized following the procedure described above from the resin Fmoc-Lys(Boc)-Lys(Boc)-Leu-Phe-Lys(CO-C≡CH)-Lys(Boc)-Ile-Leu-Lys(Boc)-Tyr(^{t}Bu)-Leu-Rink-MBHA. An aliquot of the alkynyl resin was cleaved and the respective H-Lys-Lys-Leu-Phe-Lys(CO-C≡CH)-Lys-Ile-Leu-Lys-Tyr-Leu-NH_2 (**3c**) was obtained in 80 % purity.

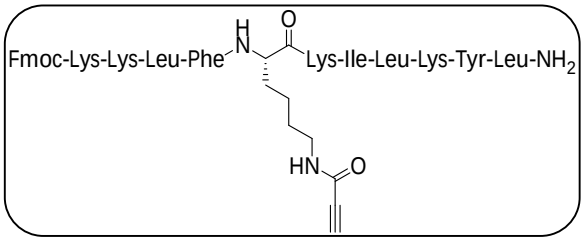

HPLC (λ=220 nm): 8.10 min [Method A]. ***ESI/MS (m/z)***: 1695.8 $[M+H]^+$.

8.4.1.4. H-Lys-Lys-Leu-Phe-Lys-Lys(CO-C≡CH)-Ile-Leu-Lys-Tyr-Leu-NH_2 (1d)

This alkynyl resin was synthesized following the procedure described above from the resin Fmoc-Lys(Boc)-Lys(Boc)-Leu-Phe-Lys(Boc)-Lys(CO-C≡CH)-Ile-Leu-Lys(Boc)-Tyr(^{t}Bu)-Leu-Rink-MBHA. An aliquot of the alkynyl resin was cleaved and the respective H-Lys-Lys-Leu-Phe-Lys-Lys(CO-C≡CH)-Ile-Leu-Lys-Tyr-Leu-NH_2 (**3d**) was obtained in 84 % purity.

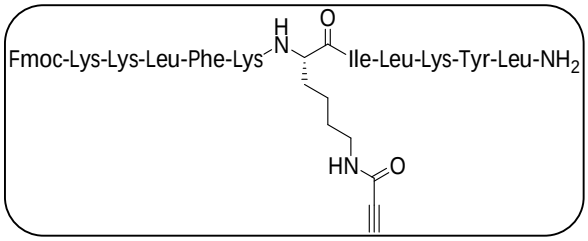

HPLC (λ=220 nm): 8.37 min [Method A]. ***ESI/MS (m/z)***: 1695.8 $[M+H]^+$.

8.4.1.5. Fmoc-Lys(Boc)-Lys(Boc)-Leu-Phe-Lys(Boc)-Lys(Boc)-Ile-Leu-Lys(CO-C≡CH)-Tyr(^{t}Bu)-Leu-Rink-MBHA (1e)

This alkynyl resin was synthesized following the procedure described above from the resin Fmoc-Lys(Boc)-Lys(Boc)-Leu-Phe-Lys(Boc)-Lys(Boc)-Ile-Leu-Lys(CO-C≡CH)-Tyr(^{t}Bu)-Leu-Rink-MBHA. An aliquot of the alkynyl resin was cleaved and the respective H-Lys-Lys-Leu-Phe-Lys-Lys-Ile-Leu-Lys(CO-C≡CH)-Tyr-Leu-NH_2 (**3e**) was obtained in 80 % purity.

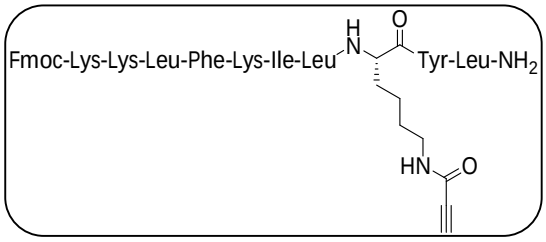

HPLC (λ=220 nm): 7.79 min [Method A]. ***ESI/MS (m/z)***: 1695.8 $[M+H]^+$.

8.4.1.6. H-Lys(Boc)-Lys(Boc)-Leu-Prg-Lys(Boc)-Lys(Boc)-Ile-Leu-Lys(Boc)-Tyr-Leu-NH_2 (2)

This alkynyl resin was synthesized following the procedure described above from the resin Fmoc-Lys(Boc)-Lys(Boc)-Leu-Prg-Lys(Boc)-Lys(Boc)-Ile-Leu-Lys(Boc)-Tyr(^{t}Bu)-Leu-Rink-MBHA. An aliquot of the alkynyl resin was cleaved and the respective H-Lys-Lys-Leu-Prg-Lys-Lys-Ile-Leu-Lys-Tyr-Leu-NH_2 (**4**) was obtained in 80 % purity.

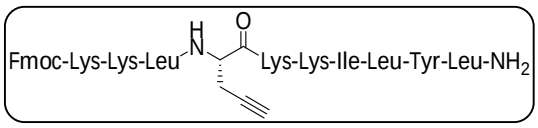

HPLC (λ=220 nm): 7.56 min [Method A]. ***ESI/MS (m/z)***: 796.0 $[M+2H]^{2+}$, 1592.1 $[M+H]^+$.

8.4.2. Synthesis of linear peptidotriazoles

Each of the alkynyl resins was swollen with CH_2Cl_2 (1 × 20 min) and DMF (1 × 20 min), and were treated with the corresponding azide (5 equiv) in the presence of ascorbic acid (5 equiv) and CuI (5 equiv) in piperidine/DMF (2:8). The reaction mixture was stirred overnight at room temperature. The resin was subsequently washed with sodium *N,N*-diethyldithiocarbamate (0.03 M in NMP, 3×15 min), DMF (6×1 min) and CH_2Cl_2 (1×20 min). Peptidotriazoles were individually cleaved from the resin with TFA/H_2O/TIS (95:2.5:2.5) and analyzed by HPLC, mass spectrometry and NMR.

8.4.2.1. Peptidotriazole BP238

The alkynyl resin Fmoc-Lys(CO-C≡CH)-Lys(Boc)-Leu-Phe-Lys(Boc)-Lys(Boc)-Ile-Leu-Lys(Boc)-Tyr(^{t}Bu)-Leu-Rink-MBHA (80 mg) was treated with NaN_3 following the general procedure described above to perform the click reaction. BP238 was obtained in 84 % purity.

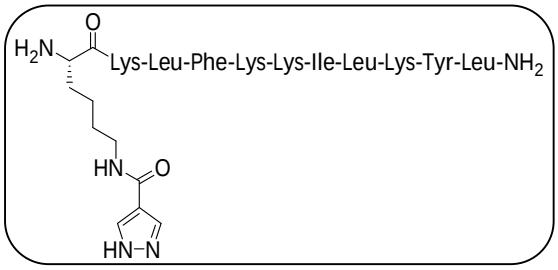

^{1}H-RMN: (*400 MHz, CD_3OD)* δ (ppm): 0.89–0.95 (m, 24H, 18 CH_3(δ)-Leu, 6 CH_3(δ)-Ile), 1.29–1.82 (m, 41H, 10 CH_2(β)-Lys, 10 CH_2(γ)-Lys, 10 CH_2(δ)-Lys, 6 CH_2(β)-Leu, 3 CH(γ)-Leu, 2 CH_2(γ)-Ile), 2.84–2.93 (m, 11H, 1 CH(β)-Ile, 8 CH_2(ε)-Lys, 1 CH_2(β)-Phe, 1 CH_2(β)-Tyr), 3.12–3.15 (m, 4H, 1 CH_2(β)-Phe, 1 CH_2(β)-Tyr, 2 CH_2(ε)-Lys), 3.47–3.49 (m, 1H, 1 CH(α)-Lys), 4.12–4.54 (m, 10H, 4 CH(α)-Lys, 3 CH(α)-Leu, 1 CH(α)-Ile, 1 CH(α)-Phe, 1 CH(α)-Tyr), 6.70 (d, *J* = 8.0 Hz, 2H, 2 CH_{arom}-Tyr), 7.10–7.25 (m, 7H, 2 CH_{arom}-Tyr, 5 CH_{arom}-Phe). ***HPLC (λ=220 nm)***: 17.70 min [Method D]. **ESI-MS (*m/z*):** 758.5 $[M+2H]^{2+}$, 1515.7 $[M+H]^+$. **HRMS (ESI):** calcd. for $C_{75}H_{129}N_{20}O_{13}$ 506.0011, found 506.0014; calcd. for $C_{75}H_{128}N_{20}O_{13}$ 758.4979, found 758.4946.

8.4.2.2. Peptidotriazole BP239

The alkynyl resin Fmoc-Lys(CO-C≡CH)-Lys(Boc)-Leu-Phe-Lys(Boc)-Lys(Boc)-Ile-Leu-Lys(Boc)-Tyr(^{t}Bu)-Leu-Rink-MBHA (80 mg) was treated with Boc-Nle(ε-N_3)-OH following the general procedure described above to perform the click reaction. BP239 was obtained in 73 % purity.

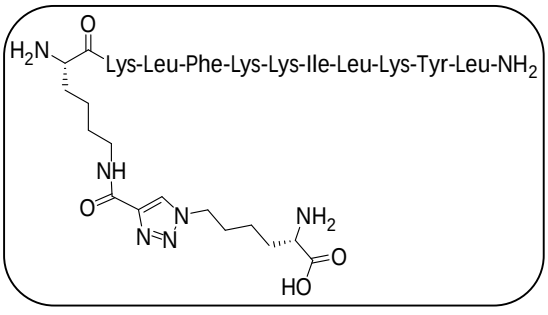

^{1}H-RMN: (*400 MHz, CD_3OD)* δ (ppm): 0.89–0.95 (m, 24H, 18 CH_3(δ)-Leu, 6 CH_3(δ)-Ile), 1.29–1.82 (m, 47H, 10 CH_2(β)-Lys, 10 CH_2(γ)-Lys, 10 CH_2(δ)-Lys, 6 CH_2(β)-Leu, 3 CH_2(γ)-Leu, 2 CH_2(γ)-Ile, 6 CH_2-Ahx), 2.87–2.95 (m, 11H, 1 CH(β)-Ile, 8 CH_2(ε)-Lys, 1 CH_2(β)-Phe, 1 CH_2(β)-Tyr), 3.12–3.15 (m, 4H, 1 CH_2(β)-Phe, 1 CH_2(β)-Tyr, 2 CH_2(ε)-Lys), 3.39–3.41 (m, 1H, 1 CH-Ahx), 3.49–3.55 (m, 1H, 1 CH(α)-Lys), 4.08–4.53 (m, 12H, 2 CH_2-Ahx, 4 CH(α)-Lys, 3 CH(α)-Leu, 1 CH(α)-Ile, 1 CH(α)-Phe, 1 CH(α)-Tyr), 6.70 (d, *J* = 8.3 Hz, 2H, 2

CH_{arom}-Tyr), 7.10 (d, *J* = 8.3 Hz, 2H, 2 CH_{arom}-Tyr), 7.22–7.28 (m, 5H, 5 CH_{arom}-Phe), 8.40 (s, 1H, CH_{Tr}). ***HPLC (λ=220 nm)***: 17.33 min [Method D]. **ESI-MS (*m/z*):** 823.4 $[M+2H]^{2+}$, 1645.7 $[M+H]^{+}$. **HRMS (ESI):** calcd. for $C_{81}H_{140}N_{21}O_{15}$ 549.0274, found 549.280; calcd. for $C_{81}H_{139}N_{21}O_{15}$ 823.0374, found 823.0338.

8.4.2.3. Peptidotriazole BP240

The alkynyl resin Fmoc-Lys(Boc)-Lys(CO-C≡CH)-Leu-Phe-Lys(Boc)-Lys(Boc)-Ile-Leu-Lys(Boc)-Tyr(^{t}Bu)-Leu-Rink-MBHA (80 mg) was treated with NaN_3 following the general procedure described above to perform the click reaction. BP240 was obtained in 84 % purity.

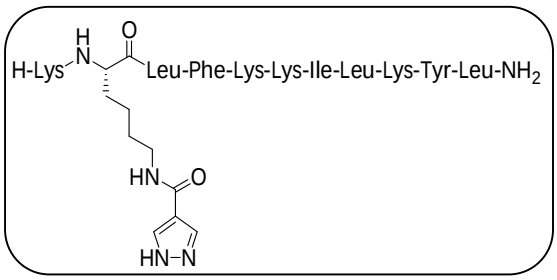

^{1}H-RMN: (*400 MHz, CD_3OD)* δ (ppm): 0.85–0.98 (m, 24H, 18 CH_3(δ)-Leu, 6 CH_3(δ)-Ile), 1.19–2.02 (m, 41H, 10 CH_2(β)-Lys, 10 CH_2(γ)-Lys, 10 CH_2(δ)-Lys, 6 CH_2(β)-Leu, 3 CH_2(γ)-Leu, 2 CH_2(γ)-Ile), 2.86–3.01 (m, 11H, 1 CH(β)-Ile, 8 CH_2(ε)-Lys, 1 CH_2(β)-Phe, 1 CH_2(β)-Tyr), 3.12–3.15 (m, 4H, 1 CH_2(β)-Phe, 1 CH_2(β)-Tyr, 2 CH_2(ε)-Lys), 3.37–3.41 (m, 1H, 1 CH(α)-Lys), 3.95–4.56 (m, 10H, 4 CH(α)-Lys, 3 CH(α)-Leu, 1 CH(α)-Ile, 1 CH(α)-Phe, 1 CH(α)-Tyr), 6.72 (d, *J* = 8.5 Hz, 2H, 2 CH_{arom}-Tyr), 7.11 (d, *J* = 8.5 Hz, 2H, 2 CH_{arom}-Tyr), 7.20–7.29 (m, 5H, 5 CH_{arom}-Phe). ***HPLC (λ=220 nm)***: 17.94 min. [Method D]. ***ESI/MS (*m/z*)***: 758.5 $[M+2H]^{2+}$, 1515.7 $[M+H]^{+}$. ***HRMS (ESI)***: calcd. for $C_{75}H_{129}N_{20}O_{13}$ 506.0011, found 506.0008; calcd. for $C_{75}H_{128}N_{20}O_{13}$ 758.4979, found 758.4940.

8.4.2.4. Peptidotriazole BP241

The alkynyl resin H-Lys(Boc)-Lys(CO-C≡CH)-Leu-Phe-Lys(Boc)-Lys(Boc)-Ile-Leu-Lys(Boc)-Tyr(^{t}Bu)-Leu-Rink-MBHA (80 mg) was treated with Boc-Nle(ε-N_3)-OH following the general procedure described above to perform the click reaction. BP241 was obtained in 82 % purity.

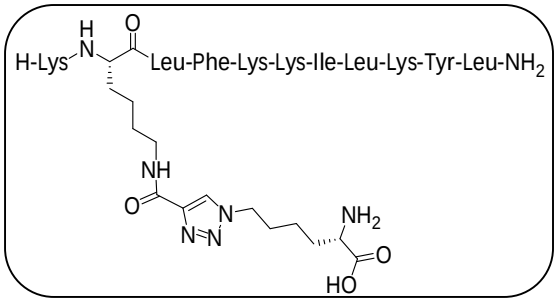

^{1}H-RMN: (*400 MHz, CD_3OD)* δ (ppm): 0.85–0.98 (m, 24H, 18 CH_3(δ)-Leu, 6 CH_3(δ)-Ile), 1.18–2.05 (m, 47H, 10 CH_2(β)-Lys, 10 CH_2(γ)-Lys, 10 CH_2(δ)-Lys, 6 CH_2(β)-Leu, 3 CH_2(γ)-Leu, 2 CH_2(γ)-Ile, 6 CH_2-Ahx), 2.84–3.01 (m, 11H, 1 CH(β)-Ile, 8 CH_2(ε)-Lys, 1 CH_2(β)-Phe, 1 CH_2(β)-Tyr), 3.10–3.17 (m, 4H, 1 CH_2(β)-Phe, 1 CH_2(β)-Tyr, 2 CH_2(ε)-Lys), 3.36–3.41 (m, 1H, 1 CH-Ahx), 3.65–3.69 (m, 1H, 1 CH(α)-Lys), 4.09–4.62 (m, 12H, 2 CH_2-Ahx, 4 CH(α)-Lys, 3 CH(α)-Leu, 1 CH(α)-Ile, 1 CH(α)-Phe, 1 CH(α)-Tyr), 6.72 (d, *J* = 8.5 Hz, 2H, 2 CH_{arom}-Tyr), 7.10 (d, *J* = 8.5 Hz, 2H, 2 CH_{arom}-Tyr), 7.21–7.29 (m, 5H, 5 CH_{arom}-Phe), 8.34 (s, 1H, CH_{Tr}). ***HPLC (λ=220 nm)***: 17.67 min [Method D]. **ESI-MS (*m/z*):** 823.5 $[M+2H]^{2+}$,1644.7 $[M+H]^+$. **HRMS (ESI):** calcd. for $C_{81}H_{140}N_{21}O_{15}$ 549.0274, found 549.0295; calcd. for $C_{81}H_{139}N_{21}O_{15}$ 823.0374, found 823.0358.

8.4.2.5. Peptidotriazole BP242

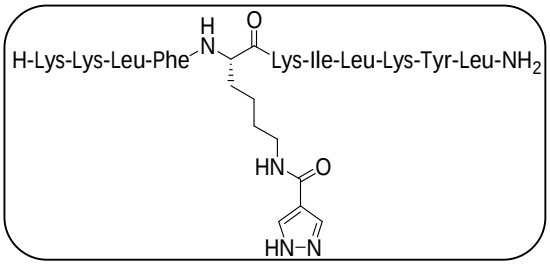

The alkynyl resin Fmoc-Lys(Boc)-Lys(Boc)-Leu-Phe-Lys(CO-C≡CH)-Lys(Boc)-Ile-Leu-Lys(Boc)-Tyr(^{t}Bu)-Leu-Rink-MBHA (80 mg) was treated with NaN_3 following the general procedure described above to perform the click reaction. BP242 was obtained in 79 % purity.

HPLC (λ=220 nm): 17.85 min [Method D]. ***ESI/MS (m/z)***: 758.4 $[M+2H]^{2+}$, 1515.7 $[M+H]^+$. ***HRMS (ESI)***: calcd. for $C_{75}H_{129}N_{20}O_{13}$ 506.0011, found 506.0025.

8.4.2.6. Peptidotriazole BP243

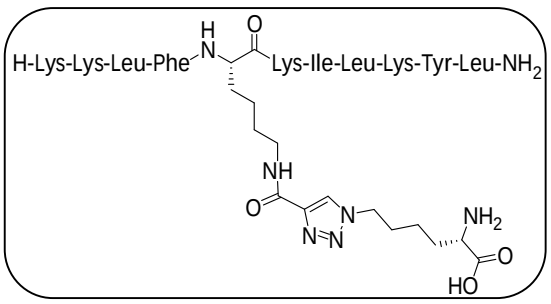

The corresponding alkynyl resin Fmoc-Lys(Boc)-Lys(Boc)-Leu-Phe-Lys(CO-C≡CH)-Lys(Boc)-Ile-Leu-Lys(Boc)-Tyr(^{t}Bu)-Leu-Rink-MBHA (80 mg) was treated with Boc-Nle(ε-N_3)-OH following the general procedure described above to perform the click reaction. BP243 was obtained in 92 % purity.

^{1}H-RMN: (*400 MHz, CD_3OD)* δ (ppm): 0.85–0.94 (m, 24H, 18 CH_3(δ)-Leu, 6 CH_3(δ)-Ile), 1.19–2.01 (m, 47H, 10 CH_2(β)-Lys, 10 CH_2(γ)-Lys, 10 CH_2(δ)-Lys, 6 CH_2(β)-Leu, 3 CH_2(γ)-

Leu, 2 CH_2(γ)-Ile, 6 CH_2-Ahx), 2.87–2.95 (m, 11H, 1 CH(β)-Ile, 8 CH_2(ε)-Lys, 1 CH_2(β)-Phe, 1 CH_2(β)-Tyr), 3.12–3.14 (m, 4H, 1 CH_2(β)-Phe, 1 CH_2(β)-Tyr, 2 CH_2(ε)-Lys), 3.39–3.43 (m, 1H, 1 CH-Ahx), 3.56–3.59 (m, 1H, 1 CH(α)-Lys), 4.09–4.56 (m, 12H, 2 CH_2-Ahx, 4 CH(α)-Lys, 3 CH(α)-Leu, 1 CH(α)-Ile, 1 CH(α)-Phe, 1 CH(α)-Tyr), 6.71 (d, *J* = 8.4 Hz, 2H, 2 CH_{arom}-Tyr), 7.11 (d, *J* = 8.4 Hz, 2H, 2 CH_{arom}-Tyr), 7.22–7.30 (m, 5H, 5 CH_{arom}-Phe), 8.42 (s, 1H, CH_{Tr}) ppm. ***HPLC (λ=220 nm)***: 17.48 min [Method D]. **ESI-MS *(m/z):*** 823.5 $[M+2H]^{2+}$, 1645.6 $[M+H]^+$. **HRMS (ESI):** calcd. for $C_{81}H_{140}N_{21}O_{15}$ 549.0274, found 549.0300; calcd. for $C_{81}H_{139}N_{21}O_{15}$ 823.0374, found 823.0352.

8.4.2.7. Peptidotriazole BP244

The alkynyl resin Fmoc-Lys(Boc)-Lys(Boc)-Leu-Phe-Lys(Boc)-Lys(CO-C≡CH)-Ile-Leu-Lys(Boc)-Tyr(^{t}Bu)-Leu-Rink-MBHA (80 mg) was treated with NaN_3 following the general procedure described above for the click reaction. BP244 was obtained in 84 % purity.

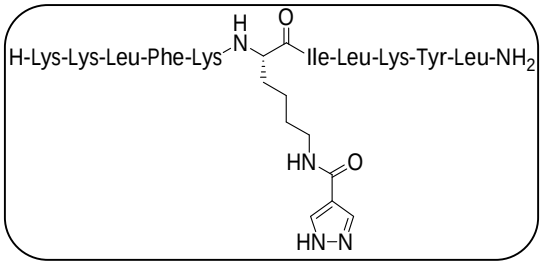

^{1}H-RMN: (*400 MHz, CD_3OD)* δ (ppm): 0.88-0.92 (m, 24H, 18 CH_3(δ)-Leu, 6 CH_3(δ)-Ile), 1.21–2.04 (m, 41H, 10 CH_2(β)-Lys, 10 CH_2(γ)-Lys, 10 CH_2(δ)-Lys, 6 CH_2(β)-Leu, 3 CH_2(γ)-Leu, 2 CH_2(γ)-Ile), 2.83–2.99 (m, 11H, 1 CH(β)-Ile, 8 CH_2(ε)-Lys, 1 CH_2(β)-Phe, 1 CH_2(β)-Tyr), 3.12-3.14 (m, 4H, 1 CH_2(β)-Phe, 1 CH_2(β)-Tyr, 2 CH_2(ε)-Lys), 3.51-3.59 (m, 1H, 1 CH(α)-Lys), 4.09-4.57 (m, 10H, 4 CH(α)-Lys, 3 CH(α)-Leu, 1 CH(α)-Ile, 1 CH(α)-Phe, 1 CH(α)-Tyr), 6.71 (d, *J* = 8.0 Hz, 2H, 2 CH_{arom}-Tyr), 7.09–7.12 (m, 2H, 2 CH_{arom}-Tyr), 7.23-7.27 (m, 5H, 5 CH_{arom}-Phe) ppm. ***HPLC (λ=220 nm)***: 17.85 min [Method D]. **ESI-MS *(m/z):*** 758.9 $[M+2H]^{2+}$, 1516.7 $[M+H]^+$. **HRMS (ESI):** calcd. for $C_{75}H_{129}N_{20}O_{13}$ 506.0011, found 506.0015.

8.4.2.8. Peptidotriazole BP245

The alkynyl resin Fmoc-Lys(Boc)-Lys(Boc)-Leu-Phe-Lys(Boc)-Lys(CO-C≡CH)-Ile-Leu-Lys(Boc)-Tyr(^{t}Bu)-Leu-Rink-MBHA (80 mg) was treated with Boc-Nle(ε-N_3)-OH following the general procedure

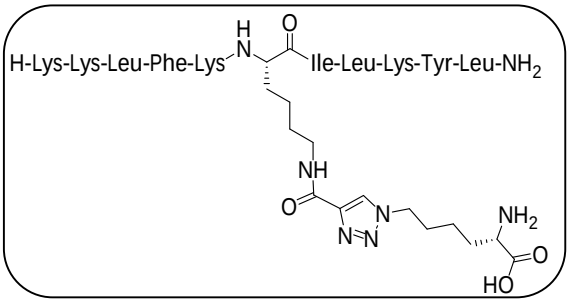

described above to perform the click reaction. BP245 was obtained in 81 % purity.

^{1}H-RMN: (*400 MHz, CD_3OD)* δ (ppm): 00.89–0.94 (m, 24H, 18 CH_3(δ)-Leu, 6 CH_3(δ)-Ile), 1.31–1.95 (m, 41H, 10 CH_2(β)-Lys, 10 CH_2(γ)-Lys, 10 CH_2(δ)-Lys, 6 CH_2(β)-Leu, 3 CH_2(γ)-Leu, 2 CH_2(γ)-Ile), 2.92–2.94 (m, 11H, 1 CH(β)-Ile, 8 CH_2(ε)-Lys, 1 CH_2(β)-Phe, 1 CH_2(β)-Tyr), 3.12–3.14 (m, 4H, 1 CH_2(β)-Phe, 1 CH_2(β)-Tyr, 2 CH_2(ε)-Lys), 3.56–3.61 (m, 1H, 1 CH(α)-Lys), 4.07–4.59 (m, 10H, 4 CH(α)-Lys, 3 CH(α)-Leu, 1 CH(α)-Ile, 1 CH(α)-Phe, 1 CH(α)-Tyr), 6.71 (d, *J* = 8.2 Hz, 2H, 2 CH_{arom}-Tyr), 7.09 (d, *J* = 8.2 Hz, 2H, 2 CH_{arom}-Tyr), 7.20–7.31 (m, 5H, 5 CH_{arom}-Phe). ***HPLC (λ=220 nm)***: 17.43 min [Method D]. **ESI-MS *(m/z):*** 758.9 $[M+2H]^{2+}$, 1515.7 $[M+H]^+$. **HRMS (ESI):** calcd. for $C_{75}H_{129}N_{20}O_{13}$ 506.0011, found 506.0034; calcd. for $C_{75}H_{128}N_{20}O_{13}$ 758.4979, found 758.4979.

8.4.2.9. Peptidotriazole BP246

The alkynyl resin Fmoc-Lys(Boc)-Lys(Boc)-Leu-Phe-Lys(Boc)-Lys(Boc)-Ile-Leu-Lys(CO-C≡CH)-Tyr(^{t}Bu)-Leu-Rink-MBHA (80 mg) was treated with NaN_3 following the general procedure described above to perform the click reaction. BP246 was obtained in 72 % purity.

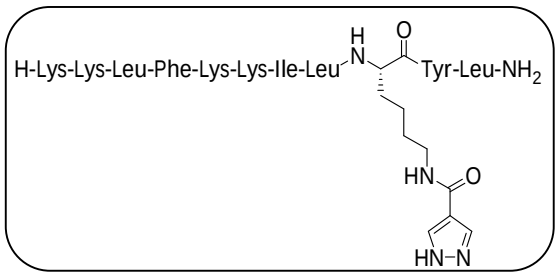

^{1}H-RMN: (*400 MHz, CD_3OD)* δ (ppm): 0.85–0.93 (m, 24H, 18 CH_3(δ)-Leu, 6 CH_3(δ)-Ile), 1.28–1.95 (m, 47H, 10 CH_2(β)-Lys, 10 CH_2(γ)-Lys, 10 CH_2(δ)-Lys, 6 CH_2(β)-Leu, 3 CH_2(γ)-Leu, 2 CH_2(γ)-Ile, 6 CH_2-Ahx), 2.88–2.93 (m, 11H, 1 CH(β)-Ile, 8 CH_2(ε)-Lys, 1 CH_2(β)-Phe, 1 CH_2(β)-Tyr), 3.12–3.15 (m, 4H, 1 CH_2(β)-Phe, 1 CH_2(β)-Tyr, 2 CH_2(ε)-Lys), 3.38–3.43 (m, 1H, 1 CH-Ahx), 3.56–3.58 (m, 1H, 1 CH(α)-Lys), 4.08–4.58 (m, 12H, 2 CH_2-Ahx, 4 CH(α)-Lys, 3 CH(α)-Leu, 1 CH(α)-Ile, 1 CH(α)-Phe, 1 CH(α)-Tyr), 6.71 (d, *J* = 8.2 Hz, 2H, 2 CH_{arom}-Tyr), 7.11 (d, *J* = 8.2 Hz, 2H, 2 CH_{arom}-Tyr), 7.21–7.26 (m, 5H, 5 CH_{arom}-Phe), 8.42 (s, 1H, CH_{Tr}). ***HPLC (λ=220 nm)***: 17.51 min [Method D]. **ESI-MS *(m/z):*** 823.0 $[M+2H]^{2+}$, 1645.7 $[M+H]^+$. **HRMS (ESI):** calcd. for $C_{81}H_{140}N_{21}O_{15}$ 549.0274, found 549.0288.

8.4.2.10. Peptidotriazole BP247

The alkynyl resin Fmoc-Lys(Boc)-Lys(Boc)-Leu-Phe-Lys(Boc)-Lys(Boc)-Ile-Leu-Lys(CO-C≡CH)-Tyr(^{t}Bu)-Leu-Rink-MBHA (80 mg) was treated with Boc-Nle(ε-N_3)-OH following the general procedure described above to perform the click reaction. BP247was obtained in 71 % purity.

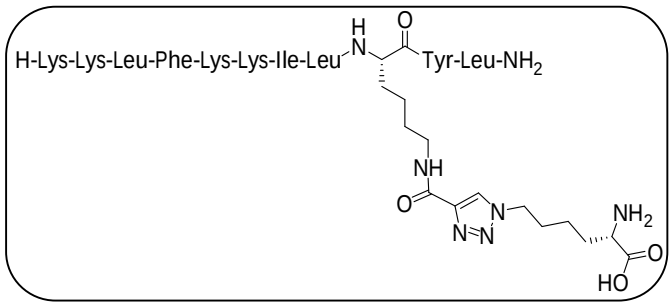

^{1}H-RMN: (*400 MHz, CD_3OD)* δ (ppm): 0.88–0.94 (m, 24H, 18 CH_3(δ)-Leu, 6 CH_3(δ)-Ile), 1.28–2.01 (m, 47H, 10 CH_2(β)-Lys, 10 CH_2(γ)-Lys, 10 CH_2(δ)-Lys, 6 CH_2(β)-Leu, 3 CH_2(γ)-Leu, 2 CH_2(γ)-Ile, 6 CH_2-Ahx), 2.89–2.99 (m, 11H, 1 CH(β)-Ile, 8 CH_2(ε)-Lys, 1 CH_2(β)-Phe, 1 CH_2(β)-Tyr), 3.12–3.15 (m, 4H, 1 CH_2(β)-Phe, 1 CH_2(β)-Tyr, 2 CH_2(ε)-Lys), 3.35–3.37 (m, 1H, 1 CH-Ahx), 3.55–3.61 (m, 1H, 1 CH(α)-Lys), 3.95–4.61 (m, 12H, 2 CH_2-Ahx, 4 CH(α)-Lys, 3 CH(α)-Leu, 1 CH(α)-Ile, 1 CH(α)-Phe, 1 CH(α)-Tyr), 6.71 (d, *J* = 8.2 Hz, 2H, 2 CH_{arom}-Tyr), 7.10 (d, *J* = 8.2 Hz, 2H, 2 CH_{arom}-Tyr), 7.21–7.27 (m, 5H, 5 CH_{arom}-Phe), 8.40 (s, 1H, CH_{Tr}). ***HPLC (λ=220 nm)***: 17.16 min [Method D]. **ESI-MS (*m/z*):** 823.5 $[M+2H]^{2+}$, 1645.7 $[M+H]^+$. **HRMS (ESI):** calcd. for $C_{81}H_{140}N_{21}O_{15}$ 549.0274, found 549.0289; calcd. for $C_{81}H_{139}N_{21}O_{15}$ 823.0374, found 823.0373.

8.4.2.11. Peptidotriazole BP248

The alkynyl resin Fmoc-Lys(Boc)-Lys(Boc)-Leu-Prg-Lys(Boc)-Lys(Boc)-Ile-Leu-Lys(Boc)-Tyr(^{t}Bu)-Leu-Rink-MBHA (80 mg) was treated with NaN_3 following the general procedure described above to perform the click reaction. BP248 was obtained in 76 % purity.

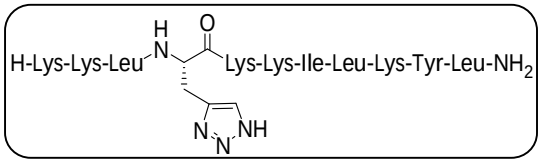

^{1}H-RMN: (*400 MHz, CD_3OD)* δ (ppm): 0.86–0.96 (m, 24H, 18 CH_3(δ)-Leu, 6 CH_3(δ)-Ile), 1.39–1.94 (m, 41H, 10 CH_2(β)-Lys, 10 CH_2(γ)-Lys, 10 CH_2(δ)-Lys, 6 CH_2(β)-Leu, 3 CH_2(γ)-Leu, 2 CH_2(γ)-Ile), 2.87–2.98 (m, 10H, 1 CH(β)-Ile, 8 CH_2(ε)-Lys, 1 CH_2(β)-Tyr), 3.12–3.14

(m, 5H, 2 CH_2(β)-Ala, 1 CH_2(β)-Tyr, 2 CH_2(ε)-Lys), 3.47–3.49 (m, 1H, 1 CH(α)-Lys), 4.27–4.62 (m, 10H, 4 CH(α)-Lys, 3 CH(α)-Leu, 1 CH(α)-Ile, 1 CH(α)-Tyr, 1 CH(α)-Ala), 6.71 (d, *J* = 8.5 Hz, 2H, 2 CH_{arom}-Tyr), 7.11 (d, *J* = 8.5 Hz, 2H, 2 CH_{arom}-Tyr). ***HPLC (λ=220 nm)***: 15.82 min [Method D]. **ESI-MS (*m/z*)**: 706.5 $[M+2H]^{2+}$, 1412.1 $[M+H]^+$. **HRMS (ESI):** calcd. for $C_{68}H_{125}N_{20}O_{12}$ 471.3256, found 471.3279; calcd. for $C_{68}H_{124}N_{20}O_{12}$ 706.4848, found 706.4847.

8.4.2.12. Peptidotriazole BP249

The alkynyl resin Fmoc-Lys(Boc)-Lys(Boc)-Leu-Prg-Lys(Boc)-Lys(Boc)-Ile-Leu-Lys(Boc)-Tyr(*t*Bu)-Leu-Rink-MBHA (80 mg) was treated with Boc-Nle(ε-N_3)-OH following the general procedure described above to perform the click reaction. BP249 was obtained in 65 % purity.

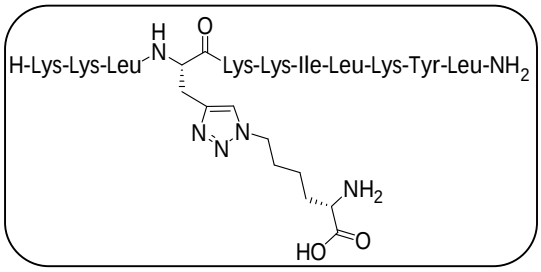

^{1}H-RMN: (*400 MHz, CD_3OD)* δ (ppm): 0.84–0.97 (m, 24H, 18 CH_3(δ)-Leu, 6 CH_3(δ)-Ile), 1.29–1.96 (m, 47H, 10 CH_2(β)-Lys, 10 CH_2(γ)-Lys, 10 CH_2(δ)-Lys, 6 CH_2(β)-Leu, 3 CH_2(γ)-Leu, 2 CH_2(γ)-Ile, 6 CH_2-Ahx), 2.87–2.99 (m, 10H, 1 CH(β)-Ile, 8 CH_2(ε)-Lys, 1 CH_2(β)-Tyr), 3.12–3.15 (m, 5H, 1 CH_2(β)-Tyr, 2 CH_2(ε)-Lys, 2 CH_2(β)-Ala), 3.38–3.43 (m, 1H, 1 CH-Ahx), 3.62–3.66 (m, 1H, 1 CH(α)-Lys), 3.95–4.55 (m, 12H, 4 CH(α)-Lys, 3 CH(α)-Leu, 1 CH(α)-Ile, 1 CH(α)-Ala, 1 CH(α)-Tyr, 2 CH_2-Ahx), 6.71 (d, *J* = 8.5 Hz, 2H, 2 CH_{arom}-Tyr), 7.13 (d, *J* = 8.5 Hz, 2H, 2 CH_{arom}-Tyr), 7.91 (s, 1H, CH_{Tr}). ***HPLC (λ=220 nm)***: 15.69 min [Method D]. **ESI-MS (*m/z*):** 771.0 $[M+2H]^{2+}$, 1540.7 $[M+H]^+$. **HRMS (ESI):** calcd. for $C_{74}H_{136}N_{21}O_{14}$ 514.3520, found 514.3538; calcd. for $C_{74}H_{135}N_{21}O_{14}$ 771.0243, found 771.0215.

8.4.2.13. Peptidotriazole BP250

In order to synthesize this peptide, BnN_3 was prepared using the following procedure.

A solution of BnBr (1.84 mL, 21 mmol), NaN_3 (1.46 g, 22.5 mmol), and H_2O (2.5 mL) in EtOH (20 mL) was stirred at room temperature overnight.

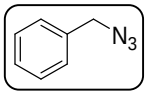

Thereafter, the mixture was diluted with H_2O (100 mL) and extracted repeatedly with diethyl ether (3×25 mL). The combined organic layers were washed with H_2O (3×25 mL), dried over anhydrous $MgSO_4$ and concentrated to give a pure colorless liquid (1.85 mg, 90 %).

Rf: 0.79, Hexane:EtOAc (3:1). ***IR*** (neat) ν (cm^{-1}): 3031.95 (≡CH st), 2090.08 (N≡N st), 1454.45 (δ CH_2), 736.87 (δ CH opp), 697.14 (δ C=C). ***^{1}H-RMN***: (*400 MHz, $CDCl_3$)* δ (ppm): 4.39 (s, 2H, CH_2), 7.36-7.41 (m, 5H, 5 CH_{arom}). ***^{13}C-RMN***: *(100MHz, $CDCl_3$)* δ (ppm): 54.61 (CH_2), 128.07 (1 CH_{arom}), 128.14 (2 CH_{arom}), 128.67 (2 CH_{arom}), 135.25 (1 C_{arom}). ***HPLC (λ=220 nm)***: 8.24 min [Method A].

Once we had BnN_3 we proceded to the synthesis of peptidotriazole BP250. The corresponding resin Fmoc-Lys(Boc)-Lys(Boc)-Leu-Prg-Lys(Boc)-Lys(Boc)-Ile-Leu-Lys(Boc)-Tyr(^{t}Bu)-Leu-Rink-MBHA (80 mg) was treated with BnN_3 following the general procedure described above to perform the click reaction. BP250 was obtained in 91 % purity.

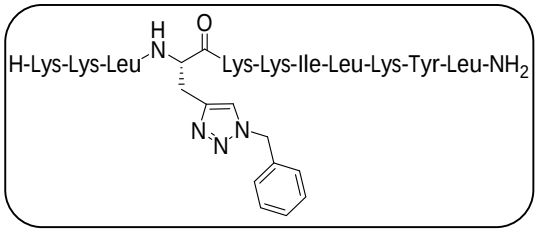

^{1}H-RMN: (*400 MHz, CD_3OD)* δ (ppm): 0.88–0.93 (m, 24H, 18 CH_3(δ)-Leu, 6 CH_3(δ)-Ile), 1.21–2.03 (m, 41H, 10 CH_2(β)-Lys, 10 CH_2(γ)-Lys, 10 CH_2(δ)-Lys, 6 CH_2(β)-Leu, 3 CH_2(γ)-Leu, 2 CH_2(γ)-Ile), 2.83–2.99 (m, 10H, 1 CH(β)-Ile, 8 CH_2(ε)-Lys, 1 CH_2(β)-Tyr), 3.11–3.14 (m, 5H, 2 CH_2(β)-Ala, 1 CH_2(β)-Tyr, 2 CH_2(ε)-Lys), 3.47–3.49 (m, 1H, 1 CH(α)-Lys), 4.06–4.49 (m, 10H, 4 CH(α)-Lys, 3 CH(α)-Leu, 1 CH(α)-Ala, 1 CH(α)-Ile, 1 CH(α)-Tyr), 5.58 (br s, 2H, 2 CH_2-Bn), 6.69 (d, *J* = 8.2 Hz, 2H, 2 CH_{arom}-Tyr), 7.08–7.13 (m, 4H, 2 CH_{arom}-Tyr, 2 CH_{arom}-Bn), 7.31–7.37 (m, 3H, 3 CH_{arom}-Bn), 7.96 (s, 1H, CH_{Tr}). ***HPLC (λ=220 nm)***: 16.91 min [Method D]. **ESI-MS (*m/z*):** 751.5 $[M+2H]^{2+}$, 1501.7 $[M+H]^+$. **HRMS (ESI):** calcd. for $C_{75}H_{131}N_{20}O_{12}$ 501.3413, found 501.3431.

8.5. Synthesis of cyclic peptidotriazoles

8.5.1. Synthesis of amino acids and scaffolds

8.5.1.1. Fmoc-Gln($CH_2C\equiv CH$)-O^{t}Bu

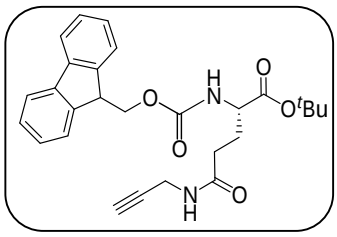

Propargylamine (110 µL, 1.56 mmol), Oxyma (404 mg, 2.84 mmol), DIPEA (720 µL, 4.22 mmol) and EDC (320 mg, 3.12 mmol) were subsequently added to a solution of Fmoc-Glu-O^{t}Bu (600 mg, 1.42 mmol) in dry THF (70 mL) under N_2. The reaction mixture was stirred at room temperature under N_2 and monitored by HPLC. After 24 h, more EDC (160 mg), Oxyma (101 mg) and DIPEA (125 µL) were added and the mixture was stirred for additional 24 h. The reaction was stopped by adding EtOH (2 mL). The removal of the solvents under vacuum gave a residue which was dissolved in EtOAc (50 mL), extracted with H_2SO_4 0.5M (4 x 50 ml), washed with distilled H_2O (2 x 50 mL), dried over anhydrous $MgSO_4$ and concentrated. Afterwards, the crude product was chromatographed on silica gel with hexane:EtOAc (2:1) to give quantitatively Fmoc-Gln($CH_2C\equiv CH$)-O^{t}Bu as a yellow oil (639 mg, 98 %).

Rf: 0.81, Hexane:EtOAc (1:5). ***IR*** (neat) ν (cm^{-1}): 3305.99 (≡CH st), 2980.46 (C≡C st), 1725.79, 1689.73 (C=O st), 1637.08 (δ NH_2), 1083.99 (C-O st), 738.99 (δ NH opp), 646.23 (δ≡CH). ***^{1}H-RMN***: *(400 MHz, $CDCl_3$)* δ (ppm): 1.51 (s, 9H, $C(CH_3)_3$), 1.90-1.97 (m, 2H, 1 CH_2(β), 1 CH_2(γ)), 2.23-2.30 (m, 3H, 1 CH_2(β), 1 CH_2(γ), 1 C≡CH), 4.07-4.09 (m, 2H, NCH_2), 4.24-4.27 (m, 2H, 1 CH_{Fmoc}, 1 CH(α)), 4.42-4.51 (m, 2H, OCH_2), 5.59 (d, J=7.6 Hz, 1H, NHCOO), 6.32 (br, 1H, CONH), 7.36 (t, J= 7.6 Hz, 2H, 2 CH_{arom}), 7.45 (t, J= 7.6 Hz, 2H, 2 CH_{arom}), 7.63 (d, J= 7.6 Hz, 2H, 2 CH_{arom}), 7.81 (d, J= 7.6 Hz, 2H, 2 CH_{arom}). ***^{13}C-RMN*** *(100MHz, $CDCl_3$)* δ (ppm): 27.92 (CH_3), 29.06, 29.19, 32.23 (CH_2(β), CH_2(γ), CH_2N), 47.15 (CH_{Fmoc}), 53.80 (CH(α)), 66.93 (OCH_2), 71.52 (≡CH), 79.41 (C≡), 82.63 ($C(CH_3)_3$), 119.94 (1 CH_{arom}), 119.97 (1 CH_{arom}), 125.01 (1 CH_{arom}), 125.06 (1 CH_{arom}), 127.04 (2 CH_{arom}), 127.70 (2 CH_{arom}), 141.25 (1 C_{arom}), 141.29 (1 C_{arom}), 143.57 (1 C_{arom}), 143.81 (1 C_{arom}), 156.42 (NHCOO), 170.96 (COO^{t}Bu), 171.71 (CONH). ***HPLC (λ=220 nm)***: 8.94 min [Method A]. ***ESI/MS (m/z)***: 463.1 $[M+H]^+$, 485.1 $[M+Na]^+$.

8.5.1.2. Fmoc-Gln($CH_2C\equiv CH$)-OH

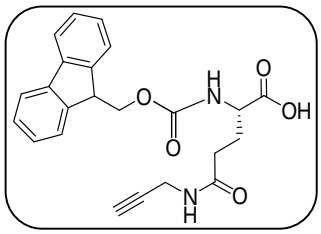

Fmoc-Gln($CH_2C\equiv CH$)-O^{t}Bu (400 mg, 0.71 mmol) was dissolved in a solution of TFA/CH_2Cl_2 (1:1) (10 mL) and stirred for 2 h at room temperature. Following TFA evaporation and diethyl ether extraction, Fmoc-Gln($CH_2C\equiv CH$)-OH was obtained as a white powder (81 mg, 58 %).

Rf: 0.32, EtOAc:NH_3:MeOH (5:1:1). ***IR*** (neat) ν (cm^{-1}): 3293.84 (≡CH st), 2923.38 (C≡C st), 1687.41 (C=O st), 1640.36 (δ NH_2), 1536.22, 1448.67 (δ CH_2), 1085.73 (C-O st), 738.22 (δ NH opp), 620.39 (δ ≡CH). ***^{1}H-RMN***: *(400 MHz, $CDCl_3$)*δ (ppm): 1.91-1.98 (m, 1H, 1 CH_2(β)), 2.12-2.24 (m, 1H, 1 CH_2(β)), 2.28-2.33 (m, 2H, CH_2(γ)), 2.56 (t, J= 3.6 Hz, 1H, ≡CH), 3.93 (d, J= 3.6 Hz, 2H, NCH_2), 4.15-4.22 (m, 2H, 1 CH_{Fmoc}, 1 CH(α)), 4.31 (dd, J= 9.4 Hz, J= 13.8 Hz, 1H, 1 OCH_2), 4.37 (dd, J= 9.4 Hz, J= 13.8 Hz, 1H, 1 OCH_2), 7.30 (td, J= 1.6 Hz, J= 9.8 Hz, 2H, 2 CH_{arom}), 7.38 (t, J= 9.8 Hz, 2H, 2 CH_{arom}), 7.64-7.68 (m, 2H, 2 CH_{arom}), 7.77 (d, J= 9.8 Hz, 2H, 2 CH_{arom}). ***^{13}C-RMN***: *(100MHz, $CDCl_3$)* δ (ppm): 28.54 (CH_2-β), 29.45 (NCH_2), 33.05 (CH_2-γ), 46.99 (CH_{Fmoc}), 54.91 (CH-α), 67.96 (OCH_2), 72.18 (≡CH), 80.51 (≡C), 120.86 (2 CH_{arom}), 126.23 (2 CH_{arom}), 128.13 (2 CH_{arom}), 128.74 (2 CH_{arom}), 142.51 (2 C_{arom}), 145.10 (1 C_{arom}), 145.27 (1 C_{arom}), 158.62 (NHCOO), 174.46 (CONH), 175.35 (COOH). ***HPLC (λ=220 nm)***: 7.70 min [Method A]. ***ESI/MS (m/z)***: 407.0 $[M+H]^+$. ***HRMS (ESI)***: calcd. for $C_{23}H_{23}N_2O_5$ 407.1601, found 407.1591; calcd. for $C_{23}H_{22}N_2NaO_5$ 429.1421, found 429.1406.

8.5.1.3. Fmoc-Lys-OH

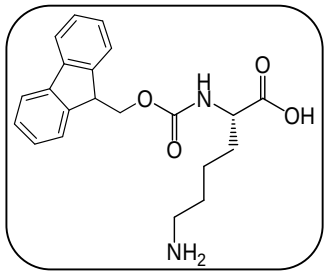

Fmoc-Lys(Boc)-OH (1.25 g, 3.40 mmol) was dissolved in a solution of TFA/CH_2Cl_2.(1:1) (75 mL) and stirred for 2 h at room temperature. Following TFA evaporation and diethyl ether extraction, Fmoc-Lys-OH was obtained quantitatively as a white powder (1.22 g, 95 %).

Rf: 0.5, $CHCl_3$:MeOH:AcOH (5:3:1). ***IR***(neat) ν (cm^{-1}): 3066.47 (≡CH st), 1670.64 (C=O st), 1519.64 (C=C), 1449.63 (δ CH_2), 1181.57 (δ C-H ip), 789.19 (γ CH_2), 738.60 (δ NH opp). ***^{1}H-RMN***: *(400 MHz, DMSO-d*6) δ (ppm): 1.344-1.430 (m, 2H, 2 CH_2(γ)), 1.48-1.71

(m, 4H, 2 CH_2(β), 2 CH_2(δ)), 2.73-2.80 (m, 2H, 2 CH_2(ε)), 3.90-3.96 (m, 1H, CH(α)), 4.21-4.26 (m, 1H, $CH_{(Fmoc)}$), 4.28-4.34 (m, 2H, $CH_{2(Fmoc)}$), 7.33 (td, J= 0.7 J= 7.2 Hz, 2H, 2 CH_{arom}), 7.42 (t, J= 7.2 Hz, 2H, 2 CH_{arom}), 7.63 (d, J= 7.2 Hz, 1H, 1 CH_{arom}), 7.71-7.74 (m, 1H, 1 CH_{arom}), 7.79 (br, 1H, CONH), 7.89 (d, J= 7.2 Hz, 2H, 2 CH_{arom}). ***^{13}C-RMN*** *(100MHz, DMSO-d*6) δ (ppm): 22.57 (CH_2(γ)), 26.51 (CH_2(β)), 30.17 (CH_2(δ)), 38.59 (CH_2(ε)), 46.66 ($CH_{(Fmoc)}$), 53.61 (CH(α)), 65.58 ($CH_{2(Fmoc)}$), 120.13 (1 CH_{arom}), 120.14 (1 CH_{arom}), 125.26 (2 CH_{arom}), 127.07 (1 CH_{arom}), 127.08 (1 CH_{arom}), 127.65 (2 CH_{arom}), 140.73 (1 C_{arom}), 140.76 (1 C_{arom}), 143.79 (1 C_{arom}), 143.81 (1 C_{arom}), 156.20 (CONH), 173.85 (COOH). ***HPLC (λ=220 nm)***: 6.99 min [Method A]. ***ESI/MS (m/z)***: 369.1 $[M+H]^+$.

8.5.1.4. Fmoc-Nle(ε-N_3)-OH

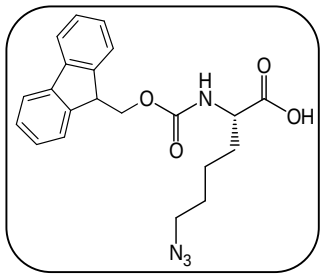

NaN_3 (883 mg, 13.58 mmol) was dissolved in a mixture of distilled H_2O (2 mL) and CH_2Cl_2 (3.5 mL). Triflic anhydride (460 µL, 2.72 mmol) was added slowly, and stirred for 2 h. The organic phase was removed and the aqueous phase was extracted with CH_2Cl_2 (2×3 mL). The organic fractions containing TfN_3 were combined, washed with a saturated aqueous solution of Na_2CO_3 (6.5 mL), and used without further purification.

Fmoc-Lys-OH (500 mg, 1.36 mmol) was dissolved in distilled H_2O (4.5 mL) and MeOH (9 mL). Thereafter, $NaHCO_3$ (1.14 g, 13.58 mmol) and $CuSO_4 \cdot 5H_2O$ (34 mg, 13 mmol) were added. TfN_3 in CH_2Cl_2 (9.5 mL) was added and the mixture was stirred under pressure at room temperature. The reaction was monitored by HPLC. After 12 h, the organic solvents were removed under vacuum, and the remaining solution was diluted with distilled H_2O (36 mL) and acidified at pH 2 by the addition of aq HCl. After extraction with EtOAc (4×20 mL), the organic fractions were combined, washed with brine (20 mL), dried over anhydrous $MgSO_4$ and concentrated. Afterwards, the crude product was digested with pentane to give quantitatively Fmoc-Nle(ε-N_3)-OH as a white powder (384.8 mg, 94 %).

Rf: 0.64, CH_2Cl_2:MeOH (7:1). ***IR*** (neat) ν (cm^{-1}): 3381.58 (≡CH st), 2095.48 (N≡N st), 1701.11 (C=O st), 1521.57 (C=C st), 1450.02 (δ CH_2), 1190.06 (δ CH ip), 739.37 (δ NH

opp). ***^{1}H-RMN***: (*400 MHz, DMSO-d*6) δ (ppm): 1.34-1.43 (m, 2H, 2 CH_2(γ)), 1.45-1.57 (m, 2H, CH_2(δ)), 1.58-1.66 (m, 1H, 1 CH_2(β)), 1.68-1.77 (m, 1H, 1 CH_2(β)), 3.32 (t, J= 6.8 Hz, 2H, CH_2(ε)), 3.91-3.97 (m, 1H, CH(α)), 4.21-4.25 (m, 1H, $CH_{(Fmoc)}$), 4.28-4.30 (m, 2H, $CH_{2(Fmoc)}$), 7.42 (td, J= 0.9 Hz, J= 7.4 Hz, 2H, 2 CH_{arom}), 7.42 (t, 2H, J= 7.4 Hz, 2 CH_{arom}), 7.65 (d, J= 7.4 Hz, 1H, 1 CH_{arom}), 7.73 (d, J= 7.4 Hz, 1H, 1 CH_{arom}), 7.89 (d, J= 7.4 Hz, 2H, 2 CH_{arom}), 8.95 (s, 1H, CONH). ***^{13}C-RMN*** *(100MHz, DMSO-d*6) δ (ppm): 23.37 (CH_2(γ)), 28.29 (CH_2(δ)), 30.74 (CH_2(β)), 47.13 ($CH_{(Fmoc)}$), 50.98 (CH_2(ε)), 54.12 (CH(α)), 66.05 ($CH_{2(Fmoc)}$), 120.56 (1 CH_{arom}), 120.58 (1 CH_{arom}), 125.73 (1 CH_{arom}), 125.76 (1 CH_{arom}), 127.52 (2 CH_{arom}), 128.10 (2 CH_{arom}), 141.20 (1 C_{arom}), 141.22 (1 C_{arom}), 144.27 (1 C_{arom}), 144.32 (1 C_{arom}), 156.63 (CONH), 174.32 (COOH). ***HPLC (λ=220 nm)***: 8.60 min [Method A]. ***ESI/MS (m/z)***: 395.1 $[M+H]^+$. ***HRMS (ESI)***: calcd. For $C_{21}H_{23}N_4O_4$ 395.1714, found 395.1727; calcd. for $C_{21}H_{22}N_4NaO_4$ 417.1533, found 417.1544.

8.5.2. Synthesis of Fmoc-Lys(Boc)-Nle(ε-N_3)-Leu-Phe-Lys(Boc)-Lys(Boc)-Ile-Leu-Lys(Boc)-Tyr(^{t}Bu)-Leu-OH (BP304)

The required amount of Fmoc-Rink-4-methylbenzhydrylamine resin (0.64 mmol/g) was swollen with CH_2Cl_2 (1×20 min) and with DMF (1×20 min). Couplings of the Fmoc-amino acids were mediated by Strategy B. An aliquot of peptide was cleaved from the resin with TFA/H_2O/TIS (95:2.5:2.5) and analyzed by HPLC and mass spectrometry obtaining the desired product with 82 % purity.

HPLC (λ=220 nm): 7.97 min. [Method A]. ***ESI/MS (m/z)***: 835.6 $[M+2H]^{2+}$, 1670.2 $[M+H]^+$.

8.5.3. Synthesis of peptidotriazoles BP253 and BP254

8.5.3.1. Fmoc-Phe-Nle(ε-N_3)-Lys(Boc)-Leu-Gln(Rink-MBHA)-OAl (26)

The required amount of Fmoc-Rink-4-MBHA (0.3 mmol/g) was swollen with CH_2Cl_2 (1×20 min) and DMF (1×20 min).

Peptidyl resin Fmoc-Phe-Nle(ε-N_3)-Lys(Boc)-Leu-Gln(Rink-MBHA)-OAl was prepared following conditions B, in section 8.2. Once chain assembly was completed, peptidyl resin was treated with 1 % TFA in CH_2Cl_2 upon which the solution became yellow. The

mixture was stirred for 5 min and the resin was then washed with CH_2Cl_2 (2×1 min), MeOH (2×1 min) and CH_2Cl_2 (2×1 min). The TFA treatment and the washes were repeated until the solution remained colorless. Then, the resin was treated with K_2CO_3 (0.4 equiv), $CuSO_4 \cdot 5H_2O$ (0.1 equiv), MeOH (40 µL) and a solution of TfN_3 in CH_2Cl_2, previously synthesised as described in section 8.5.1.4.

The reaction mixture was stirred at room temperature for 18 h. After this time, the resinwas treated again with the above reagents for additional 18h. The resin was subsequently washed with CH_2Cl_2 (1×3 min), MeOH (1×3 min), DMF (3×1 min), sodium *N,N*-diethyldithiocarbamate (0.03 M in NMP, 3×15 min) and CH_2Cl_2 (1×3 min). The reaction was followed by the ninhydrin test. An aliquot of the resulting resin was cleaved with TFA/H_2O/TIS (95:2.5:2.5) and the crude analyzed by HPLC and mass spectrometry. Fmoc-Phe-Nle(ε-N_3)-Lys-Leu-Gln-OAl (BP252) was obtained in 94 % purity.

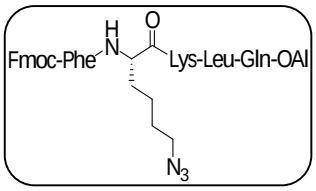

HPLC (λ=220 nm): 8.29 min [Method A]. ***ESI/MS (m/z)***: 951.4 $[M+H]^+$.

8.5.3.2. Peptidotriazole BP253

The azidopeptidyl resin Fmoc-Phe-Nle(ε-N_3)-Lys(Boc)-Leu-Gln(Rink-MBHA)-OAl (50 mg) was swollen with CH_2Cl_2 (1×20 min) and DMF (1×20 min) and then it was treated with the heptyne (5 equiv) in presence of ascorbic acid (5 equiv) and CuI (5 equiv) in piperidine/DMF (2:8). The reaction mixture was stirred at room temperature for 5 h. The resin was subsequently washed with sodium *N,N*-diethyldithiocarbamate (0.03 M in NMP, 3×15 min), DMF (6×1 min) and CH_2Cl_2 (1×20 min). The resin was cleaved with TFA/H_2O/TIS (95:2.5:2.5) and the crude was analyzed by HPLC, mass spectrometry and NMR. BP253 was obtained in 96 % purity.

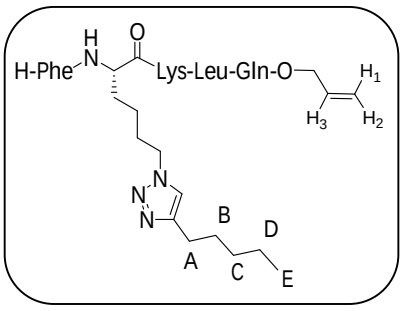

^{1}H-RMN: (*400 MHz, CD_3OD)* δ (ppm): 0.9-0.93 (m, 6H, 3 CH_3(δ)-Leu, 3 CH_3(E), 0.97 (d, J= 6.8 Hz, 3H, 3 CH_3(δ)-Leu), 1.33-1.40 (m, 8H, 2 CH_2(γ)-Lys[2], 2 CH_2(B), 2 CH_2(C), 2 CH_2(D), 1.46 (quint, J= 7.7 Hz, 2H, 2 CH_2(γ)-Lys[3]), 1.61 (t, J= 7.6 Hz, 2H, 2 CH_2(β)-Leu),

1.65-2.00 (m, 11H, 1 CH(γ)-Leu, 4 CH_2(β)-Lys, 4 CH_2(δ)-Lys, 2 CH_2-Glu), 2.31-2.36 (m, 2H, 2 CH_2-Glu), 2.68 (t, J= 7.6 Hz, 2H, 2 CH_2(A)), 2.95 (t, J= 7.2 Hz, 2H, 2 CH_2(ε)-Lys^3), 2.98-3.04 (m, 1H, CH_2(β)-Phe), 3.27-3.28 (m, 1H, CH_2(β)-Phe), 4.13- 4.17 (m, 1H, 1 CH(α)-Phe), 4.31- 4.42 (m, 5H, 2 CH(α)-Lys, 1 CH(α)-Leu, 2 CH_2(ε)-Lys^2), 4.46 (dd, J= 5.2 Hz, J= 9.2 Hz, 1H, 1 CH(α)-Glu), 4.61 (dq, J= 1.4 Hz, J= 5.7 Hz, 2H, 2 OCH_2), 5.33 (dq, J= 1.4 Hz, J= 17.2 Hz, 1H, 1 =CH_2^1), 5.24 (dq, J= 1.4 Hz, J= 10.4 Hz, 1H, 1 =CH_2^2), 5.93 (ddt, J= 5.7 Hz, J= 10.4 Hz, J= 17.2 Hz, 1H, 1 $CH=^3$), 7.29-7.37 (m, 5H, 5 CH_{arom}), 7.75 (s, 1H, CHTr). ***^{13}C-RMN***: *(100MHz, CD_3OD)* δ (ppm): 22.14, 23.04, 23.38, 23.42, 23.49, 23.57, 23.74, 25.75, 26.27 (CH_2(A), 28.08, 30.28, 30.73, 32.40, 32.47, 32.53, 38.56, 40.46 (CH_2(ε)-Lys^3), 41.79 (CH_2(β)-Leu), 50.86, 53.23, 53.30, 54.40, 54.50, 55.52 (CH(α)-Phe), 66.97 (OCH_2), 118.98 (=CH_2), 128.94, 130.17, 130.58 (CH_{arom}), 133.18 (C_{arom}), 135.48 (CH=), 169.73 (CO), 172.67 (CO), 173.23 (CO), 173.74 (CO), 174.93 (CO), 177.58 (CO). ***HPLC (λ=220 nm)***: 6.46 min [Method A]. ***ESI/MS (m/z)***: 413.2 $[M+2H]^{2+}$, 825.5 $[M+H]^+$, 847.4 $[M+Na]^+$. ***HRMS (ESI)***: calcd. for $C_{42}H_{70}N_{10}O_7$ 413.2709; found 413.2720; calcd. for $C_{42}H_{69}N_{10}O_7$ 825.5345; found 825.5314; calcd. for $C_{42}H_{69}N_{10}NaO_7$ 847.5165; found 847.5131.

8.5.3.3. Peptidotriazole BP254

BP254 was prepared following the protocol described for BP253 using tetrahydro-2-(prop-2-ynyloxy)-2*H*-pyran as alkyne, being obtained in 99 % purity.

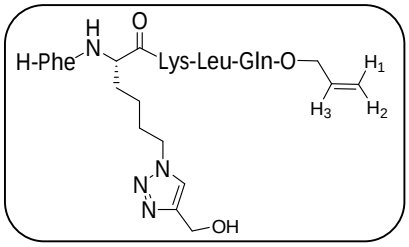

HPLC (λ=220 nm): 13.54 min [Method C]. ***ESI/MS (m/z)***: 393.1 $[M+2H]^{2+}$, 785.3 $[M+H]^+$. ***HRMS (ESI)***: calcd. for $C_{38}H_{62}N_{10}O_8$ 393.2371; found 393.2368; calcd. for $C_{38}H_{61}N_{10}O_8$ 785.4668; found 785.4624; calcd. for $C_{38}H_{60}N_{10}NaO_8$ 807.4488; found 807.4439.

8.5.4. Synthesis of peptidotriazoles BP286-BP289

8.5.4.1. Fmoc-Gln(CH_2CΞCH)-Leu-Glu(Rink-MBHA)-OAl (13)

Peptidyl alkynyl resin Fmoc-Gln(CH_2-CΞCH)-Leu-Glu(Rink-MBHA)-OAl was prepared following the

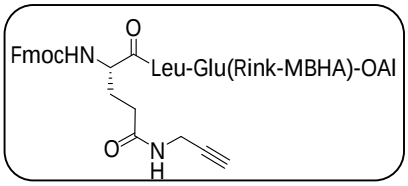

general procedure described above (Conditions B, section 8.2). Once chain assembly was completed, an aliquot of the resin was cleaved and the respective Fmoc-Gln($CH_2C\equiv CH$)-Leu-Gln-OAl was obtained in 97 % purity.

HPLC (λ=220 nm): 8.14 min [Method A].

8.5.4.2. Peptidotriazole BP288

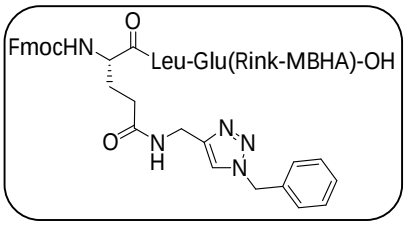

The alkynylpeptidyl resin Fmoc-Gln(CH_2-$C\equiv CH$)-Leu-Glu(Rink-MBHA)-OAl (**13**) (50 mg) was treated with $Pd(PPh_3)_4$ (3 equiv) in $CHCl_3$/AcOH/NMM (3:2:1) under stirring for 3 h at room temperature in order to remove the C-terminal allyl ester. After this time, the resin was washed with THF (3×2 min), NMP (3×2 min), DIPEA/CH_2Cl_2 (1:19, 3×2 min), sodium *N,N*-diethyldithiocarbamate (0.03 M in NMP, 3×15 min), NMP (10×1 min) and CH_2Cl_2 (3×2 min). Afterwards, the click reaction was carried out by treating the resin with BnN_3 for 5 h following the general procedure described in section 8.5.3. BP288 was obtained in 76 % purity.

HPLC (λ=220 nm): 16.88 min. [Method D]. ***ESI/MS (m/z)***: 559.3 $[M+H]^+$, 581.3 $[M+Na]^+$. ***HRMS (ESI)***: calcd. for $C_{26}H_{39}N_8O_6$ 559.2987; found 559.3014; calcd. for C $C_{26}H_{38}N_8NaO_6$ 581.2807; found 581.2828.

8.5.4.3. Peptidotriazole BP286

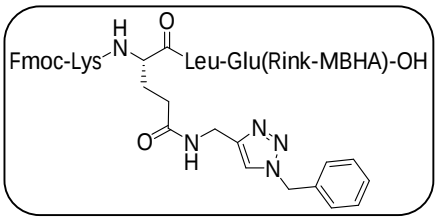

Peptidyl alkynyl Fmoc-Gln(CH_2-$C\equiv CH$)-Leu-Glu(Rink-MBHA)-OAl was swollen with CH_2Cl_2 (1×20 min) and DMF (1×20 min) and then Fmoc-Lys(Boc)-OH was coupled following conditions B described above (section 8.2). Once the chain assembly was completed, the alkynylpeptidyl resin Fmoc-Lys-Gln(CH_2-$C\equiv CH$)-Leu-Glu(Rink-MBHA)-OAl (**14**) (50 mg) was treated with $Pd(PPh_3)_4$ (3 equiv) in $CHCl_3$/AcOH/NMM (3:2:1) under stirring for 3 h at room temperature in order to remove the C-terminal allyl ester. After this time, the resin was washed with THF (3×2 min), NMP (3×2 min), DIPEA/CH_2Cl_2 (1:19, 3×2 min), sodium *N,N*-

diethyldithiocarbamate (0.03 M in NMP, 3×15 min), NMP (10×1 min) and CH_2Cl_2 (3×2 min). Afterwards, the click reaction was carried out by treating the resin with BnN_3 for 5 hours following the general procedure described in section 8.5.3. BP286 was obtained in 70 % purity.

HPLC (λ=220 nm): 16.09 min [Method D]. ***ESI/MS (m/z)***: 687.4 $[M+H]^+$. ***HRMS (ESI)***: calcd. for $C_{32}H_{51}N_{10}O_7$ 687.3937, found 687.3930.

8.5.4.4. Fmoc-Prg-Leu-Glu(Rink-MBHA)-OAl (15)

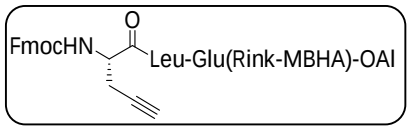

Peptidyl alkynyl resin Fmoc-Prg-Leu-Glu(Rink-MBHA)-OAl was prepared following the general procedure described above (Conditions B, section 8.2). Once chain assembly was completed, an aliquot of the resin was cleaved and the regarding Fmoc-Prg-Leu-Gln-OAl was obtained in 99 % purity.

HPLC (λ=220 nm): 8.41 min [Method A].

8.5.4.5. Peptidotriazole BP289

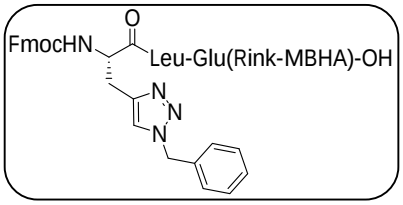

The alkynylpeptidyl resin Fmoc-Prg-Leu-Glu(Rink-MBHA)-OAl (**15**) (50 mg) was treated with $Pd(PPh_3)_4$ (3 equiv) in $CHCl_3$/AcOH/NMM (3:2:1) under stirring for 3 h at room temperature in order to remove the C-terminal allyl ester. After this time, the resin was washed with THF (3×2 min), NMP (3×2 min), DIPEA/CH_2Cl_2 (1:19, 3×2 min), sodium *N,N*-diethyldithiocarbamate (0.03 M in NMP, 3×15 min), NMP (10×1 min) and CH_2Cl_2 (3×2 min). Afterwards, the click reaction was carried out by treating the resin with BnN_3 for 5 h following the general procedure described in section 8.5.3. BP289 was obtained in 86 % purity.

HPLC (λ=220 nm): 16.23 min [Method D].***ESI/MS (m/z)***: 488.2 $[M+H]^+$. ***HRMS (ESI)***: calcd. for $C_{23}H_{34}N_7O_5$ 488.2616; found 488.2608; calcd. for $C_{23}H_{33}N_7NaO_5$ 510.2435; found 510.2426.

8.5.4.6. Peptidotriazole BP287

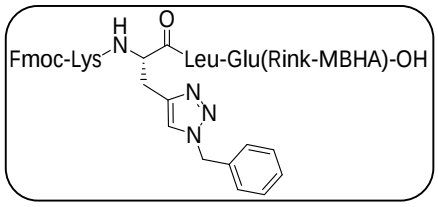

Peptidyl alkynyl Fmoc-Prg-Leu-Glu(Rink-MBHA)-OAl (**15**) was swollen with CH_2Cl_2 (1×20 min) and DMF (1×20 min) and then Fmoc-Lys(Boc)-OH was coupled following conditions B described above (section 8.2). Once the chain assembly was completed, the alkynylpeptidyl resin Fmoc-Lys-Prg-Leu-Glu(Rink-MBHA)-OAl (**16**) (50 mg) was treated with $Pd(PPh_3)_4$ (3 equiv) in $CHCl_3$/AcOH/NMM (3:2:1) under stirring for 3 h at room temperature in order to remove the C-terminal allyl ester. After this time, the resin was washed with THF (3×2 min), NMP (3×2 min), DIPEA/CH_2Cl_2 (1:19, 3×2 min), sodium *N,N*-diethyldithiocarbamate (0.03 M in NMP, 3×15 min), NMP (10×1 min) and CH_2Cl_2 (3×2 min). Afterwards, the click reaction was carried out by treating the resin with BnN_3 for 5 hours following the general procedure described in section 8.5.3. BP287 was obtained in 85 % purity.

HPLC (λ=220 nm): 15.71 min [Method D]. ***ESI/MS (m/z)***: 616.4 $[M+H]^+$.

8.5.5. Synthesis of cyclic peptidotriazoles from an alkynyl resin

8.5.5.1. Synthesis of alkynyl resins

Fmoc-Rink-4-MBHA resin (0.3 mmol/g) was swollen with CH_2Cl_2 (1×20 min) and DMF (1×20 min). Couplings of the Fmoc-amino acids were mediated using conditions B described in section 8.2. After chain assembly was completed, the C-terminal allyl ester was cleaved by treatment with $Pd(PPh_3)_4$ (3 equiv) and in $CHCl_3$/AcOH/NMM (3:2:1) under stirring for 3 h at room temperature. After this time, the resin was washed with THF (3×2 min), NMP (3×2 min), DIPEA/CH_2Cl_2 (1:19, 3×2 min), sodium *N,N*-diethyldithiocarbamate (0.03 M in NMP, 3×15 min), NMP (10×1 min) and CH_2Cl_2 (3×2 min). The Fmoc removal was performed by exposure of the peptidyl resin to a mixture of piperidine/DMF (3:7, 2+10 min). The cyclization was carried out by treating the resin with Oxyma (5 equiv), PyOxim (5 equiv) and DIPEA (10 equiv) using stirring during 24 h followed by washes with NMP (6×1 min) and CH_2Cl_2 (6×1 min).

8.5.5.1.1. c(Lys(Boc)-Lys(Boc)-Gln($CH_2C\equiv CH$)-Lys(Boc)-Lys(Boc)-Phe-Lys(Boc)-Lys(Boc)-Leu-Glu(Rink-MBHA)) (7)

This alkynyl peptidyl resin was synthesized following the procedure described above incorporating Gln($CH_2C\equiv CH$) at position 3. An aliquot of the resin was cleaved with TFA/H_2O/TIS (95:2.5:2.5) at room temperature for 2 h. The resulting peptide (**BPC280**) was obtained in 99 % purity.

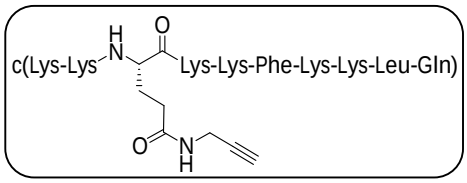

HPLC (λ=220 nm): 6.08 min [Method A], ***ESI/MS (m/z)***: 1324.0 $[M+H]^+$, 1346.0 $[M+Na]^+$.

8.5.5.1.2. c(Lys(Boc)-Lys(Boc)-Prg-Lys(Boc)-Lys(Boc)-Phe-Lys(Boc)-Lys(Boc)-Leu-Glu(Rink-MBHA)) (5)

This alkynyl peptidyl resin was synthesized following the procedure described above incorporating Prg at position 3. An aliquot of the resin was cleaved with TFA/H_2O/TIS (95:2.5:2.5) at room temperature for 2 h. The resulting peptide (**BPC466**) was obtained in 96 % purity.

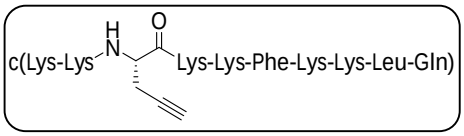

HPLC (λ=220 nm): 5.81 min [Method A]. ***ESI/MS*** (m/z): 1253.0 $[M+H]^+$, 1274.9 $[M+Na]^+$. ***HRMS (ESI):*** calcd. for $C_{61}H_{108}N_{17}O_{11}$ 418.2799, found 418.2794; calcd. for $C_{61}H_{107}N_{17}O_{11}$ 626.9163, found 626.9150.

8.5.5.1.3. c(Lys(Boc)-Lys(Boc)-Leu-Lys(Boc)-Prg-Phe-Lys(Boc)-Lys(Boc)-Leu-Glu(Rink-MBHA)) (6)

This alkynyl peptidyl resin was synthesized following the procedure described above incorporating Prg at position 5. An aliquot of the resin was cleaved with TFA/H_2O/TIS (95:2.5:2.5) at room temperature for 2 h. The resulting peptide (**BPC574**) was obtained in 92 % purity.

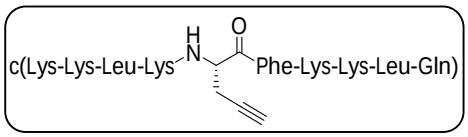

HPLC (λ=220 nm): 6.41 min [Method A]. ***ESI/MS (m/z)***: 1238.0 $[M+H]^+$, 1260.0 $[M+Na]^+$.

8.5.5.1.4. c(Lys(Boc)-Lys(Boc)-Lys(COC≡CH)-Lys(Boc)-Lys(Boc)-Phe-Lys(Boc)-Lys(Boc)-Leu-Glu(Rink-MBHA)) (8)

Peptidyl resin c(Lys(Boc)-Lys(Boc)-Lys(Mtt)-Lys(Boc)-Lys(Boc)-Phe-Lys(Boc)-Lys(Boc)-Leu-Glu(Rink-MBHA)) (50 mg) was prepared following the general procedure descrived above. After cyclization the peptidyl resin was treated with 1 % TFA in CH_2Cl_2 upon which the solution became yellow. The mixture was stirred for 5 min and the resin was then washed with CH_2Cl_2 (2×1 min), MeOH (2×1 min) and CH_2Cl_2 (2×1 min).

The TFA treatment was repeated until the solution remained colorless. Then, the N^{ε}-amino group was acylated with propiolic acid following conditions B (section 8.2). An aliquot of the resulting resin was cleaved with TFA/H_2O/TIS (95:2.5:2.5) at room temperature for 2 h. The resulting peptide (**BP468**) was obtained in 99 % purity.

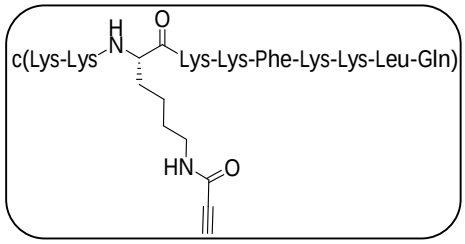

HPLC (λ=220 nm): 5.98 min [Method A]. ***ESI/MS (m/z)***: 1337.7 [M+H]+, 1359.7 [M+Na]+.

8.5.5.1.5. c(Lys(Boc)-Lys(Boc)-Leu-Lys-Lys(COC≡CH)-Phe-Lys(Boc)-Lys(Boc)-Leu-Glu(Rink-MBHA)) (9)

Peptidyl resin c(Lys(Boc)-Lys(Boc)-Leu)-Lys(Boc)-Lys(Mtt)-Phe-Lys(Boc)-Lys(Boc)-Leu-Glu(Rink-MBHA)) (50 mg) was prepared following the general procedure descrived above. After cyclization the peptidyl resin was treated with 1 % TFA in CH_2Cl_2 upon which the solution became yellow. The mixture was stirred for 5 min and the resin was then washed with CH_2Cl_2 (2×1 min), MeOH (2×1 min) and CH_2Cl_2 (2×1 min). The TFA treatment was repeated until the solution remained colorless.

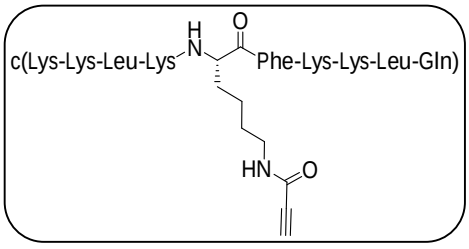

Then, the N^{ε}-amino group was acylated with propiolic acid following conditions B (section 8.2). An aliquot of the resulting resin was cleaved with TFA/H_2O/TIS (95:2.5:2.5) at room temperature for 2 h. The resulting peptide (**BPC578**) was obtained in 97 % purity.

HPLC (λ=220 nm): 6.05 min. [Method A]. ***ESI/MS (m/z)***: 1323.0 $[M+H]^+$, 1345.0 $[M+Na]^+$.

8.5.5.2. Synthesis of cyclic preptidotriazoles

The corresponding alkynyl resin was treated with an azide (5 equiv) in presence of ascorbic acid (5 equiv) and CuI (5 equiv) in piperidine/DMF (2:8) as described in section 8.4.2. The reaction mixture was stirred overnight at room temperature. The resin was subsequently washed with sodium *N,N*-diethyldithiocarbamate (0.03 M in NMP, 3×3 min), DMF (6×1 min) and CH_2Cl_2 (1×20 min). Peptidotriazole was cleaved from the resin with TFA/H_2O/TIS (95:2.5:2.5) and analyzed by HPLC and mass spectrometry.

8.5.5.2.1. Cyclic peptidotriazole BPC456

The alkynyl resin c(Lys(Boc)-Lys(Boc)-Prg-Lys(Boc)-Lys(Boc)-Phe-Lys(Boc)-Lys(Boc)-Leu-Glu(Rink-MBHA)) (50 mg) was treated with NaN_3 following the general procedure described above. There were required two treatments of 10 h. **BPC456** was obtained in 96 % purity.

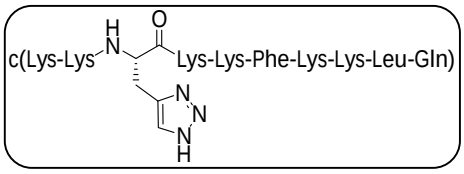

HPLC (λ=220 nm): 5.87 min [Method A]. ***ESI/MS (m/z)***: 1295.7$[M+H]^+$. ***HRMS (ESI)***: calcd. for $C_{61}H_{109}N_{20}O_{11}$ 432.6189, found 432.6211; calcd. for $C_{61}H_{108}N_{20}O_{11}$ 648.4248, found 648.4263.

8.5.5.2.2. Cyclic peptidotriazole BPC458

The alkynyl resin c(Lys(Boc)-Lys(Boc)-Prg-Lys(Boc)-Lys(Boc)-Phe-Lys(Boc)-Lys(Boc)-Leu-Glu(Rink-MBHA)) (50 mg) was treated with BnN_3 following the general procedure described above. **BPC458** was obtained in 94 % purity.

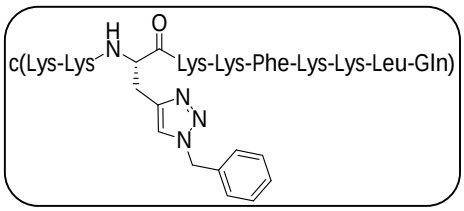

HPLC (λ=220 nm): 5.98 min [Method A]. ***ESI/MS (m/z)***: 1385.7 $[M+H]^+$, 1426.7 $[M+K]^+$. ***HRMS (ESI)***: calcd. for $C_{68}H_{115}N_{20}O_{11}$ 462.6346, found 462.6365; calcd. for $C_{68}H_{114}N_{20}O_{11}$ 693.4482, found 693.4478.

8.5.5.2.3. Cyclic peptidotriazole BPC460

The alkynyl resin c(Lys(Boc)-Lys(Boc)-Prg-Lys(Boc)-Lys(Boc)-Phe-Lys(Boc)-Lys(Boc)-Leu-Glu(Rink-MBHA)) (50 mg) was treated with Boc-Nle(ε-N_3)-OH following the general procedure described above to perform the click reaction. **BPC460** was obtained in 90 % purity.

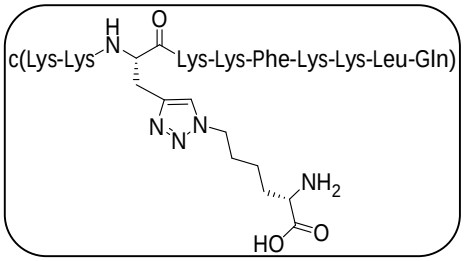

HPLC (λ=220 nm): 5.85 min [Method A]. ***ESI/MS (m/z)***: 1424.7 $[M+H]^+$. ***HRMS (ESI)***: calcd. for $C_{67}H_{120}N_{21}O_{13}$ 475.6453, found 475.6464; calcd. for $C_{67}H_{119}N_{21}O_{13}$ 712.9643, found 712.96439.

8.5.5.2.4. Cyclic peptidotriazole BPC518

The alkynyl resin c(Lys(Boc)-Lys(Boc)-Prg-Lys(Boc)-Lys(Boc)-Phe-Lys(Boc)-Lys(Boc)-Leu-Glu(Rink-MBHA)) (50 mg) was treated with *p*-azidoaniline following the general procedure described above to perform the click reaction. **BPC518** was obtained in 95 % purity.

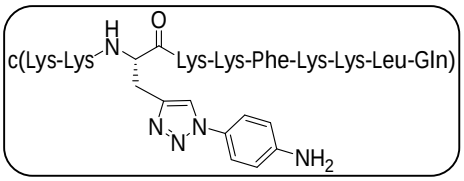

HPLC (λ=220 nm): 5.89 min [Method A]. ***ESI/MS (m/z)***: 1387.0 $[M+H]^+$, 1409.0 $[M+Na]^+$. ***HRMS (ESI)***: calcd. for $C_{67}H_{115}N_{21}O_{11}$ 347.4766, found 347.4763; calcd. for $C_{67}H_{114}N_{21}O_{11}$ 462.9663, found 462.9660; calcd. for $C_{67}H_{113}N_{21}O_{11}$ 693.9459, found 693.9462.

8.5.5.2.5. Cyclic peptidotriazole BPC542

The alkynyl resin c(Lys(Boc)-Lys(Boc)-Prg-Lys(Boc)-Lys(Boc)-Phe-Lys(Boc)-Lys(Boc)-Leu-Glu(Rink-MBHA)) (50 mg) was treated with *p*-azidoanisole following the general procedure described above to perform the click reaction.

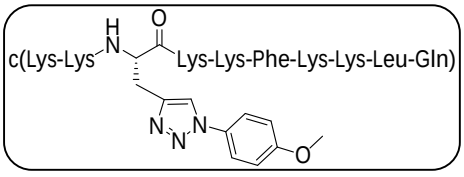

BPC542 was obtained in 96 % purity.

HPLC (λ=220 nm): 6.09 min [Method A]. ***ESI/MS (m/z)***: 1402.1 $[M+H]^+$, 1424.0 $[M+Na]^+$. ***HRMS (ESI)***: calcd. for $C_{68}H_{115}N_{20}O_{12}$ 467.9662, found 467.9699; calcd. for $C_{68}H_{114}N_{20}O_{12}$ 701.4457, found 701.4479.

8.5.5.2.6. Cyclic peptidotriazole BPC544

The alkynyl resin c(Lys(Boc)-Lys(Boc)-Prg-Lys(Boc)-Lys(Boc)-Phe-Lys(Boc)-Lys(Boc)-Leu-Glu(Rink-MBHA)) (50 mg) was treated with *p*-azidobenzene following the general procedure described above to perform the click reaction. **BPC544** was obtained in 92 % purity.

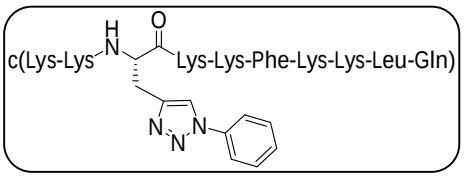

HPLC (λ=220 nm): 6.07 min [Method A]. ***ESI/MS (m/z)***: 1372.1 $[M+H]^+$, 1394.0 $[M+Na]^+$. ***HRMS (ESI)***: calcd. for $C_{67}H_{113}N_{20}O_{11}$ 457.9627, found 457.9658; calcd. for $C_{67}H_{112}N_{20}O_{11}$ 686.4404, found 686.4421.

8.5.5.2.7. Cyclic peptidotriazole BPC540

The alkynyl resin c(Lys(Boc)-Lys(Boc)-Prg-Lys(Boc)-Lys(Boc)-Phe-Lys(Boc)-Lys(Boc)-Leu-Glu(Rink-MBHA)) (50 mg) was treated with *p*-azidotoluene following the general procedure described above to perform the click reaction. **BPC540** was obtained in 99 % purity.

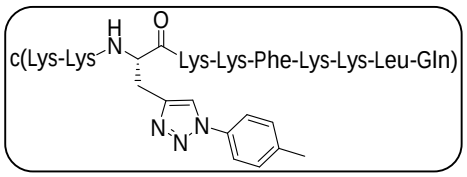

HPLC (λ=220 nm): 6.20 min [Method A]. ***ESI/MS (m/z)***: 1386.1 $[M+H]^+$, 1408.1 $[M+Na]^+$. ***HRMS (ESI)***: calcd. for $C_{68}H_{115}N_{20}O_{11}$ 462.6346, found 462.6360; calcd. for $C_{68}H_{114}N_{20}O_{11}$ 693.4482, found 693.4490.

8.5.5.2.8. Conjugated peptide BPC472

The alkynyl resin c(Lys(Boc)-Lys(Boc)-Prg-Lys(Boc)-Lys(Boc)-Phe-Lys(Boc)-Lys(Boc)-Leu-Glu(Rink-MBHA)) (50 mg) was treated with Fmoc-Phe-Nle(ε-N_3)-Lys-Leu-Gln-OH (BP252) following the general procedure described above to perform the click reaction. The resulting peptide **BPC472** was obtained in 98 % purity.

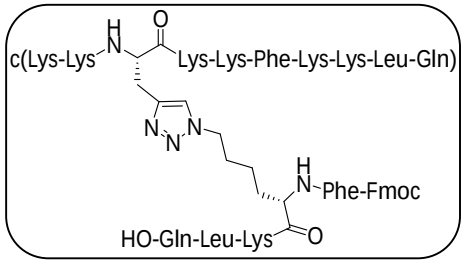

HPLC (λ=220 nm): 6.15 min [Method A]. ***ESI/MS (m/z)***: 1981.6 $[M+H]^+$. ***HRMS (ESI)***: calcd. for $C_{96}H_{165}N_{27}O_{18}$ 496.0701; found 496.0741; calcd. for $C_{96}H_{164}N_{27}O_{18}$ 661.0910, found 661.0941; calcd. for $C_{96}H_{163}N_{27}O_{18}$ 991.1329, found 991.1351.

8.5.5.2.9. Cyclic peptidotriazole BPC510

The alkynyl resin c(Lys(Boc)-Lys(Boc)-Leu-Lys(Boc)-Prg-Phe-Lys(Boc)-Lys(Boc)-Leu-Glu(Rink-MBHA)) (50 mg) was treated with BnN_3 following the general procedure described above to perform the click reaction. **BPC510** was obtained in 77 % purity.

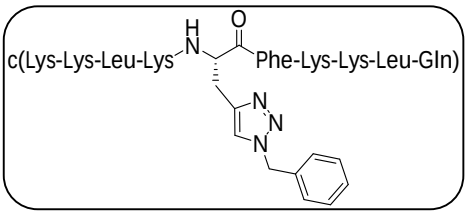

HPLC (λ=220 nm): 6.53 min [Method A]. ***ESI/MS (m/z)***: 1371.0 $[M+H]^+$, 1393.0 $[M+Na]^+$. ***HRMS (ESI)***: calcd. for $C_{68}H_{114}N_{19}O_{11}$ 457.6310, found 457.6337; calcd. for $C_{68}H_{113}N_{19}O_{11}$ 685.9428, found 685.9444.

8.5.5.2.10. Cyclic peptidotriazole BPC512

The alkynyl resin c(Lys(Boc)-Lys(Boc)-Leu-Lys(Boc)-Prg-Phe-Lys(Boc)-Lys(Boc)-Leu-Glu(Rink-MBHA)) (50 mg) was treated with Boc-Nle(ε-N_3)-OH following the general procedure described above to perform the click reaction. **BPC512** was obtained in 95 % purity.

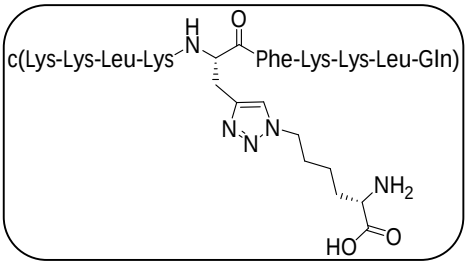

HPLC (λ=220 nm): 6.14 min [Method A]. ***ESI/MS (m/z)***: 1410.0 $[M+H]^+$, 1432.0 $[M+Na]^+$. ***HRMS (ESI)***: calcd. for $C_{67}H_{119}N_{20}O_{13}$ 470.6416, found 470.6447; calcd. for $C_{67}H_{118}N_{20}O_{13}$ 705.4588, found 705.4623.

8.5.5.2.11. Cyclic peptidotriazole BPC514

The alkynyl resin c(Lys(Boc)-Lys(Boc)-Leu-Lys(Boc)-Prg-Phe-Lys(Boc)-Lys(Boc)-Leu-Glu(Rink-MBHA)) (50 mg) was treated with *p*-azidoaniline following the general procedure described above to perform the click reaction. **BPC514** was obtained in 90 % purity.

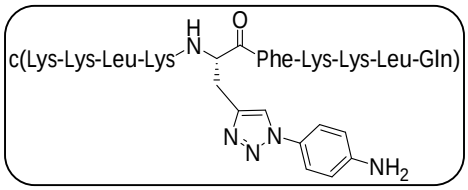

HPLC (λ=220 nm): 6.29 min [Method A]. ***ESI/MS (m/z)***: 1372.0 $[M+H]^+$, 1394.0 $[M+Na]^+$. ***HRMS (ESI)***: calcd. for $C_{67}H_{114}N_{20}O_{11}$ 343.7239, found 343.7239; calcd. for $_{67}H_{113}N_{20}O_{11}$ 457.9627, found 457.9644; calcd. for $C_{67}H_{112}N_{20}O_{11}$ 686.4404, found 686.4411.

8.5.5.2.12. Cyclic peptidotriazole BPC564

The alkynyl resin c(Lys(Boc)-Lys(Boc)-Leu-Lys(Boc)-Prg-Phe-Lys(Boc)-Lys(Boc)-Leu-Glu(Rink-MBHA)) (50 mg) was treated with *p*-azidotoluene following the general procedure described above to perform the click reaction. **BPC564** was obtained in 88 % purity.

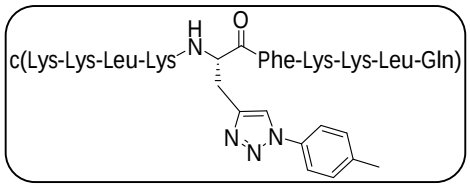

HPLC (λ=220 nm): 6.59 min [Method A]. ***ESI/MS (m/z)***: 1371.1 $[M+H]^+$, 1393.1 $[M+Na]^+$. ***HRMS (ESI)***: calcd. for $C_{68}H_{114}N_{19}O_{11}$ 457.6310, found 457.6310; calcd. for $C_{68}H_{113}N_{19}O_{11}$ 685.9428, found 685.9422.

8.5.5.2.13. Cyclic peptidotriazole BPC566

The alkynyl resin c(Lys(Boc)-Lys(Boc)-Leu-Lys(Boc)-Prg-Phe-Lys(Boc)-Lys(Boc)-Leu-Glu(Rink-MBHA)) (50 mg) was treated with *p*-azidoanisole following the general procedure described above to perform the click reaction.

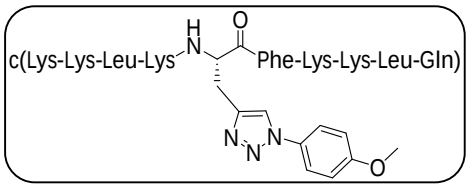

BPC544 was obtained in 80 % purity.

HPLC (λ=220 nm): 6.49 min [Method A]. ***ESI/MS (m/z)***: 1387.1 $[M+H]^+$, 1409.1 $[M+Na]^+$. ***HRMS (ESI)***: calcd. for $C_{68}H_{114}N_{19}O_{12}$ 462.9626, found 462.9635; calcd. for $C_{68}H_{113}N_{19}O_{12}$ 693.9403, found 693.9410.

8.5.5.2.14. Cyclic peptidotriazole BCP568

The alkynyl resin c(Lys(Boc)-Lys(Boc)-Leu-Lys(Boc)-Prg-Phe-Lys(Boc)-Lys(Boc)-Leu-Glu(Rink-MBHA)) (50 mg) was treated with *p*-azidobenzene following the general procedure described above to perform the click reaction. **BPC568** was obtained in 78 % purity.

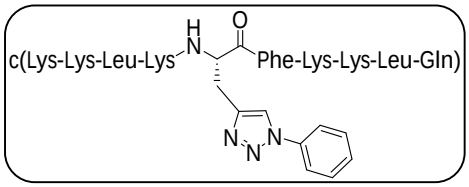

HPLC (λ=220 nm): 6.48 min [Method A]. ***ESI/MS (m/z)***: 1357.1 $[M+H]^+$, 1380.1 $[M+Na]^+$. ***HRMS (ESI)***: calcd. for $C_{67}H_{112}N_{19}O_{11}$ 452.9591, found 452.9607; calcd. for $C_{67}H_{111}N_{19}O_{11}$ 678.9350, found 678.9377.

8.5.5.2.15. Cyclic peptidotriazole BPC532

The alkynyl resin c(Lys(Boc)-Lys(Boc)-Gln($CH_2C\Xi CH$)-Lys(Boc)-Lys(Boc)-Phe-Lys(Boc)-Lys(Boc)-Leu-Glu(Rink-MBHA)) (50 mg) was treated with NaN_3 following the general procedure described above to perform the click reaction. **BPC532** was obtained in 98 % purity.

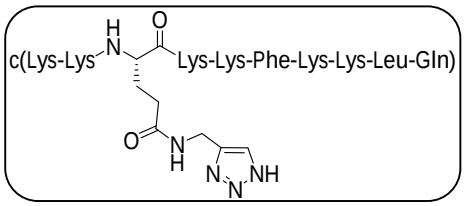

HPLC (λ=220 nm): 5.79 min [Method A]. ***ESI/MS (m/z)***: 1367.0 $[M+H]^+$, 1388.9 $[M+Na]^+$. ***HRMS (ESI)***: calcd. for $C_{64}H_{114}N_{21}O_{12}$ 456.3047, found 456.2980; calcd. for $C_{64}H_{113}N_{21}O_{12}$ 683.9433, found 683.9527.

8.5.5.2.16. Cyclic peptidotriazole BPC520

The alkynyl resin c(Lys(Boc)-Lys(Boc)-Gln($CH_2C\Xi CH$)-Lys(Boc)-Lys(Boc)-Phe-Lys(Boc)-Lys(Boc)-Leu-Glu(Rink-MBHA)) (50 mg) was treated with BnN_3 following the general

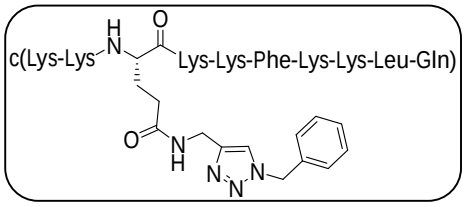

procedure described above to perform the click reaction. **BPC520** was obtained in 98 % purity.

HPLC (λ=220 nm): 6.04 min [Method A]. ***ESI/MS (m/z)***: 1457.0 $[M+H]^+$, 1479.0 $[M+Na]^+$. ***HRMS (ESI)***: calcd. for $C_{71}H_{120}N_{21}O_{12}$ 486.3136, found 486.3156; calcd. for $C_{71}H_{119}N_{21}O_{12}$ 728.9668, found 728.9709.

8.5.5.2.17. Cyclic peptidotriazole BPC522

The alkynyl resin c(Lys(Boc)-Lys(Boc)-Gln($CH_2C\equiv CH$)-Lys(Boc)-Lys(Boc)-Phe-Lys(Boc)-Lys(Boc)-Leu-Glu(Rink-MBHA)) (50 mg) was treated with Boc-Nle(ε-N_3)-OH following the general procedure described above to perform the click reaction. **BPC522** was obtained in 94 % purity.

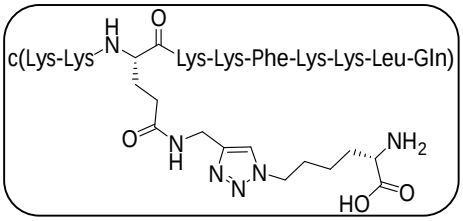

HPLC (λ=220 nm): 5.66 min [Method A]. ***ESI/MS (m/z)***: 1496.0 $[M+H]^+$,1518.0 $[M+Na]^+$. ***HRMS (ESI)***: calcd. for $C_{70}H_{125}N_{22}O_{14}$ 499.3243, found 499.3279; calcd. for $C_{70}H_{124}N_{22}O_{14}$ 748.4828, found 748.4891.

8.5.6. Synthesis of cyclic peptidotriazoles from an azidopeptidyl resin

8.5.6.1. Synthesis of azido peptidyl resins

8.5.6.1.1. c(Lys(Boc)-Lys(Boc)-Nle(ε-N_3)-Lys(Boc)-Lys(Boc)-Phe-Lys(Boc)-Lys(Boc)-Leu-Glu(Rink-MBHA)) (10)

This azidopeptidyl resin was synthesized following the procedure described in section 8.5.5.1 incorporating Fmoc-Nle(ε-N_3)-OH at position 3. An aliquot of the resulting resin was cleaved with TFA/H_2O/TIS (95:2.5:2.5) at room temperature for 2 h. The resulting peptide (**BPC464**) was obtained in 94 % purity.

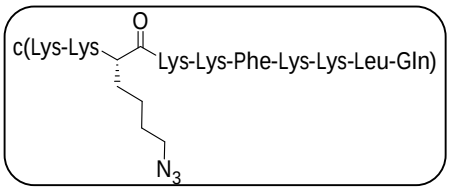

HPLC (λ=220 nm): 6.00 min [Method A]. ***ESI/MS (m/z)***: 1312.0 $[M+H]^+$, 1334.0 $[M+Na]^+$.

8.5.6.1.2. c(Lys(Boc)-Lys(Boc)-Leu-Lys(Boc)-Nle(ε-N_3)-Phe-Lys(Boc)-Lys(Boc)-Leu-Glu(Rink-MBHA)) (11)

This azidopeptidyl resin was synthesized following the procedure described in section 8.5.5.1 incorporating Fmoc-Nle(ε-N_3)-OH at position 5. An aliquot of the resulting resin was cleaved with TFA/H_2O/TIS (95:2.5:2.5) at room temperature for 2 h. The resulting peptide (**BPC576**) was obtained in 94 % purity.

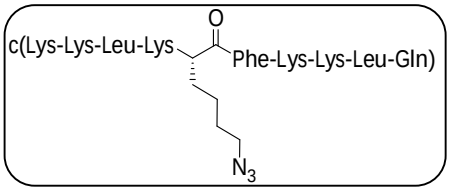

HPLC (λ=220 nm): 6.57 min [Method A]. ***ESI/MS (m/z)***: 1297.0 $[M+H]^+$, 1319.0 $[M+Na]^+$.

8.5.6.2. Synthesis of cyclic peptidotriazoles

The corresponding azido peptidyl resin was treated with an alkyne (5 equiv) in the presence of ascorbic acid (5 equiv) and CuI (5 equiv) in piperidine/DMF (2:8), as described in section 8.5.5.2. The reaction mixture was stirred at room temperature. The resin was subsequently washed with sodium *N,N*-diethyldithiocarbamate (0.03 M in NMP, 3×15 min), DMF (6x1 min) and CH_2Cl_2 (1×20 min). Peptidotriazole was individually cleaved from the resin with TFA/H_2O/TIS (95:2.5:2.5) and analyzed by HPLC and mass spectrometry.

8.5.6.2.1. Cyclic peptidotriazole BPC470

The corresponding azido peptidyl resin c(Lys(Boc)-Lys(Boc)-Nle(ε-N_3)-Lys(Boc)-Lys(Boc)-Phe-Lys(Boc)-Lys(Boc)-Leu-Glu(Rink-MBHA)) (50 mg) was treated with heptyne following the general procedure described in section 8.5.5.2. It was required one treatment of 5h followed by two treatments of 18h. **BPC470** was obtained in 99 % purity.

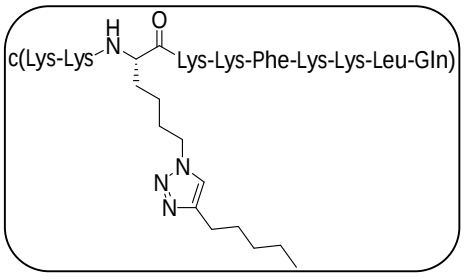

HPLC (λ=220 nm): 6.12 min [Method A]. ***ESI/MS (m/z)***: 1408.1 $[M+H]^+$, 1431.0 $[M+Na]^+$. ***HRMS (ESI)***: calcd. for $C_{69}H_{126}N_{20}O_{11}$ 352.7473, found 352.7464; calcd. for

$C_{69}H_{125}N_{20}O_{11}$ 469.9940, found 469.9940; calcd. for $C_{69}H_{124}N_{20}O_{11}$ 704.4874, found 704.4833.

8.5.6.2.2. Cyclic peptidotriazole BCP516

The corresponding azido peptidyl resin c(Lys(Boc)-Lys(Boc)-Nle(ε-N_3)-Lys(Boc)-Lys(Boc)-Phe-Lys(Boc)-Lys(Boc)-Leu-Glu(Rink-MBHA)) (50 mg) was treated with phenylacetylene following the general procedure described in section 8.5.5.2. **BPC516** was obtained in 97 % purity.

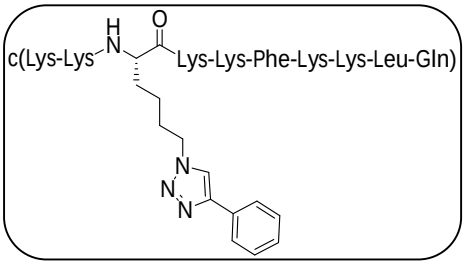

HPLC (λ=220 nm): 6.09 min [Method A]. ***ESI/MS (m/z)***: 1414.0 $[M+H]^+$, 1436.0 $[M+Na]^+$. ***HRMS (ESI)***: calcd. for $C_{70}H_{119}N_{20}O_{11}$ 471.9784, found 471.9825; calcd. for $C_{70}H_{118}N_{20}O_{11}$ 707.4639, found 707.4658.

8.5.6.2.3. Cyclic peptidotriazole BPC546

The corresponding azido peptidyl resin c(Lys(Boc)-Lys(Boc)-Nle(ε-N_3)-Lys(Boc)-Lys(Boc)-Phe-Lys(Boc)-Lys(Boc)-Leu-Glu(Rink-MBHA)) (50 mg) was treated with *p*-ethynylpentylbenzene following the general procedure described in section 8.5.5.2. **BPC546** was obtained in 81 % purity.

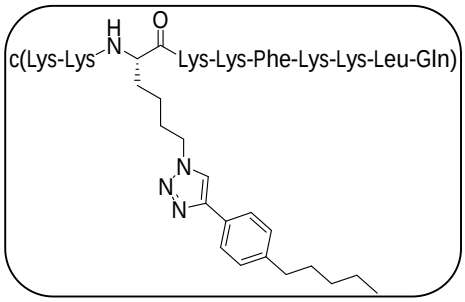

HPLC (λ=220 nm): 6.61 min [Method A]. ***ESI/MS (m/z)***: 1484.2 $[M+H]^+$, 1506.2 $[M+Na]^+$. ***HRMS (ESI)***: calcd. for $C_{75}H_{129}N_{20}O_{11}$ 495.3378, found 495.3411; calcd. for $C_{75}H_{129}N_{20}O_{11}$ 743.0069, found 743.0065.

8.5.6.2.4. Cyclic peptidotriazole BPC538

The corresponding azido peptidyl resin c(Lys(Boc)-Lys(Boc)-Nle(ε-N_3)-Lys(Boc)-Lys(Boc)-Phe-Lys(Boc)-Lys(Boc)-Leu-Glu(Rink-MBHA) (50 mg) was treated with *p*-ethynylaniline following the general procedure described in section

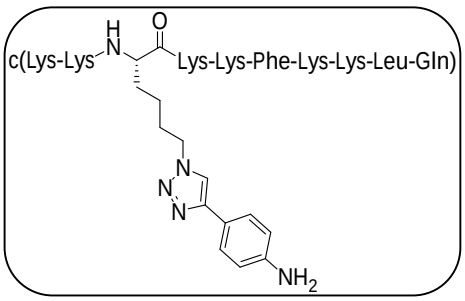

8.5.5.2. **BPC538** was obtained in 95 % purity.

HPLC (λ=220 nm): 5.83 min [Method A]. ***ESI/MS (m/z)***: 1429.1 $[M+H]^+$, 1451.1 $[M+Na]^+$. ***HRMS (ESI)***: calcd. for $C_{70}H_{120}N_{21}O_{11}$ 476.9820, found 476.9834; calcd. for $C_{70}H_{119}N_{21}O_{11}$ 714.9693, found 714.9706.

8.5.6.2.5. Cyclic peptidotriazole BPC548

The corresponding azido peptidyl resin c(Lys(Boc)-Lys(Boc)-Nle(ε-N_3)-Lys(Boc)-Lys(Boc)-Phe-Lys(Boc)-Lys(Boc)-Leu-Glu(Rink-MBHA)) (50 mg) was treated with *p*-ethynyltoluene following the general procedure described in section 8.5.5.2. **BPC548** was obtained in 95 % purity.

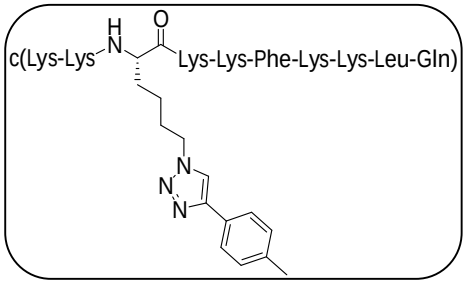

HPLC (λ=220 nm): 6.35 min [Method A]. ***ESI/MS (m/z)***: 1428.2 $[M+H]^+$, 1450.1 $[M+Na]^+$. ***HRMS (ESI)***: calcd. for $C_{71}H_{121}N_{20}O_{11}$ 476.6502, found 476.6542; calcd. for $C_{71}H_{120}N_{20}O_{11}$ 714.4717, found 714.4729.

8.5.6.2.6. Cyclic peptidotriazole BPC550

The corresponding azido peptidyl resin c(Lys(Boc)-Lys(Boc)-Nle(ε-N_3)-Lys(Boc)-Lys(Boc)-Phe-Lys(Boc)-Lys(Boc)-Leu-Glu(Rink-MBHA)) (50 mg) was treated with *p*-ethynylanisole following the general procedure described in section 8.5.5.2. **BPC550** was obtained in 86 % purity.

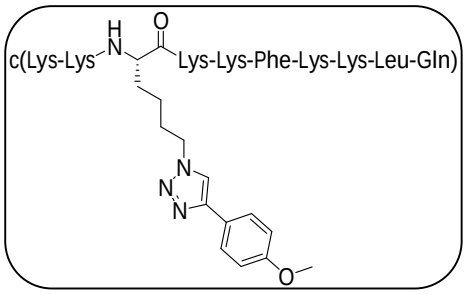

HPLC (λ=220 nm): 6.23 min [Method A]. ***ESI/MS (m/z)***: 1444.1 $[M+H]^+$, 1466.1 $[M+Na]^+$. ***HRMS (ESI)***: calcd. for $C_{71}H_{121}N_{20}O_{12}$ 481.9819, found 481.9831; calcd. for $C_{71}H_{120}N_{20}O_{12}$ 722.4692, found 722.4717.

8.5.6.2.7. Cyclic peptidotriazole BPC552

The corresponding azido peptidyl resin c(Lys(Boc)-Lys(Boc)-Nle(ε-N_3)-Lys(Boc)-Lys(Boc)-Phe-Lys(Boc)-Lys(Boc)-Leu-Glu(Rink-MBHA)) (50 mg) was treated with tetrahydro-2-(prop-2-ynyloxy)-2*H*-pyran following the general procedure described in section 8.5.5.2. **BPC522** was obtained in 90 % purity.

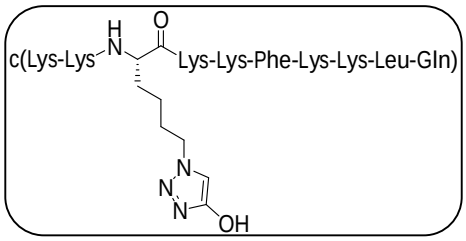

HPLC (λ=220 nm): 5.77 min [Method A]. ***ESI/MS (m/z)***: 1368.1 $[M+H]^+$, 1386.1 $[M+NH_4]^+$, 1408.1 $[M+Na+H_2O]^+$. ***HRMS (ESI)***: calcd. for $C_{65}H_{117}N_{20}O_{12}$ 456.6381, found 456.6401; calcd. for $C_{65}H_{116}N_{20}O_{12}$ 684.4535, found 684.4579.

8.5.6.2.8. Cyclic peptidotriazole BPC570

The corresponding azido peptidyl resin c(Lys(Boc)-Lys(Boc)-Leu-Lys(Boc)-Nle(ε-N_3)-Phe-Lys(Boc)-Lys(Boc)-Leu-Glu(Rink-MBHA)) (50 mg) was treated with heptyne following the general procedure described in section 8.5.5.2. **BPC570** was obtained in 94 % purity.

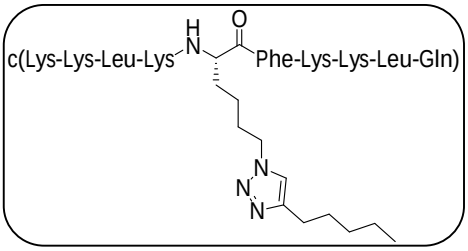

HPLC (λ=220 nm): 6.54 min [Method A]. ***ESI/MS (m/z)***: 1393.1 $[M+H]^+$, 1415.0 $[M+Na]^+$, 1427.1 $[M+K]^+$, 1449.0 $[M+K+H_2O]^+$, 1504.1 $[M+TFA]^+$, 1526.1 $[M+TFA+Na]^+$, 1545.1 $[M+TFA+K]^+$. ***HRMS (ESI)***: calcd. for $C_{69}H_{125}N_{19}O_{11}$ 348.9946, found 348.9970; calcd. for $C_{69}H_{124}N_{19}O_{11}$ 464.9904, found 464.9921; calcd. for $C_{69}H_{123}N_{19}O_{11}$ 696.9819, found 696.9847.

8.5.6.2.9. Cyclic peptidotriazole BPC572

The corresponding azido peptidyl resin c(Lys(Boc)-Lys(Boc)-Leu-Lys(Boc)-Nle(ε-N_3)-Phe-Lys(Boc)-Lys(Boc)-Leu-Glu(Rink-MBHA)) (50 mg) was treated with *p*-ethynylaniline following the general procedure described in section 8.5.5.2. **BPC572** was obtained in 99 % purity.

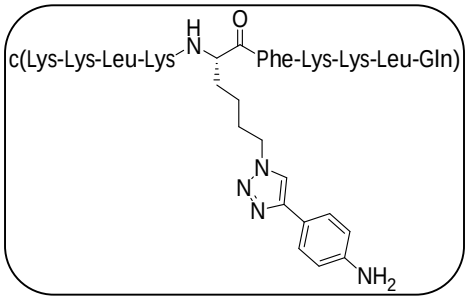

HPLC (λ=220 nm): 6.34 min [Method A]. ***ESI/MS (m/z)***: 1414.0 $[M+H]^+$, 1436.0 $[M+Na]^+$, 1449.0 $[M+K]^+$. ***HRMS (ESI)***: calcd. for $C_{70}H_{119}N_{20}O_{11}$ 471.9784, found 471.9817; calcd. for $C_{70}H_{118}N_{20}O_{11}$ 707.4639, found 707.4663.

8.5.6.2.10. Cyclic peptidotriazole BPC554

The corresponding azido peptidyl resin c(Lys(Boc)-Lys(Boc)-Leu-Lys(Boc)-Nle(ε-N_3)-Phe-Lys(Boc)-Lys(Boc)-Leu-Glu(Rink-MBHA)) (50 mg) was treated with *p*-ethynylpenthylbenzene following the general procedure described in section 8.5.5.2. **BPC554** was obtained in 76 % purity.

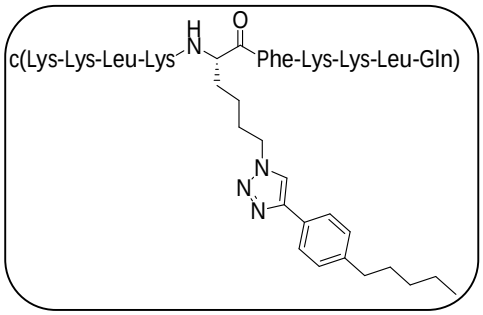

HPLC (λ=220 nm): 7.46 min [Method A]. ***ESI/MS (m/z)***: 1469.2 $[M+H]^+$, 1491.2 $[M+Na]^+$. ***HRMS (ESI)***: calcd. for $C_{75}H_{128}N_{19}O_{11}$ 490.3341, found 490.3360; calcd. for $C_{75}H_{127}N_{19}O_{11}$ 734.9976, found 734.9988.

8.5.6.2.11. Cyclic peptidotriazole BPC556

The corresponding azido peptidyl resin c(Lys(Boc)-Lys(Boc)-Leu-Lys(Boc)-Nle(ε-N_3)-Phe-Lys(Boc)-Lys(Boc)-Leu-Glu(Rink-MBHA)) (50 mg) was treated with *p*-ethynyltoluene following the general procedure described in section 8.5.5.2. **BPC556** was obtained in 85 % purity.

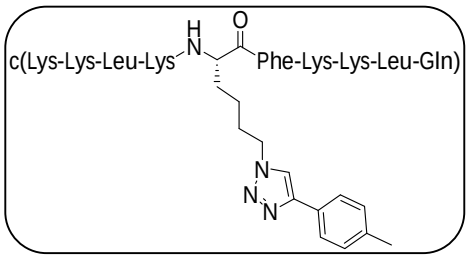

HPLC (λ=220 nm): 6.71 min [Method A]. ***ESI/MS (m/z)***: 1413.1 $[M+H]^+$, 1435.1 $[M+Na]^+$. ***HRMS (ESI)***: calcd. for $C_{71}H_{120}N_{19}O_{11}$ 471.6466, found 471.6499; calcd. for $C_{71}H_{119}N_{19}O_{11}$ 706.9663, found 706.9708.

8.5.6.2.12. Cyclic peptidotriazole BPC558

The corresponding azido peptidyl resin c(Lys(Boc)-Lys(Boc)-Leu-Lys(Boc)-Nle(ε-N_3)-Phe-Lys(Boc)-Lys(Boc)-Leu-Glu(Rink-MBHA)) (50 mg) was treated with *p*-ethynylanisole following the

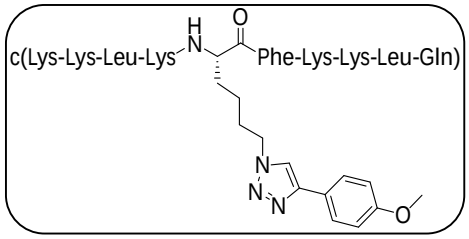

general procedure described in section 8.5.5.2. **BPC558** was obtained in 95 % purity.

HPLC (λ=220 nm): 6.72 min [Method A]. ***ESI/MS (m/z)***: 1429.1 $[M+H]^+$, 1451.1 $[M+Na]^+$. ***HRMS (ESI)***: calcd. for $C_{71}H_{120}N_{19}O_{12}$ 476.9782, found 476.9813; calcd. for $C_{71}H_{119}N_{19}O_{12}$ 714.9637, found 714.9675.

8.5.6.2.13. Cyclic peptidotriazole BPC560

The corresponding azido peptidyl resin c(Lys(Boc)-Lys(Boc)-Leu-Lys(Boc)-Nle(ε-N_3)-Phe-Lys(Boc)-Lys(Boc)-Leu-Glu(Rink-MBHA)) (50 mg) was treated with tetrahydro-2-(prop-2-ynyloxy)-2*H*-pyran following the general procedure described in section 8.5.5.2. **BPC560** was obtained in 96 % purity.

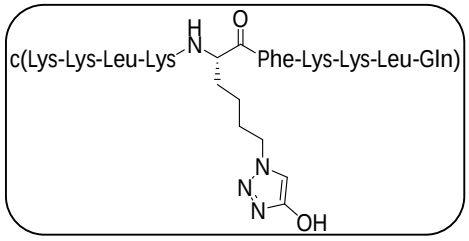

HPLC (λ=220 nm): 6.37 min [Method A]. ***ESI/MS (m/z)***: 1353.1 $[M+H]^+$, 1376.1 $[M+Na]^+$. ***HRMS (ESI)***: calcd. for $C_{65}H_{116}N_{19}O_{12}$ 451.6345, found 451.6364; calcd. for $C_{65}H_{115}N_{19}O_{12}$ 676.9481, found 676.9513.

8.5.6.2.14. Cyclic peptidotriazole BPC562

The corresponding azido peptidyl resin c(Lys(Boc)-Lys(Boc)-Leu-Lys(Boc)-Nle(ε-N_3)-Phe-Lys(Boc)-Lys(Boc)-Leu-Glu(Rink-MBHA)) (50 mg) was treated with phenylacetylene following the general procedure described in section 8.5.5.2. **BPC562** was obtained in 90 % purity.

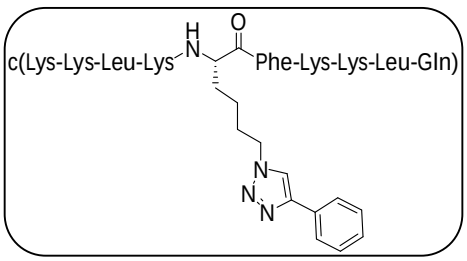

HPLC (λ=220 nm): 6.65 min [Method A]. ***ESI/MS (m/z)***: 1399.0 $[M+H]^+$, 1421.0 $[M+Na]^+$. ***HRMS (ESI)***: calcd. for $C_{70}H_{118}N_{19}O_{11}$ 466.9747, found 466.9772; calcd. for $C_{70}H_{117}N_{19}O_{11}$ 699.9584, found 699.9620.

8.6. Synthesis of carbopeptides

8.6.1. Synthesis of peptide aldehyde

TentaGel S NH_2 (TG) resin (0.27 mmol/g) was placed in a syringe and swollen with CH_2Cl_2 (3×10 min) and DMF (3×10 min). The Ortho-Backbone Amide Linker (*o*-BAL) was incorporated by treating the resin twice with 5-(2-formyl-3,5-dimethoxyphenoxy)pentanoic acid (4.0 equiv), HBTU (3.8 equiv), HOBt (4.0 equiv), and DIPEA (7.8 equiv) in DMF at room temperature for 12 h. Washings were performed with DMF (3×1 min), CH_2Cl_2 (3×1 min) and DMF (3×1 min). Next a reductive amination was performed using aminoacetaldehyde dimethyl acetal (10 equiv) and $NaBH_3CN$ (10 equiv) suspended in AcOH/DMF (1:99). This suspension was added to the *o*-BAL-TG resin and the mixture was heated under microwave irradiation at 60 °C for 10 min. The resin was washed with DMF (3×1 min), CH_2Cl_2 (3×1 min) and DCE (3×1 min) and the reductive amination step was repeated. Then, Fmoc-Leu-OH (10 equiv) was dissolved in DCE-DMF (10:1), DIPCDI (5 equiv) was added, and after preactivation for 10 min, transferred to the resin. The reaction mixture was heated in a microwave oven to 60 °C for 2×10 min, and then the resin was washed with DMF (3×1 min), CH_2Cl_2 (3×1 min) and DMF (3×1 min). Peptide elongation was performed on the fully automatic synthesizer by repeated cycles of amino acid coupling, Fmoc group removal and washings. The amino acid couplings were carried out using the corresponding Fmoc-amino acid (6 equiv), HBTU (5.8 equiv), HOBt (6 equiv) and DIPEA (11.7 equiv) shaking the mixture for 2 h at room temperature. DMF was used as solvent for all the couplings except for Fmoc-Phe-OH and Fmoc-D-Phe-OH which was coupled in NMP. Each coupling step was repeated twice. The Fmoc group was removed by treating the resin with piperidine/DMF (2:3, 3 min) followed by two treatments of piperidine/DMF (1:4, 12 + 15 min). After coupling and deprotection steps the resin was washed with DMF (3×1 min), CH_2Cl_2 (1×1 min) and DMF (3×1 min). Once the second amino acid was coupled, Fmoc quantification was performed to estimate the overall loss in loading. Peptide elongation was performed by repeated cycles of Fmoc group removal, coupling and washings.

Once the synthesis was completed, peptides were individually cleaved from the resin with TFA/H_2O (95:5) for 2h. Following TFA evaporation and diethyl ether extraction, the crude peptides were dissolved in H_2O, analyzed by high-performance liquid chromatography (HPLC), purified by a preparative HPLC using Method B and characterized by LC/MS.

8.6.1.1. KKLFKKILKYLG-H (42)

HPLC (λ=220 nm): 2.08 min (99 % purity) [Method A]. **ESI/MS** (m/z): 366.7 $[M+4H]^{4+}$, 488.6 $[M+4H]^{3+}$.

8.6.1.2. KKLfKKILKYLG-H (43)

HPLC (λ=220 nm): 2.20 min (99 % purity) [Method A]. **ESI/MS** (m/z): 366.6 $[M+4H]^{4+}$, 488.5 $[M+3H]^{3+}$.

8.6.2. Preparation of the aminooxy-functionalized template cDTE (41)

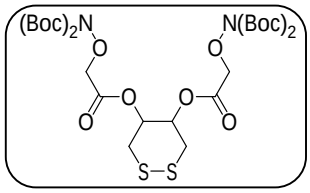

(S,R)-Cyclodithioerythritol (19.5 mg, 0.13 mmol) and *N,N*-di-Boc-aminooxyacetic acid (125.7 mg, 0.43 mmol) were dissolved in pyridine/CH_2Cl_2 (1:1, 3 mL). The reaction was stirred with molecular sieves (4 Å) for 1 h before DIPCDI (67 µL, 0.43 mmol) and 4-dimethylaminopyridine (DMAP) (10 mg, 0.081 mmol) were added. After 2 h, additional DIPCDI (106 µL, 1.38 mmol) was added and the reaction was stirred for an additional 30 min. Finally, the molecular sieves were removed and the reaction mixture was concentrated in vacuo. The solution was dissolved in ACN, centrifuged and purified by preparative HPLC using Method A (Materials and Methods) (62.5 mg, 70 %).

^{1}H-NMR ($CDCl_3$, 300 MHz) δ (ppm): 1.41 (s, 36H), 2.4–3.41 (m, 4 H), 4.45 (s, 4H), 5.10–5.22 (m, 2H); **^{13}C NMR (300 MHz, $CDCl_3$) δ (ppm)**: 28.04, 72.17, 84.51, 150.07, 166.26. ***HPLC (λ=220 nm)***: 6.93 min (93 % purity) [Method A]. ***ESI/MS (m/z)***: 721.2 $[M+H]^+$

8.6.3. Synthesis of carbopeptides cDTE(BP100)$_2$, cDTE(BP143)$_2$ and Galp(BP100)$_4$

8.6.3.1. cDTE(BP100)$_2$

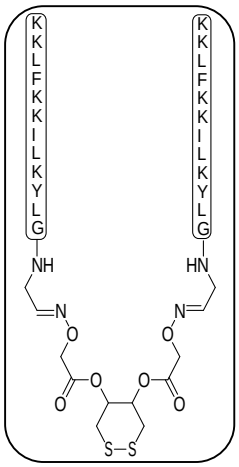

Template cDTE (**41**) (12.7 mg, 18.2 μmol) was dissolved in TFA/CH_2Cl_2 (1:1, 2 mL) and stirred for 1 h. The solution was then concentrated in vacuo, redissolved in a small amount of water and lyophilized to afford the deprotected template **39** as a white powder. This template and the peptide aldehyde **42** (65.7 mg, 45 μmol) were dissolved in 6.2 mL of a 1:1 solution of ACN and an acetate buffer (0.1 M, pH 4.76) containing aniline (100 mM). The reaction mixture was stirred for 3 h and purified by preparative HPLC using Method C (Materials and Methods) (24.3 mg, 42 % yield).

HPLC (λ=220 nm): 2.50 min (98 % purity) [Method C]. ***ESI/MS (m/z)***: 1594.5 $[M+2H]^{2+}$, 1063.5 $[M+3H]^{3+}$, 797.8 $[M+4H]^{4+}$, 638.4 $[M+5H]^{5+}$, 532.2 $[M+6H]^{6+}$. ***HRMS (MALDI-MS)*:** calcd. for $C_{156}H_{264}N_{36}O_{30}S_2$ 3186.9753, found 3186.9749.

8.6.3.2. cDTE(BP143)$_2$

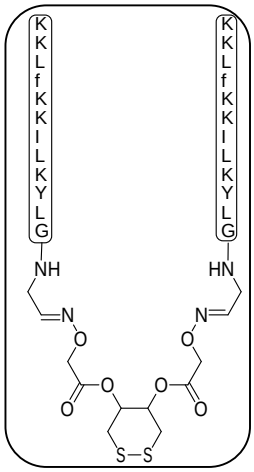

Template cDTE (**41**) (4.8 mg, 6.9 μmols) was dissolved in TFA/CH_2Cl_2 (1:1, 1 mL) and stirred for 1 h. The solution was then concentrated in vacuo, redissolved in a small amount of water and lyophilized to afford the deprotected template **41** as a white powder. This template and the peptide aldehyde **43** (30.2 mg, 20.6 μmol) were dissolved in 2 mL of a 1:1 solution of ACN and an acetate buffer (0.1 M, pH 4.76). containing aniline (100 mM) The reaction mixture was stirred for 3 h and purified by preparative HPLC using Method C (Materials and Methods) (13.6 mg, 62 % yield).

HPLC (λ=220 nm): 2.51 min (98 % purity) [Method C]. ***ESI/MS (m/z)***: 1594.1 $[M+2H]^{2+}$, 1063.5 $[M+3H]^{3+}$, 797.9 $[M+4H]^{4+}$, 638.4 $[M+5H]^{5+}$, 532.2 $[M+6H]^{6+}$. ***HRMS (MALDI-MS)*:** calcd. for $C_{156}H_{264}N_{36}O_{30}S_2$ 3186.9753, found 3186.9820.

8.6.3.3. Gal*p*(BP100)$_4$

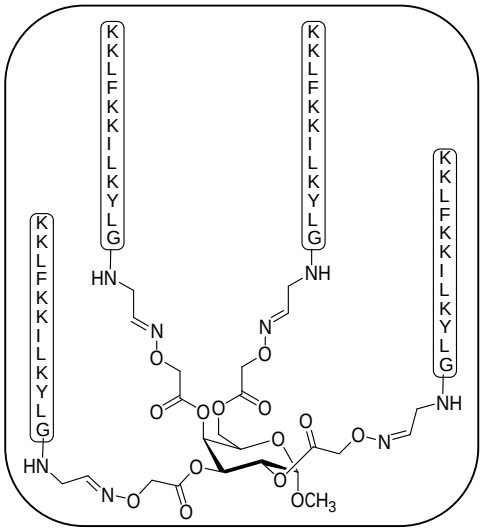

Template Galp (Brask 2000) (3.4 mg, 2.6 μmol) was dissolved in TFA/CH_2Cl_2 (1:1, 0.5 mL) and stirred for 30 min at room temperature. The solution was then concentrated to dryness, redissolved in a small amount of water and lyophilized to afford the deprotected template **40** as a white powder. This lyophilized template was dissolved in 1.2 mL of a solution of 1:1 ACN and an acetate buffer (0.1 M, pH 4.76). Peptide aldehyde **42** (19.27 mg, 13.2 μmol) was added and the mixture was stirred at room temperature. The reaction was followed by HPLC (Analysis B). After 4 h, an additional amount of peptide aldehyde **42** (20 mg, 13.7 μmol) dissolved in 1.1 mL of a 1:1 solution of ACN and an acetate buffer (0.1 M, pH 4.76) containing aniline (100 mM) was added. After further 2.5 h, the reaction was completed. The reaction mixture was purified by HPLC using Method D (Materials and Methods) (10.7 mg, 64 % yield).

HPLC (λ=220 nm): 6.23 min (90 % purity) [Method D]. ***ESI/MS (m/z)***: 1566.3 $[M+4H]^{4+}$, 1253.8 $[M+5H]^{5+}$, 1045.1 $[M+6H]^{6+}$, 895.7 $[M+7H]^{7+}$, 784.2 $[M+8H]^{8+}$, 697.2 $[M+9H]^{9+}$, 627.5 $[M+10H]^{10+}$ (calcd for $C_{311}H_{526}N_{72}O_{62}$: 6262.02 Da).

8.7. Biological tests

8.7.1. Bacterial strains and growth conditions

For the analysis of the *in vitro* activity of peptides, the following plant pathogenic bacterial strains were used: *Erwinia amylovora* PMV6076 (Institut National de la Recherche Agronomique, Angers, France), Pseudomonas *syringae* EPS94 (INTEA, Institut de Tecnología Agroalimentària, Universitat de Girona, Spain) and *Xanthomonas*

vesicatoria 2133-2 (IVIA, Institut Valencià d'Investigacions Agràries, València, Spain). Human bacteria used in this study were: *Listeria monocytogenes* ATCC15313, *Staphylococcus aureus* ATCC9144, *E. coli* ATCC5934 and *Salmonella typhimurium* ATCC43971 (American Type Culture Collection). Other plant beneficial bacteria were included: *Bacillus subtilis* EPS2017 (INTEA) and *Leuconostoc mesenteroides* CM160 (INTEA). All bacteria were stored in Luria Bertani broth (LB) supplemented with glycerol (20 %) and maintained at 80 °C except for *L. monocytogenes,* which was stored in Brain Heart Infusion broth (BHI) and *L. mesenteroides* that was stored in Man Rogosa Sharpe broth (MRS). All strains were routinely grown in the same solid media (LB, BHI or MRS agar) and incubated at 25 °C. All strains were scraped from the corresponding agar plates after 24 h growth except for *X. vesicatoria* that was after 48 h. The cell material was suspended in sterile water to obtain a suspension of 10^8 CFU ml^{-1} (absorbance at 620 nm of 0.2, except for Bacillus that it was 0.5).

8.7.2. Fungal strains and growth conditions

The plant pathogenic fungal strains *Penicillium expansum* EPS 26 (INTEA, University of Girona) and *Fusarium oxysporum* f. sp. *lycopersici* FOL 3 race 2 (ATCC 201829, American Type Culture Collection) were used. Strains were cultured on potato dextrose agar (PDA) plates (Difco) using aseptic procedures to avoid contamination. Conidia from *P. expansum* mycelium were obtained from 5-day-old PDA cultures of the fungus incubated at 25 ºC. Inoculum was prepared by scraping spore material from the culture surfaces with a wet cotton swab and resuspending it in distilled water containing 0.5‰ of Tween 80. Microconidia of *F. oxysporum* were obtained from 1-week-old potato dextrose broth (PDB) cultures (Oxoid) of the fungus incubated at 25 ºC in the dark in a rotary shaker at 125 rpm. After incubation, the culture was filtered through several layers of sterile cheesecloth to eliminate macroconidia and mycelial growth of the fungus. Then, the effluent was centrifuged at 8000 x g for 20 min at 4 ºC, and the pellet was resuspended in sterile water. The concentration of conidia was determined using a hemacytometer and adjusted to 10^4 conidia ml^{-1} for *F. oxysporum* and 10^3 conidia ml^{-1} for *P. expansum*.

8.7.3. Antibacterial activity assays

Lyophilized peptides were solubilized in sterile distilled water to a concentration of 1000 μM and filter sterilized through a 0.22 μm-pore-size filter. For MIC assessment, dilutions of the synthetic peptides were made to obtain a final concentration of 500, 250, 125, 75, 62, 50, 31, 25, 16, 12.5 and 6.25 μM. Twenty microliters of each dilution were mixed in a microliter plate well with 20 μL of the corresponding suspension of the bacterial indicator at 10^8 CEU ml^{-1} and with 160 μL of Trypticase Soy Broth (TSB) (BioMèrieux, France) to a total volume of 200 μL. Final peptide concentrations assayed were 50, 25, 12.5, 7.5, 5.0, 3.1, 2.5, 1.6, 1.25 and 0.62 μM. Three replicates for each strain, peptide and concentration were used. Positive controls contained water instead of peptide and negative controls contained peptide without bacterial suspension.

Microbial growth was automatically determined by optical density measurement at 600 nm (Bioscreen C, Labsystem, Finland). Microplates were incubated at 25 ºC with 20 s shaking before hourly absorbance measurement for 48 h. The experiment was repeated twice. The MIC was taken as the lowest peptide concentration with no growth at the end of the experiment.

8.7.4. Antifungal activity assays

Lyophilized peptidotriazoles were solubilized in sterile Milli-Q water to a final concentration of 1 mM and filter sterilized through a 0.22-μm pore filter (Sartorius). For MIC assessment, stock solutions of peptidotriazoles were made to obtain final concentrations of 500, 250, 125, and 62.5 μM. Twenty microliters of each dilution were mixed in a microliter plate well with 80 μl of the corresponding suspension of the fungal pathogen and 100 μL of double-concentrated PDB to a total volume of 200 μL containing 0.003 % (wt/vol) of chloramphenicol. The final peptide concentrations assayed were 50, 25, 12.5, and 6.2 μM. Three replicates for each strain, peptide, and concentration combination were used. Positive controls contained water instead of peptide, and negative controls contained peptides without the fungal pathogen. Microbial growth was automatically determined by optical density measurement at 600 nm (Bioscreen C; Labsystems, Helsinki, Finland). Microplates were incubated at

20°C with 1 min/9 min on/off shaking cycles, and the measurements were done every 2 h for 6 days. The MIC was taken as the lowest peptide concentration without growth at the end of the experiment.

8.7.5. Hemolytic activity

The hemolytic activity of peptides was evaluated by determining hemoglobin release from erythrocyte suspensions of fresh human blood (5 % vol/vol). Blood was aseptically collected using a BD vacutainer K2E System with EDTA (Belliver Industrial State, Plymouth, U.K.) and stored for less than 2 h at 4 ºC. Blood was centrifuged at 6000 x g for 5 min, washed three times with TRIS buffer (10 mM TRIS, 150 mM NaCl, pH 7.2) and ten fold diluted in the same buffer.

Peptides were solubilized in TRIS buffer to a concentration of 500 μM. Sixty five microliters of human red blood cells were mixed with 65 μL of the peptide solution (final concentration of 250 μM) in a 96-well reaction plate and incubated under continuous shaking for 1 h at 37 ºC. Then, the plates were centrifuged at 3500 x g for 10 min. Eighty microliter aliquots of the supernatant were transferred to 100-well microplates and diluted with 80 μL of sterile distilled water. Three replicates for each peptide were used. Hemolysis was measured as the absorbance at 540 nm with a microplate reader.

Complete hemolysis was determined in TRIS buffer plus melittin at 200 μM (Sigma-Aldrich Corporation, Spain) as a positive control. The percentage of hemolysis (*H*) was calculated using the equation: $H = 100x[(Op - Ob)/(Om - Ob)]$, where *Op* is the density for a given peptide concentration, *Ob* for the buffer, and *Om* for the melittin-positive control.

8.7.6. *Ex vivo* assays

The efficacy of peptides was determined using infection assays in detached plant organs. Immature pear fruits (cv. Passe Crassane) were used for *E. amylovora*, detached pear leaves (cv. Conference) for *P. syringae* and detached pepper leaves (cv. Dulce Italiano) for *X.* vesicatoria. Immature pear fruits obtained from commercial

orchards were collected in early June at the 6 weeks stage from fruit set, and kept in the dark at 0 to 4 °C.

Fruits were used before one month of storage to avoid significant physiological changes which could affect the assay. Before inoculation, fruits were surface-disinfected by immersion for 1 min in a diluted solution of sodium hypochlorite (1 % active chlorine), washed twice in distilled water, and let under air flow in a sterile cabinet to remove excess water. Each fruit was wounded four times in opposite sides with a cork borer (approximately 2 mm diameter and 5 mm depth). Fruits were placed in polystyrene tray packs into boxes.

Leaves of pear or pepper were obtained from potted plants cultivated in the greenhouse. The youngest leaves were selected and surface-disinfected following the same procedure described above for immature fruits. Leaves were wounded approximately in the middle by a double transverse incision (~1 mm) to the midrib and placed in plastic boxes over a humidified paper towel. Then, 10 µl of a 200 µM solution of the corresponding peptide was delivered onto the wounds of leaves or immature fruits, and the treated material was left at room temperature for 1 h. The treated materials were inoculated with 10 µl of a suspension of *E. amylovora* EPS101 (10^7 CFU ml^{-1}), *P. syringae,* EPS31 (10^7 CFU ml^{-1}) or *X. vesicatoria* 1779 (10^8 CFU ml^{-1}). The inoculated plant material was incubated at 23 °C and high relative humidity for 5 days.

The experimental design consisted of 3 replicates of 8 immature fruits or 9 leaves per each treatment. A non-treated control inoculated only with the corresponding pathogen and a control treated with 100 mg/L of streptomycin were included. Controls for phytotoxicity assessment consisted of uninoculated immature fruits or leaves, treated only with the peptides. Infection severity levels were determined for each fruit using a scale of severity from 0 to 3 according to the symptoms observed: 0, no symptoms; 1, local necrosis around the wound or presence of exudates; 2, necrosis progression around the wound with a diameter between 3 to 5 mm; 3, necrosis progression around the wound with a diameter higher than 5 mm. Infection severity levels were determined for each leaf using a scale of severity from 0 to 3 according to the symptoms observed: 0, no symptoms; 1, leaf necrosis localized around the wound;

2, necrosis progression far from the wound; 3, necrosis of the whole leaf. The mean severity was calculated for each replicate. Two independent experiments were done.

8.7.7. *In planta* assays

The efficacy of peptides was determined using whole plant infection assays with pear plants (cv. Conference) inoculated with *E. amylovora* or *P. syringae*, and with pepper plants (cv. Dulce Italiano) inoculated with *X. vesicatoria*. Two-to-three year old pear plants grown in 20-cm-diameter plastic pots in the greenhouse were used. Plants were pruned to leave 3-to-4 shoots per plant and were forced to bud in the greenhouse. Plants were fertilized once a week with a 200 ppm N-P-K solution (20-10-20) and were used when the shoots were about 3-to-4 cm length and had 5-to-6 young leaves per shoot. Pepper plants were obtained from seeds grown in 10-cm-diameter plastic pots in the greenhouse, fertilized as for pear plants, and used when they achieved 25-30 cm height. Standard insecticide and miticide sprays were applied to pear and pepper plants. Fungicides or bactericides were not applied to prevent interference with the assays.

For the assays, the three youngest expanded leaves of each shoot were wounded approximately in the middle of the leaf by a double transverse incision (~1 mm) to the midrib. Then, 10 µl of a 200 µM solution of the corresponding peptide were delivered onto the wounds and plants were left at room temperature for 1 h. Each leaf wound of the treated plants was inoculated with 10 µl of a suspension of the corresponding bacteria as for the ex vivo assays.

Plants were incubated in a controlled environment greenhouse for 9 days in the case of pear plants and 12 days for pepper plants at 23 ± 2 ºC during day and 15 ± 2 ºC at night. Photoperiod was of 16 h of light and 8 h of dark. The experimental design consisted of three replicates of three plants per treatment. Appropriate non-treated, non-inoculated and reference controls were used as described for the ex vivo assays. Activity was assessed according to the incidence of infection, i.e. appearance of necrosis at the inoculation point. The mean incidence was calculated for each replicate. Two independent experiments were performed.

8.7.8. Susceptibility to protease degradation

Digestion of the peptides was carried out by treating 50 or 100 µg/ml peptide with 1 or 2 µg/ml proteinase K (Sigma–Aldrich Corporation, Madrid, Spain), respectively, in 100 mM TRIS buffer, pH 7.6, at room temperature. The peptide cleavage after 5, 10, 15, 30, 45 and 60 min was monitored by HPLC using a Kromasil C18 reversed-phase column (4.6 mm x 40 mm; 3.5 µm particle size) or by MALDI-TOFF. The linear gradients of 0.1 % aqueous TFA and 0.1 % TFA in ACN were run from 0.98:0.02 to 0:1 over 7 min with UV detection at 220 nm. The digestion was estimated as the percentage of degraded peptide calculated from the decrease of the HPLC peak area of the native peptide. Samples were lyophylized previous to MALDI-TOF analysis.

8.8. Cytotoxicity by a peptidotriazole infiltration assay (Tobacco assays)

Peptidotriazole solutions of 25 and 50 µM concentration in H_2O were prepared and infiltrated (100 µL) into the mesophylls of fully expanded tobacco leaves using a syringe without a needle. Three infiltrations were done for each peptide at each concentration. Control infiltrations with water (negative control) or mellitin (positive control) at the same molar concentration were performed. The appearance of symptoms on the leaves was followed for 48 h after infiltration.

Supplementary data

The material listed below is attached as supplementary material on the CD accompanying the report:

- PhD thesis in pdf format.
- All the spectra characterized in the experimental section: Annex.pdf

9. REFERENCES

Adessi, C.; Soto, C. *Curr. Med.Chem.*, **2002**, *9*, 963-978.

Agrios G. N. 2005. Plant pathology, 5th ed. Academic Press, San Diego, California.

Alexander, M. 1977. Introduction to Soil Microbiology. John Wiley and Sons, Inc., New York.

Ali G. S.; Reddy A. S. N. *Mol. Plant-Microbe Interact*. **2000**, *13,* 847-859.

Andreu, D.; Merrifield, R. B.; Steiner, H.; Boman, H. G. *Proc. Natl. Acad. Sci. USA* **1983**, *80*, 6475-6479.

Appukkuttan, P.; Van der Eycken, E. *Eur. J. Org. Chem.* **2008**, 1133-1155.

Arnusch, C. J.; Branderhorst, H.; de Kruijff, B.; Liskamp, R. M. J.; Breukink, E.; Pieters, R. J. *Biochemistry* **2007**, *46*, 13437-13442.

Aufort, M.; Herscovici,J.; Bouhours,P.; Moreau,N.; Girard,C.*Bioorg.Med. Chem. Lett.* **2008,** *18*, 1195-1198.

van Baal, I.; Malda, H.; Synowsky, S. A.; van Dongen, J. L. J.; Hackeng, T. M.; Merkx, M. Miejer, E. W. *Angew. Chem.* **2005**, *117*, 2-7.

Badosa, E.; Ferre, R.; Planas, M.; Feliu, L.; Besalú, E.; Cabrefiga, J.; Bardají, E.; Montesinos, E. *Peptides* **2007**, *28,* 2276–2285.

Badosa, E.;Ferre, R.; Francés, J.; Bardají, E.; Feliu, L.; Planas, M.; Montesinos, E. *Appl. Environ. Microbiol.* **2009**, *75*, 5563–5569.

Bardají, E.; Montesinos, E.; Planas, M.; Badosa, E.; Feliu, L.; Ferre, R. April 2006. Antimicrobial linear peptides.Patent WO/2007/125142 A1.

Bechinger, B.; Lohner, K. *Biochim. Biophys. Acta* **2006**, *1758*, 1529-1539.

Blondelle, S. E.; Lohner, K. *Biopolymers* **2000**, *55*, 74-87.

Bock, V. D.; Speijer, D.; Hiemstra, H.; Maarseveen, J. H. *Org. Biomol. Chem*. **2007***, 5*, 971-975.

Boturyn, D.; Coll, J. L.; Garanger, E.; Favrot, M. C.; Dumy, P. *J. Am. Chem. Soc.* **2004**, *126*, 5730-5739.

Brask, J.; Jensen, K. J. *J. Peptide Sci*. **2000**, *6*, 290-299.

Brask, J.; Jensen, K. J. *Bioorg. Med. Chem. Lett.* **2001**, *11*, 697-700.

Brogden, K. A.; Ackermann, M.; McCray, P. B.; Tack, B. F. *Int. J. Antimicrob. Agents* **2003**, *22,* 465–478.

Brogden, K. A. *Nature Rev. Microbiol.* **2005**, *3*, 238-250.

Cabrefiga, J.; Francés, J.; Montesinos, E.; Bonaterra, A. *Appl. Environ. Microbiol.* **2011**, *77*, 3174–3181.

Cantel, S.; Chevalier Isaad, A.; Scrima, M.; Levy, J.J.; DiMarchi, R.D.;Rovero, P.; Halperin, J.A. D'Ursi, A.M.; Papini, A.M.; Chorev, M. *J. Org. Chem.* **2008**, *73*, 5663–5674.

Cavallarin, L.; Andreu, D.; San Segundo, B. *Mol. Plant-Microbe Interact.* **1998**, *11*,218-227.

Chevalier Isaad, A.; Barbetti, F.; Rovero, P.; D'Ursi, A. M.; Cheli, M.; Papini, A. M. Eur. *J. Org. Chem.* **2008**, *73*, 5308-5314.

Chittaboina, S.; Xie, F.; Wang, Q. *Tetrahedron Lett.* **2005**, *46*, 2331-2336.

Choi, S.-K. 2004. Synthetic Multivalent Molecules, Wiley-VCH, New York.

Compant, S.; Duffy, B.; Nowak, J.; Clément, C.; Barka, E. A. *Appl. Environ. Microbiol.* **2005**, *71*, 4951-4959.

Coulson, D. R. *Inorg. Synth.* **1990**, *28*, 107-109.

Dawson, P. E.; Muir, T. W.; Clark-Lewis, I.; Kent, S. B.H. *Science* **1994**, *266*, 776-779.

Dawson, P. E.; Kent, S. B.H. *Annu. Rev. Biochem.* **2000**, *69*, 923-960.

Diamond, G.; Beckloff, N.; Weinberg, A.; Kisich, K. O. *Curr. Pharm. Des.* **2009**, *15*, 2377-2392.

Dirksen, A.; Hackeng, T. M.; Dawson, P. E. *Angew. Chem. Int. Ed.* **2006**, *45*, 7581-7584.

Djedaïni-Pilard, F.; Désalos, J.; Perly, B.; *Tetrahedron Lett.* **1993**, *34*, 2457-2460.

El-Faham, A.; Subirós-Funosas, R.; Prohens, R.; Albericio, F. *Chem. Eur. J.* **2009**, *15*, 9404-9416.

El-Faham, A.; Albericio, F. *J Pept. Sci.* **2010**, *16*, 6-9.

Evans, R. A. *Aust. J. Chem*. **2007**, *60*, 384-395.

Fan, W. Q.; Katritzky A. R. in *Comprehensive Heterocyclic Chemistry II*,*Vol. 4 (*Eds.: Katritzky, A. R.; Rees, C. W.; Scriven,V. E. F. B.), Elsevier Science, Oxford, **1996**, pp. 1-126.

Ferre, R.; Badosa, E.; Feliu, L.; Planas, M.; Montesinos, E.; Bardají, E. *Appl. Environ. Microbiol*. **2006**, *72*, 3302-3308.

Ferre, R.; Melo, M. N.; Correia, A. D.; Feliu, L.; Bardají, E.; Planas, Castanho, M. A. R. B. M. *Biophys. J.* **2009**, *96*, 1815-1827.

Fletcher, S.; Hamilton, A. D. *Curr. Opin. Chem. Biol.* **2005**, *9*, 1-7.

Forget, D.; Boturyn, D.; Defrancq, E.; Lhomme, J.; Dumy, P. *Chem. Eur. J.* **2001**, *7*, 3976-3984.

Franke, R.; Doll, C.; Eichler, J. *Tetrahedron Lett.* **2005**, *46*, 4479-4482.

Fung, S; Hruby, V. J. *Curr. Opin. Chem. Biol*. **2005**; *9*, 352-358.

Gerhardson, B. *Trends in Biotechnol*. **2002**, *20*, 338-343.

Grant, G. A. *Synthetic Peptides. A User's Guide.;* W.H. Freeman and Company: New York, 1992.

Güell, I.; Cabrefiga, J.; Badosa, E.;Ferre, R.; Talleda, M.; Bardají, E.; Planas, M.; Feliu, L.; Montesinos, E. *Appl. Environ. Microbiol.* **2011**, *77*, 2667-2675.

Guibé, F. *Tetrahedron* **1998**, *54*, 2967-3042.

Hackenberger, C. P. R.; Schwarzer, D. *Angew. Chem. Int. Ed.* **2008**, *47*, 10030-10074

Hancock, R.E.W. *Lancet Infect. Dis.* **2001**, *1*, 156-164.

Hancock, R. E. W.; H. G. Sahl. Nature Biotechnol. **2006**, *24,* 1551-1557.

Hang, H. C.; Bertozzi, C. R. *Acc. Chem. Res*. **2001,** *34*, 727-736.

Haridas, V.; Sharma, Y. L.; Sahu, S.; Verma, R. P.; Sadanandan, S.; Kacheshwar, B. G. *Tetrahedron* **2011,** *67*, 1873-1884.

Hein, J. E.; Fokin,V. V. *Chem. Soc. Rev.* **2010**, *39*, 1302-1315.

Hirschmann, R.; Nicolaou, K. C.; Pietranico, S.; Salvino, J.; Leahy, E. M.; Sprengeler, P. A,; Furst, G.; Smith, A. B.; Strader, C. D.; Cascieri, M. A.; Candelore, M. R.; Donaldson, C.; Vale, W.; Maechler, L. *J. Am. Chem. Soc*. **1992**, *114*, 9217–9218.

Hirschmann, R.; Nicolaou, K. C.; Pietranico, S.; Leahy, E. M.; Salvino, J.; Arison, B.; Cichy, M. A.; Spoors, P. G.; Shakespeare, W. C.; Sprengeler, P. A.; Hamley, P.; Smith, A. B.; Reisine, T.; Raynor, K.; Maechler, L.; Donaldson, C.; Vale, W.; Freidinger, R. M.; Cascieri, M. R.; Strader, C. D. *J. Am. Chem. Soc*. **1993**, *115*, 12550–12568.

Høiberg-Nielsen, R.; Tofteng, A. P.; Sørensen, K. K.; Roessle, M.; Svergun, D.; Thulstrup, P. W.; Jensen, K. J.; Arleth, L. *ChemBioChem* **2008**, *9*, 2663-2672.

Hoffmann, R. W. *Synthesis* **2006**, *21*, 3531–3541.

Holub, J. M.; Kirshenbaum, K. *Chem. Soc. Rev.* **2010**, *39*, 1325-1337.

Hong, S. Y.; Oh, J. E.; Lee, K. H. *Biochem.Pharmacol.* **1999**, *58*, 1775-1780.

Huang, H. W. *Biochemistry* **2000**, *39*, 8347-8352.

Huang, H. W. *Biochim. Biophys. Acta* **2006**, *1758*, 1292-1302.

Hudson R. F. *Angew. Chem.* **1973**, *85*, 63–84.

Janiszewska, J.; Swieton, J.; Lipkowski, A. W.; Urbanczyk-Lipkowska, Z. *Bioorg. Med. Chem. Lett.* **2003**, *13*, 3711-3713.

James, I. W. *Tetrahedron,* **1999***, 55,* 4855-4946.

Jensen, K.J.; Barany, G. *J. Peptide Res*. **2000**, *56*, 3-11.

Jensen, K. J.; Brask, J. *Cell. Mol. Life Sci*. **2002**, *59*, 859-869.

Jensen, K. J.; Brask, J. *Biopolymers* **2005**, *80*, 747-761.

Jenssen, H.; Hamil, P.; Hancock, R. E. W. *Clin. Microbiol. Rev.* **2006**, *19*, 491-511.

Kaiser, E.; Colescott, R. L.; Bossinger, C. D.; Cook, P. *Anal.Biochem*. **1970**, *34*, 595-598.

Kappe, C. O. *Angew. Chem. Int. Ed.* **2004**, *43*, 6250-6284.

Katayama, H.; Hoja, J.; Ohira, T.; Nakahara, Y. Tetrahedron Lett. **2008**, *59*, 5492-5494.

Kates, S.A.; Albericio, F. *Solid-Phase Synthesis: A Practical Guide*. Marcel Dekker, Inc., 2000.

Kiessling, L. L.; Gestwicki, J. E.; Strong, L. E. *Angew. Chem. Int. Ed.* **2006**, *45*, 2348-2368.

Kimmerlin, T.; Seebach, D. *J. Peptide Res.* **2005**, *65*, 229-260.

Kobayashi, S.; Jørgensen, K. A. *Cycloaddition Reactions in Organic Synthesis*. Wiley-VCH: Weinheim, Germany, 2002.

Le, T.; Cheah, W. C.; Wooda, K.; Black, D. S. C.; Willcox, M. D.; Kumar, N. *Tetrahedron Letters* **2011**, *52*, 3645–3647.

Lemieux, G. A.; Bertozzi C. R. *Trends Biotechnol.* **1998**, *16*, 506-513.

Li, D; Elbert, D. L. *J. Peptide Res.* **2002**, *60*, 300-303.

Lin, F. L.; Hoyt, H. M.; van Halbeek, H.; Bergman, R. G.; Bertozzi, C. R. *J. Am. Chem. Soc.* **2005**, *127*, 2686-2695

Liu, L.; Hong, Z. Y.; Wong, C. H. *ChemBioChem* **2006**, *7*, 429-432.

Liu, Z.; Deshazer, H.; Rice, A. J.; Chen, K.; Zhou, C.; Kallenbach, N. R. *J. Med. Chem*. **2006**, *49*, 3436-3539.

Liu, Y.; Zhang,L.; Wang, J.; Li, Y.; Xu, Y.; Pan, Y. *Tetrahedron* **2008**, *64*, 10728-10734.

Lundquist, J. T.; Pelletier, J. C. *Org. Lett.* **2001**, *3*, 781–783.

Makovitzki, A.; Viterbo, A.; Brotman, V.; Chet, I.; Shai, Y. *Appl. Environ. Microbiol.* **2007**, *73*, 6629-6636.

Mamidyala, S. K.; Finn,M. G. *Chem. Soc. Rev*. **2010***, 39*, 1252-1261.

Martos, V.; Castreno, P.; Valero, J.; Mendoza, J. *Curr. Opin. Chem. Biol.* **2008**, *12*, 698-706.

Marcos, J. F.; Gandia, M. *Expert. Opin. Drug Discov.* **2009**, *4*, 659-671.

Matsuzaki, K. *Biochim. Biophys.Acta* **2009**, *1788,* 1687–1692.

McManus, P. S.; Stockwell, V. O.; Sundin, V. O.; Jones, A. L. *Annu. Rev. Phytopathol*. **2002**, *46*, 443-465.

Meldal, M.; Tornøe,C. W. *Chem. Rev*. **2008**, *108*, 2952-3015.

Melo, M. N.; Ferre, R.; Castanho, M. A. R. B. *Nature Rev. Microb.* **2009**, *7*, 245-250.

Miranda, L. P.; Alewood, P. F. *Biopolymers* **2000**, *55*, 217-226.

Monroc, S.; Badosa, E.; Feliu, L.; Planas, M.; Montesinos, E.; Bardají, E. *Peptides* **2006**, *27***,** 2567–2574.

Monroc, S.; Badosa, E.; Besalú, E.; Planas, M.; Bardají, E.; Montesinos, E.; Feliu, L. *Peptides* **2006**, *27***,** 2575–2584.

Montesinos, E.; Bardají, E. *Chem. Biodivers.* **2008**, *5*, 1225-1237.

Montesinos, E.; Vilardell, P. *Eur. J. Plant Pathol*. **2001**, *107***,** 787–794.

Moses, J. E.; Moorhous, A. D. *Chem. Soc. Rev*. **2007**, *36*, 1249-1262.

Nicolas, P**.** *FEBS J.* **2009**, *276,* 6483-6496.

Nilsson, B. L.; Kiessling, L. L.; Raines, R. T. *Org. Lett.* **2000**, *2*, 1939-1941.

Oh, D.; Shin, S. Y.; Lee, S.; Kang, J. H.; Kim, S. D.; Ryu, P. D.; Hahm, K. S.; Kim, Y. *Biochemistry* **2000**, *39*, 11855-11864.

Ortoneda, M.; Guarro, J.; Madrid, M. P.; Caracuel, Z.; Roncero, M. I. G.; Mayayo, E.; Di Pietro, A. *Infect. Immun.* **2004**, *72*, 1760-1766.

Otvos, L., Jr. *J. Pept. Sci.* **2000***, 6,* 497–511.

Oyelere, A. K.; Chen, P. C.; Yao, L. P.; Boguslavsky, N. *J. Org. Chem.***2006**, *71*, 9791-9796.

Papo, N.; Oren, Z.; Pag, U.; Sahl, H. G.; Shai, I. *J. Biol. Chem.* **2002**, *277*, 33913-33921.

Pedersen, A. S.; Abell, A. *Eur. J. Org. Chem*. **2011**, 2399-2411.

Pieters, R. J.; Arnusch, C. J.; Breukink, E. *Protein Pept. Lett.* **2009**, *16*, 736-742.

Powers, J. P. S.; Hancock, R. E. W. *Peptides* **2003**, *24,* 1681–1691.

Reck, F.;Zhou, F.; Girardot,M.; Kern, G.; Eyermann, C. J.; Hales, N. J.; Ramsay, R. R.; Gravestock, M. B.*J. Med. Chem*. **2005**, *48*, 499-506.

Rijkers, D. T. S.; Van Vugt, R. H. H.; Jacobs, H. J. F.; Liskamp, R. M. J. *Tetrahedron Lett.* **2002**, *43*, 3657-3660.

Roberts, K. D.; Lambert, J. N.; Ede, N. J.; Bray, A. M. *J. Peptide Sci.* **2004,** *10*, 659-665.

Roedern, E.G.V.; Kessler, H. *Angew. Chem. Int. Ed. Engl.* **1994***,* 33, 687-698.

Rose, K. *J. Am. Chem. Soc.* **1994**, *116*, 30-33.

Rostovtsev, V. V.; Green, L. G.; Fokin, V. V.; Sharpless, K. B. *Angew. Chem. Int. Ed.* **2002**, *41*, 2596-2599.

Rotem, S.; Mor, A. *Bichim. Biophys. Acta* **2009**, *1788*, 1582-1592.

Rundberget, T.; Skaar, I.; Flåøyenm, A. *Int. J. Food Microbiol.* **2004**, *90*, 181-188.

Sanzani, S. M.; Girolamo, A.; Schena, L.; Solfrizzo, M.; Ippolito, A.; Visconti, A. *Eur. Food Res. Technol.* **2009**, *228*, 381-389.

Saxon, E.; Armstrong, C.R.; Bertozzi, C.R. *Org. Lett.* **2000**, *2*, 2141-2143.

Scrima,M.; Chevalier-Isaad,A.; Rovero,P.; Papini, A. M.; Chorev,M.; D'Ursi,A. M. *Eur. J. Org. Chem.* **2010**, 446-457.

Shao, J.; Tam J. P. *J.* Am. Chem. Soc. **1995***, 117*, 3893-3899*.*

Sharma, R. K.; Sundriyal, S.; Wangoo, N.; Tegge, W.; Jain, R. *Chem. Med. Chem.* **2010**, *5*, 86-95.

Steiner, H.; Hultmark, D.; Engstrom, A.; Bennich, H.; Boman, H. G. *Nature* **1981**, *292*, 246-248.

Subirós-Funosas, R; Prohens, R.; Barbas, R.; El-Faham, A.; Albericio, F. *Chem. Eur. J.* **2009**, *15*, 9394-9403.

Sung, M.; Poon, G. M. K.; Gariépy, J. *Biochim. Biophys. Acta* **2006**, *1758*, 355-363.

Sureshbabu, V. V.; Narendra, N.; Hemantha, H. P.; Chennakrishnareddy, G. *Protein Peptide Lett.* **2010**, *17*, 499-506.

Tofteng, A. P.; Hansen, T.H.; Brask, J.; Nielsen, J.; Thulstrup, P. W.; Jensen, K. *J. Org. Biomol. Chem.* **2007**, *5*, 2165-2320.

Toke, O. *Biopolymers*, **2005** *80*, 717-735.

Tornøe, C. W.; Christensen, C.; Meldal, M. *J. Org. Chem.* **2002**, *67*, 3057-3064.

Tornøe, C. W.; Sanderson, S. J.; Mottram, J. C.; Coombs, G. H.; Meldal, M. *J. Comb. Chem.* **2004**, *6*, 312-324.

Tron,G. C.; Pirali,T.; Billington, R. A.; Canonico, P. L.; Sorba,G.; Genazzani,A. A. *Med. Res. Rev.* **2008**, *28*, 278-308.

Tossi, A.; Sandri, L.; Giangaspero, A. *Biopolymers* **2000**, *55*, 4–30.

Turner, A.; Oliver, A. *Org. Lett*. **2007**, *9*, 5011-5014

Vadas, O.; Rose, K. *J. Pept. Sci.* **2007**, *13*, 581-587.

Valeur, E.; Bradley, M. *Chem. Soc. Rev.* **2009**, *38*, 606-631.

Vidaver, A. K. *Clin. Infect. Dis.* **2002**, *34*, S107-110.

Wan,Q.; Chen, J.; Chen,G.; Danishefsky, S. J .*J. Org. Chem.* **2006**, *71*, 8244-8249.

Wehrstedt, K. D.; Wandrey, P.A.; Heitkamp, D. *J. Hazard. Mater.* **2005**, *A126*, 1-7.

Whiting, M.; Muldoon, J.; Lin, Y. C.; Silverman, S. M.; Lindstrom, W.; Olson, A. J.; Kolb, H. C.; Finn, M. G.; Sharpless, K. B.; Elder, J. H.; Fokin, V. V.*Angew. Chem. Int. Ed.* **2006**, *45*, 1435-1439.

Zaiou, M *J. Mol. Med.* **2007**, *85*, 317-329.

Zasloff, M. *N. Engl. J. Med.* **2002**, *347*, 1199-1200.

Zasloff, M. *Nature* **2002**, *415*, 389-395.

Zatsepin, T. S.; Stetsenko, D. A.; Gait, M. J.; Oretskaya, T. S. *Bioconjugate Chem.* **2005**, *16*, 471-489.

Zhang, Y.; Mi, J.; Zou, X. *Eur. J. Med. Chem*. **2011**, *46*, 4391-4402.

Zhu, W. L.; Nan, Y. N.; Hahm, K. S. M.; Shin, S. Y. *J. Biochem. Mol. Biol.* **2007**, *40*, 1091-1094.